THE DIATOM RECORD:

RECONSTRUCTING HISTORICALLY RECENT ENVIRONMENTAL CHANGE IN THE KNYSNA ESTUARY

Helen Grace Antonopoulos

Supervisors: Prof. Michael E. Meadows & Dr. Kelly L. Kirsten

Dissertation submitted in the fulfilment of the requirements for the degree Master of Science in the Department of Environmental and Geographical Science

University of Cape Town

PLAGIARISM DECLARATION

1. I know the meaning of plagiarism and declare that all of the work in the dissertation (or thesis), save for that which is properly acknowledged, is my own.
2. I have used the Harvard convention for citation and referencing. Each contribution to, and quotation in this thesis from the work(s) of other people ahs been attributed, and has been cited and referenced.
3. I have not allowed, and will not allow, anyone to copy my work with the intention of passing it off as their own work.

Signature: Signed by candidate

Date: 10 October 2022

ABSTRACT

Estuaries are highly productive systems responsible for many vital ecosystem goods and services. Therefore, it is not surprising that the diversity and abundance of exploitable estuarine resources have attracted human settlers for centuries. Increased anthropogenic pressures have placed much stress on estuarine and coastal ecosystems. This is the case of the Knysna Estuary, which is South Africa's highest-rated estuary in terms of biodiversity and conservation importance. This study represents the first high-resolution diatom record from the Knysna Estuary encompassing the last ~680 years. Diatom analysis was employed to reconstruct salinity, nutrients, and saprobity variables in addition to inferring community structure and trophic status over time by creating an age-depth model based on a combination of ^{210}Pb and radiocarbon dates. The record is divided into three distinctive phases, namely the Pre-Colonial (~610 to ~200 cal BP), Colonial (~200 cal BP to ~1900 CE), and Anthropogenically Impacted Lagoon Phase (~1900 CE to Present). These phases correspond with the Little Ice Age (LIA), the arrival of colonialists, and anthropogenic impacts linked to rapid population growth and land use change. More specifically, the dominance of marine species illustrate that the first phase of the LIA is associated with drier conditions, whereas a growing dilute and eutrophic assemblage reveals a wetter second phase of the LIA coinciding with the arrival of colonialists in the 1700s. Consequently, it is challenging to disentangle natural climate change with the effects of deforestation and agriculture during the Colonial Phase. A shift towards an increasingly fresh, hypertrophic, and polysaprobic diatom assemblage is indicative of the intensification of agricultural practices in the catchment from ~1900 CE to present, stormwater inflow, the inefficiency of the Knysna Waste Water Treatment Works (WWTW), and sewage entering the estuary via streams during the final phase of the estuary's development. This high-resolution record is of vital importance, as it is one of a few palaeoestuarine studies in the Southern Hemisphere to illuminate the effects of natural climate change and human-induced impacts on an estuarine system. Despite the limitations, this study illustrates that diatoms are a useful tool for tracking environmental change in estuaries.

Keywords

Diatoms, estuaries, historically recent change, Little Ice Age, land use change, anthropogenic impact

ACKNOWLEDGEMENTS

This project would not be possible without the patience and kindness of my supervisors, Prof. Michael Meadows and Dr. Kelly Kirsten. Thank you for the support, motivation, and various opportunities sent my way. To Kelly – thank you for always going above and beyond. I wouldn't have been able to do this without you.

I would like to express my gratitude to everyone who helped out in the field, particularly to Sayed Hess who is always willing to lend a hand. Thank you, Prof. Kunshan Bao, for supplying the grain-size data and for assisting me with the methodology thereof. Regarding the chronology, I'd like to thank Prof. Kunshan Bao again for dating the very-many samples. To Dr. Kelly Kirsten and Dr. Lauren Pretorius - thank you for all the hours spent on the age-depth models. Additional thanks to Dr. Marco Aquino-López for availing himself for discussions. It is safe to say that there would be no study without all of your efforts.

I'd also like to thank the Post-Graduate Funding Office for financial support, especially when it came to extending this degree in the midst of a global pandemic.

Last but not least, a special thanks is due to my family and friends who have supported, encouraged, and inspired me throughout this project.

TABLE OF CONTENTS

LIST OF FIGURES

LIST OF TABLES

CHAPTER 1 - INTRODUCTION

The coastal zone is a dynamic interface where estuaries and coastal wetlands form a critical transitional zone between the land, rivers, and oceans (Zhao *et al.,* 2004; Bianchi and Allison, 2009). Despite accounting for a surface area of only 1.1 x 10^6 km² globally (Dürr *et al.,* 2009), estuaries are highly productive systems responsible for many vital ecosystem goods and services (Day *et al.,* 2013). Consequently, it is not surprising that the diversity and abundance of exploitable estuarine resources have attracted human settlers for centuries (Day *et al.,* 2013; Teichert *et al.,* 2016). From the 1900s to present, rapid growth in the human population led to large-scale changes in estuaries (Day *et al.,* 2013). In addition to undermining an estuary's ability to execute ecological functions, increased anthropogenic pressures have placed much stress on estuarine and coastal ecosystems (Van Damme *et al.,* 2005; Wachnicka *et al.,* 2010; Lemley *et al.,* 2016). A rise in contaminants from domestic, industrial, aquaculture, and agricultural activities has led to excessive amounts of nutrients (particularly nitrogen and phosphorous) and organic material, which can be, but is not limited to, wastewater treatment works and sewerage from informal settlements, within the estuary's catchment (Van Niekerk *et al.,* 2012; Lemley *et al.,* 2016). This, in turn, has a direct impact on the biomass and community composition of phytoplankton, which includes diatoms (Lemley *et al.,* 2016). Diatoms are the first organisms to react to environmental changes and have long been used as biological indicators of water quality due to their rapid response rate (Bellinger and Sigee, 2015; Dalu and Froneman, 2016; Ryabushko *et al.*, 2017; Temizel *et al.*, 2017). Hence, they are an effective proxy in discerning natural and anthropogenic impacts, such as eutrophication and industrial pollution, on aquatic ecosystems (Bellinger and Sigee, 2015; Lemley *et al.,*2016; Ryabushko *et al.*, 2017). The diatom community acts as a repository for the effect of human activities on changes in environmental conditions in estuaries. Therefore, the analysis of fossilised diatoms deposited in the sediment of vegetated and unvegetated coastal wetlands can aid in the reconstruction of estuarine environments and determine the extent of environmental change and anthropological disturbance (Fox *et al.,* 1999; Parsons *et al.,* 1999).

Thus far, much international research has focused on the taxonomy and identification of diatoms, laboratory cultivation, their sensitivity to certain parameters (Werner, 1977; Mann, 1990; Battarbee *et al.,* 2002), and the use of diatoms in palaeoclimate reconstruction studies (Crosta *et al.,* 1998; Potapova and Charles, 2002; Obrezkova, 2007). Additionally, a wide variety of research exists on the use of diatoms as bioindicators of water quality in lakes (Guzkowska and Gasse, 1990; Blanco *et al.,* 2004), rivers

(Kwadrans *et al.,* 2004; Salomoni *et al.,* 2006; Szczepocka and Szulc, 2009), and streams (Winter and Duthi, 2000; Jüttner *et al.,* 2003). In contrast, studies of the estuarine diatom community and their responses to environmental change, especially in relation to the historically recent past, are much scarcer than that of freshwater studies (Lemley *et al.,* 2016). It must be noted that the number of studies corresponding to estuarine environmental change over time has increased at a noticeably slower pace as compared to studies related to the value (both socio-economic and environmental) of estuaries (Starratt, 2007). This is the case of the Knysna Estuary (34°04'35" S, 23°03'40" E) - a functional shallow estuary located on the south coast of South Africa, approximately 485km from Cape Town (Van Niekerk *et al.,* 2012; Bate *et al.,* 2013, Pollard *et al.,* 2018). At present, the Knysna Estuary is threatened by anthropogenic activities, such as urban expansion, tourism development, and land use change (Marker, 2003; Marker and Holmer, 2005). Notwithstanding, the estuary is of high scientific and socioeconomic importance to South Africa (Marker, 2003; Marker and Holmer, 2005; Coastal and Environmental Services (CES), 2007).

Despite the importance of the estuary, only two diatom studies have been conducted (Bate *et al*., 2013; Else, 2018). Bate *et al.* (2013) broadly aimed to use diatoms as a proxy to identify salinity characteristics of South African estuaries. The results did not focus on Knysna specifically, nor was any reference made to the diatom assemblage of the estuary. The most recent and more comprehensive study is a postgraduate project (Else, 2018) that determined the diatom distribution in the estuary and attributed the distribution pattern mostly to salinity and partly to nutrient availability or pollution. No research has been conducted on the historically recent diatom assemblages of the Knysna Estuary, thus only a limited temporal understanding of environmental change - and the impact of anthropogenic activity - over time is known. Inferring environmental conditions prior to extensive human settlement can provide management authorities with a baseline of physical, chemical, or biological conditions (Watson *et al.,* 2011). Although it is not within the scope of this study, reconstructive studies have the potential to steer sustainable conservation decisions by informing mitigation and rehabilitation targets (Gillson and Marchant, 2014). This is particularly important, especially since the Knysna Estuary is one the most important estuaries in terms of biodiversity (Adams *et al.,* 2020).

1.1. RESEARCH QUESTIONS

- What are the recent environmental changes that have taken place in the Knysna Estuary?
- What are the main environmental drivers responsible for the observed changes in the study sites?

- Through the analyses of diatom samples, what is the nature and scale of the changes in the diatom assemblage at the sites and what are the inferred anthropogenic influences?
- What might these environmental changes and inferred water quality conditions mean in relation to human activities?
- How does the diatom assemblage of the study sites compare with that of other regional studies?
- Can an understanding of the recent environmental changes assist in guiding future efforts towards restoring water quality?

1.2. AIM AND OBJECTIVES

1.2.1. Aim

This research aims to use fossilised diatoms as biological indicators of environmental conditions to explore historically recent changes in the Knysna Estuary. Diatom analysis is applied alongside well-refined age models to provide an indication of which environmental parameters are responsible for the change detected in the estuary. It is anticipated that this research will illuminate the changes that have occurred during the geologically recent past, specifically in terms of water quality. Moreover, it is expected to produce a high temporal resolution study of environmental change in the Knysna Estuary, while highlighting the extent of anthropogenically-induced change.

1.2.2. Objectives

Bearing the above aim in mind, the following objectives were determined:

- Obtain shallow sediment cores from the Knysna Estuary
- Create a refined age-depth model for these sediments using Carbon-14 and Lead-210 dating techniques
- Sub-sample cores to obtain samples for diatom analysis
- Illustrate the temporal changes in diatom communities by using percentage diatom representation against depth and age
- Reconstruct water quality indices over the temporal scale
- Describe the historically recent diatom assemblages whilst taking historical records into consideration
- Relate the changes in diatom composition to human-induced environmental changes

1.2. THESIS STRUCTURE

This introductory chapter (**Chapter 1)** places the research into perspective, as well as explains the need to determine environmental change over geologically recent timeframes in estuaries, especially when considering their immense value. **Chapter 2** examines the literature regarding estuaries and diatoms, while emphasising the various uses of diatoms as biological indicator species. **Chapter 3** describes the physical and hydrological setting of the Knysna Estuary, in addition to its contemporary setting in terms of climate, vegetation, land use, and anthropogenic influences. **Chapter 4** outlines the methodology employed to achieve the aims and objectives of the research. **Chapter 5** presents the results obtained by implementing the methodology outlined in chapter 4. **Chapter 6** provides a discussion of the results by outlining key findings. Finally, **Chapter 7** contains concluding thoughts and remarks regarding the research.

CHAPTER 2 - THE RELATIONSHIP BETWEEN ESTUARIES AND DIATOMS

Estuaries are subject to manifold anthropological pressures (Day *et al.,* 2013; Teichert *et al.,* 2016), which have led to large-scale changes in estuarine functioning, biodiversity, and water quality (Lamberth and Turpie, 2003; Lotze *et al.,* 2006). Sediment deposits in estuaries have long been used in reconstructive studies, by reason that mudflats and salt marshes act as depositional sinks for the accumulation of sediment layers (Fox *et al.,* 1999). These layers contain various contaminants, as well as fossilised diatoms (Underwood *et al.*, 1998; Cantwell *et al.,* 2007). Diatoms preserved in estuarine sediments have been used widely in reconstructive and contemporary studies as they provide a rapid indication of environmental change due to their short regeneration time (Wachnicka *et al.,* 2010; Gordon *et al.,* 2012). This chapter will elaborate on the relationship between estuarine systems and diatoms by elucidating the above-mentioned information.

2.1. ESTUARIES

2.1.1. Definition

The coastal zone forms a dynamic interface between the land and the ocean (Bianchi and Allison, 2009). More specifically, the coastal zone is a region where the atmosphere, land, freshwater, and oceans interact to form "one of the most active interfaces of the biosphere" (Bianchi and Allison, 2009; Dürr *et al.,* 2009:441). In particular, estuaries and coastal wetlands form the critical transitional zone between land, rivers, and oceans (Zhao *et al.,* 2004), where estuaries – and the various habitat types they are comprised of, including sand and mudflats, salt marshes, water bodies, and plant and rock communities – essentially operate as a transitional zone between marine and freshwater systems (Van Damme *et al.,* 2005). According to Whitfield (1992:89), the definition of an estuary, as proposed by Day (1980:198), is the most applicable to southern African estuaries. The definition is as follow:

> "An estuary is a partially enclosed body of water which is either permanently or periodically open to the sea, and within which there is a measurable variation of salinity due to the mixture of seawater with freshwater derived from land drainage."

This definition accounts for seasonal droughts when a low or negligible amount of fluvial discharge forms a sandbar that isolates an estuary from the ocean – consequently creating a fresh or hypersaline lake or lagoon (Van Niekerk *et al.,* 2012). In contrast, during the rainy season, flooding may cause complete flushing of the estuary leading to limited mixing between marine and fresh waters within the system to the extent that some southern African estuaries turn into a river mouth (Van Niekerk *et al.,* 2012).

2.1.2. The Value of Estuaries

Despite accounting for a relatively small surface area, estuaries are widely recognised for their economic value, productivity, and biodiversity (Dürr *et al.,* 2009; Adams *et al.,* 2012; Department of Environmental Affairs [DEA], 2015). This, in turn, is responsible for many vital ecosystem services estimated to be worth roughly $30 000 per hectare in 2011 (Constanza *et al.,* 2014). The Millennium Ecosystem Assessment (MEA, 2005; Reid *et al.,* 2005) broadly defines ecosystem services as the benefits human populations derive from ecosystems. Stated otherwise, this includes the direct and indirect ecosystem goods and services obtained from ecosystem functions (Constanza *et al.,* 1997; Barber *et al.,* 2011). Ecosystem services are divided into four main categories, namely provisioning services (including food, water, timber, and other resources), regulating services (such as air and water filtration, carbon sequestration, and erosion control), supporting services (for example, soil formation, nursery areas, nutrient cycling, and waste treatment) and cultural services (consisting of spiritual, educational, aesthetic, cultural, and recreational benefits) (Zhao *et al.,* 2004; MEA, 2005; Reid *et al.,* 2005; Turpie and Clark, 2007; Van Niekerk *et al.*, 2012). Waste treatment is a highly important supporting service, since an estuary's high retention rate renders them effective in breaking down waste and detoxifying pollution, whereas tidal and fluvial flushing assists with the dilution and transportation of pollutants (Van Niekerk *et al.,* 2012). According to Lamberth and Turpie (2003:131), estuaries are particularly valuable in terms of the role they play in fisheries, as the South African fishing industry in estuarine systems alone was valued at approximately R1251 billion in 2002, partly owing to the fact that estuaries act as nursery areas for various fish species that depend on the estuary during the early stages of their growth. For example, the Cape stumpnose (*Rhabdosargus holubi*) uses the Knysna estuary as its nursery grounds during its juvenile years (Napier *et al*, 2009).

2.1.3. Estuary Functionality

Estuaries are regarded as dynamic and inherently variable owing to elements such as winds, tidal forces, and fluvial discharge subjecting them to constant change over a manifold of temporal and spatial scales (Schumann *et al.,* 1999; Trobajo and Sullivan, 2010). Essentially, the complex dynamics and steep chemical gradients are a major feature of estuaries that cause constant fluctuation in the amount, type, and temporal qualities of material within the system (Van Damme *et al.,* 2005). Estuaries are characterised by the variability of their physicochemical parameters, such as fluctuations in salinity, temperature, conveyor belt circulation, turbidity and wave action, and the distinctive biogeochemistry of estuarine sediment (Cooper *et al.*, 2010). Bearing this in mind, a specific estuary's characteristics are often a combination of the distinguishing physical and chemical characteristics, as outlined below (Schumann *et al.*, 1999).

First and foremost, salinity fluctuations are pronounced in estuaries, as salinity can vary between 0 g kg^{-1} - being freshwater - and 35 g kg^{-1} - being marine (Whitfield, 1992; Schumann *et al*, 1999). Variation in salinity is usually horizontal, as rivers introduce freshwater from the upper reaches of the estuary and saline water enters via the mouth (Schumann *et al.*, 1999). Secondly, temperature fluctuations are one of the main parameters of estuaries. Generally, there is temperature variation from the lower reaches to the upper reaches (Whitfield, 1992). In turn, temperature and salinity both determine water density, although salinity is the dominant constituent (Schumann *et al.*, 1999). This results in the vertical estuarine stratification of estuarine waters, where an increase in depth is associated with higher salinity levels and lower temperatures (Schumann *et al.*, 1999). Subsequently, variation in water density drives the characteristic conveyor belt circulation pattern present in estuarine systems (Schumann *et al.*, 1999). This circulation pattern occurs when dense, deep seawater flows inland, while concurrently the less dense riverine input flows towards the mouth of the estuary due to a seaward slant in the water surface (Schumann *et al.*, 1999). The horizontal stratification, as determined by water density, is perturbed by tides and currents - a combination of marine tidal and river flows - as they are responsible for the majority of the turbulence and mixing between different layers (Whitfield, 1992).

Lastly, estuaries are characterised by distinctive biogeochemistry within the sediment (Cooper *et al.*, 2010). The sediments create a substrate with unique chemistry and benthic communities, where anoxic sediments and high carbon dioxide partial pressures are generally distinctive of estuaries (Boschker *et al.*, 2005; Cooper *et al.*, 2010). Furthermore, the trophic status of aquatic habitats is determined by the

following factors: nitrogen and phosphorous concentrations, oxygen budget, transparency, primary production, and chlorophyll concentration, which is indicative of phytoplankton biomass (Van Dam *et al.*, 1994; Istvanovics, 2010). The upper reaches of the estuaries tend to be net heterotrophic, whereas the portion with a stronger marine influence may be more susceptible to algal blooms, since nutrients released by mineralisation are transported to this area, subsequently stimulating primary production (Boschker *et al.*, 2005). At present, primary production and associated algal blooms are further abetted by land-use change or effluent discharge, as these activities cause enhanced nutrient loading in estuaries (Bianchi and Allison, 2009; Cooper *et al.*, 2010; Van Niekerk *et al.,* 2012).

2.1.4. Coastal Migration and Associated Threats

Estuaries are highly productive systems, as indicated by the large diversity of goods and services that they provide (Day *et al.,* 2013). This, in addition to the beneficial position of estuaries and coastal zones in terms of maritime transportation routes (Teichert *et al.,* 2016), has attracted human settlement for centuries (Day *et al.,* 2013). For example, the presence of archaeological remains indicates that settlements have developed alongside estuaries and lower river valleys for millennia, where many of these have given rise to major cities, including Venice, Calcutta, and Shanghai (Day *et al.,* 2013). Almost half of all major cities are located in the coastal boundary and accommodate approximately two-thirds of the global population (MEA, 2005; Reid *et al.,* 2005; Bianchi and Allison, 2009). The figure is still growing rapidly – it is projected that three-quarters of the population will reside in the coastal zone by 2025, whereas the remaining 25% will inhabit areas surrounding major rivers (Bianchi and Allison, 2009; Dürr *et al.*, 2011).

Based on the above, it is evident that an increasing amount of the population resides in the coastal zone, in effect rendering estuarine and coastal ecosystems one of the most “heavily used and threatened” systems in the world, as human activities have a direct and indirect influence on estuarine biodiversity and resources (Lamberth and Turpie, 2003; Barbier *et al.,* 2011:169). Consequently, the structure and functioning of estuaries have been significantly altered by anthropogenic impacts, such as resource overexploitation, urbanisation, infrastructure developments, land use change, sea level rise, and pollution (Dürr *et al.*, 2011; Van Niekerk *et al.,* 2005; Cooper, Gaiser and Wachnicka, 2010; Teichert *et al.,* 2016).

The rapid population growth in coastal areas is particularly reflected by land-use change and the increased discharge of effluent by faulty municipal wastewater treatment works, thus leading to enhanced nutrient loading (or eutrophication) in estuaries (Bianchi and Allison, 2009; Cooper *et al.*, 2010; Van Niekerk *et al.,*

2012). The elevated concentration of various forms of nitrogen and phosphorus in estuaries is of major concern, considering that it imperils systems in the coastal zone (Cooper *et al.*, 2010; Trobajo and Sullivan, 2010). Eutrophication causes environmental issues that include algal blooms, hypoxia and anoxia (Bianchi and Allison, 2009; Wallace *et al.,* 2014), biodiversity decline, and habitat loss, all of which ultimately places socioeconomic, environmental, cultural and human health at risk (Cooper *et al.*, 2010). According to Van Damme *et al.* (2005), ecological functioning is of the utmost importance, seeing that it is the final opportunity to address water quality issues prior to it developing into a refractory issue in the coastal zone. Furthermore, variation in the amount of nutrients entering the system has a detrimental impact on primary producers, such as phytoplankton and benthic diatoms, thus influencing the food web as a whole.

2.2. ESTUARIES AND DIATOMS

2.2.1. Description, Habitat, and Ecological Function

Diatoms are unicellular, eukaryotic algae, and are either solitary or live in colonies (Round *et al.,* 1990; Dixit *et al.,* 1992; Battarbee *et al.,* 2002). Current records indicate that this extremely diverse group consists of roughly 60 000 species and is distinguished by siliceous cell walls termed frustules, brown-yellow colouration, and photosynthetic pigments (Battarbee *et al.,* 2002; Potapova and Charles, 2002; Smol and Stoermer, 2010). According to Round *et al.* (1990:7), most diatoms have simplistic shapes, where the valves are radially or bilaterally symmetrical, parallel to one another, and linked by a cylindrical girdle (Dixit *et al.,* 1992; Mann, 1999; Battarbee *et al.,* 2002). Their frustules consist of two roughly identical thecae or valves, which have unique morphological features aiding in species identification (Gordon *et al.,* 2012).

Diatoms occur in most aquatic and subaerial environments, including rivers, lakes, wetlands, salt marshes, oceans, and estuaries (Round *et al.,* 1990; Dixit *et al.,* 1992; Battarbee *et al.,* 2002; Gordon *et al.,* 2012). In estuaries, benthic epipelic diatoms form the largest group of photoautotrophic organisms living in the fine intertidal sediments (Underwood *et al.*, 1998). To a lesser extent, diatoms also occur in planktonic habitats and are present in a majority of microhabitats within aquatic systems including on plants, rocks, sand, and animals (Round *et al.,* 1990; Dixit *et al.,* 1992; Reid *et al.,* 1995).

Lemley *et al.* (2016:12), describe microalgae which include diatoms, as “one of the most important components of estuarine ecosystems.” This is due to diatoms in the littoral zone having high productivity

and photosynthetic rates, thus rendering them important primary producers located at the base of all aquatic food webs (Hoagland *et al.,* 1993; Underwood, 1994; Lemley *et al.,* 2016). As a result, various heterotrophs, especially demersal fish and other nektobenthic species (Petrov and Nevrov, 2007), are dependent on diatoms as a source of sustenance, in that diatoms contain high-energy fat reserves or lipid contents (Mann, 1999; Potapova and Charles, 2002; Battarbee *et al.,* 2010; Smol and Stoermer, 2010) that produce short food chains powered by algal blooms (Falkowski *et al.,* 2004).

2.2.2. Diatoms as Bioindicators

Bioindicators are biological ecosystem components that depict physicochemical variables within the aquatic environment and are indicative of the overall state of the ecological conditions (Weilhoefer and Pan, 2007; Desrosiers *et al.,* 2013). Subsequently, bioindicators quantify the functional and structural shifts (or qualitative and quantitative changes) in community components and function as an "integrative tool" that communicates complex information and offers insight into trends and phenomena that are not easily distinguished (Desrosiers *et al.,* 2013:26). The foremost benefit of utilising a biological approach lies in its ability to study biological components that have sustained contact with pollutants in aquatic environments and represent past and contemporary water quality conditions (Dalu and Froneman, 2016).

Suitable bioindicator groups are highly responsive to environmental changes and must react in a predictable manner to physicochemical changes in aquatic systems (Reid *et al.,* 1995; Lemley *et al.,* 2016). Diatoms meet both these requirements and provide a rapid indication of environmental change due to their short generation time (Dixit *et al.,* 1992; Harding *et al.,* 2005; Wachnicka *et al.,* 2005; Gordon *et al.,* 2012). This is a consequence of their sensitivity to abrupt environmental change and their general preference for narrow ecological ranges (Smol and Stoermer, 2010). Benthic diatoms are highly sensitive to water chemistry parameters, as well as acidification, metal contamination, salinification, and land use (Dixit and Smol, 1994; Potapova and Charles, 2002). Furthermore, diatoms' vast species diversity, widespread occurrence, and fast immigration rates offer substantial ecological information, where the presence or absence of certain taxa can be also used to make environmental inferences (Dixit *et al.,* 1992; Wachnicka *et al.,* 2005).

Diatom species have disparate habitat needs in terms of structural and physicochemical features (Bere and Tundisi, 2011). A change in habitat features affects niche composition because species differ in their sensitivity and resistance to environmental change (Bere and Tundisi, 2011). Ultimately, the more resistant species are able to tolerate environmental pressures, however, changes within a species

threshold of tolerance will not lead to their imminent disappearance (Bere and Tundisi, 2011). Instead, these changes will decrease the relevant species percentage by preventing their multiplication, whilst promoting the multiplication and introduction of others (Bere and Tundisi, 2011). In effect, the environmental change affects the species percentage composition of biological indicator species (Bere and Tundisi, 2011). For example, a rise in species associated with high salinity levels in conjunction with a decrease in less saline tolerant species could, amongst others, be an indication of secondary salinisation – i.e., an anthropogenic increase in salinity owing to industrial activities or the construction of dams (Cañedo-Argüelles *et al.,* 2013).

Diatom-based biological indices were first created in the early 20th century to study water quality changes in Europe (Temizel *et al.*, 2017). Studies have shown that diatoms are among the most effective of bioindicators in the world (Reid *et al.,* 1995) and have commonly been used as biological indicators of water quality since the seventies (Desrosiers *et al.,* 2013). They are effective proxies in discerning anthropogenic impacts on aquatic ecosystems (Lemley *et al.,* 2016) and are therefore regularly used in ecological assessments to track pollution and environmental change (Weilhoefer and Pan, 2007). Moreover, diatom indices have a long history of determining estuarine trophic conditions and productivity. Diatoms represent measures of numerous environmental parameters, such as salinity, conductivity, pH, nutrients, and water level (Lemley *et al.,* 2016). Specific structural factors and their related classification system are described below.

2.2.3. Structural Factors in Diatom Assemblages

2.2.3.1. Life Form and Habitat

In terms of life form, diatoms are classified as either benthic or planktonic and their life forms and habitat preferences can provide information on water levels and tidal energy regimes (Anderson and Vos, 1992; Finné *et al.,* 2010). Benthic diatom species form the largest group of photoautotrophic organisms and can colonise benthic substrates to form photosynthetic biofilms (Underwood *et al.*, 1998; Jesus *et al.,* 2009; Wang *et al.,* 2013). The biofilms form on various substrates in the majority of microhabitats within an aquatic system, including plants (epiphytic), rocks (epilithic), fine sediment (epipelic), and sand (epipsammic), thus the type of substrate forms the basis on which benthic diatoms are grouped (Dixit *et al.,* 1992; Lemley *et al.,* 2016). Biofilms play a vital role in the ecology and ecosystem functioning of estuarine mudflats and coastal environments owing to their stabilisation properties and ability to sustain

fluctuations between oxygen, nutrients, and sediments in coastal areas (Underwood *et al.*, 1998; Petrov and Nevrova, 2007; Jesus *et al.,* 2009).

In an estuarine setting, benthic species are indicative of shallow littoral habitats in close proximity to shores (Heinsalu *et al.,* 2007; Shirey *et al.,* 2008). For example, an abundance of epiphytic species, such as *Cocconeis scutellum,* is associated with a permanently submerged low-energy environment, such as a pond or lagoon, as they occur on macroalgae and tracheophytes (Anderson and Vos, 1992). Epiphytic species are linked to the depth of the photic zone for the reason that a substantial portion of the substrate is exposed to sunlight, which increases benthic habitat and macrophyte growth (Wolin and Stone, 2010). A predominantly epipsammic diatom community is characteristic of an intertidal zone, since they attach to sand grains, while epipelic species dominate in salt marshes and mudflats (Anderson and Vos, 1992). In comparison to benthic species, planktonic species are free-floating diatoms suspended in the water column (Shirey *et al.,* 2008) and are associated with deep open-water environments and wetter conditions (Finné *et al.,* 2010; Wolin and Stone, 2010; Wang *et al.,* 2013).

2.2.3.2. Salinity

Salinity refers to the total concentration of dissolved inorganic ions in water and is a key constituent of all aquatic bodies (Cañedo-Argüelles *et al.,* 2013; Schröder *et al.,* 2015) and is one of the primary structuring variables in most estuaries and shallow coastal environments (Wachnicka *et al.,* 2010; Potapova, 2011; Nodine and Gaiser, 2014). In these environments, diatom assemblages display spatial variation congruous with an axial salinity gradient, meaning that less saline assemblages are present at the head, whereas more saline or even marine species are prevalent at the mouth (Figure 1) (Parsons *et al.,* 1999; Bate *et al.*, 2013; Dalu *et al.*, 2016).

Changes in marine and freshwater influxes affect salinity concentrations in estuaries, which in turn reflect in the diatom assemblage (Nodine and Gaiser, 2014). For example, a rise in the relative percentage of freshwater species is indicative of increased freshwater influxes and a decrease in the estuary's salinity concentration (Nodine and Gaiser, 2014). This could be as a result of increased seasonal precipitation rates in the river catchment, thus leading to higher riverine input, as illustrated in Figure 2 (Zong *et al.,* 2010). On the contrary, a reduction in freshwater input can cause elevated salinity levels and a higher prevalence of saline-tolerant species (Nodine and Gaiser, 2014). Furthermore, a strong marine influence

in the form of tidal action transports marine species into more brackish (1.8 to 9.0 ‰) environments (Starratt, 2007).

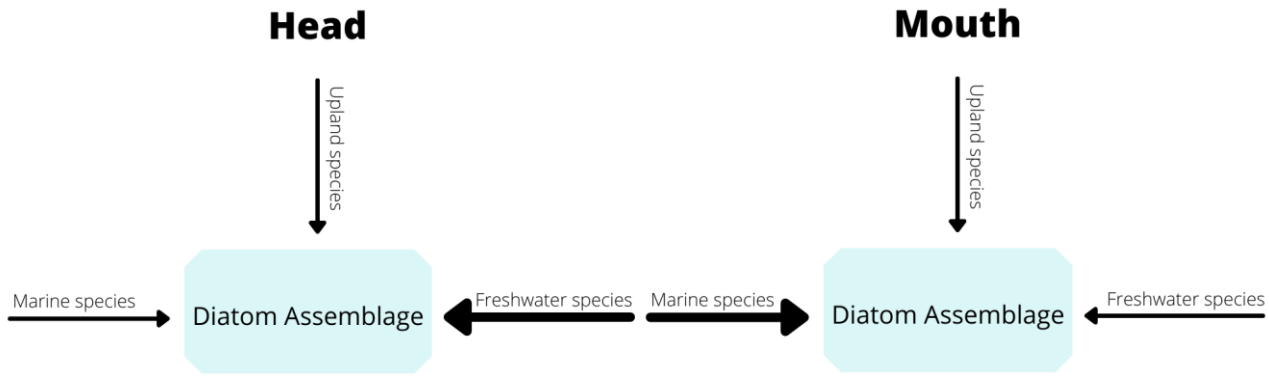

Figure 1. Diatom assemblage composition according to a salinity gradient in a typical estuary. Arrow size corresponds to each source's relative input. Adapted from Starratt (2007:89).

The unequivocal correlation between diatom communities and salinity has led to their widespread use as recorders of salinity fluctuation, freshwater inflow, and tidal exposure both contemporarily and within a palaeoenvironmental setting (Vos and de Wolf, 1993; Gasse *et al.,* 1997; Bate *et al.*, 2013), due to their sensitivity to salinity variability (Schröder *et al.,* 2015). Certain species, such as *Seminavis strigosa* and *Halamphora coffeaeformis,* are saline-tolerant, whereas other species are saline-sensitive to the extent that they promptly disappear when salinity concentrations increase (Schröder *et al.,* 2015). Due to their specific salinity preferences, it is possible to categorise diatoms according to the salinity environment in which they are usually present (Lemley *et al.,* 2016). Diatoms can be grouped as per Van der Werff's salinity classification system, which classifies diatoms as fresh, fresh-brackish, brackish-fresh, brackish, marine-brackish, or marine.

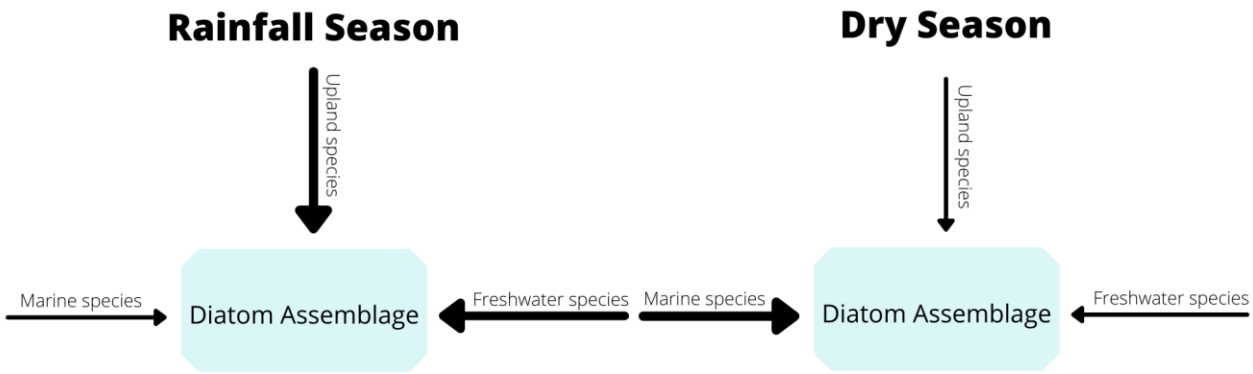

Figure 2. Diatom assemblage response to changes in seasonal freshwater influx in a typical estuary. Arrow size corresponds to each source's relative input. Adapted from Starratt (2007:89).

2.2.3.3. Trophic status, Nutrient Loads, and Water Quality

Trophic state refers to the productivity or nutrients of a water body in terms of organic carbon produced in a specific area over a specific time and is a powerful indicator of anthropogenic-induced changes in estuaries, coastal, and oceanic waters (Lobo *et al.,* 2010; Lemley *et al.,* 2016; Beiras, 2018). Changes in nutrient loads, such as nitrogen, phosphorus, organic matter, etc., and ratios are central in structuring diatom assemblages and community compositions, thus rendering diatoms sound indicators of bio-available nutrients within water bodies as nutrient input affects the trophic status or productivity of an aquatic ecosystem (Sanders *et al.,* 1987; Taff *et al.*, 2017; Beiras, 2018). Subsequently, diatoms have long been used in short and long-term assessments of environmental change both locally and globally and form one of the most important components in eutrophication evaluation (Harding *et al.,* 2005; Montoya Moreno and Aguirre Ramírez, 2013).

Factors, such as urbanisation, agriculture, and industrial pollution (Lamberth and Turpie, 2003; Dürr *et al.*, 2011), give rise to eutrophication in that they are responsible for introducing disproportionately high nutrient loads - particularly nitrogen and phosphorus - into estuarine systems (Garcia-Rodriguez *et al.,* 2011; Logan and Taffs, 2013; Lemley *et al.,* 2016). Since diatoms are primary producers and photoautotrophs, changes in nutrient content and light availability have an immediate and direct impact on diatoms' growth response to the point where assemblage change can occur within two to four days after enrichment (Sanders *et al.,* 1987; Harding *et al.*, 2005). Consequently, benthic diatoms are globally accepted as indicators of eutrophication and organic pollution (Lobo *et al.,* 2010). Diatoms can therefore

be classified according to their preferred trophic status using the classification system below (Taylor *et al.*, 2007):

1) Dystrophic — Rich in organic matter, usually in the form of suspended plant colloids, but of a low nutrient content.
2) Oligotrophic — Low levels or primary productivity, containing low levels of mineral nutrients required by plants.
3) Mesotrophic — Intermediate levels of primary productivity, with intermediate levels of mineral nutrients required by plants.
4) Eutrophic — High primary productivity, rich in mineral nutrients required by plants.
5) Hypereutrophic — Very high primary productivity, constantly elevated supply of mineral nutrients required by plants.

According to Lemley *et al.* (2016:14), estuaries experiencing eutrophication are host to diatom assemblages with low species diversity (Figure 3). This is due to only the most resistant diatom species being able to endure the change in conditions (Lemley *et al.,* 2015). For example, *Nitzchia frustulum* and *N. sigma* are quintessential indicators of nutrient-enriched waters, and their relative abundance increases during these conditions (Lemley *et al.,* 2016). Furthermore, high nutrient loads promote the dominance of diatoms, while lower nutrient content supports the dominance of dinoflagellates (Sanders *et al.,* 1987).

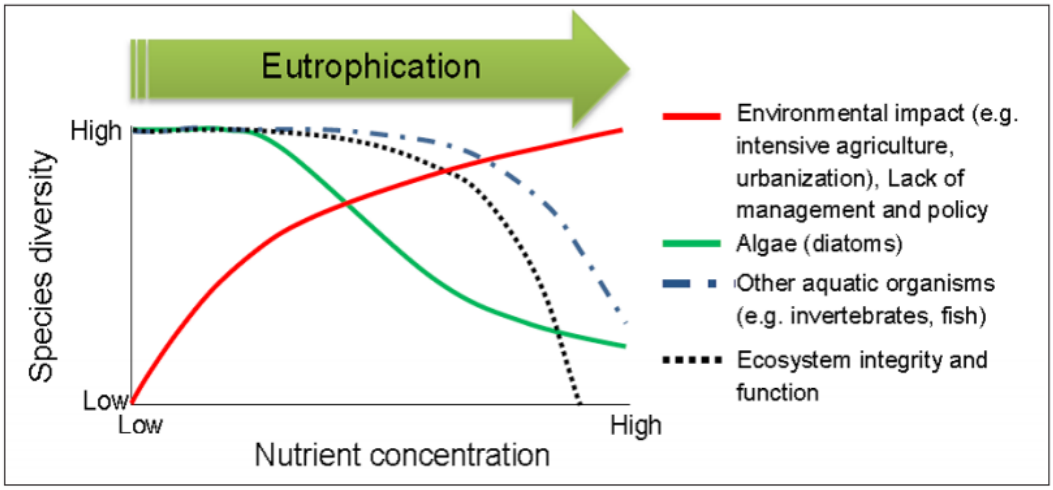

Figure 3. Relationship between species diversity and nutrient concentration within an estuary (Dalu and Froneman, 2016).

2.2.3.4. Saprobity

Dokulil (2003) simply defines saprobity as "the intensity of heterotrophic activity" and is distinguished by communities that display the degree and intensity of organic matter decomposition (Brabec *et al.,* 2004). The saprobity system was originally identified by Kolkwitz and Marsson (1908) as a means to gauge organic pollution downstream of a pollution source (Reid *et al.,* 1995). Saprobic levels are illustrative of the intensity of organic matter decomposition and oxygen concentrations in aquatic ecosystems (Van Dam *et al.*, 1994; Brabec *et al.,* 2004). Diatoms and other members of the benthic community are particularly responsive to saprobity, therefore contributing to their effectiveness as bioindicators (Sládecek, 1986; Tagliapietra *et al.*, 2012). Additionally, saprobity is a vital factor in structuring benthic communities, as different species have different saprobity optimums (Tagliapietra *et al.*, 2012).

Diatoms are classified into categories based on their tolerance to pollution using Van Dam, Mertens, and Sinkeldam's (1994) saprobic system:

1) Polysaprobic — Characteristic of the zone of degradation and putrefaction, oxygen is usually absent or low in concentration.
2) Mesosaprobic — Characteristic of the zone where oxidation of organic load is proceeding.
   - α-mesosaprobic — Range of stronger pollution, nitrogen is in the form of amino acids.
   - β-mesosaprobic — Range of weaker pollution, nitrogen is in the form of ammonia compounds.
3) Oligosaprobic — Characteristic of the zone where oxidation of biodegradable compounds is complete. The concentration of inorganic nutrients is usually high.

High saprobity, i.e., polysaprobic conditions, is associated with system impairment, which in turn conditions toward diatom species, such as *Nitzschia frustulum* and *Navicula tenelloides*, that can tolerate reduced water quality conditions and increased levels of toxicity (Tagliapietra *et al.*, 2012).

2.3. LIMITATIONS OF DIATOMS ANALYSIS IN ESTUARIES

Per Storme *et al.* (2020), reconstructing estuarine environments is a challenging undertaking due to the nature of marine, riverine, and anthropological interactions within the system. The sedimentary record, and thus fossilised diatoms within the sediment, is affected by wave energy, dominant water flow

direction, reworking, sediment transportation, and bioturbation (Storme *et al.,* 2020; Taffs *et al.*, 2017; Starratt, 2007), all of which contribute to a highly dynamic zone where sediment mixing is common (Cooper *et al.*, 2010; Trobajo and Sullivan, 2010; Bianchi and Allison, 2009). For this reason, the sediment integrity may be disturbed, thus thwarting the ability to obtain a continuous and unperturbed sediment record (Taffs *et al.*, 2017)

Taking the above into consideration, a major limitation of estuarine diatom analysis lies in the fact that the surficial sediment layer is a highly energised depositional environment, which in turn hinders the preservation of diatom frustules (Reid *et al.,* 1995). This environment furthers the fragmentation of frustules and increases the rate at which silica is released from the surface sediments to the water column, where the latter is exacerbated under eutrophic conditions (Reid *et al.,* 1995). Moreover, the degree of preservation is reduced by additional natural processes, viz prolonged subaerial exposure, predation, chemical leaching, extreme temperature shifts, compaction, and diagenesis (Starratt, 2007; Vos and Wolf, 1988).

Diatom frustules also face chemical preservational challenges in the form of dissolution (Reid *et al.,* 1995). Chemical dissolution is common in waters with an elevated salinity content or a high pH and disproportionately affects smaller elongated or weakly silicified diatoms to the point where it inhibits precise identification (Reid *et al.,* 1995). Conversely, round and strongly silicified valves are less prone to breakage (Vos and Wolf, 1988), while freshwater species are better preserved than brackish and marine species, reason being that they usually have stronger silicified valves (Cooper *et al.*, 2010).

The dynamic and variable nature of sedimentation - along with poor physical or chemical preservation in estuaries - is widespread and can lead to preservation bias in the diatom assemblage (Cooper *et al.*, 2010; Starratt, 2007). Preservation bias is expressed as a decrease in species diversity and is particularly common in older samples, which can hinder ecological interpretations (Starratt, 2007). Despite these challenges, diatoms generally preserve well in sediment and are a good biological indicator species of environmental change in estuaries on the same grounds as to why they prove useful in a manifold of other aquatic environments (Nodine and Gasser, 2014; Cooper *et al.*, 2010). It is also possible to address some of these obstacles by identifying favourable depositional environments in an estuary, such as marshes, mudflats, lagoons, or channels (Taffs *et al.*, 2017; Cooper *et al.*, 2010). Consequently, it is possible to use fossilised diatoms in estuaries to gain insights into environmental conditions before and after the occurrence of anthropological impacts (Nodine and Gasser, 2014).

2.4. CONCLUSIONS

This chapter describes the main physicochemical properties of estuaries, as well as highlighted the values and ecosystem services associated with estuarine systems. Furthermore, the chapter calls attention to the manifold of anthropogenic pressures estuaries face. Diatoms' status as bioindicators permits that reconstructed diatom assemblages, which are based on numerous structural factors and their related classification systems, can provide invaluable insights into environmental change over time. Despite the limitations of diatom analysis in estuaries, it is evident that they remain effective proxies in discerning anthropogenic impacts and environmental change in aquatic systems (Weilhoefer and Pan, 2007; Lemley *et al.,* 2016). This is particularly important, considering that there is a growing emphasis placed on the deterioration of estuarine health (Taffs *et al.*, 2017).

CHAPTER 3 - STUDY SITE: KNYSNA ESTUARY, WESTERN CAPE, SOUTH AFRICA

The Knysna Estuary is of high scientific and socioeconomic importance to South Africa, in part owing to its high biodiversity - almost half of South Africa's total estuarine biodiversity is found within the Knysna Estuary (Marker, 2003). Although the Knysna Estuary is clearly a functional estuary, it is threatened by anthropogenic activities, such as urban expansion, tourism development, and land use change (Marker and Holmer, 2005; CES, 2007). Hence, it is imperative to study the extent of the environmental change of the estuary. This chapter describes the physical and hydrological setting of the Knysna Estuary and its catchment, in addition to its coeval setting in terms of climate, vegetation, land use, and anthropogenic influences. The chapter also examines previous diatom studies that were conducted in the region.

3.1. CLIMATE

South Africa overlies the subtropics at the point at which tropical, subtropical, and temperate atmospheric pressure systems meet, thus forming three pronounced rainfall zones (Roffe *et al.*, 2021). The summer rainfall zone (SRZ) covers a substantial portion of the interior and east coast, the winter rainfall zone (WRZ) encompasses the southwestern Cape and western coast, while the yearly rainfall zone (YRZ) receives both summer and winter rainfall zones and spans the southern Cape (Roffe *et al.*, 2019). Rainfall over the YRZ

stems from mid-latitude systems, tropical systems, convection from the north, and interchanges amongst these various systems (Engelbrecht *et al.,* 2015). Meso-scale circulation systems also influence the YRZ, as well as mid-latitude weather systems, such as cold fronts, west-wind troughs, cut-off lows, and ridging high-pressure systems (Engelbrecht *et al.,* 2015). Furthermore, regional climatic patterns are further impacted by the Indian Ocean and the associated warm Agulhas current, which supplies a source of moisture causing high humidity along the coastline (Cohen and Tyson, 1995).

According to the Köppen-Geiger climate classification scheme, Knysna is classified as Cfb - temperate, without a dry season (or wet all seasons), and having warm summers (Engelbrecht and Engelbrecht, 2016). The temperate climate ranges from a mean summer temperature of 25^{o}C in January and an average winter temperature of 7^{o}C in July (Marker, 2003; Kraaij *et al.,* 2018). The equitable temperatures are partly attributed to the presence of bergwinds - a local term for hot, dry katabatic winds - during winter and cold fronts during spring and fall (Tyson, 1964; Geldenhuys, 1991). The area's climate can also be described as transitional owing to the fact Knysna is situated between the summer and winter rainfall zones (Human *et al.,* 2020). Harvey (2019) used historical daily rainfall data from 1900 to 2018 for Rainfall Station 0014063W (Knysna TNK), found on Thesen Island, to generate an average monthly rainfall chart of the area (Figure 4). Based on this chart, the rainfall station yields a mean annual precipitation of 748 mm. Monthly rainfall is mostly evenly distributed, though annual rainfall loosely adheres to seasonal patterns, owing to cold fronts in fall resulting in more rainfall than early spring (Marker, 2003; Harvey, 2019). Bergwinds occur in fall and winter and are linked to a sudden rise in winter temperatures, along with a decrease in humidity, thereby increasing the danger of forest fires (Tyson, 1964; Van Wilgen, 1984; Kraaij *et al.,* 2018).

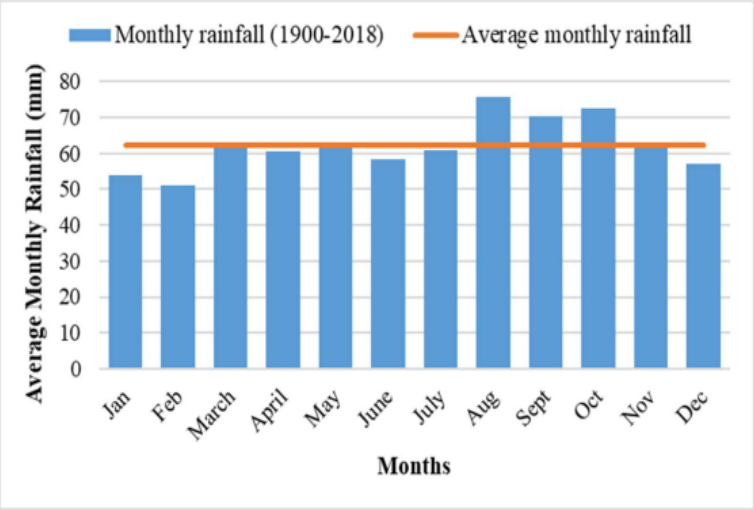

Figure 4. Average monthly rainfall for Knysna (1900 - 2018) (Harvey, 2019).

3.2 PHYSICAL SETTING

3.2.1. Topography

The catchment area is located in the southern portion of the Cape Fold Belt - a 1300 km long fold-and-thrust mountain belt situated along the south and west coast of South Africa (Blewett and Phillips, 2016). More specifically, the coastal mountains are located between 13 to 32 km inland and reach elevations of up to 1500 m above sea level (Martin, 1959; Russel *et al.*, 2012; Petermann *et al.,* 2018). Consequently, the proximity of mountainous terrain renders the majority of the Knysna Basin rugged, where the relief is "dominated by three discontinuous mountain ridges trending approximately west to east" (Marker, 2003).

South of the Cape Fold Belt, the Coastal Platform is the most significant geomorphic macro-feature of the southern coastal region, extending from Bot River (34° 14′ S, 19° 12′ E) in the west to Gqeberha (33° 58′ S, 23° 36′ E) in the east (Marker, 2003; Marker and Holmes, 2005; Marker and Holmes, 2010). In the Knysna Basin, the most uninterrupted portions of the Coastal Platform are found in areas where it overlies Cape Supergroup rocks (Marker, 2003; Marker and Holmes, 2005; Marker and Holmes, 2010). Particularly, the northern section of the Coastal Platform is aligned north-west to southeast across the Knysna Basin, adjacent to the mountains, at 280 m to 290 m above mean sea level (Marker, 2003). A remainder of the Coastal Platform forms a desiccated plateau (ranging between 200 to 240 metres above mean sea level) inland of the Knysna Amphitheatre (Marker, 2003). The Amphitheatre constitutes the southern portion of the Knysna Basin and is comprised of the Eastern and Western Heads abutting the estuary (Figure 5) (Marker, 2003). The Heads border an aperture in the surrounding sandstone ridge, thereby creating a gap that permits permanent tidal exchange (Marker, 2003).

3.2.2. Geology

The geological framework of the northern and eastern section of the catchment is predominantly set by Paleozoic and Mesozoic fractured rocks, whereas the west, southwest, and coastal plain is set by intergranular Cenozoic deposits (Petermann *et al.,* 2018). The largest portion of the catchment, including Knysna and its surroundings, is mostly composed of Paleozoic rocks of the Table Mountain Group and Uitenhage Group that make up the larger Cape Supergroup (Russel *et al.*, 2012; Petermann *et al.,* 2018). Per Petermann *et al.* (2018:955), this portion of the catchment is dominated by quartzitic sandstones of the Table Mountain Group, specifically the basal Ordovician Peninsula Formation, the Silurian primarily argillaceous Cederberg Formation, and sandstones of the uppermost Silurian/ Devonian Nardouw

Subgroup. The quartzites also overlie the Knysna half-graben and its Cretaceous and younger sediments (Marker and Holmes, 2005; Russel *et al.*, 2012).

The northern portion of the estuary is comprised of Mesozoic rocky outcrops consisting of upfaulted blocks of sandstone that ultimately decompose into sand and mud, whereas the southern portion (Brenton dune) consists of a steep dune complex that originates from the Tertiary and Pleistocene period (Marker, 2003; Russel *et al.*, 2012). The grey clay Brenton beds on the western section of the estuary are comparable to fanglomerates, while the Amphitheatre mostly overlies soft sediments (Marker, 2003).

3.3. HYDROLOGICAL SETTING

3.3.1. The Knysna Basin

The Knysna Basin covers an area of 480 km² and has its source in the Outeniqua Mountain at an altitude of 1100 m, approximately 34 km inland of the Indian Ocean (Marker and Holmes, 2005). The basin includes the Knysna River catchment and Knysna Estuary in the south, in addition to the northerly positioned Klein Langkloof Mountain crests (Coastal and Environmental Service, 2007). The Knysna River catchment is host to the Knysna River - a roughly 60 km-long sixth order master drainage line with three main tributaries, *viz.* the Kruis, Rooi-els, and Gouna Rivers (Largier *et al.,* 2000; Marker 2003; CES, 2007). A streamflow gauging station at Charlesford Wier (station K5H003) measures the mean annual runoff of the Knysna River at 3 $m^3 s^{-1}$, although streamflow is usually below 1 $m^3 s^{-1}$ (Largier *et al.,* 2000). The catchment consists of quaternary catchments K50A and K50B, both of which form part of the Gouritz Water Management Area 16 (Coastal and Environmental Service, 2007). The Knysna River is largely responsible for freshwater inflow to the estuary, however two smaller streams, namely the Salt River and Bigai Stream, also drain directly into the Knysna Estuary (CES, 2007).

3.3.2. The Knysna Estuary

The Knysna Estuary (34°04’35” S, 23°03’40” E) is a shallow estuary, situated alongside the town of Knysna (Figure 5). The Knysna Estuary is the only estuary that is classified as a natural estuarine-bay system in South Africa (Whitfield, 1992). Freshwater enters the S-shaped drowned river valley estuary via the Knysna River, whereas tidal seawater exchange occurs at the Heads (Largier *et al.,* 2000; Switzer, 2008; Petermann *et al.,* 2018). The estuary starts at Charlesford Wier and ends at the Knysna Heads where it

opens into the Indian Ocean (Largier *et al.,* 2000; Switzer, 2008). Ultimately, the system stretches roughly 19 km and covers an area of 18.27 km², however, the surface area increases and decreases depending on the tides (Largier *et al.,* 2000; Switzer, 2008). Water depth ranges between 2 and 5 m below mean low water along the main channel and the estuary has an average water depth of 1.8 m, though tidal scour holes of up to 13 m are present within 2 km of the mouth (Largier *et al.,* 2000).

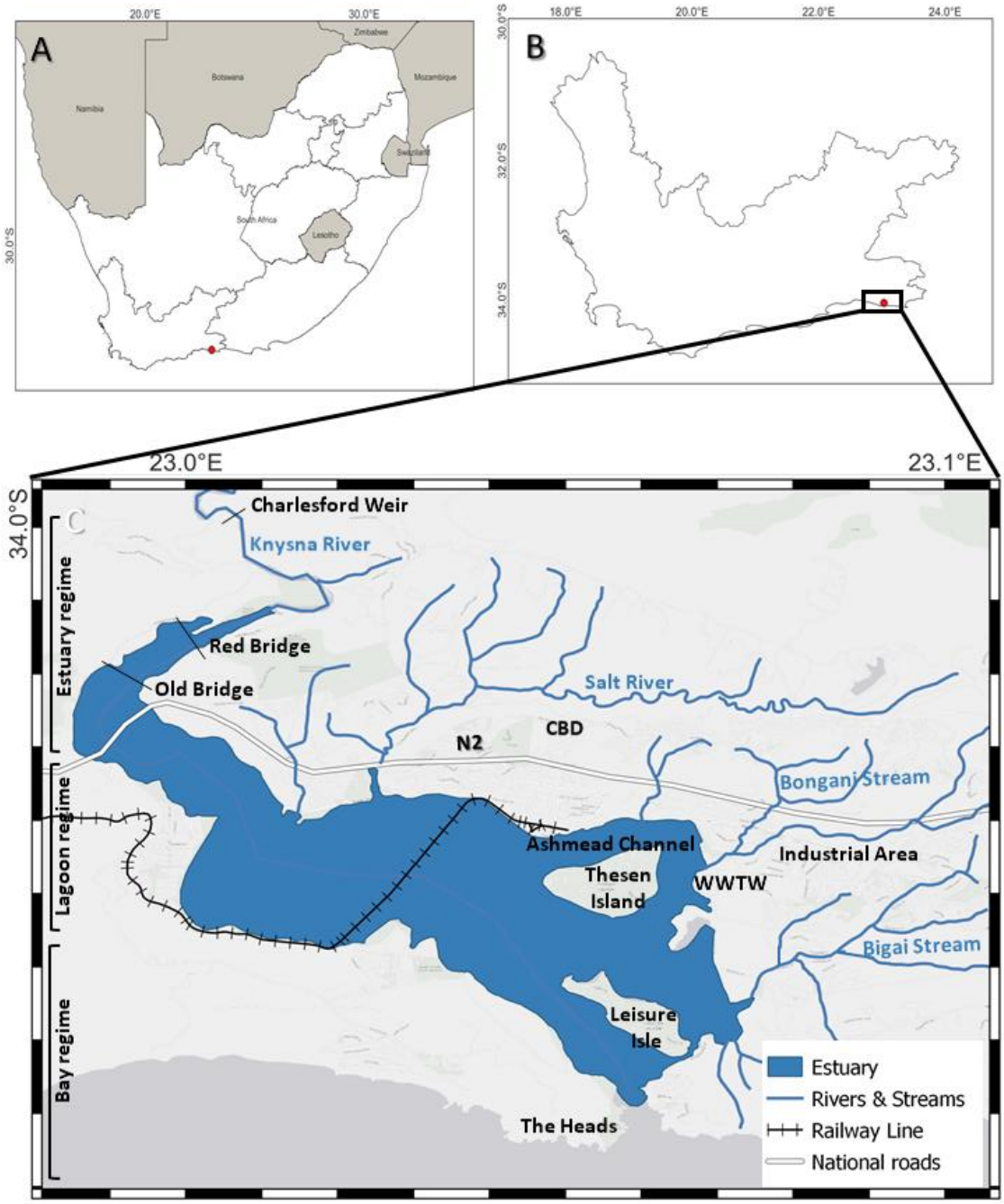

Figure 5. Map of the study site. a) Inset of South Africa. b) Location of the study site within the Western Cape. c) The Knysna Estuary.

The estuary is classified as a permanently open estuary because the Knysna Heads create a narrow 120m passage that obstructs the formation of a barrier, and the strong tidal currents restrict the transportation and deposition of marine sediment in the mouth (Largier *et al.,* 2000; Cooper, 2001). However, subtidal and intertidal sand bars are present during ebb and flood tides, especially on the shores adjacent to the mouth (Largier *et al.,* 2000). The shores of the inner estuary are bordered by intertidal flats, in addition to the marine and riverine sediments (Cooper, 2001). The eastern shore of the estuary serves as the entry point of the Ashmead Channel - a warm, shallow channel that contains stormwater runoff from the Knysna Central Business District (CBD), inflow from the Bongani River, as well as effluent from the Knysna Waste Water Treatment Works (WWTW) (Switzer, 2008). The Ashmead Channel enters the estuary along its eastern shore and encircles most of Thesen Island, apart from the island's western flank, which is bordered by the main estuary. Similar to Thesen Island, Leisure Isle is another suburban outlier that is linked to the mainland by a causeway.

3.2.3. Main Physical and Chemical Characteristics of the Knysna Estuary

The Knysna Estuary can be subdivided into three sections (Figure 5), as per Largier *et al.* (2000), to facilitate the description of its main physicochemical traits:

a) Bay regime: Adjacent to the Indian Ocean; includes The Knysna Heads and the mouth. Forms the outer part of the estuary, spanning seaward from the railway bridge.
b) Lagoon regime: Encompasses the portion between the bay regime and the estuary regime. The lagoon regime acts as a transitional zone between these two sections.
c) Estuary regime: Abuts the Knysna River and constitutes the upper reaches of the estuary, spanning landward from the N2 or white bridge.

3.2.3.1. Salinity

The Knysna Estuary experiences a natural horizontal salinity gradient, meaning that the bay regime's salinity is comparable to that of the ocean (34g kg^{-1}), the lagoon regime has salinity levels lower than that of the ocean (30 - 34g kg^{-1}), and estuary regime has the lowest salinity (<30g kg^{-1}), as the Knysna River introduces freshwater into the estuary (Largier *et al.,* 2000; Marker, 2003). Typically, freshwater inflow dominates an entire estuarine system, however, the Knysna Estuary is an exception to this rule, aside from

periods where sustained freshwater flows from storm events and rainfall can extend the estuary regime (Largier *et al.,* 2000).

3.2.3.2. Temperature

The Knysna Estuary undergoes noticeable temperature variation owing to tidal fluctuations and seasonal temperature change of freshwater (Largier *et al.,* 2000; Schumann, 2000). The bay regime experiences temperatures similar to that of the Indian Ocean (Largier *et al.,* 2000), where temperatures range between 13.5 and 22.4 ℃, although data from a study by Russel (1997) indicated that temperatures at the mouth are occasionally higher than that of the ocean temperature, potentially caused by warmer water flowing from the upper reaches of the estuary. Lastly, the lagoon regime is distinguished by water temperatures that are several degrees warmer than that of the bay regime (Largier *et al.,* 2000).

3.2.3.3. Tidal Regime

The Knysna Estuary's tidal range varies between 0.4 m and 2 m and is therefore categorised under a microtidal regime with a tidal water area of roughly 20 km², where tidal height fluctuations within the lower reaches are usually comparable to that of the ocean (Whitfield, 1992; Largier *et al.,* 2000; Marker, 2003). Strong stratification is present during neap tides in the lagoon and estuary regime, whereas high tide facilitates mixing in turn leading to poor stratification in the estuary (Whitfield, 1992; Largier *et al.,* 2000).

3.4. HISTORICAL SETTING

Archaeological studies have revealed that indigenous populations have resided in the region for millenia (Hart and Halkett, 1998; Sealy, 2003; Keller, 2019). Excavations in the Knysna Eastern Heads cave 1 revealed a habitual and dense occupation by nomadic societies going as far back as ~46 ka (Keller, 2019), whereas a sedentary hunter-gatherer society settled near Knysna approximately 4500 years ago (Sealy, 2003). Although there is no evidence of prehistoric material on Thesen Island, Hart and Halkett (1998:6) state that it is possible that ancestors of the San and Khoi Khoi accessed the island during low tide to hunt birds and to gather seafood upon transporting it back to their occupation sites.

The first five farms were established in the Knysna area in the latter half of the 1700s following the exploitation of surrounding indigenous forests in the area (Caveney, 2015; Collinson, 2020; Joubert, 2021). Subsequently, George Rex was granted Thesen Island (historically known as Paarden Island) in the early 1800s, as well as all of the farms encircling the Knysna Estuary (Hart and Halkett, 1998). From that point onwards, Thesen Island was mainly used for grazing cattle (Hart and Halkett, 1998). The exploitation of forests rose exponentially, particularly by the 1840s, as a result of timber shipping had shifted to Knysna and the government exercised a negligible amount of supervision over the forests (Hart and Halkett, 1998; Joubert, 2021). From 1817, the estuary became the main shipping point for transporting timber to Cape Town (Matthews, 2019; Joubert, 2021). This period coincides with population growth associated with a gold rush, as well as the introduction of industrial activities, including a sawmill, and infrastructure development (Caveney, 2015; Joubert, 2021). Infrastructure included the construction of a wooden jetty on the southwest side of Thesen Island, which was linked to the mainland by a causeway, while the first permanent bridge over the Knysna River was officially opened in 1893 after the previous bridge was washed away by floods (Hart and Halkett, 1998; Collinson, 2020).

Industrial development on Thesen Island began with the Thesen and Co. Sawmill, likely stimulated by population growth and the fact that the only deepwater wharf was located on the island (Hart and Halkett, 1998). The Thesen family raised the level of the island in the 1920s via infilling and installed a dyke system to prevent tidal penetration onto the island (Hart and Halkett, 1998; Clark *et al.,* 2002). Subsequently, a hardwood mill, power station, softwood mill, and workshops were erected on the island (Hart and Halkett, 1998). By this point, Midgley *et al.* (1997) estimate that 3 million m^3 of timber was removed from the forests between 1776 and 1939. The dairy farm on Thesen Island moved to Charlesford farm in the 1940s, while major infrastructure projects, such as the construction of railways, bridges, roads, and causeways, started from 1904 onwards and are responsible for much of the habitat loss around the edge of the estuary (Clark *et al.,* 2002; Collinson, 2020; Joubert, 2021). Prior to this, most bridges were constructed of wood or stone and washed away during floods (Collinson, 2020).

3.5. CONTEMPORARY SETTING

3.5.1. Vegetation

Much of the indigenous tall Afromontane Forest has been destroyed by human activities and the only remaining portions can be found in the Sparrebos Forest Reserve and Brenton-on-Lake (Marker, 2003). In

areas of lower rainfall, such as the Western and Eastern Heads, fynbos supersedes forest (Figure 6) (Marker, 2003). In relation to the estuary itself, the main components are intertidal wetlands, intertidal salt marshes, and supratidal marshes (Figure 6) (Mucina *et al.,* 2006). Intertidal wetlands cover 10 km², including 3.55 km² of submerged *Zostera capensis* (Mucina *et al.,* 2006). This is the largest area of *Z. capensis* in South Africa, as it constitutes 49% of the national total (Pollard *et al.*, 2018). Overall, the intertidal salt marshes at Thesen Island, George Rex Drive, and Brenton-on-Lake cover 4.84 km² (Mucina *et al.,* 2006). Covering 0.6 km², the supratidal marsh is considerably reduced (Mucina *et al.,* 2006). The marshes in the upper reaches of the estuary are mostly comprised of *Juncus kraussii,* which spans 1.5 km² (Mucina *et al.,* 2006).

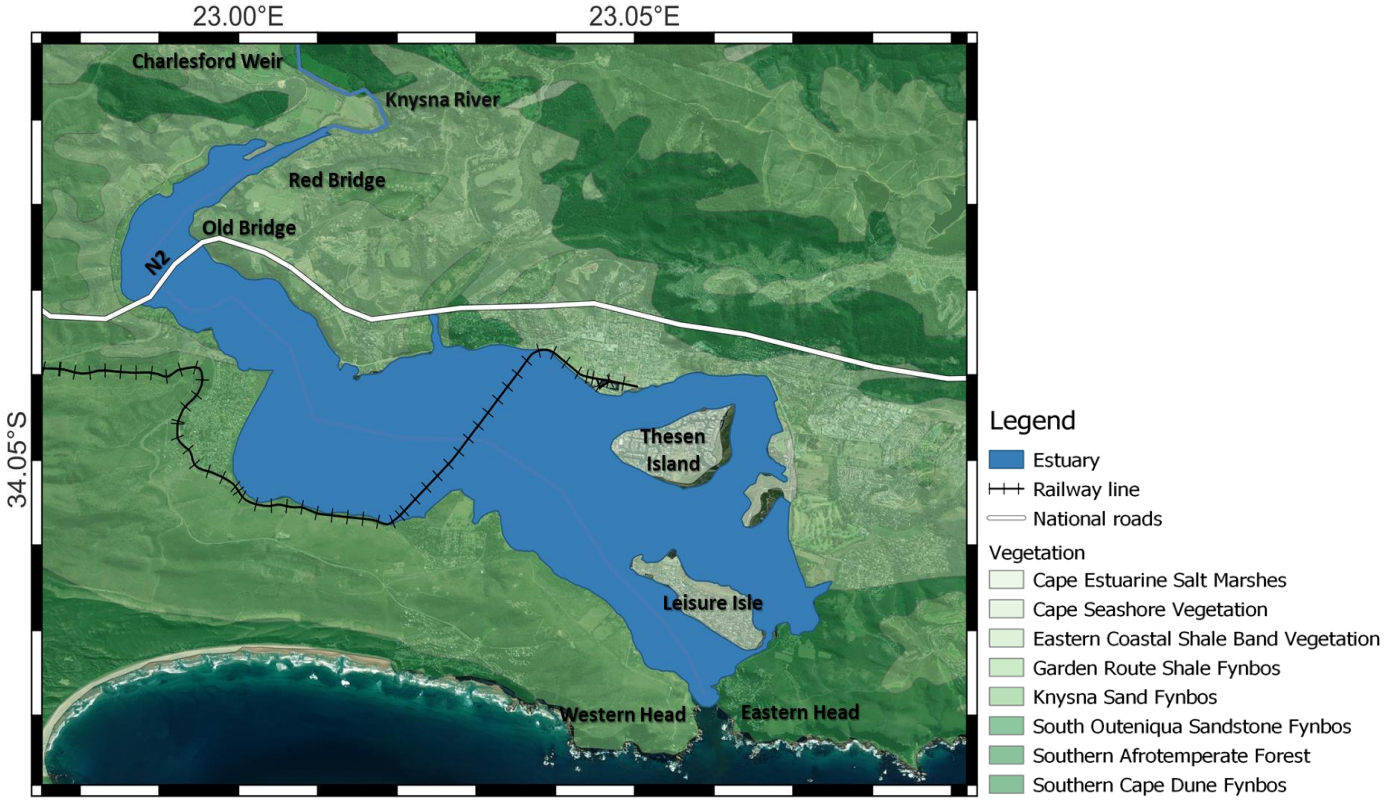

Figure 6. Map of the vegetation surrounding the Knysna Estuary.

3.5.2. Land Use

Over a third of the Knysna Basin is used for forest plantations (Figure 7) (Lombard *et al.,* 2005; CES, 2007). Agriculture in the form of cattle grazing is the second most common land use practice, representing 8% of the land use (Lombard *et al.,* 2005; CES, 2007; Switzer, 2008). Agriculture development is mostly restricted to farms, such as Portland, Charlesford, Westford, Eastford, Simola, and on the Gouna Commonage, where most cattle farms are less than 100 hectares each (CES, 2007; Switzer, 2008). Urban

areas account for 4% of the catchment area (Petermann *et al.,* 2018). The establishment of the N2 highway in 1952 prompted urban growth and densification, while the 1990s onwards saw the construction of holiday and retirement homes (Marker, 2004). Formal development is centred around the CBD and its eastward and westward expansions, in addition to outlying suburban areas that include the Knysna Heads, Leisure Isle, Thesen Island, Belvidere, and Brenton-on-Lake (Marker, 2003).

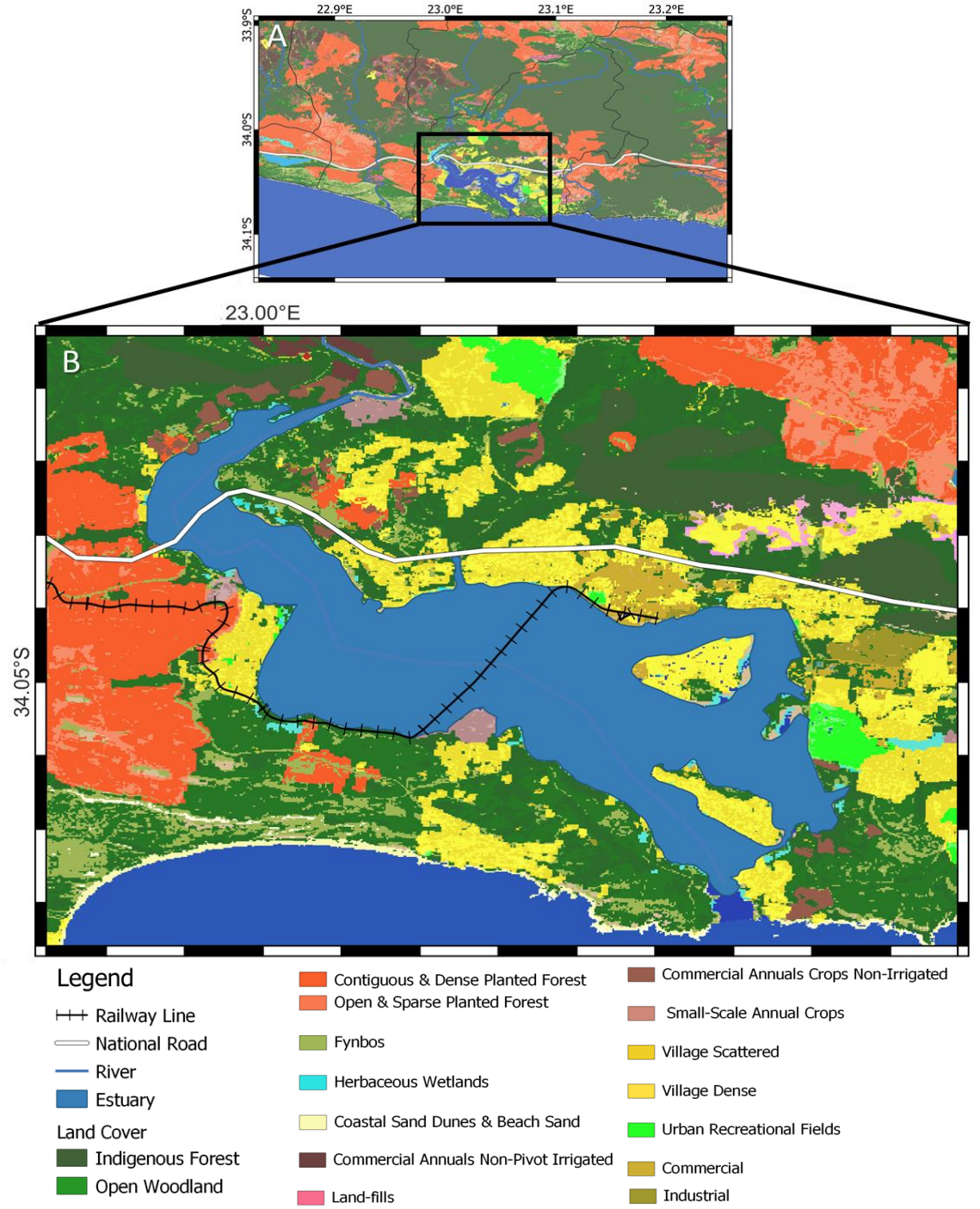

Figure 7. Regional and local land use. a) Regional land use. b) Land use surrounding the Knysna Estuary.

3.5.3. Anthropogenic Influences

The Knysna catchment has a high degree of landscape sensitivity and is vulnerable to anthropogenic and climatic impacts (Marker, 2004). Specifically, population and urban growth, tourism development, and land use change threaten the functioning of the estuary (Marker, 2003). Essentially, the factors that attract people to reside and work alongside the estuary are currently under threat by human impacts (Largier *et al.,* 2000).

Knysna's rapidly growing population has had a severe impact on the estuary. In particular, the population increased from roughly 40 000 residents in 1999 to 75 000 in 2016, most of which occupy formal dwellings (80.4%) (Knysna Municipality, 2020; Human *et al.,* 2020). The exact number of residents in informal settlements, including White Location, Nekkies East, Dam-se-Bos, and Bongani, is unknown, though it is estimated that approximately 5000 households live in informal dwellings where a third of households do not have access to flush toilets and adequate wastewater disposal systems (Knysna Municipality, 2020; Human *et al.,* 2020). Specifically, the larger population, as well as holiday periods where the population multiplies fourfold, places pressure on the availability of freshwater inflow as more water is abstracted to meet the needs of a larger population (Marker, 2003).

It is estimated that almost 20% of the estuary's Functional Zone is impacted by development, whereas 80% of the banks consist of impermeable surfaces (Claassens *et al.,* 2020). A larger area of impermeable surfaces associated with urban expansion has led to increased stormwater runoff, thereby increasing siltation and the amount of suspended sediments entering the estuary (Marker, 2003). Furthermore, encroachment, reclamation, and siltation have reduced the salt marsh over the last half a century (Marker and Holmes, 2005). More specifically, almost 70% of the supratidal marsh has been lost (Claassens *et al.,* 2020; Raw *et al.,* 2020), while *Z. capensis* has experienced large changes in surface area, particularly in the Ashmead Channel (Adams, 2016). This is particularly alarming, considering that the estuarine food chain largely relies on the salt marsh, in turn impacting biodiversity (Marker and Holmes, 2005).

Population growth and urban expansion further threaten the estuary in terms of chemical and biological pollutants, as the WWTW has to treat higher quantities of sewerage (Marker, 2003). WWTW effluent and urban runoff amount to 6500 m^3 of contaminated water entering the estuary per day, which has resulted in heavily modified water quality of high severity (Adams *et al.,* 2020). In short, this has caused anoxic sediment, ammonium release, weak flushing, macroalgal growth, and the dieback of *Z. capensis* (Adams

et al., 2020). The WWTW releases the effluent into the Ashmead Channel, giving rise to a high nutrient load (CES, 2007). Therefore, it is not surprising that a macroalgal bloom (or green tide) occurred in the estuary in the summers of 2014 and 2015, where it is generally accepted that nitrogen and phosphorus are the main drivers of the green macroalgal blooms (Allanson *et al.,* 2016). Apart from the WWTW and urban runoff, the eastern shore of the estuary receives pollution and solid waste from informal settlements that rely on pit toilets and open sewers, as the stormwater outlets are inefficient in retaining the solid waste (Marker, 2003; Switzer, 2008).

Freshwater inflow from the Knysna River also influences nutrient loads in the system, owing to the fact that runoff from cattle farming and other agricultural activities ultimately flow into the estuary (CES, 2007). The cattle farmers, in addition to golf courses and residential properties, in the catchment enrich their pastures with inorganic and organic (urea-based) fertilisers (CES, 2007; Switzer, 2008). A study by Switzer (2008:66) indicates that spring storms notably contribute large amounts of nitrogen to the estuarine system, seeing as it is the period when farmers fertilise their land. Moreover, the study suggests that the nutrient enrichment may be responsible for the large dinoflagellate blooms that take place in the estuary during the late summer months (Switzer, 2008).

Despite the high nutrient inputs derived from agricultural runoff, WWTW, and urban runoff, the contribution of these sources to the total nutrient budget of the estuary remains relatively low (CES, 2007). This is mostly attributed to the fact that vast quantities of nutrient-poor water enter the estuary twice a day (CES, 2007). Nevertheless, it cannot be overlooked that human activities elevate the nutrient loads in the estuary to the point where it experiences eutrophic conditions and macroalgal blooms, particularly seeing that the estuary is ranked as the most important in the country for ecosystem services and biodiversity conservation (CES, 2007; Adams *et al.,* 2020).

3.6. PREVIOUS DIATOM STUDIES

In relation to previous diatom studies at Knysna, most of the comprehensive studies were conducted in the Wilderness Lakes Complex (Martin, 1956; 1959; Kirsten, 2008; 2014). The first diatom studies in the region were conducted in the 1950s by Anthony Martin, who studied the ecology and history of Groenvlei, which is located approximately 15 km west of Knysna (Martin, 1956; Martin, 1959). Only one sediment core was obtained and diatoms were used to make salinity inferences. Five decades later, sediment cores were obtained from Groenvlei, Eilandvlei, and Swartvlei (situated 30km west of Knysna) to reconstruct

the palaeolimnotic and palaeoclimatic conditions during the Holocene (Kirsten, 2008; Kirsten, *et al.,* 2018; Haberzettl *et al.,* 2019). As far as diatom studies at the Knysna Estuary are concerned, only two previous studies have been located. Bate *et al.* (2013) broadly aimed to use diatoms as a proxy to identify salinity characteristics of South African estuaries. The results did not focus on Knysna specifically, nor was any reference made to the diatom assemblage of the Knysna Estuary. The most recent and comprehensive study is UCT BSc Honours project (Else, 2018) that determined the diatom distribution in the estuary and attributed the distribution pattern mostly to salinity and partly to nutrient availability or pollution. In summary no previous research has been conducted on the historically recent diatom assemblages of the Knysna Estuary.

3.7. CONCLUSIONS

The Knysna Basin, including the estuary, in particular, has been subjected to vast anthropogenic pressures over the last few decades. It is believed that some of these environmental changes are likely to be reflected in the fossilised diatom assemblage preserved within the estuarine sediment. An appropriate methodology is required to reveal such changes, which therefore form the main content of the following chapter.

CHAPTER 4 - METHODOLOGY

This project aims to reconstruct the historically recent diatom communities, thus concomitantly reconstructing the environmental changes that have occurred in the Knysna Estuary over time. Specifically, this includes changes in nutrient status, salinity, and saprobity. As outlined in this chapter, appropriate methodology was employed to accomplish the aims and objectives.

4.1. SEDIMENT SAMPLING

The soft sediments of the Knysna estuary permitted the manual extraction of seven short cores (KNY19-A to KNY19-H) from various sites in the estuary during July 2019. One metre long aluminium tubes (with a diameter of 7.8 cm) were inserted into the sediment and extracted using an adjustable lever that was mounted onto the core tubing (Figure 8). A core-catcher was manufactured from shim stock and attached to the bottom of the core to prevent sediment loss by permitting the unidirectional entry of sample material during core insertion. Upon the extraction of the cores, excess piping was removed with a handsaw, sealed, and labelled (Figure 9). Cores were stored at the Environmental and Geographical Science Department laboratory, University of Cape Town prior to being split lengthwise. KNY19-B and KNY19-G were included in this study, as they were representative of the marine and riverine environment, respectively. KNY19-A is roughly illustrative of intermediary conditions, however, the core was excluded due to poor diatom concentrations.

Figure 8. Manual coring device, along with adjustable lever. **Figure 9.** Cores were labelled and sealed.

4.2. CORE SITES

4.2.1. Ashmead Channel - KNY19-B (34° 2' 28.2078"S; 23° 3' 55.9656"E)

Core site KNY19-B was selected for the reason that it is representative of a marine-influenced section of the estuary. KNY19-B is located on the outer bend of the lower section of the Ashmead Channel, approximately 155 m west of George Rex Drive (Figures 10a, c, and 11). Core site KNY19-B is roughly 110 m south of the bank of the Ashmead Channel between Central Knysna and Old Place, where a gravel road separates the urbanised area from the bank. The core site is situated on a tidally exposed mudflat with aquatic vegetation to the east.

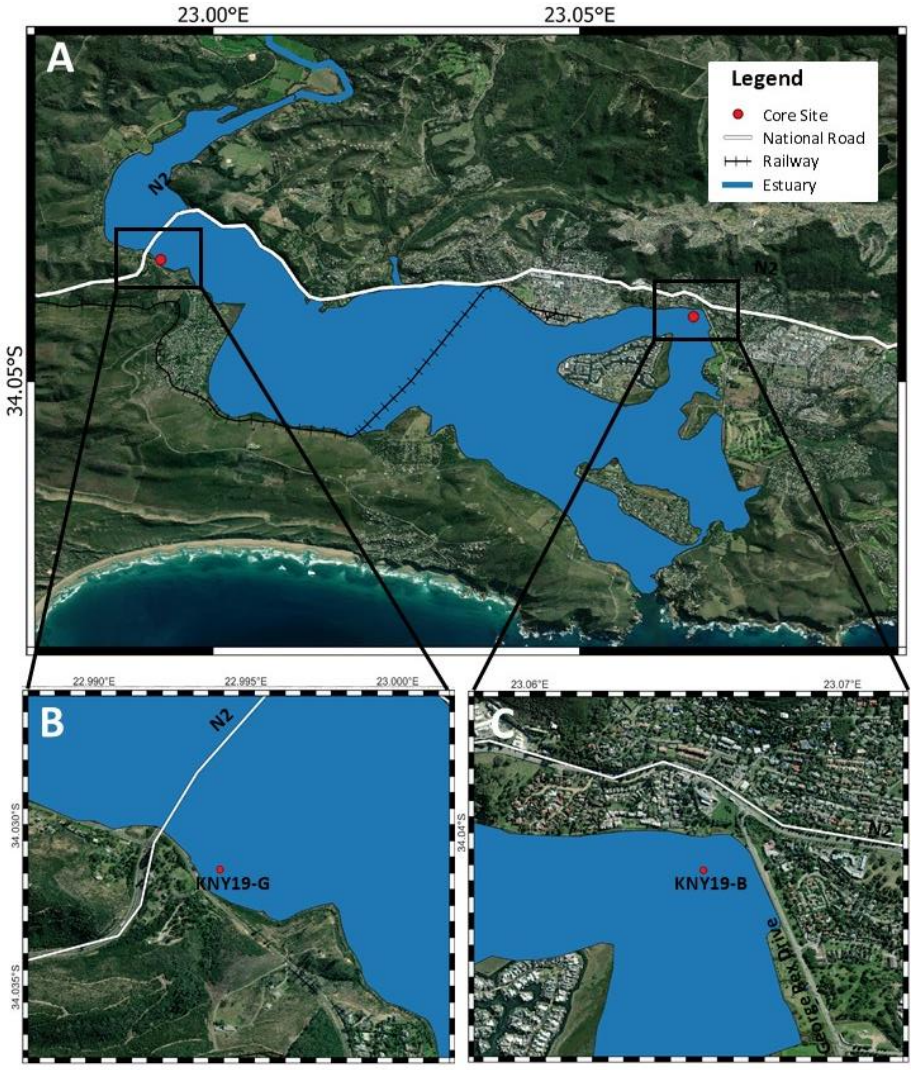

Figure 10. Map of the core site locations within the Knysna Estuary. a) Core sites within the estuary. b) KNY19-G. c) KNY19-B. Note that the outline of the estuary is representative of high tide, thereby obscuring the mudflats.

The aluminium core tube penetrated the sediment with ease. The retrieved sediment core measured 57 cm, while the top of the core tube to the uppermost portion of the sediment core measured 19 cm. There was a 16 cm difference between the ground (mudflat surface) and the top of the core tube, therefore the compaction factor is 3 cm or 5,26%.

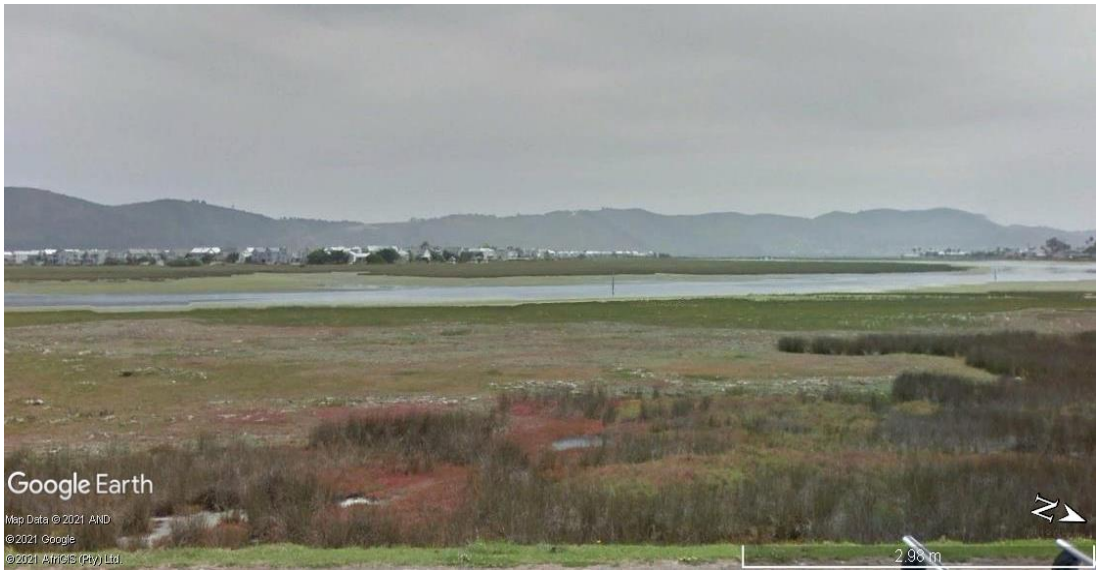

Figure 11. Core site KNY19-B as viewed from George Rex Drive (Google Earth, 2021).

4.2.2. KNY19-G (34° 2' 0.1896"S; 22° 59' 34.3782"E)

KNY19-G was identified as a second core site as it is subject to more riverine influence in comparison to KNY19-B. KNY19-G is located 230 m southeast of the N2 highway (Figures 10a, b, and 12) or roughly 85 m east of Rexton Road. The site is situated in a *Phragmites* bed approximately 30 m east of the western shore of the Knysna River.

The aluminum core tube penetrated the sediment with relative ease. The retrieved sediment core measured 37 cm, while the top of the core tube to the uppermost portion of the sediment core measured 24 cm. There was a 10 cm difference between the ground (surface of the reed bed) and the top of the core tube, therefore the compaction factor is 14 cm or 37,84%.

Figure 12. Core site KNY19-G as viewed from the N2 (Google Earth, 2021).

4.3. CORE DESCRIPTION

4.3.1. Lithology and Colour

Once cores were split lengthwise, a stratigraphical description based on lithology, colour, and texture was determined. The lithology was described using the Troels-Smith sediment classification scheme (1955), whereas a Munsell Soil Colour chart was used to describe colouration.

4.3.2. Texture

Texture was described by means of visual and tactile inspection that consisted of rubbing small quantities of sediment between the fingers as outlined by Schnurrenberger, Russel, and Kelts (2003:144). This information was supplemented by data obtained from grain size analysis conducted by Prof. Kunshan Bao at the South China Normal University in Guangzhou, China. Sediment grain size analysis was determined through Mastersizer 2000 Laser Particle Size Analyser (Malvern Ltd., Worcestershire, UK) working on the principle of laser diffraction to detect sizes across the range of 0.02 to 2000 µm. Continuous subsamples were pretreated with 10% hydrogen peroxide (H_2O_2) and 10% hydrochloric acid (HCl) to remove organic material and carbonate content, respectively. The samples' nominal diameter was measured three times upon which the average was used to identify three categories, namely clay (< 4 µm), silt (4-64 µm), and sand (> 64 µm) content. The repeated measurement error is generally less than 3%.

According to López (2017), grain size analysis should always be used in conjunction with other analyses in order to deepen the understanding of the sedimentary context. Consequently, grain size analysis is merely a supportive and complementary analysis to this study.

4.4. DATING METHODS

4.4.1. Carbon-14 (^{14}C)

In total, four suitable samples (three samples were obtained in 2019, while an extra sample was taken in 2021) (Table 1) were sent to Beta Analytic Inc.'s testing laboratory in Miami, United States. Each sample was analysed using the Accelerator Mass Spectrometric (AMS)-Standard delivery method, while Conventional Radiocarbon Ages were corrected for total fractionation effects where applicable. Calibration was performed using the Marine20 calibration database for Southern Hemisphere samples by Heaton *et al.* (2020).

Table 1. Samples submitted for ^{14}C dating.

Core	Depth (cm)	Sample Year	Material type
KNY19-B	48 - 49	2019	Coastal estuarine sediment
KNY19-G	35 - 36	2019	Organic sediment

^{14}C is a commonly applied dating technique, considering that its half-life of approximately 5730 years can date samples that were deposited relatively recently between 200 and 55 000 years ago before present (1950) (Goh, 1991; Walker, 2005; Heaton *et al.,* 2020). ^{14}C can be found in all biological material, including sediment, hence adding to its practicality (Goh, 1991).

^{14}C is constantly produced in the upper atmosphere when cosmic ray neutrons strike Nitrogen-14 atoms (Coleman and Corbin, 1991; Walker, 2005). The underlying assumptions behind ^{14}C dating goes as follows (Walker, 2005):

- There are three carbon isotopes, where ^{14}C is the most abundant and ^{13}C is the rarest.
- ^{12}C and ^{13}C are stable isotopes, while ^{14}C is unstable and decays at a known rate into Nitrogen-14 via the emission of beta (β) particles.

Ages are inferred using the AMS technique, which uses particle accelerators such as mass spectronometers to measure the ratio of unstable ^{14}C to stable ^{12}C and ^{13}C isotopes (Goh, 1991; Walker, 2005). Subsequently, the ratio is compared to modern ^{14}C in standard material to determine the age of the sample (Walker, 2005). However, past variation in the amount of atmospheric ^{14}C renders ^{14}C years (which is simply a measurement of isotope ratios) disparate to calendar years (Ramsey, 2009; Blaauw, 2010; Reimer *et al.,* 2013). Therefore, a statistical analysis in the form of a calibration curve is required to interpret ^{14}C as calendar dates (Ramsey, 2009; Blaauw, 2010; Reimer *et al.,* 2013). As a result, Bacon was used to calibrate the ^{14}C dates in R (R Core Team, 2020) - an open-source statistical environment - as well as produce an age-model using the marine calibration curve Marine20. The ^{14}C dates were corrected to accommodate for the marine reservoir effect. Maboya *et al*. (2018) calculated the regional marine reservoir correction values by administering ^{14}C age determinations on 15 shells of known age and integrating the results with formerly published values. The study yielded a weighted mean marine carbon reservoir value of 187 ± 18 ^{14}C for the south coast of South Africa. It must be noted that determining the age-depth model for cores KNY19-B and KNY19-G is the object of another related project by Dr. Kelly Kirsten and Dr. Lauren Pretorious.

4.4.2. Lead-210 (^{210}Pb)

Both cores were sampled at 1 cm intervals, thereby generating 93 samples, and submitted for ^{210}Pb determination. All samples were prepared by Prof. Kunshan Bao in his laboratory at the South China Normal University in Guangzhou, China.

^{210}Pb is a naturally occurring isotope with a short half-life of 22.26 years (Battarbee, 1984; Valette-Silver, 1993). Consequently, ^{210}Pb is the most widely used radionuclide employed in dating sediment samples that were recently deposited within the last 100 to 150 years (Battarbee, 1984; Schelske *et al.,* 1994; Aquino-López *et al.,* 2020; Barsanti *et al.,* 2020). Similar to ^{14}C dating, this timeframe is host to important environmental changes (Goh, 1991). The quantification of ^{210}Pb activity and the subsequent use of dating models can establish continuous age-depth relationships that provide reliable sediment chronologies (Appleby, 1993; Schelske *et al.,* 1994).

The principle of the methodology lies in the fact that natural ^{210}Pb radionuclides can be found in all environmental compartments (Barsanti *et al.,* 2020) and belong to the Uranium-238 natural decay series (Aquino-López *et al.,* 2020). Furthermore, the ^{210}Pb in sediments originates from two sources (Figure 13). First, ^{210}Pb is produced by the decay of Radium-226 in sediment minerals or the lithosphere, also known

as “supported ^{210}Pb” ($^{210}Pb_{sup}$) (Kirchner, 2011; Aquino-López *et al.,* 2020). Second, atmospheric Radon-222 decays into ^{210}Pb before it is transferred to sediments, which is otherwise called “unsupported” or “excess ^{210}Pb” ($^{210}Pb_{ex}$) (Kirchner, 2011; Aquino-López *et al.,* 2020). Since the $^{210}Pb_{ex}$ is deposited on the surface sediment and decays over time with a known half-life, the activity declines with an increase in sediment core depth, thus permitting the establishment of geochronologies (Aquino-López *et al.,* 2020).

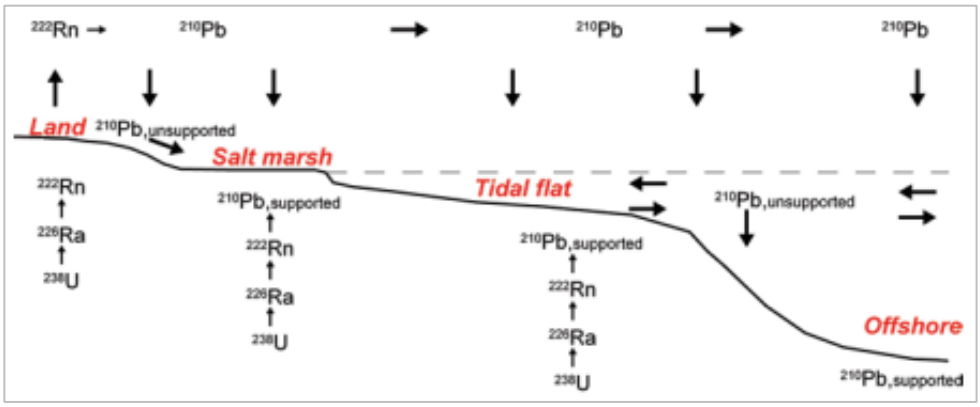

Figure 13. Supply of $^{210}Pb_{sup}$ and $^{210}Pb_{ex}$ in a hypothetical estuary (Andersen, 2017).

The ^{210}Pb dates were established by Dr. Kirsten and Dr. Pretorious using the Plum model in R statistical software version 4.0 (R Core Team, 2020). Plum is the Bayesian formulation of the “constant flux” or “constant rate of supply” (CRS) ^{210}Pb dating model and offers more precise dates, in addition to a more dependable measure of uncertainty (Aquino-López *et al.,* 2018; Iurian *et al.,* 2021). Plum can be used in tandem with other radioactive isotopes, for this reason, Plum was used in conjunction with the ^{14}C dates in order to obtain “more robust, realistic, and statistically better-defined age estimates” (Aquino-López *et al.,* 2018:317; Iurian *et al.,* 2021).

4.5. DIATOM ANALYSIS

4.5.1. Extraction

KNY19-B and KNY19-G were subsampled at 2 cm intervals in order to produce a high-resolution depiction of environmental change over time. Every second sample was processed, in total generating 48 samples, with the aim of generating microscope slides sufficient for analysis. Only two samples (KNY19-B: 55-56cm and KNY19-G:25-26 cm) were excluded due to low diatom concentrations and poor clarity. The samples were chemically treated in accordance with standard laboratory protocol, as modified by Battarbee

(1986), to concentrate fossilised diatoms by removing organic material, carbonates, salts, and coarser-grained sediments. The following laboratory procedures were followed:

1. Approximately 1 cm^3 of sediment sample was decanted into a marked test tube.
2. Subsequently, 20 mℓ of 30% hydrogen peroxide (H_2O_2) was added to each sample to remove organic matter, upon which the samples were heated in a hot water bath that was adjusted to 80^oC.
3. Once the chemical reactions subsided, 25 mℓ of distilled water was used to dilute each sample.
4. Samples were then left overnight as a means of allowing the diatom sample to settle.
5. Afterwards, the supernatant was decanted from the test tubes prior to treating the samples with 20 mℓ of 10% hydrochloric acid (HCl) to remove all carbonates. The rest of the step was executed in the same manner as described in the initial step.
6. As a means of eradicating coarser-grained materials, such as sand particles and roots, each sample was sieved through a 300 µm sieve.
7. Furthermore, each sample was swirled in a 100 mℓ beaker in order to bring the content into suspension and then waiting for five counts – or until most of the coarser-grained material settled – and then decanting the content back into the test tube.
8. The supernatant was decanted every eight hours over the course of two weeks in order to remove suspended solids and finer materials, such as clay. This was achieved by refilling the test tube with distilled water, swirling the remaining sample into suspension after decanting the supernatant.
9. Once the diatom solution was sufficiently devoid of extraneous material, a pipette was used to transfer approximately three drops of each sample onto a clean coverslip.
10. Coverslips were then placed on a hot plate that was set at 40^oC to slowly evaporate the water from the diatom solution.
11. Lastly, the coverslips were mounted onto clean microscope slides using Pleurax (R.I. = 1.73) – a resin used to increase the visibility of the diatoms to the human eye by alternating the light refraction as it passes through the Pleurax.

4.5.2. Counting, Identification, Nomenclature, and Classification

In order to obtain statistically significant results, 300 diatom valves per sample were counted along random transects. 300 is considered the minimum amount of diatoms per sample, as this number is large enough to illuminate ecologically important species that might be adumbrated by heavily prevalent species. Fragmentary diatom valves were also counted, given that more than half of the valve was identifiable in order to prevent double counting of a diatom. Polycounter version 3.2.2 (Nakagawa, 2007) software aided the counting process. Diatoms were identified under a Zeiss light microscope at a magnification of 1000x. Images of diatoms were captured by mounting a Xiaomi Redmi Note 7 Pro onto the microscope's eyepiece with a Celestron NeXYZ Universal Smartphone Adapter, thereby expediting the creation of diatom plates for the core sites (Appendix 1).

Diatoms were identified to species level using South African diatom catalogues by Taylor *et al.* (2007) and Bate *et al.* (2004). Furthermore, diatom identification was aided by the *Stuart R. Stidolph Diatom Atlas* (Stidolph *et al.,* 2012), which is an extensive volume of international diatom taxa identified and micrographed from a manifold of marine sites located in numerous geographical areas with a variety of climate types. Lastly, online resources, such as Plankton Net (n.d.) and Diatoms of North America (n.d.), were also utilised.

Open nomenclature taxonomic terminology was used as a means of conveying additional information regarding species identification. Instances of uncertainty regarding the identification of a species (or more specifically where a species could not be conclusively identified by the literature) are declared within the given species name. The uncertainty is illustrated by including "cf" in the scientific name, for example, *Auliscus cf. sculptus.* Moreover, when a particular morphology is present amongst potentially more than one species with identical ecological characteristics, the species morphology is grouped together as an aggregate, for instance, *Diploneis* aggregate (= *Diploneis bombus, D. crabro, D. interrupta).*

Autoecological classification of diatom species (according to preferences for life form, salinity, nutrients, saprobity, etc.) was determined by using checklists and coded indicator values by Denys (1991), Vos and De Wolf (1993), Van Dam *et al.* (1994), and Taylor *et al.* (2007). Omnidia software (version 5) (Lecointe *et al.*, 1993) facilitated the classification process, as well as electronic databases, namely the World Register of Marine Species (n.d.) and AlgaeBase (n.d.). Ecological preferences were supplemented by literature where information was absent in previously mentioned resources. Ultimately, the percentage of occurring diatom species within each sample was calculated. Tilia version 2.6.1. (Grimm, 1997) was used to create

a visual representation of diatom species percentages along with environmental parameters and to perform a Constrained Incremental Sum of Squares (CONISS) stratigraphically constrained cluster analysis to display the results (i.e., the zonation and relationships between zones) in the form of a dendrogram (Grimm, 1997).

4.5. STATISTICAL ANALYSES

4.5.1. Principal Component Analysis (PCA)

A PCA was performed on the dataset using the programme PAleontological STatistics (PAST) version 4.05 (Hammer *et al.,* 2001) because the length of Axis 1's gradient was less than 3 standard deviation units in an initial detrended correspondence analysis (DCA) (Dale and Dale, 2002). Consequently, a linear PCA was chosen to illustrate the main directions of variation within KNY19-B and KNY19-G's diatom assemblages.

The PCA was applied to find hypothetical variables (or components) that can account for the variance within multivariate data. More specifically, PCA was used to determine which environmental variables have the greatest impact on the system (Hassan *et al*., 2006). PCA was used to reduce the diatom dataset to the two first components for plotting purposes, where the two suggested components were influential to the system and correlated with underlying variables. The PCA routine also identified the eigenvalues of the variance-covariance (Hammer *et al.,* 2001). Eigenvalues were used to quantify (in percentages) the variance caused by the corresponding components.

4.5.2. Shannon-Wiener Diversity Index

Although species richness and species diversity are often used interchangeably, it is useful to differentiate between the two terms (Spellerberg and Fedor, 2003). Species richness measures the variety of species and thus applies to the number of species in a certain area or sample, whereas species diversity is conveyed as a diversity index (Spellerberg and Fedor, 2003). Species richness has an insignificant impact on species diversity, whereas diversity indices are strongly associated with evenness scores (Gao and Song, 2005).

The Shannon-Wiener diversity index is one of the most common diversity indices (Gao and Song, 2005). This proportional statistic is rooted in information and communication theory and measures uncertainty by calculating the Shannon Function or H' (Gao and Song, 2005; Masisi *et al.*, 2008; Ortiz-Burgos, 2016).

In ecological studies, H' measures the community structure or species diversity of a diatom assemblage by combining species richness and evenness indices, where evenness refers to how evenly individuals are distributed between the species (De la Rey, 2008). H' was calculated with the following equation by Shannon *et al.* (1949):

$$H' = -\sum_{i=1}^{S} Pi\ log_2 Pi\ (Pi = Ni/N); \quad J = H'/log_2 S$$

where "S" refers to diatom species richness (Goa and Song, 2005), "Pi" denotes relative diatom abundance (Cheng and Song, 2014), which is calculated from Ni/N as the proportion of the total population of individuals (N) that form part of the ith species (Ni) (De La Rey, 2008), and "J" signifies evenness.

There are various benefits associated with using H'. H' is seen as a more practical index than solely relying on species richness as an indication of environmental change, as that would entail counting a minimum of 8000 specimens, while species diversity can be determined by counting hundreds of specimens (Patrick *et al.,* 1954). H' takes into account the number of species and the distribution of the data by combining species richness and evenness indices, thereby adding to its advantages by generating informative results (Wu *et al.*, 2014). These results can be readily interpreted and compared with other values or results in the literature, owing to H's popularity as a diversity index in ecological studies (Wu *et al.*, 2014).

Bearing these benefits in mind, H' was applied to samples in Omnidia to provide an insight into community structure and population variation, as well as to complement diatom species' autoecological information.

4.6. TROPHIC DIATOM INDEX (TDI)

Omnidia version 5 (Lecointe *et al.*, 1993) calculated the TDI and the percentage pollution tolerant values (%PTV), as based on Kelly and Whiton (1995) and Kelly (1998), to create a bioindicator of water quality in the Knysna Estuary.

In essence, TDI is an index used for monitoring the trophic status of water bodies and is centred on using changes in the composition of taxa in diatom communities (Kelly and Whitton, 1995). Consequently, the taxonomic change acts as a quantification of the impact of nutrients on water bodies (Atazadeh *et al.*, 2007). In cases of extreme organic pollution, it is worth noting that TDI is less effective in distinguishing between eutrophication and other effects, which is why TDI complements the %PTV, as this value

indicates the percentage of the sample that consists of organic pollution tolerant diatom species (Table 2) (Kelly and Whitton, 1995). Therefore, TDI cannot be applied without taking %PTV into account, as %PTV impacts TDI's proficiency in correctly determining the effect of inorganic nutrients on eutrophication (Wu *et al.*, 2014).

Table 2. Interpretation of the %PTV score as a complement to TDI (Adapted from Kelly and Whitton, 1995).

Water Quality Conditions	**%PT Range**
No significant organic pollution	0 – 20%
Some indication of organic pollution	21 – 40%
Eutrophication caused by the significant contribution of organic pollution	41 – 60%
Severe contamination by organic pollution	61 – 100%

The TDI formula is as follows: $TDI = \Sigma asv / \Sigma sv$

"s" sensitivity of the species (from 1 – 5)
"v" indicator value of the species (1 – 3)
"a" abundance of species in the sample

TDI varies between 1 ("clean water" or oligotrophic conditions) and 5 ("grossly polluted water" or eutrophic conditions) (Lecointe *et al.*, 1993), however, the results also generate a percentage value ranging from 0 to 100 for each sample. The values are subsequently divided into subclasses that are based on the proportion of the count belonging to %PTV, thereupon providing an interpretation of trophic status or a measure of eutrophication (Kelly and Whitton, 1995) as illustrated in Table 3.

Table 3. TDI percentage range and the associated trophic status (Adapted from Kelly and Whitton, 1995).

Trophic Status	**TDI Range (%)**
Oligotrophic	0 – 20
Oligo-mesotrophic	21 – 40
Mesotrophic	41 – 60
Meso-eutrophic	61 – 80
Eutrophic	81 – 100

4.7. CONCLUSIONS

It is imperative to grasp the above methodology in full, as it provides a solid underlying structure that can be used to determine environmental change over time in the Knysna Estuary. Fundamentally, the methodological framework is used to underpin the research aim and achieve the objectives.

CHAPTER 5 - RESULTS

This chapter presents the results obtained using the described methodological approach. Specifically, the results of core KNY19-B - a strongly marine-influenced section of the estuary located in the Ashmead Channel - is compared to core KNY19-G, which is located in the middle reaches of the estuary and is subject to a greater degree of fluvial influence.

5.1. CORE KNY19-B: THE ASHMEAD CHANNEL

5.1.1. Chronology and Sediment Accumulation

The age-depth model, which is the objective of another related project, is based on a combination of ^{210}Pb and radiocarbon dating and is graphically presented in Figure 14. A basal sample returned a ^{14}C date of 1330 BP and included the lower and upper calibrated age ranges and their associated relative probabilities (Table 4). Subsequent to applying the calibration curve and marine reservoir effect for the southern Cape coast, the results indicate that the core spans 680 years.

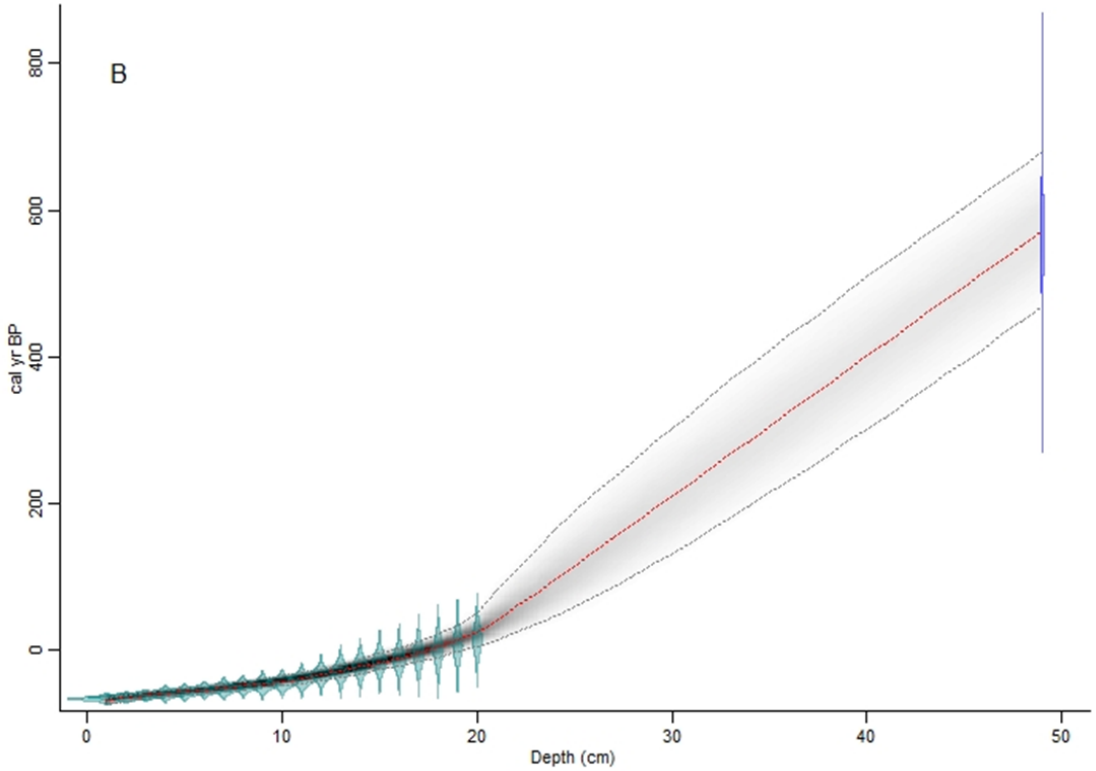

Figure 14. Age-depth model for KNY19-B.

The mean sediment accumulation rate for KNY19-B is 13.09 yr/cm^{-1} (0.14 cm/year) (Figure 14). However, prior to 25 cal BP, sediment accumulation rates were significantly lower at an average of 19.04 yr/cm^{-1} (0.05 cm/yr), after which the deposition of sediment accelerates to 2.69 yr/cm^{-1} (0.41 cm/yr) during the 21st century (upper 7 cm).

Table 4. Information on ^{14}C basal age including error margins, lower and upper probability ranges, and the relative probability.

Lab Code	Depth (cm)	^{14}C age (yr BP)	Error (± yr)	95.4% (2σ) probability range (cal BP)		
				Lower	Upper	Relative probability
Beta-553445	48 – 49	1330	30	1292	1172	0.941
				1141	1107	0.059

5.1.2. Stratigraphy

KNY19-B is 57 cm in length and consists primarily of *Substantia humosa* and silt deposits (Figure 15). From roughly 1975 CE onwards, the percentage of silt increases in favour of clay and sand. A distinct incursion of sand is discernible at approximately 400 to 400 cal BP at the expense of the proportion of silt and clay. Organic matter lenses intrude throughout the core at depths, but most notably at 0 to 3 cm, 8 to 11 cm, 17 to 18 cm, and 28 cm. The core colouration is predominantly classified as 10YR 5/1 (greyish-brown), whereas the markedly darker intrusions were categorised as 10YR 2/1 (dark brownish-black).

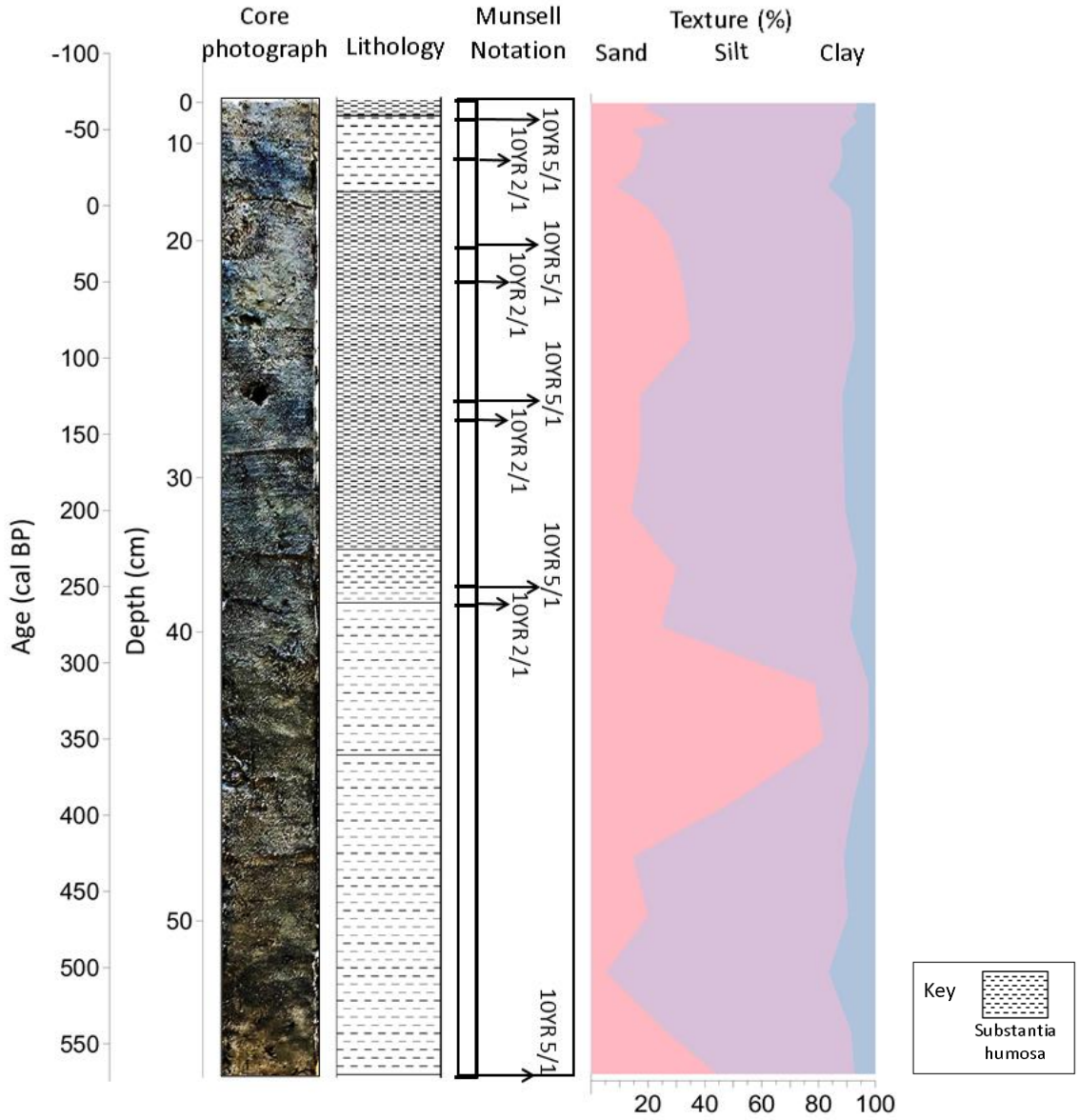

Figure 15. Core description of KNY19-B in terms of lithology, colour, and texture. Note that the varying degrees of shading in the lithology corresponds to the relative abundance of *S. humosa.*

5.1.3. Diatom Assemblage Zones

Stratigraphically constrained cluster analysis (CONISS) identified three main diatom assemblage zones in both KNY19-B and KNY19-G. Although species with a relative abundance of >3% were excluded from the relative percentage diagrams on the grounds that they were considered rare, their autoecological relationships form part of the total percentage on the diagrams. A comprehensive list of each species' autoecological preferences can be found in Appendix 2 (Table 11, pp. 143). The zones are labelled alphabetically according to age - commencing at the base of the core with zone C and concluding with zone A at the top of the core. Results obtained from the diatom analysis are discussed based on the diatom

assemblage zones as illustrated by the relative percentage diagrams based on salinity (Figure 16), trophic status, and saprobity preferences, where the latter two diagrams can be found in Appendix 2 (Figures 36 and 37).

In all, 75 diatom species were identified in 28 samples, although only 23 are commonly occurring (>3%). Very low diatom preservation was observed in the lowermost sample, 56 cm, therefore this sample was excluded from the count. Overall, the diatom assemblage is dominated by a strong marine, oligotrophic, β-mesosaprobic signal. A complete record of all the diatom species identified in KNY19-B, as well as their autoecological preferences based on salinity, trophic status, and saprobity, can be found in Appendix 2. Cluster analysis divided the assemblage into five zones, namely Zone KNY19-B-A (∼610 to ∼450 cal BP; 54 - 42 cm), Zone KNY19-B-B (∼450 to ∼225 cal BP; 42 - 31 cm), and Zone KNY19-B-C (∼225 cal BP to present; 31 - 0 cm). This final zone is subdivided into three subzones, *viz.* Zone KNY19-B-C1 (∼225 to ∼30 cal BP; 31 - 21 cm), Zone KNY19-B-C2 (∼30 to ∼-50 cal BP or ∼1915 to ∼2007 CE; 21 - 4 cm), and Zone KNY19-B-C3 (∼-60 to ∼-70 cal BP or ∼2007 to present; 4 - 0 cm) (Figure 16). A description of each diatom assemblage zone follows for KNY19-B.

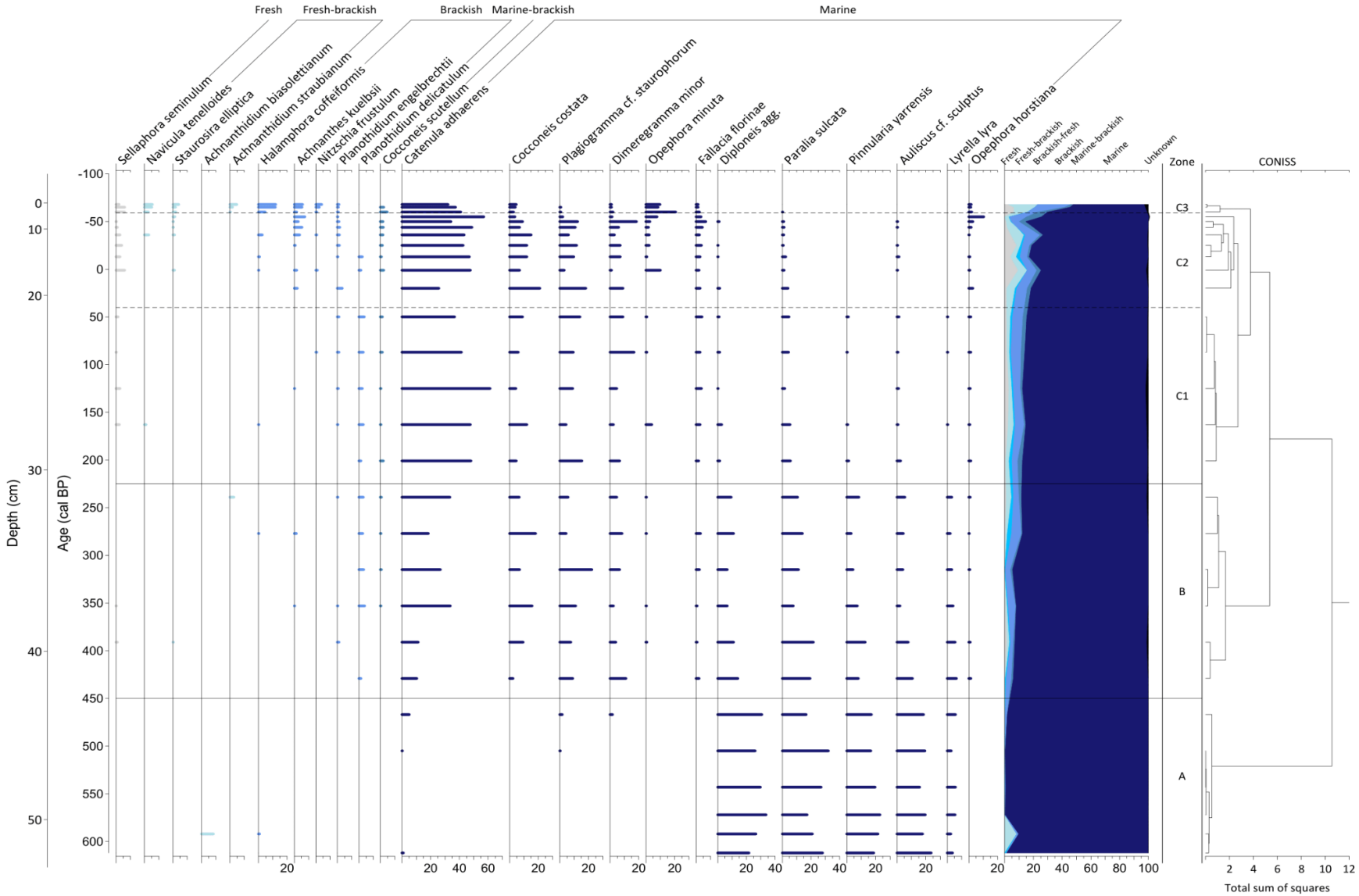

Figure 16. KNY19-B diatom relative percentage diagram against age (cal BP) and depth (cm) where species are grouped according to salinity preferences.

Zone KNY19-B-A: 54 - 42 cm; ~ 610 to ~450 cal BP

Diatom fossil assemblage Zone KNY19-B-A encompasses the basal section of the sedimentary record and lasted ~160 years. Low fossil preservation occurred throughout. This zone is characterised by low species richness and the highest relative abundance of marine species (97.67% average) to the extent that the entire zone is dominated by marine intertidal species, except at ~590 cal BP (52 cm) when fresh-brackish *Achnanthiduim biasolettianum* (8.33%) makes its only fleeting appearance in the entire sequence alongside brackish *Halamphora coffeaeformis* (0.67%) (Figure 16 and Appendix 1, Figure 34Y). In addition, there is a minor increase in brackish and marine-brackish species toward the top of this zone, from ~460 cal BP. Zone KNY19-B-A is further distinguished by containing the highest relative proportion of oligosaprobic (21.67% - 33.67%) and oligotrophic (16.67% - 23%) species (Appendix 2, Figures 36 and 37).

The most common species in the assemblage are Diploneis aggregate (= *Diploneis bombus, D. crabro, D. interrupta*) (Appendix 1, Figure 34P) and *Paralia sulcata* (Appendix 1, Figure 35FF) (in total comprising >60% of the diatom assemblage) - both marine species present in near-similar concentrations throughout the zone (Figure 16). *D.* agg is a warm-water, epipelic species characteristic of coastal environments (Zalat and Al-Wosabi, 2011), while cosmopolitan cold-water *P. sulcata* is typical of estuarine conditions under salt-wedge influence and tidal channels (Espinosa and Isla, 2015). *P. sulcata* has a complicated palaeoecological application and ecology seeing that its heavily silicified frustules are resistant to dissolution, thereby being partly responsible for its relative profusion in coastal sediment records and rendering it complicated to use in palaeoenvironmental reconstructions (Jiang, 1996; McQuoid and Nordberg, 2003; Novak, 2017). Moreover, *P. sulcata* is a true benthic or bottom dwelling species, where the frustules are easily suspended in the water column by daily tides or storm events and ultimately dispersed throughout all tidal environments (Buzer, 1981; Zong, 1997; Sawai *et al.,* 2016). Consequently, *P. sulcata* may indicate strong velocity flow as it is brought in with the tide, therefore it is considered allochthonous in this assemblage (Sato *et al.,* 1998; Sawai and Nagumo, 2003; Kirsten *et al.,* 2020). Ranging between 15.67% to 23.67%, marine epipsammic *Auliscus* cf. *sculptus* (Appendix 1, Figure 35EE) and epipelic *Pinnularia yarrensis* (Appendix 1, Figure 35AA) further co-dominate the assemblage albeit to a slightly lesser degree compared to *D.* agg and *P. sulcata. P. yarrensis* has a preference for low nutrient concentrations, in effect giving rise to the strong oligotrophic component of this zone. *Lyrella lyra,* a sublittoral benthic marine species, also has a fairly consistent average abundance (4.22%) throughout Zone KNY19-B-A (Korotky *et al.,* 1997; Ganzey *et al.,* 2015; Zalat *et al.,* 2021). Although the species is

adapted to various substrates, *L. lyra* has been observed as epiphytes on macroalgae in subtidal zones (Mitlehner, 1992; Zalat *et al.,* 2021). Lastly, *Catenula adhaerens* (5%) (Appendix 1, Figure 32F) and *Plagiogramma* cf. *staurophorum* (1.67%) (Appendix 1, Figure 32B), make their first appearance in relatively low concentration towards the top of the zone at 500 cal BP (45 cm), while *Dimeregramma minor* (1.67%) (Appendix 1, Figure 32A) first emerges at ~470 cal BP (44 cm).

Zone KNY19-B-B: 42 - 31 cm; ~ 450 to ~225 cal BP

Zone KNY19-B-B, spanning 220 years, is distinguished by a decreasing trend of marine species. Marine species reach a maximum value of 94% at the bottom of the zone at ~450 cal BP (42 cm), followed by a steady decline to 87.33% at the top of the zone at ~240 cal BP (32 cm), thus giving way to an increasing proportion of fresh-brackish, brackish-fresh, and brackish taxa (Figure 16). Regarding trophic characteristics, eutrophic species increase to roughly 5% of the assemblage, thereby signalling the establishment of steadily increasingly eutrophic conditions throughout the zone and sequence as a whole (Appendix 2, Figure 36). Meanwhile, β-mesosaprobic conditions experience a substantial rise from 12.33% to 41% (Appendix 2, Figure 37).

This zone is dominated by epipsammic marine sublittoral diatoms, such as *Catenula adhaerens* (22.28%) and *Cocconeis costata* (9.83%) (Appendix 1, Figure33J), while epipelic *D.* (agg) (9.78%) lives freely on sediment surfaces (Moss, 1977; Buzer, 1981; Hudon and Bourget, 1983). Again, *P. sulcata* (14.11%) is well represented, thereby reinforcing the prominence of marine littoral diatoms in this zone (Erikkson *et al.,* 1999). However, there is a noticeable reduction in previously dominant marine species, such as *D.* (agg), *P. sulcata, P. yarrensis,* and *A. sculptus*, due to the dramatic increase in *C. adhaerens.* Epipsammic *Opephora minuta, Fallacia florinae,* and *Planothidium delicatulum* (Appendix 1, Figure 32I) each make their first appearance in the sequence around the commencement of the zone (~430 to ~390 cal BP).

Zone KNY19-B-C: 31 - 0 cm; ~ 225 to ~-70 cal BP

Zone C is the largest diatom assemblage zone and extended for almost three centuries from ~225 cal BP. It is divided into three sub-zones, KNY19-B-C1 (~225 to ~35 cal BP), KNY19-B-C2 (~35 to ~-60 cal BP), and KNY19-B-C3 (~-60 to ~-70 cal BP).

Zone KNY19-B-C1: 31 - 21 cm; ~ 225 to ~35 cal BP

Zone KNY19-B-C1 encompasses 190 years and is characterised by relatively stable conditions throughout. There is a slight decrease in the relative abundance of marine species from 87.33% to 84.33% owing to the continuous presence of brackish species, as well as the increasing frequency of fresh species (Figure 16). The ratio between oligotrophic and eutrophic species remains more or less constant throughout the sub-zone. There are exceptions at ~200 cal BP (30 cm) when oligotrophic species reach their lowest values (1.66%) and at ~165 cal BP (28 cm) when eutrophic species (7.32%) and polysaprobic (8%) species peak (Appendix 2, Figures 36 and 37).

The diatom assemblage of Zone KNY9-B-C1 is primarily dominated by the β-mesosaprobic *C. adhaerens,* which peaks at 61.33% in this zone at ~125 cal BP or 1825 CE (26 cm). At 10.4%, benthic-planktonic *P.* cf. *staurophorum* is subdominant. The distribution of *P. yarrensis* and *L. lyra* culminates at the top of the zone. It is noteworthy that polysaprobic *Sellaphora seminulum* and the first appearance of *Navicula tenelloides* (Appendix 1, Figure 34S) contribute towards the maximum value of eutrophic species in this zone.

Zone KNY19-B-C2: 21 - 4 cm; ~ 35 to ~-60 cal BP (~1915 to ~2005 CE)

The following 92 years are defined by major fluctuations in the community structure. This is a cumulative result of minor fluctuations in the levels of the less dominant taxa, with only dominant marine taxa displaying major variations. Specifically, the relative abundance of marine species fluctuates significantly in the zone due to pulses of freshwater and fresh-brackish inputs. Consequently, it is evident that there is a decrease in the abundance of marine species from an average of 85.53% in Zone KNY19-B-C1 to 79.04% in the current zone (Figure 16). Similarly, these fluctuations are reflected in the abundance of oligotrophic species (Appendix 2, Figure 36). The abundance of eutrophic and hypertrophic continues to increase, with a deviation in ~2000 and ~2005 CE, when eutrophic species reach their lowest abundance (1.33%) since ~430 cal BP (42 cm). Simultaneously, polysaprobic and α-mesosaprobic species also decline towards the top of the zone (Appendix 2, Figure 37).

In total, *C. adhaerens, C. costata,* and *P.* cf. *staurophorum* consist of over 60% of the biological community, where *C. costata* peaks at 21% in ~1930 CE (20 cm). The constant presence of supratidal *D.* (agg) and sublittoral *A.* cf. *sculptus* throughout the core concludes at the end of the zone. Interestingly, eutrophic

and polysaprobic *S. seminulum* steadily disappears at the top of the zone after achieving maximum percentage values (6%) in ~1950 CE (18 cm), whereas *P. delicatulum* abruptly vanishes in ~1965 CE (16 cm). Both *N. tenelloides* and *N. frustulum* also dissipate towards the top of the zone after having made sudden reappearances in the assemblage in ~1980 CE and ~1950 CE respectively. Other eutrophic species, such as *P. engelbrechtii* and *C. scutellum,* remain relatively stable throughout the zone.

Zone KNY19-B-C3: 4 - 0 cm; ~-60 to ~-70 cal BP (~2005 to Present)

Zone KNY19-B-C3, the upper part of Zone KNY19-B-C, lasts for about a decade. Marine taxa drastically decrease to an average of 57%, while fresh-brackish and brackish species display an upward trend (Figure 16). The zone is further distinguished by strong mesotrophic to hyper-eutrophic conditions. Specifically, the most recent sample in the sequence is host to the highest average abundance of mesotrophic species (8.67%), eutrophic (22.89%), and hypereutrophic (3.67%) species in the entire core (Appendix 2, Figure 36). Furthermore, this zone sees the reemergence of increased α-mesosaprobic to polysaprobic conditions (Appendix 2, Figure 37).

C. adhaerens continues to dominate the assemblage at 36.78%*,* whereas marine *O. minuta* and α-mesosaprobic *H. coffeaformis* are subdominant at 12.98% and 9.44%, respectively. Eutrophic *H. coffeaeformis, S. seminulum, N. tenelloides* and *N. frustulum* reach their highest abundances in this zone. Lastly, *P.* cf. *staurophorum* and *D. minor* were present in their lowest abundances in the core and allochthonous *P. sulcata* is absent from ~-65 cal BP (~2015 CE) (2 cm) onwards.

5.1.4. Statistical Analysis

5.1.4.1. Principal Component Analysis (PCA)

At first, a PCA was conducted on the entire species list of KNY19-B. The high abundance of certain marine species skewed the interpretation of the results and was therefore excluded from the analysis as they were also deemed as allochthonous and not a true representation of *in situ* conditions, along with the 2% of the rare species. A subsequent PCA (Figure 17) containing 20 out of the original 77 species determined the principal species behind the environmental conditions at KNY19-B. Ultimately, 87.71% of the total variance is explained by the first two principal components (Table 5), whereas the remaining 17

components were deemed insignificant. Furthermore, Table 5 illustrates that PC1 and PC1 have significantly larger eigenvalues than the remaining components.

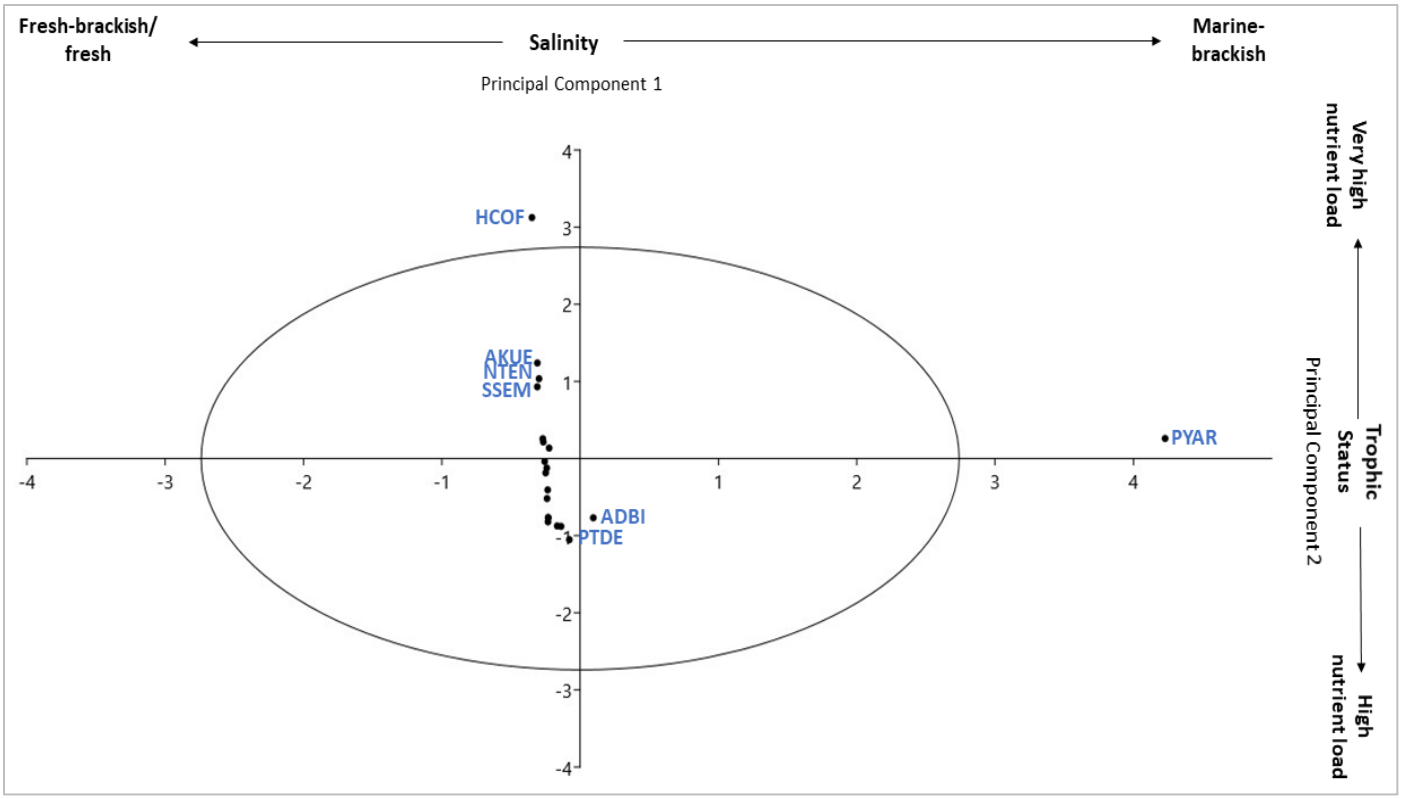

Figure 17. Principal component analysis illustrating the main environmental variables impacting the system at KNY19-B.

PC1 accounts for 76.2% of the variability in KNY19-B's assemblage (Table 5). *Pinnularia yarrensis* has by far the highest positive score along this axis (Figures 17 and 18). *Achnanthidium biasolettianum* was the only other species with a positive loading on the first axis, though the species is considerably less positive compared to *P. yarrensis*. Negative loadings are observed for *Halamphora coffeaeformis*, *Sellaphora seminulum,* A*chnanthes kuelbsii,* and *Navicula tenelloides. H. coffeaeformis*'s factor loading is only marginally lower than the rest.

Table 5. PCA results indicating the first four and last principal components of KNY19-B, as well as the eigenvalues and variance, explained by each.

Principal Component (PC)	1	2	3	4	...	19
Eigenvalue	1129.27	170.64	60.6	34.46	...	0.005
Variance (%)	76.2	11.51	4.09	2.33	...	0.00

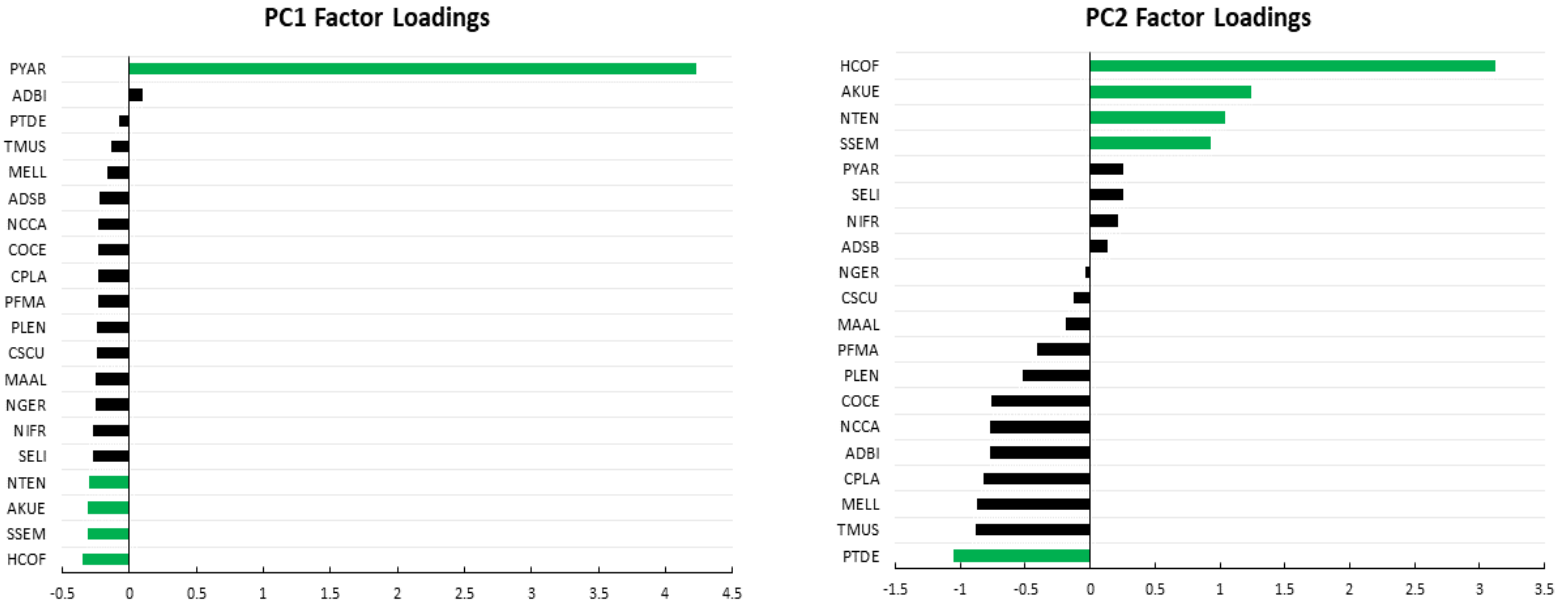

Figure 18. Factor loadings for the first two principal components at KNY19-B. Significant loadings are indicated in green. (HCOF = *Halamphora coffeaeformis*; ADBI = *Achnanthidium biasolettianum*; ADSB = *Achnanthidium straubianum*; AKUE = *Achnanthes kuelbsii*; COCE = *Cocconeis engelbrechtii*; CPLA = *Cocconeis placentula*; CSCU = *Cocconeis scutellum*; MAAL = *Mayamaea atomus*; MELL = *Mastogloia elliptica;* NCCA = *Navicula cincta*; NGER = *Navicula germainii*; NIFR = *Nitzschia frustulum*; NTEN = *Navicula tenelloides*; PFMA = *Planothidium frequentissimum*; PLEN = *Planothidium engelbrechtii*; PTDE = *Planothidium delicatulum*; PYAR = *Pinnularia yarrensis*; SSEM = *Sellaphora seminulum*; TMUS = *Terpsinoë musica*).

P. yarrensis is a marine species commonly found in tidal flats or salt marsh environments (Chibo *et al.,* 2016; Sawai and Nagumo, 2003). This is echoed by Sitoe *et al.* (2017:309), who state that *P. yarrensis* is recurrently found in near-shore and intertidal areas. Negatively loaded *H. coffeaeformis* is a brackish species that is globally known for tolerating hypersaline conditions (Gell *et al.*, 2002; Taukulis and John, 2002; Luly *et al.*, 2006), while *A. kuelbsii* is a brackish estuarine species (Bate *et al.,* 2004). *N. tenelloides* is a fresh-brackish species, whereas *A. kuelbsii* and *S. seminulum* are freshwater species (Guiry, 2021;

Taylor *et al.,* 2007). This suggests that PC1 can be interpreted as an expression of salinity, since the positive score is associated with the only brackish-marine element, whereas the negative loadings are linked to lower salinity levels (ranging from fresh to brackish).

PC2 accounts for 11.51% of the variation in KNY19-B's diatom assemblage (Table 16). *H. coffeaeformis* has the highest positive loading, while *A. kuelbsii* has the second highest positive value on this axis (Figures 22 and 23). It is worth noting that *N. tenelloides* and *S. seminulum* also have high positive loading on this axis, albeit to a lesser extent. Pertaining to the negative loadings, various species, such as *Terpsinoë musica*, *Mastogloia elliptica*, *Cocconeis placentula* (Appendix 1, Figure 33L), have negative loadings on this axis. Despite the conglomeration, *Planothidium delicatulum* has the lowest factor loading.

H. coffeaeformis is a eurythermal species capable of surviving in stagnant or running water (Zalat and Al-Wosabi, 2011; Hafner *et al.*, 2018; Zalat *et al.*, 2019). *H. coffeaeformis* is polytrophic, meaning that the species is connected to elevated nutrient loads, which is not surprising considering that the species can present itself in drainages with moderate agricultural activity (Van Dam *et al.*, 1994; Blinn and Bailey, 2001). *N. tenelloides* is also polytrophic and occurs in extremely polluted waters, similar to *S. seminulum* (Taylor *et al.*, 2007; Noga *et al.,* 2016; Rimet *et al.*, 2016). Furthermore, inputs of nutrients induce an increase in *S. seminulum*, thereby making the taxa characteristic of higher nutrient concentrations or heavy organic matter pollution (Stewart *et al.*, 2018; Soeprobowati *et al.*, 2019*).* A significant negative loading is seen for *P. delicatulum* - a eutrophic species representative of tidal flat environments and typical for shallow littoral waters (Sawai *et al.*, 2004; Witkowski *et al.,* 2005; Chiba *et al.,* 2016). *C. placentula*, another eutrophic species, also has a negative score. Evidently, this axis has a strong relationship with nutrient loads because polytrophic conditions are more frequently associated with positive factor loadings, whereas significant negative factor loadings are linked to a eutrophic state. Therefore, PC2 may represent the influence of nutrient loads, which is an indication of land use change and natural estuarine nutrient fluctuation, on the diatom species composition in KNY19-B.

5.1.4.2. Shannon-Wiener Diversity Index and Evenness

On average, the Shannon-Wiener diversity index of KNY19-B is high at 2.98 (Figure 19). The highest diversity value is 3.62 at ~275 cal BP (33 cm), although similarly high values are observed at ~-70 cal BP (3.56) and ~40 cal BP (3.51), while the lowest diversity value is 2.2 during ~575 cal BP (49 cm). Generally,

diversity decreases towards the base of the core (~505 to ~610 cal BP, 45 - 54 cm) in comparison to the noticeable increase in diversity from ~-55 to ~-70 cal BP (5 - 0 cm) at the top of the core. Consequently, it seems as though there is a gradual increase in diatom community diversity over time. The average species evenness was 0.71 and evenness peaked at 0.84 (~430 cal BP, 41 cm) (Figure 19). The lowest evenness value was measured at ~125 cal BP (25 cm) (0.53) due to the overwhelming dominance of *C. adhaerens* (>50%) in the sample. As a result, there is a discernible drop in diversity during this time. For the most part, diversity and evenness fluctuate together (Figure 19), except during the last century where evenness scores diverge from the diversity scores. During this period, a low species richness (10 species on average) contributed to the continual low diversity, while high evenness scores are attributed to species occurring in equal proportion.

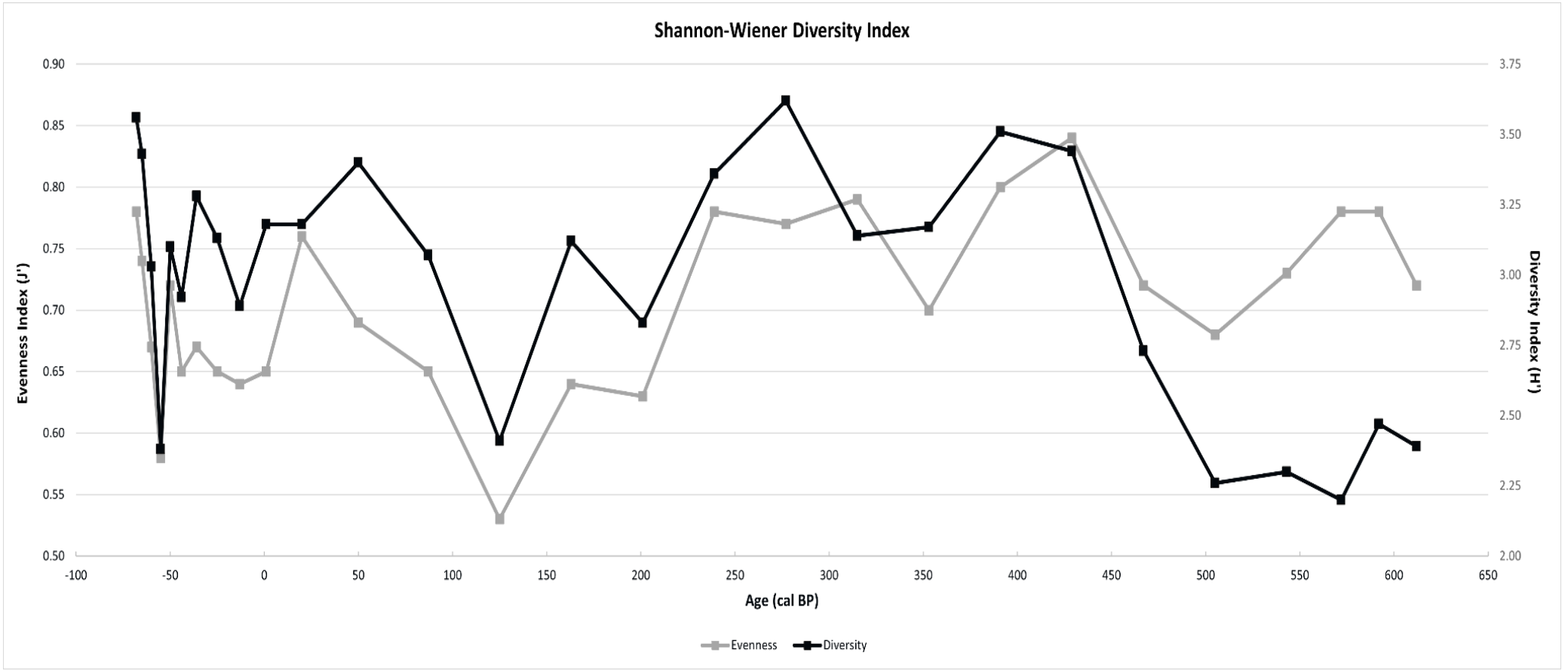

Figure 19. Shannon-Wiener Diversity and Evenness Index of KNY19-B.

5.1.5. Trophic Diatom Index (TDI)

The Trophic Diatom Index values ranged from 0% to 82.9% (Figure 20) and the percentages of taxa tolerant to organic pollution (%PTV) were all below 20% (Table 6). It is apparent that the TDI values have increased over time, thereby indicating that over time the trophic status has shifted from oligotrophic conditions to predominantly mesotrophic and meso-eutrophic conditions. TDI values were low (0% - 16.8%) from ~610 to ~300 cal BP (54 - 39 cm), indicating oligotrophic conditions. It is likely that the values of zero are attributed to the fact that the TDI was originally developed to monitor the trophic status of rivers based on diatom composition in England and Wales (Kelly and Whitton, 1995) and therefore does not take marine species, which dominate the assemblage at this point, into account. Subsequently, there was a shift to oligo-mesotrophic values from ~355 to ~240 cal BP (38 - 31 cm). The first instance of meso-eutrophic TDI values (63.6%) appears at ~125 cal BP or ~1825 CE (26 cm) and is followed by a period of instability where TDI values fluctuate between mesotrophic, meso-eutrophic, and eutrophic conditions. The TDI peaked at 82% and 82.9%, representing the first occurrence of eutrophic conditions, from ~-55 to ~-60 cal BP or from ~2005 to ~2010 CE (6 - 3 cm), after which the two most recent samples return values consistent with meso-eutrophic conditions. In relation to the pollution tolerant values (%PTV), the low values (<20%) (Table 6) signal that all samples are free of significant organic pollution. It is clear that the most recent PTV%s (7.7%, 10.7%, and 7.7%) are higher than their precursors.

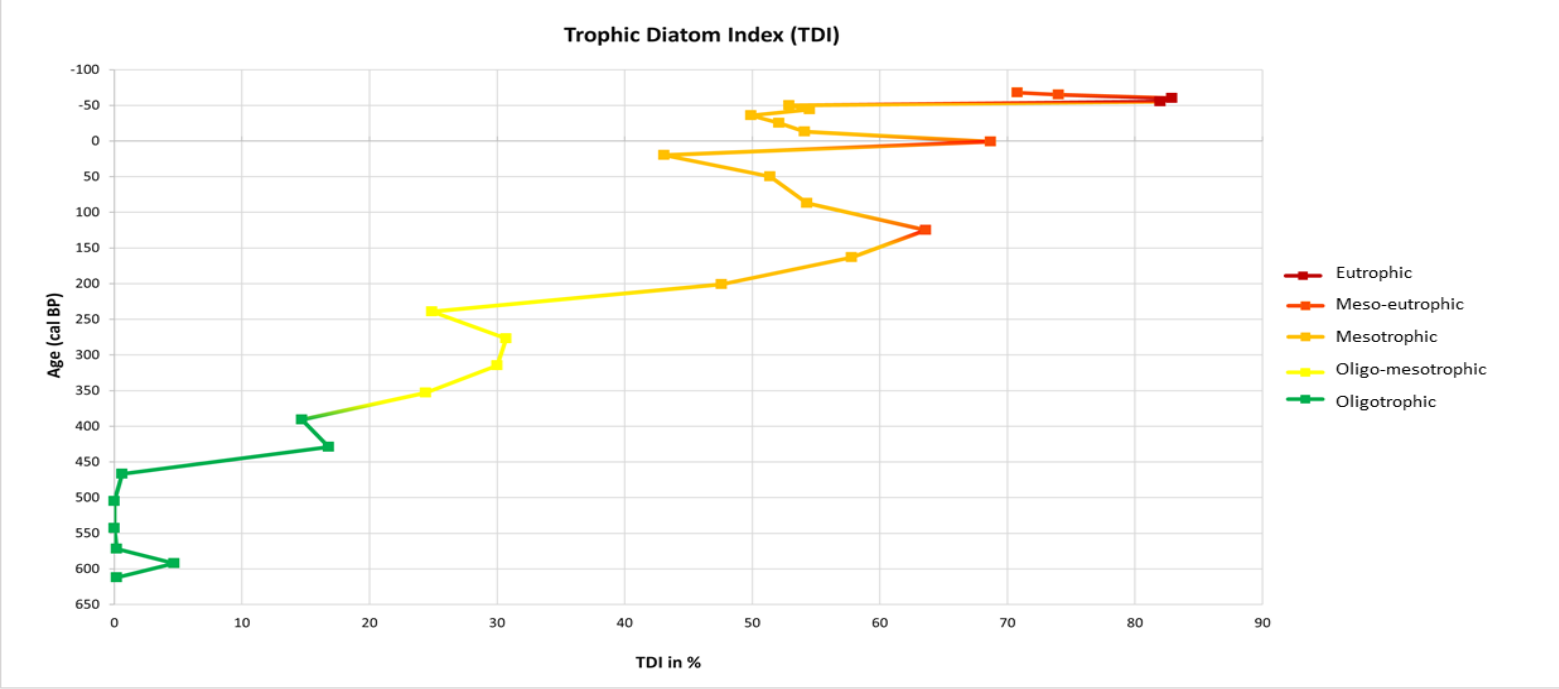

Figure 20. Trophic Diatom Index of KNY19-B.

Table 6. Percentage pollution tolerant values for samples in KNY19-B.

Age (cal BP)	-68	-65	-60	-55	-50	-44	-36	-25	-13	1	20	50	87	125
%PTV	7.7	10.7	7.7	0	0.3	1.3	4.7	5	2.7	7.3	0	1.3	1	2.7

Age (cal BP)	163	201	239	277	315	353	391	429	467	505	543	572	592	612
%PTV	3.3	0.3	0	0	0	0.3	1	0	0	0	0	0	0	0

5.2. CORE KNY19-G: THE MIDDLE REACHES

5.2.1. Chronology

The age-depth model is based on a combination of ^{210}Pb and radiocarbon dating, which is graphically presented in Figure 21. A basal sample of organic sediment returned a ^{14}C date of 1320 BP (Table 7). Subsequent to applying the calibration curve and marine reservoir effect for the southern Cape coast, the results indicate that the core spans 620 years.

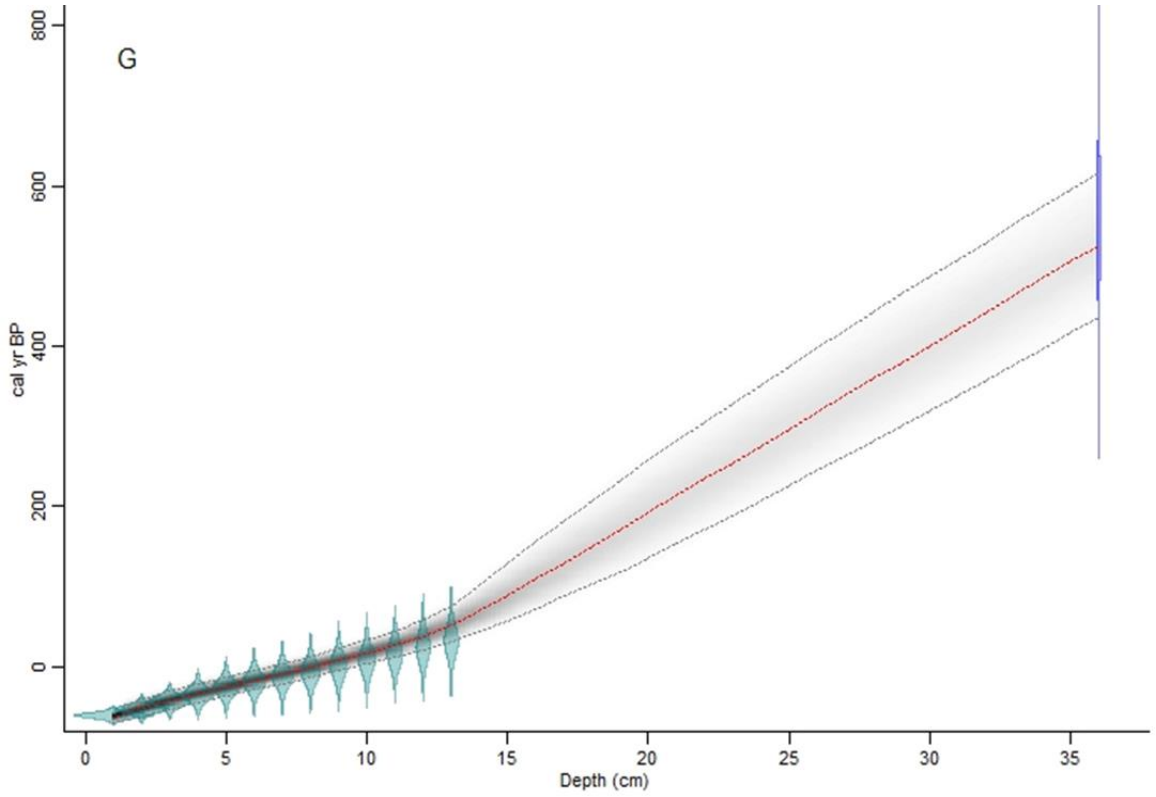

Figure 21. Age-depth model for KNY19-G.

The mean sediment accumulation rate for KNY19-B is 16.49 yr/cm^{-1} (0.7 cm/year) (Figure 21). Although, at an average of 20.81 yr/cm^{-1} (0.05 cm/yr), sediment accumulation rates were considerably lower prior to 68 cal BP, sediment accumulation rates were significantly lower. Subsequently, sediment deposition rapidly increases to 9.27 yr/cm^{-1} (0.11 cm/yr) during the 20th and 21st centuries (last 13 cm).

Table 7. Information on ^{14}C basal age including error margins, lower and upper probability ranges, and the relative probability.

Lab Code	Depth (cm)	^{14}C age (yr BP)	Error (± yr)	95.4% (2σ) probability range (cal BP)		
				Lower	Upper	Relative probability
Beta-553444	35 – 36	1320	30	1278	1141	0.879
				1146	1093	0.121

5.2.2. Stratigraphy

KNY19-G has a length of 37 cm (Figure 22). The stratigraphy is heterogenous showing variation in lithology and colour. The sediment mostly consists of *Substantia humosa*, while roots of herbaceous plants (*Turfa herbacea*) are present throughout the first nine centimetres, as well as at the base of the core. In terms of colouration, the first 15 cm is predominantly classified as 7.5YR 3/1 (dark brown), with an oxidised layer present at approximately 10 to 12 cm. The remainder of the core is distinctly darker grading from 10YR 2/2 (dark brownish-black) to 10YR 3/2 (dark greyish-brown). Overall, the majority of KNY19-G is associated with silty to sandy sediments and there is a general decrease of clay towards the top of the core. Furthermore, the percentage of sand increases from roughly 1960 CE onwards, while the percentage of silt decreases. Lastly, a heterogenous depositional layer comprised of mottled clay-like sediments occurs at ~70 to ~150 cal BP.

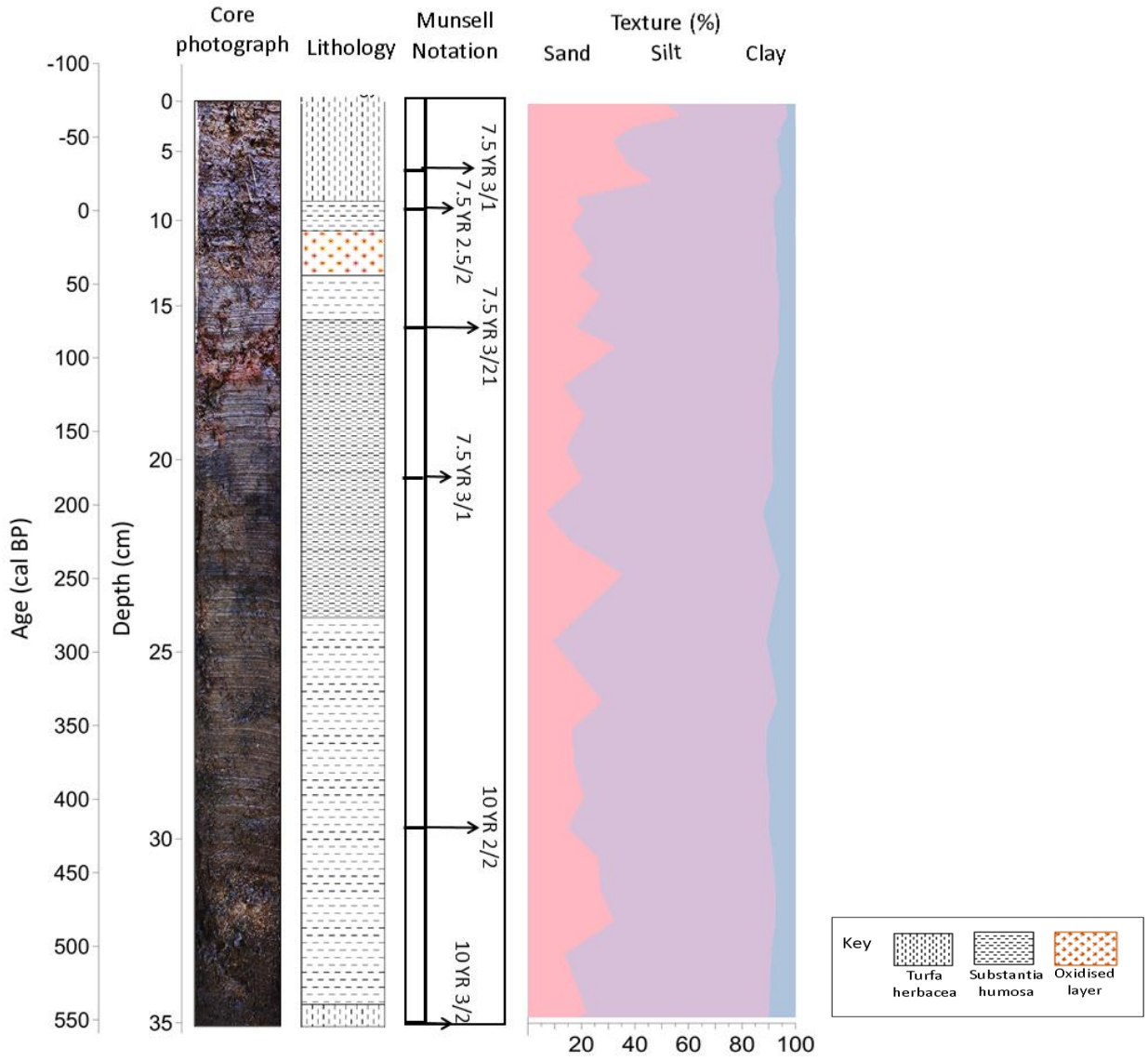

Figure 22. Core description of KNY19-G in terms of lithology, colour, and texture.

5.2.3. Diatom Assemblage Zones

A total of 109 diatom species were identified in 19 samples, however, only 26 were common (>3%). Low diatom preservation was observed between 25 to 26 cm, therefore the sample was excluded from the count. Overall, the diatom assemblage is dominated by strong marine, eutrophic, and oligosaprobic signals. A complete record of all the diatom species identified in KNY19-G, as well as their autoecological preferences based on habitat preferences, salinity, trophic status, and saprobity, can be found in Appendix 3 (Table 13). Cluster analysis divided the assemblage into five zones, namely Zone KNY19-G-A (~555 to ~300 cal BP; 38 - 26 cm), Zone KNY19-G-B (~300 to ~-30 cal BP; 26 - 5 cm). Diatom assemblage zone B is subdivided into three groups, *viz.* Zone KNY19-G-B1 (~300 to ~200 cal BP; 26 - 21 cm), Zone KNY19-G-B2

(∼200 to ∼ 0 cal BP; 21 - 9 cm), and Zone KNY19-G-B3 (∼0 to ∼-30 cal BP or ∼1950 to ∼1980 CE; 9 - 5 cm). The final zone is Zone KNY19-G-C (∼-30 to ∼-65 cal BP or ∼1980 to Present; 5 - 0 cm) (Figure 23, Appendix 3, Figures 38 and 39). A description of each diatom assemblage zone follows.

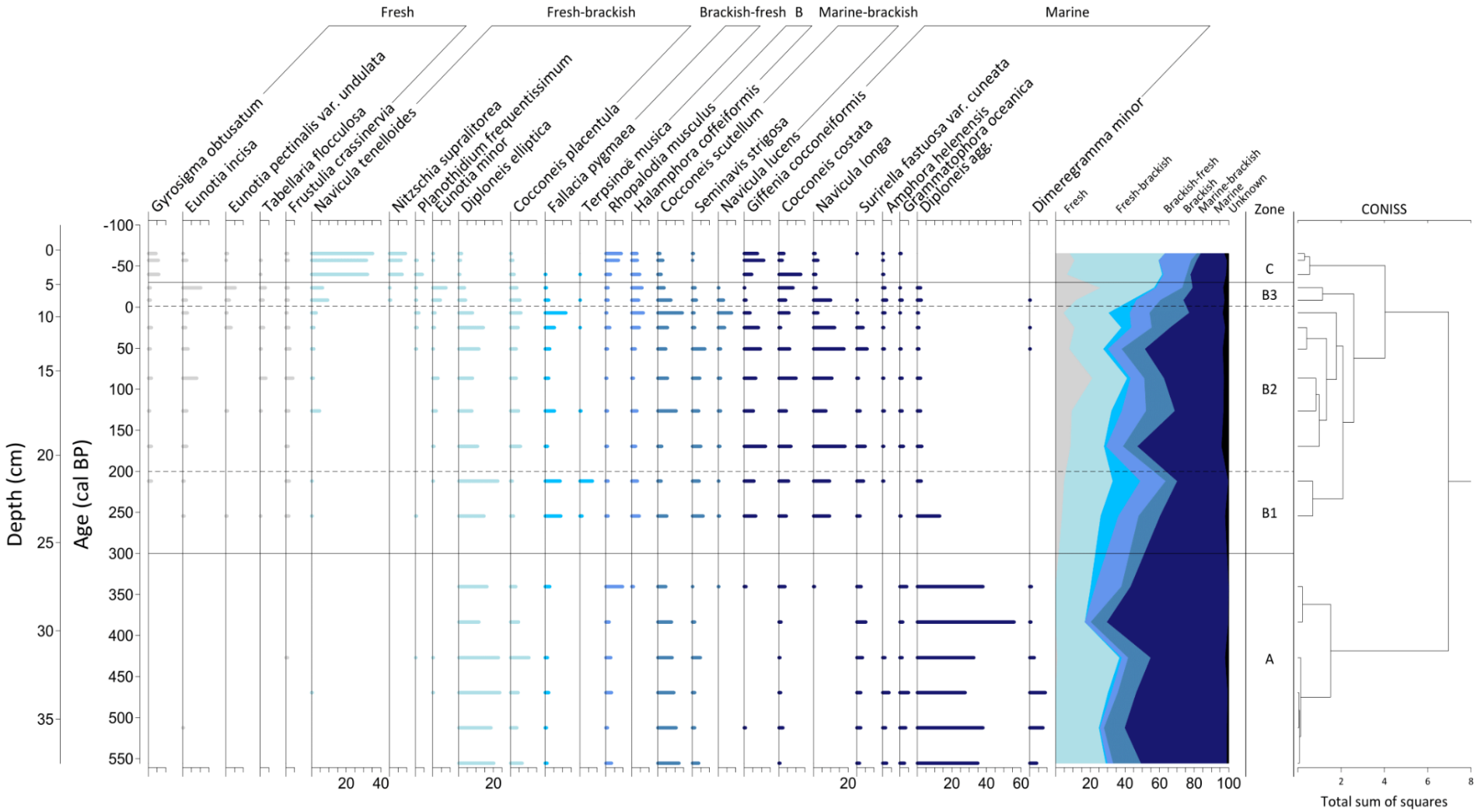

Figure 23. KNY19-G diatom relative percentage diagram against age (cal BP) and depth (cm) where species are grouped according to salinity preferences.

Zone KNY19-G-A: 38 - 26 cm; ~555 to ~300 cal BP

Diatom fossil assemblage Zone KNY19-G-A encompassed the basal section of the sedimentary record and lasted ~255 years. The zone is primarily dominated by marine species (average relative abundance of 55.17%), however, there is a continual presence of fresh-brackish (26.22%) and marine-brackish species (11.05%), as well as an increase in brackish taxa (3.33% to 15%) towards the top of the zone (Figure 23). Concurrently, oligotrophic and eutrophic species fluctuate together in near similar occurrences (21.34% and 21.55%, respectively), where the maximum proportion of eutrophic species (25.33%) occur at the base of the core at ~555 cal BP (38 cm) and at ~425 cal BP (32 cm) (Appendix 3, Figure 38). In relation to saprobity, the assemblage is dominated by a strong oligosaprobous signal due to the dominance of marine species. Furthermore, there is a decline in β-mesosaprobic species over time (from 20% in ~555 cal BP to 12.01% in ~340 cal BP) along with an increase in α-mesosaprobic species (from 1.67% to 7.34%) (Appendix 3, Figure 39).

The *Diploneis* aggregate (= *Diploneis bombus, D. crabro, D. interruptus*) dominates the assemblage reaching a maximum value of 56%, while *Diploneis elliptica* (Appendix 1, Figure 34O) averages at 18.94%. Marine-brackish, cold water *Cocconeis scutellum* (8.89% average) (Appendix 1, Figure 33K) is the third most dominant species in this zone. Although *C. scutellum* is described as one of the most frequently recorded diatom taxon on all substrates, including hydrophytes, fauna, and rocks (Car *et al.,* 2019), it is well-known for its prominence as an epiphyte, like *D. elliptica,* particularly on *Zostera marina* (Sieburth and Thomas, 1973; Ruocco *et al.,* 2019). The presence of *C. scutellum* is related to complexity in palaeoecological reconstructions owing to its ability to attach to macrophytes via its raphid valve (R-valve), however, after death the rapheless valve (P-valve) - which does not attach to macrophytes - may separate itself, thus enabling the transportation of P-valves across the whole tidal environment by daily tides (Sawai, 2001; Sawai *et al.*, 2004). Regardless, the fossil assemblage of core KNY19-G contains both R-valves and P-valves, hence *C. scutellum* is considered autochthonous in this assemblage. Epiphytic species, such as *Cocconeis placentula* (average relative abundance of 5.5%) and *Rhopalodia musculus* (3.72%) (Appendix 1, Figure 35CC), as well as tychoplanktonic *Dimeregramma minor* (4.17%) and planktonic/ epiphytic *Grammatophora oceanica* (3%) (Appendix 1, Figure 32C), are present in notable concentrations throughout the zone. Interestingly, *D. minor* declines and disappears after peaking (9%) at ~470 cal BP (34 cm) prior to re-emerging in the later phase of Zone KNY19-G-B2. This peak coincides with the first appearance of aerophilic, eutrophics *Navicula tenelloides* and *Eunotia minor,* while hypertrophic

Planothidium frequentissimum subsequently occurs once at ~430 cal BP (32 cm) alongside a maximum value of *C. placentula* (10.67%). *Navicula longa* and *Navicula lucens* (Appendix 1, Figures 34T and 34U) first appear towards the termination of the zone at ~340 cal BP (28 - 27 cm).

Zone KNY19-G-B: 26 - 5 cm; ~300 to ~-30 cal BP

Zone KNY19-G-B spanned 330 years and is divided into three subzones, *viz.* KNY19-G-B1 (~300 to ~200 cal BP), KNY19-G-B2 (~200 to ~ 0 cal BP), and KNY19-G-B3 (~ 0 to ~-30 cal BP).

Zone KNY19-G-B1: 26 - 21 cm; ~300 to ~200 cal BP

The next ~100 years are predominantly defined by a drastic decrease in marine species to an average relative abundance of 33.51% (Figure 23). This shift is accompanied by the establishment of a freshwater species community (>5%), which is an expression of high species richness instead of dominance by a few species. Additionally, there is an overall peak in brackish-fresh species (16%) at ~210 cal BP (22 cm). In relation to trophic status preferences, a noticeable proportion of hypertrophic species (3.07% average) enter the assemblage in this zone and mesotrophic species also make their first appearance (Appendix 3, Figure 38). This coincides with a growing preference for α-mesosaprobic (from an average of 2.95% in Zone KNY19-G-A to 14.5%) and polysaprobic (<1% to 4.68%) conditions due to the increasing presence of *Fallacia pygmaea* and *N. tenelloides* (Appendix 3, Figure 39).

The relative abundance of *D.* (agg) suddenly and drastically depreciated at the start of the zone from an average relative abundance of 37.89% to 7.67%, thereby shifting the dominance to epiphytic *D. elliptica, N. longa,* and eutrophic *Fallacia pygmaea* (Appendix 1, Figure 34R) - in total accounting for >30% of the biological community. Brackish-fresh species are well-represented in this zone, since *F. pygmaea* reaches a maximum average relative abundance of 8.84% and *Terpsinoë musica* achieves a maximum of 7.33% at the end of the zone at ~210 cal BP. The widely distributed aerophilic *N. tenelloides* - a species that is characteristic of shallow water basins, moistened surfaces, the moss substratum and liverworts - has a constant presence throughout the zone (Stroemer, 1963; Razjigaeva *et al.,* 2014b). The abundance of epiphytic and epipsammic marine sublittoral *C. costata* and *Giffenia cocconeiformis* (Appendix 1, Figure 33M) also increased in comparison to the former sone. Cold water *G. oceanica* contradicts the dominant warm water preferring species, it exhibits lower frequencies (0.67%) prior to disappearing. Meanwhile,

marine *A. helenensis* (Appendix 1, Figure 34Z) re-enters the assemblage in low concentration (0.67%) at the top of the zone after an absence of 215 years, while *Surirella fastuosa* var. *cuneata* (Appendix 1, Figure 35DD) and *D. elliptica* remain relatively constant. Again, it is worthwhile to note the once-off presence of hypereutrophic *P. frequentissimum* (0.67%) within the zone.

Zone KNY19-G-B2: 21 - 9 cm; ~200 to 0 cal BP

Zone KNY19-G-B2 spanned two centuries and is characterised by a dramatic decrease in marine species from 48.66% at the top of the zone at ~170 cal BP (20 cm) to 19.33% at the bottom of the zone at ~1950 CE (Figure 23). This low value of marine species is concurrent with the highest percentage of marine-brackish species (23%) in the core. The marine and freshwater components occur in approximately equal proportions, as marine species account for an average of 34.55% of the biological community, while fresh and fresh-brackish species combined comprise 32.99%. Pertaining to the classification of species according to their trophic status, the zone is further defined by a rise in the proportion of eutrophic species over time to the extent that eutrophic species occupy more than half (52.32%) of the assemblage at ~0 cal BP (Appendix 3, Figure 38). Moreover, this period also features a peak (21.33%) in α-mesosaprobic species (Appendix 3, Figure 39). At ~125 cal BP (18 cm), eutrophic species comprise 42.32%, which coincides with the highest value of polysaprobic (9.67%) and hypereutrophic (4%) species in the zone. Oligotrophic species reached their highest value (34.64%) in the entire core at 85 cal BP (16 cm).

N. longa (average relative abundance of 11.5%), *D. elliptica* (10.11%), *C. scutellum* (7.22%), and *G. cocconeiformis* (7.56%) are the main constituents of Zone KNY19-G-B2. Sublittoral, epiphytic *S. fastuosa* var. *cuneata* is common on tidal flats and persists throughout the zone, peaking (6%) at 51 cal BP (14 - 13 cm) (Sawai and Nagumo, 2003; Beltrones and Fuerte, 2006; Razjigaeva *et al.,* 2014). This peak in *S. fastuosa* var. *cuneata* corresponds with the reappearance of epipsammic *D. minor,* which also survives well in turbulent waters with active mixing of the water column (Vos and De Wolf, 1993; Pereira *et al.,* 2010; Matos *et al.,* 2011). Regarding trophic status, the strong oligotrophic signal is a result of an increase in *Eunotia incisa* (8%), *Tabellaria flocculosa* (3.33%), *Eunotia minor* (3%), and *Frustulia crassinervia* (4%) (Appendix 1, Figures 32E and 34Q) - most of which reached their highest relative abundances in this zone at ~85 cal BP or 1865 CE (16 cm). Both eutrophic *C. placentula* and *C. scutellum* occur in greater concentrations compared to Zone KNY19-G-B1, where sublittoral *C. scutellum* peaks at 14.33% at the top of the zone. At the commencement of the zone, eutrophic *F. pygmaea* exhibited lower frequencies

compared to the previous zone, however, the nutrient tolerant species reached its highest relative abundance (12%) at the top of the zone. Likewise, the re-emergence of *P. frequentissimum* at ~50 cal BP or ~1900 CE (14 cm) is also noteworthy.

Zone KNY19-G-B3: 9 - 5 cm; ~0 to ~-30 cal BP (~1950 to ~1980 CE)

Zone KNY19-G-B3 is a brief 30-year period distinguished by the strong influence of freshwater and fresh-brackish species as opposed to marine and marine-brackish species (30.31%), as well as an ever-growing eutrophic (41.65%) and polysaprobic (12.49%) component (Figure 23, Appendix 3, Figures 38 and 39).

The zone is dominated by a variety of species that occur in small quantities, *viz.* fresh-brackish, pollution-tolerant *N. tenelloides* (average relative abundance of 7.83%), fresh *E. incisa* (6.17%), marine *C. costata* (6.17%), fresh-brackish *E. minor* (6%), and marine *N. longa* (5.83%). Acidophilic *E. incisa* (10.33%)*, Eunotia pectinalis* var. *undulata* (5.33%) (Appendix 1, Figure 32D)*,* and *E. minor* (7.67%) all obtain their highest relative abundance at the top of the zone at ~-25 cal BP or ~1975 CE (6 cm). Epipsammic *D.* (agg), *D. minor,* and *N. lucens* all make their final appearance in the zone, while epiphytic *G. cocconeiformis* and *N. longa* are present in markedly lower concentrations in contrast to zone KNY19-G-B2. Dominant *N. tenelloides* and *E. minor* contribute towards the increasingly eutrophic conditions, while pollution tolerant *Nitzschia supralitorea* makes a first appearance at the bottom of the zone at ~-10 cal BP or ~1960 CE (8 cm).

Zone KNY19-G-C: 5 - 0 cm; ~-30 cal BP to Present (~1980 CE to Present)

The final zone is characterised by fresh-brackish, eutrophic, and polysaprobic taxa. At 13.66%, the lowest average relative abundance of marine species was recorded in KNY19-G-C, whereas fresh-brackish species account for more than half (52.87%) of the assemblage (Figure 25). On the whole, eutrophic species peak (65.64%) at the top of the zone in ~2015 CE (1 cm), while hypereutrophic species also obtain their highest concentrations (8%) in the core at the bottom of the zone in 1990 CE (4 cm) (Appendix 3, Figure 38). Consequently, oligotrophic species reach their lowest concentration in KNY19-G within this zone at approximately 12%. Prior to Zone KNY19-G-C, polysaprobic species comprised an average of 4.1% of the entire biological community, after which polysaprobic taxa increased to 36.55%. α-mesosaprobic species also peak (14%) in the most recent zone of the assemblage (Appendix 3, Figure 39).

N. tenelloides constitutes more than a third of the assemblage (33.11%), thereby dominating the zone, whereas *N. supralitorea* and *G. cocconeiformis* are sub-dominant. After occurring in trace amounts for the last three centuries, thermophilic *Rhopalodia musculus* (Appendix 1, Figure 35 CC) increased in abundance to an average of 6.33%. Furthermore, *Gyrosigma obtusatum* (Appendix 1, Figure 33N) also increased in prevalence, reaching its highest value at 6% in 1990 CE (4 cm), whereas *C. placentula, C. scutellum,* and *C. costata* decreased in abundance.

5.2.4. Statistical Analyses

5.2.4.1. Principal Component Analysis (PCA)

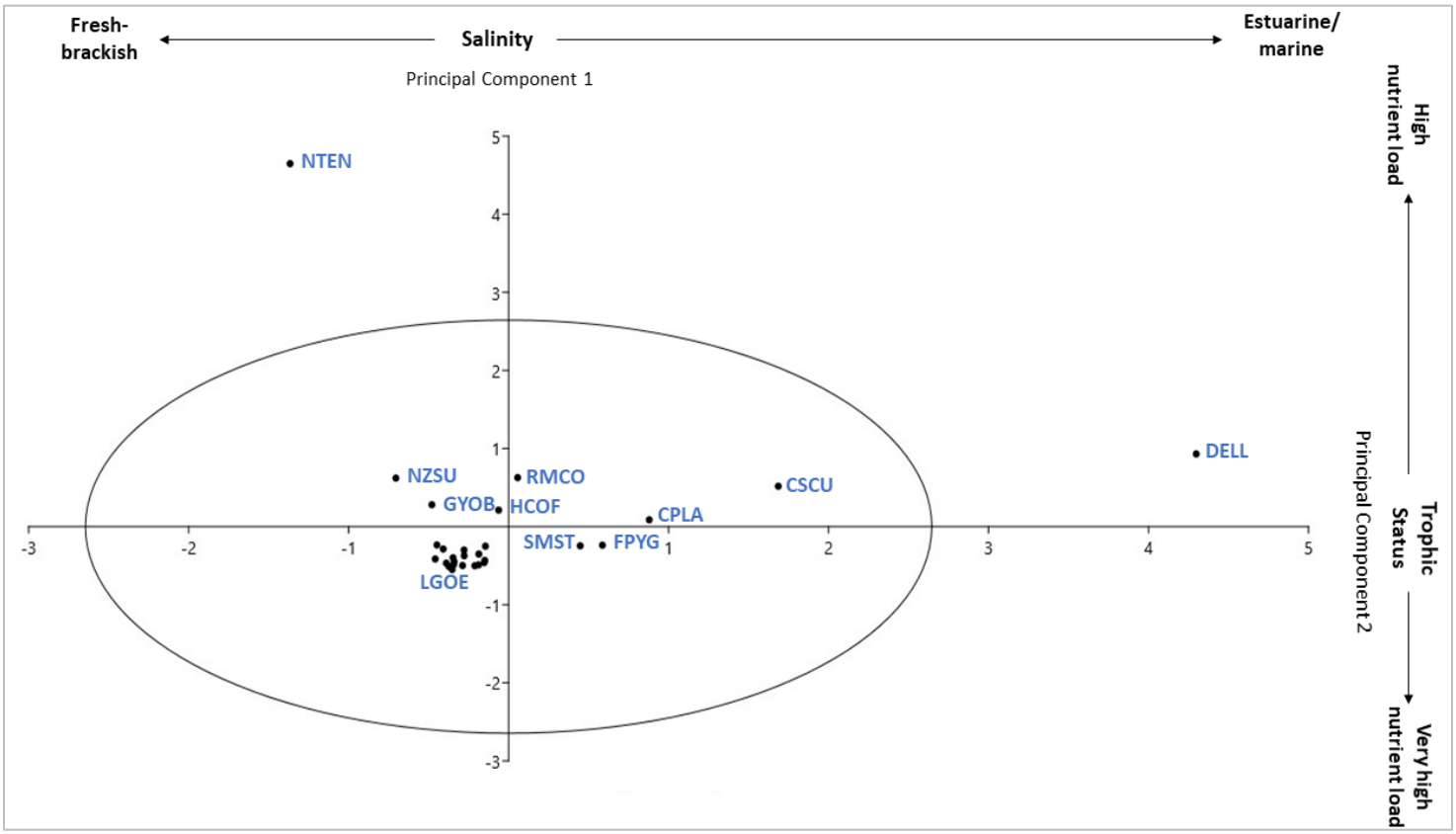

Figure 24. Principal component analysis illustrating the main environmental variables impacting the system at KNY19-G.

Initially, PCA was conducted on the entire species list of KNY19-G. Similar to conditions at KNY19-B, the high prevalence of marine species obscured the interpretation of the results and these taxa were therefore eliminated from the analysis, along with the 2% of rare species. A subsequent PCA (Figure 24) containing 28 out of the original 109 species was used to determine the principal species behind the

environmental conditions at KNY19-G. Ultimately, 86.18% of the total variance is explained by the first two principal components (Table 8), whereas the remaining 17 components were deemed insignificant. Furthermore, Table 8 illustrates that PC1 and PC2 have significantly larger eigenvalues than the remaining components.

Table 8. PCA results indicating the first four and the last principal components of KNY19-G, as well as the eigenvalues and variance, explained by each.

Principal Component (PC)	**1**	**2**	**3**	**4**	**...**	**19**
Eigenvalue	1344.35	1096.34	137.56	84.51	...	0.09
Variance (%)	47.36	38.62	4.85	2.98	...	0.00

PC1 accounts for 47.36% of the variability in KNY19-G's diatom assemblage. *Diploneis elliptica* has the highest significant positive loading along this axis, whereas *Cocconeis scutellum* is noticeably less positive, as illustrated by Figures 24 and 25. The largest negative loading is associated with *N. tenelloides*, and to a lesser extent, *Nitzschia supralitorea*.

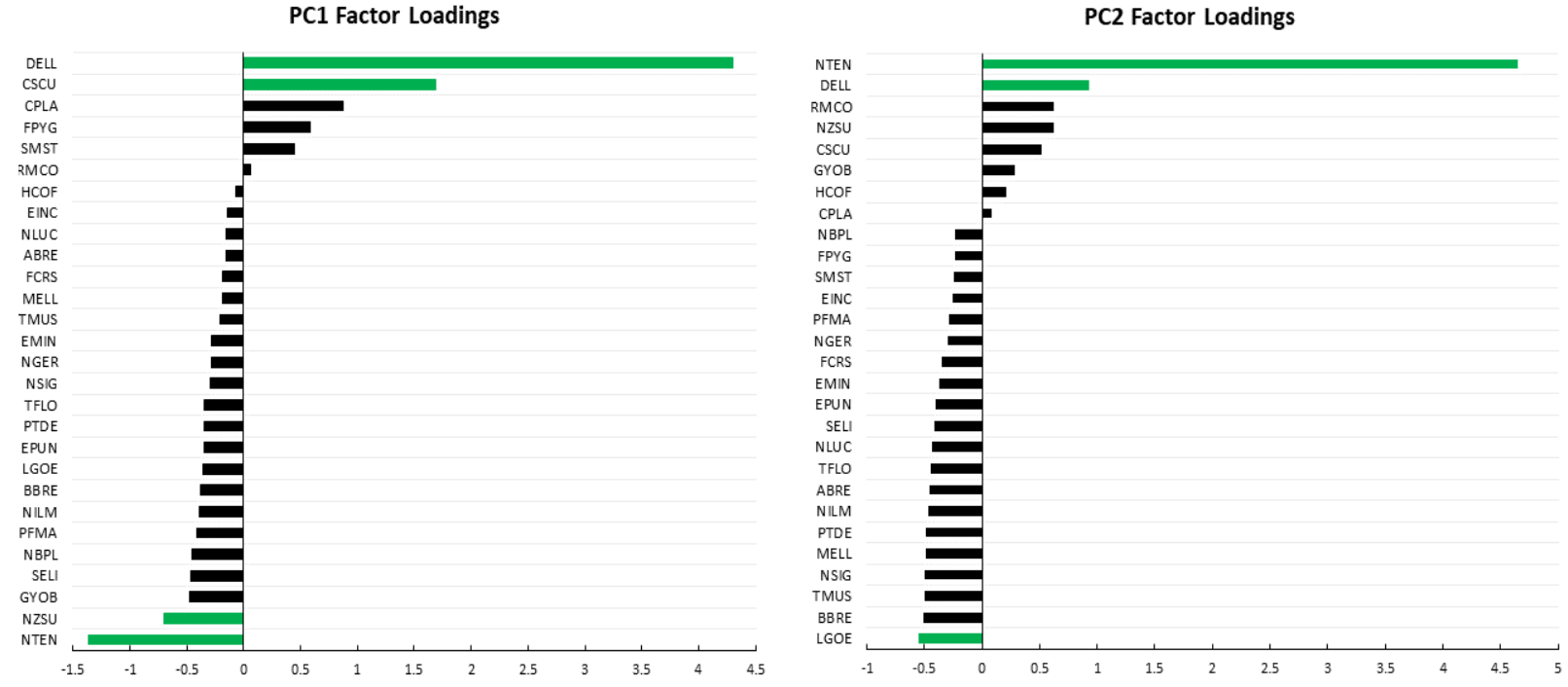

Figure 25. Factor loadings for the first two principal components at KNY19-G. Significant loadings are indicated in green. ABRE = *Achnanthes brevipes*; HCOF = *Halamphora coffeaeformis*; BBRE = *Brachysira brebissonii*; CPLA = *Cocconeis placentula*; CSCU = *Cocconeis scutellum*; DELL = *Diploneis elliptica*; EINC =

Eunotia incisa; EMIN = *Eunotia minor*; EPUN = *Eunotia pectinalis var. undulata*; FCRS = *Frustulia crassinervia*; FPYG = *Fallacia pygmaea*; GYOB = *Gyrosigma obtusatum*; LGOE = *Luticola goeppertiana*; MELL = *Mastogloia elliptica*; NBPL = *Navicymbula pusilla*; NGER = *Navicula germainii;* NILM = *Nitzschia liebertruthii;* NLUC = *Navicula lucens*; NSIG = *Nitzschia sigma*; NTEN = *Navicula tenelloides*; NZSU = *Nitzschia supralitorea*; PFMA = *Planothidium frequentissimum*; PTDE = *Planothidium delicatulum*; RMCO = *Rhopalodia musculus*; SELI = *Staurosira elliptica*; SMST = *Seminavis strigosa*; TFLO = *Tabellaria flocculosa*; TMUS = *Terpsinoë musica*

In relation to the most positively loaded species, *D. elliptica* is a cosmopolitan species that commonly occurs as marine phytoplankton (Taylor *et al.*, 2007; Hendrarto and Nitisuparjo, 2011), while *C. scutellum* is mainly an estuarine species found across the entire tidal zone, however, as an epiphyte, its preferred habitat is macrophytes (Sawaii, 2011; Tsoy *et al.,* 2015; Yuce 2017; Hafner *et al.,* 2018). With regards to the negatively loaded species, both *N. tenelloides* and *N. supralitorea* are fresh-brackish species (Taylor *et al.*, 2007). As a result, the high positive scores are indicative of elevated salinity levels, while the negative factor loadings illustrative lower salinity levels. Therefore, comparable to KNY19-B, PC1 can be interpreted as an expression of salinity.

PC2 explains less variation (38.62%) variation in KNY19-G's diatom assemblage than PC1 (Table 8). *N. tenelloides* clearly has the highest positive factor loading, while *D. elliptica* is considerably less positive (Figures 24 and 25). Pertaining to the negative loadings, various species, such as *Brachysira brebissonii*, *Nitzschia sigma*, *Terpsinoë musica*, and *Mastogloia elliptica*, have negative loadings on this axis. Although, despite the accumulation, *Luticola goeppertiana* has a marginally lower negative score.

As previously mentioned, *N. tenelloides* is a polytrophic, polysaprobic species tolerant of extremely polluted conditions (Van Dam *et al.*, 1994; Taylor *et al.*, 2007). Similar to *N. tenelloides*, *L. goeppertiana* is also classified as polysaprobic - the difference between the two species being *L. goeppertiana*'s tolerance of hypertrophic environments (Van Dam *et al.*, 1994). Additionally, *L. goeppertiana* is indicative of low concentrations of dissolved oxygen and waters with greater anthropogenic impact (Schneck *et al.,* 2007; Bere and Tundisi, 2011). Ultimately, high positive factor loadings are associated with polytrophic species, while negative loadings are linked to hypertrophy. Consequently, PC2 may represent the influence of nutrient concentration on the species composition of KNY19-G, indicating natural nutrient fluctuation and land use change.

5.2.4.2. Shannon-Wiener Species Diversity and Evenness

The mean Shannon-Wiener diversity index at KNY19-G is high (3.99) (Figure 26). KNY19-G has a wide range in diversity (2.44 to 5.14) where the highest diversity value occurred at ~-10 cal BP (8 cm) and the lowest value at ~385 cal BP (30 cm). There appears to be a gradual increase in diatom community diversity with time with a distinguishable decrease from the peak until the present day (~-65 cal BP, 1 cm). The dominance of *N. tenelloides* from ~-10 (8 cm) to ~-65 cal BP (1 cm) resulted in said diversity loss, as well as a decrease in evenness. Evenness averaged at 0.77 and peaked at two points, namely ~-10 and ~125 cal BP (0.87) (8 and 18 cm) (Figure 26). The lowest evenness score (0.6) coincides with the lowest diversity score at ~385 cal BP. Diversity and evenness fluctuate together throughout the core with one exception at ~515 cal BP (36 cm) where evenness increases while diversity decreases as a result of a decline in diatom species richness.

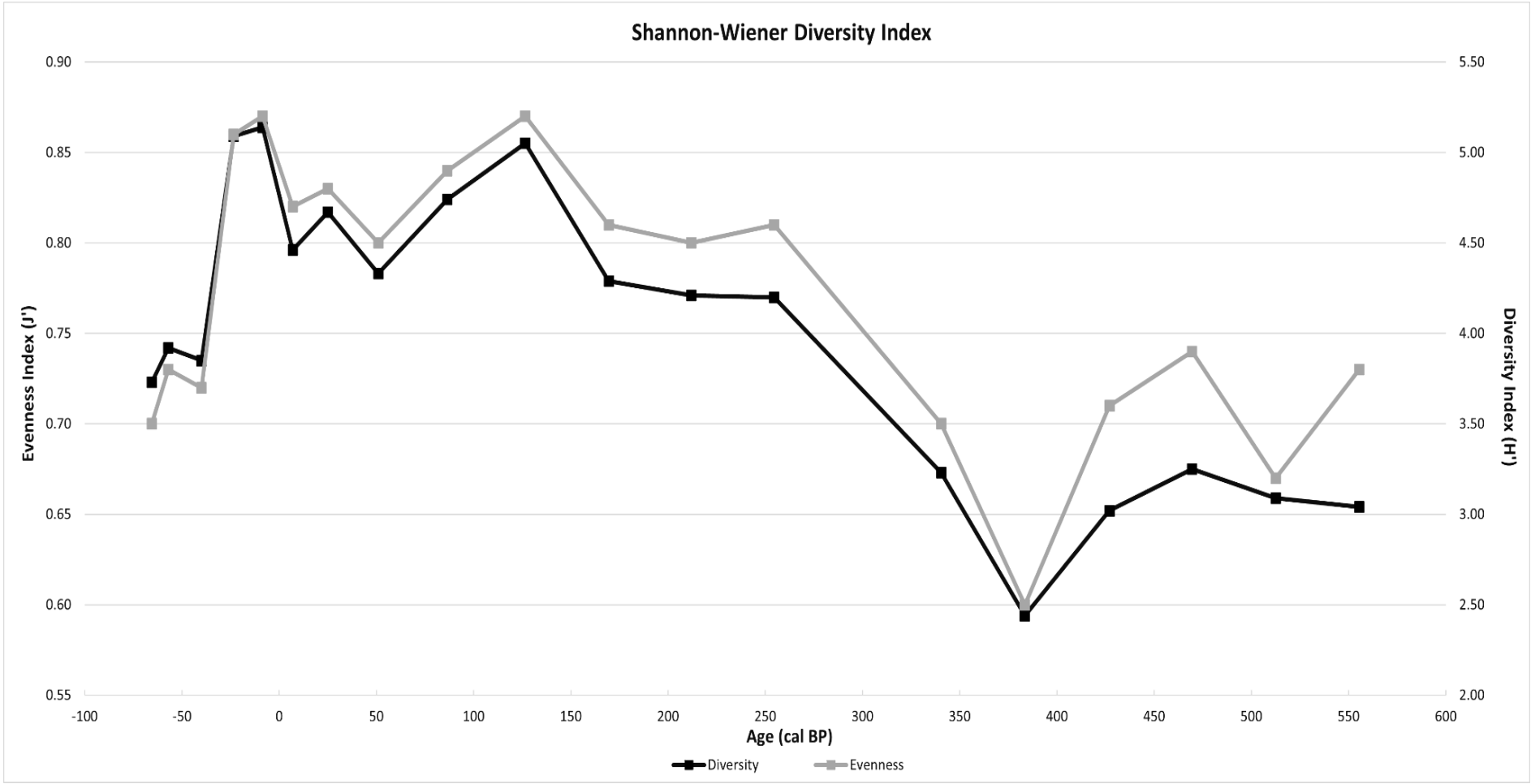

Figure 26. Shannon-Wiener Diversity and Evenness Index of KNY19-G.

5.2.5. Trophic Diatom Index (TDI)

The Trophic Diatom Index values ranges from 11.8% to 64% (Figure 27) and the percentages of taxa tolerant to organic pollution (%PTV) were all below 20% (Table 9). It is apparent that the TDI values have increased over time, thereby indicating that over time the trophic status has shifted from oligotrophic to mesotrophic and meso-eutrophic. TDI values are low (ranging from 11.8% to 19.5%) from ~555 to ~340 cal BP (38 - 27 cm), indicating oligotrophic conditions. The shift to oligo-mesotrophic values occurs at ~255 cal BP or ~1695 CE (24 cm) after which TDI values for the entire core are predominantly indicative of mesotrophic conditions, although there were instances at ~125 (18 cm), ~85 (16 cm), ~-8.5 (8 cm), and ~-23.5 cal BP (6 cm) when the TDI values reverted back to oligo-mesotrophic status. The TDI values peaks at 64% at ~-40 cal BP or ~1990 CE (3 cm), representing the first and only occurrence of meso-eutrophic conditions at KNY19-G. In relation to the %PTV, the low values (<20%) (Table 9) signal that all samples are free of significant organic pollution. It is clear that the most recent %PTV% (11.9%, 10.8%, and 10.4%) are higher than their predecessors.

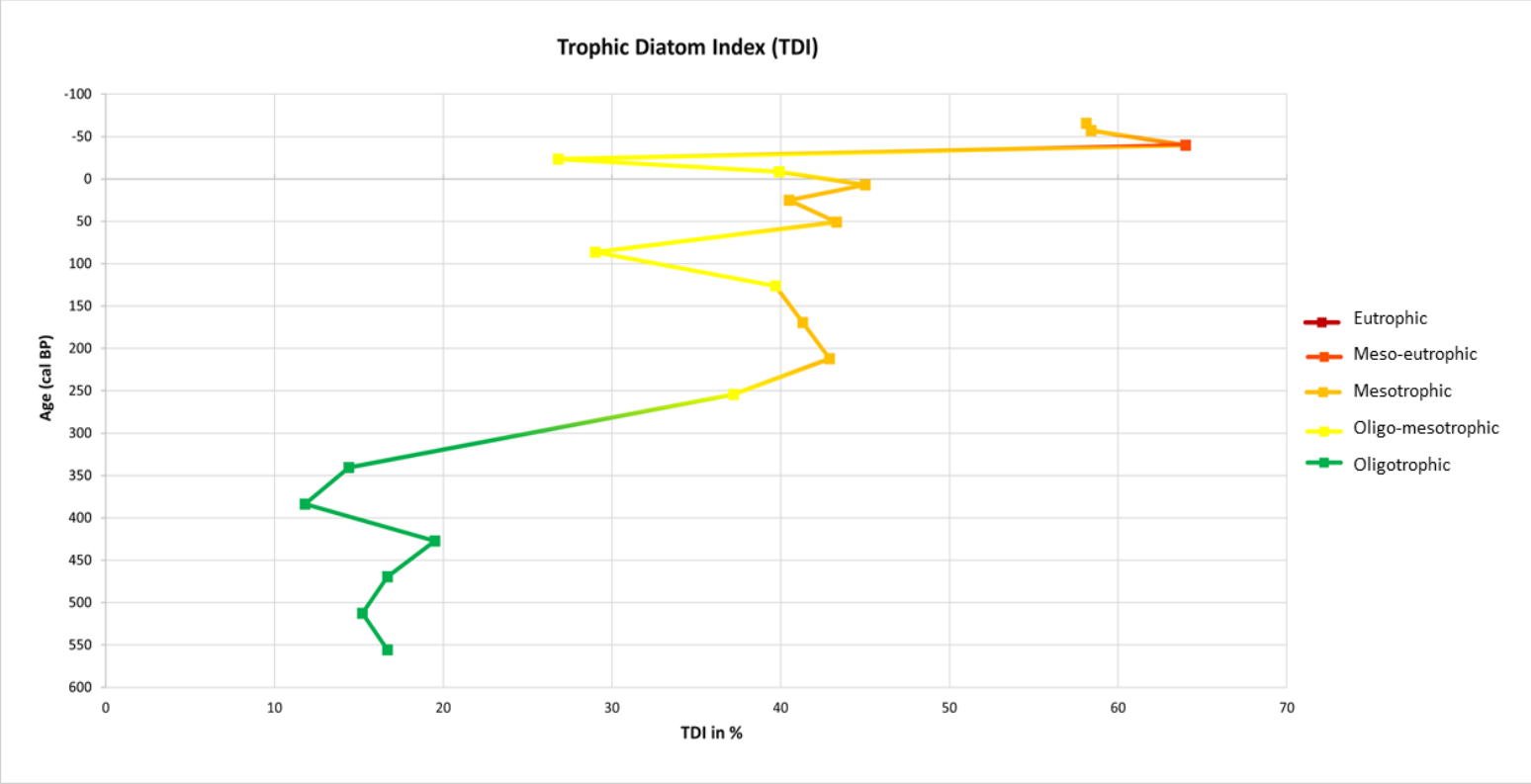

Figure 27. Trophic Diatom Index of KNY19-G.

Table 9. Percentage pollution tolerant values for samples in KNY19-G.

Age (cal BP)	-65.5	-57	-40	-23.5	-8.5	7	25	51	86.5	126.5
%PTV	11.9	10.8	10.4	3.4	4.1	2	4.7	4.5	4.9	4.4

Age (cal BP)	169.5	212	254.5	340.5	383.5	427	469.5	512.5	555.5
%PTV	2.4	5.1	3.4	2	1.3	0	0.3	0.7	0

5.3. INTER-CORE COMPARISON

It is possible to compare the data between the two cores, as well as between samples and indices, since the same numbers of diatom frustules were counted on each slide. Consequently, KNY19-B (representative of marine influence in the lower reaches) and KNY19-G (illustrative of fluvial influence in the middle reaches) are compared with regards to their diatom assemblage zones, statistical analyses, and Trophic Diatom Index scores.

5.3.1. Texture

Both cores predominantly consist of silt, followed by sand and clay. KNY19-B experiences an increase in the amount of silt (in favour of sand) towards the top of the core, whereas the opposite is seen at KNY19-G. The percentage of sand fluctuates gradually in both cores, with an exception at KNY19-B when a sand intrusion occurs in the basal half of the core. From roughly 15 cm onwards, the gradual changes in the percentage of sand give way to a rapid fluctuation in both cores. Specifically, the middle reaches experience a rapid increase in the percentage of sand, whereas the lower reaches are characterised by a decrease in the percentage of sand along with major fluctuations.

5.3.2. Diatom Assemblage Zones

Despite the KNY19-B diatom assemblage having a lower species richness (75 species) compared to KNY19-G (109 species), a more substantial proportion (30%) of the community is classified as common, whereas

only 23.8% of KNY19-G's assemblage exhibit an abundance exceeding 3%. Both assemblages share common marine, marine-brackish, and fresh-brackish species. Prior to roughly 250 cal BP, marine *D.* (agg) is the most prominent species shared between both cores, after which *C. costata* occurs in both records. Marine-brackish *C. scutellum* is also present in both assemblages, albeit to a lesser degree in KNY19-B, while fresh-brackish *N. tenelloides* is common towards the surface of both sites.

At approximately ~200 cal BP, the first two zones of both cores terminate. At this point, an overwhelmingly marine component subsides at both sites and gives way to an increasingly dilute composition. Although the remaining three zones differ somewhat in their timing, they have similar trends. For example, fluctuating freshwater assemblages are common from ~1950 CE for KNY19-B and ~1865 CE for KNY19-G. ~1950 CE marks a major shift towards eutrophic and polysaprobic species at both sites, whereas KNY19-G's shift towards a rapidly changing species composition (final zone) predates KNY19-B by two decades.

5.3.3. Statistical Analyses

5.3.3.1. Principal Component Analysis

Both KNY19-B and KNY19-G had positive and negative species loadings on Principal Component 1 consistent with an expression of salinity. Similarly, species loadings on Principal Component 2 were indicative of nutrient concentrations at both sites. As a result, salinity and nutrient concentration are the main structuring variables in both the marine-dominated and riverine-influenced regions of the estuary.

5.3.3.2. Shannon-Wiener Diversity Index and Evenness

Based on the diversity scores, KNY19-G (3.99) is more diverse compared to KNY19-B (2.98). There is a slightly more even spread of diatom populations at KNY19-G than KNY19-B as confirmed by the evenness index scores where KNY19-G scored 0.77 (on a scale of 0 to 1) and KNY19-B scored 0.71. It appears as though both cores illustrate an overall increase in diversity over time, however, there is a notable difference between KNY19-B and KNY19-G's diversity index in relation to the three most recent samples. There is a distinct increase in diversity at KNY19-B, while the opposite is true for KNY19-G.

5.3.4. Trophic Diatom Index (TDI)

Both KNY19-B and KNY19-G illustrate that the TDI values have increased in the Knysna Estuary over time, although the results are more pronounced at KNY19-B, as there are more instances of meso-eutrophic and eutrophic conditions. In addition, both cores have percentage pollution tolerant values (%PTV) below 20%. The three most recent samples, equating to approximately the last 20 years, in each core have a significantly higher value compared to their precursors, thereby possibly demonstrating an increase in the amount of organic pollution in the estuary.

5.4. CONCLUSIONS

This chapter presents the results of Core KNY19-B and Core KNY19-G spanning the historically recent period of approximately ~610 to ~-70 cal BP and approximately ~555 to ~-65 cal BP, respectively. Autoecological and statistical parameters indicate that both cores initially experienced stable conditions consisting of marine, oligotrophic, and oligosaprobic to β-mesosaprobic conditions. However, the species composition drastically shifted over the last 150 years to include an increasingly fresh, fresh-brackish, and brackish-fresh population with preferences for eutrophic and polysaprobic conditions. The results are discussed in more detail in the following chapter.

CHAPTER 6 - DISCUSSION

The fossil diatom record of cores KNY19-B and KNY19-G's spans the historically recent past, specifically the pre-colonial, colonial, and contemporary periods. Chapter 6 interprets the results of changing diatom community structure with the aim of exploring historically recent changes in the Knysna Estuary. The chapter commences with a description of the Knysna Estuary's development in response to climatic and anthropogenic influence, followed by an explanation of the drivers of the environmental change. In particular, the diatom assemblage provides inferences about the environmental conditions of the estuary prior to human occupation (Phase 1), and during the colonial period (Phase 2), aids the establishment of pre-intensive anthropogenic physical, chemical, and biological baselines, and offers reference conditions beyond what is provided by current historical records, which are often difficult to obtain or incomplete (Watson *et al.,* 2011). Moreover, analysis of the diatom record offers insights into environmental change - be it natural variability or anthropogenically-induced - such as land use change and industrial pollution, on the Knysna Estuary (Starratt, 2007; Bellinger and Sigee, 2015; Lemley *et al.,* 2016; Ryabushko *et al.*, 2017). Lastly, the chapter explores the structural variables that influence the diatom assemblage, as well as the relationship between diversity and trophic status.

It is valuable to use the diatom record to explore the historically recent changes in the Knysna Estuary, as a multi-century perspective can ultimately inform conservation goals that include ecological, environmental, and economic sustainability due to the incorporation of ecosystem dynamics and tipping points (Gillson and Marchant, 2014). This is particularly important considering that the estuary is ranked as the most important estuary in the country in terms of its socio-economic importance and high biodiversity (Marker, 2003; Adams *et al.,* 2020). Despite its protected status, the estuary is threatened by anthropogenic activities, including urban expansion, tourism development, and land use change (Marker and Holmer, 2005; CES, 2007). Therefore, it is imperative to study the extent of the environmental change in the estuary in order to provide management authorities with a baseline or reference of aquatic conditions prior to anthropogenic influence. This can inform mitigation targets and can assist management's decision-making regarding restoration and rehabilitation to prevent the emergence of diminished aesthetic value, human illness, and economic loss (McGuirk and Flynn, 2008).

6.1. ESTUARINE PHASES

6.1.1. Phase 1 - Pre-colonial Lagoon: ~610 to ~200 cal BP

6.1.1.1. General Estuarine Conditions

The dominance of *Diploneis* aggregate (= *Diploneis bombus, D. crabro, D. interruptus*) and benthic species suggests shallow water levels with the possibility of recurrent desiccation events leading to the exposure of the tidal flats across the estuary as a whole. The habitat requirements of *D.* (agg) allude to a predominantly warm water, marine, and oligotrophic environment, which may experience subaerial exposure and an extensive supralittoral zone, tidal channels, and estuarine conditions under salt-wedge influence (Vos and De Wolf, 1988; Long and Tooley, 1995; Espinosa *et al.*, 2006; Cressey *et al.,* 2010; Zalat and Al-Wosabi, 2011; Espinosa and Isla, 2015; Gomes *et al.,* 2017). These trends suggest that intertidal environmental conditions were established by ~610 cal BP at both the lower (KNY19-B) and upper estuary (KNY19-G). The presence of marine *D.* (agg) and *Dimeregramma minor* at both sites suggests that strong marine inflow gives rise to higher salinity levels, thereby enabling the expansion of the lagoon regime (or marine environment). The composition and diversity within the marine diatom assemblage suggest they were deposited *in situ* likely surviving in the higher salinity as a result of the inflow of saline marine waters. During this phase, Thesen Island presumably resembled a very low sandbar that was largely inundated with water during spring tides, seeing that this period predates the anthropogenically-induced infilling of the island that occurred during the 1900s (Hart and Halkett, 1998). For this reason, there were also no infrastructural obstructions in the estuary. As a result, there was more through flow in the estuary, hence accounting for the high salinity values in the middle reaches of the estuary (KNY19-G) during this phase. Low freshwater inflow, as illustrated by the low percentage of freshwater species at KNY19-G from ~550 to ~250 cal BP in Figure 23, would have further enabled the expansion of the lagoon regime into the upper reaches of the estuary. This is in line with contemporary flow dynamics, which are mostly dominated by marine inflow, particularly during periods where freshwater flows from storm events and rainfall are insufficient to extend the estuary regime (Largier *et al.,* 2000).

Turbulent waters and an active mixing of the water column define Phase 1 - an ideal habitat for *D. minor* - as the species' cells are surrounded by a thick mucilage coating, thus aiding the survival of the species

during periods of high hydrodynamics (Pereira *et al.,* 2010; Matos *et al.,* 2011; Costa *et al.,* 2013). Furthermore, tidal influence in the lower estuary is evident in the abundance of allochthonous *Paralia sulcata* in the Ashmead Channel between ~610 to ~200 cal BP (Figure 16), as the species introduced through strong velocity inflow under tidal dynamics (Sato *et al.,* 1998; Sawai and Nagumo, 2003; Kirsten *et al.,* 2020). *P. sulcata* is deemed allochthonous because it is likely that this cold-water diatom was introduced into the warmer estuary (indicated by the presence of the warm-water *D.* (agg)) by the tides. High flow rates are also experienced in the upper estuary, although these flow rates are associated with riverine inputs. This is supported by the existence of the fresh-brackish, epiphyte *Cocconeis placentula,* which prefers medium to high over low current velocities, mostly as a result of their reduced cell size and strong surface attachment abilities (Zalat, 2000; Plenković-Moraj *et al.,* 2008; Holmes and Taylor 2015). The occurrence of *C. placentula* corroborates the environmental conditions inferred by *D.* (agg), by reason that both species reflect shallowing and the presence of salt marsh fringes (Sato *et al.,* 1998; Espinosa *et al.,* 2006).

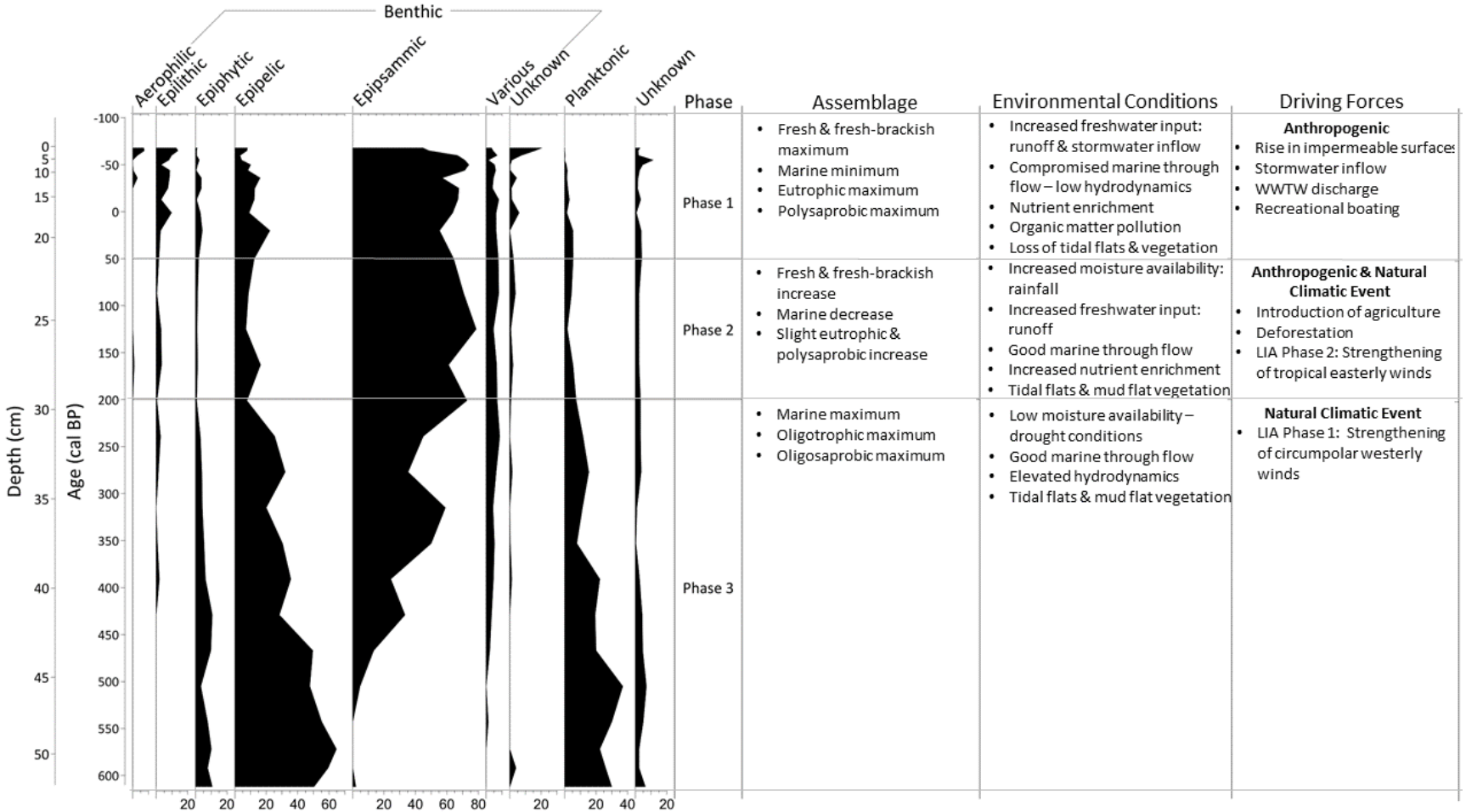

Figure 28. Summary classification of diatoms in KNY19-B based on habitat preferences, in addition to the main assemblage characteristics, inferred environmental conditions, and the driving forces responsible for the discernible environmental change.

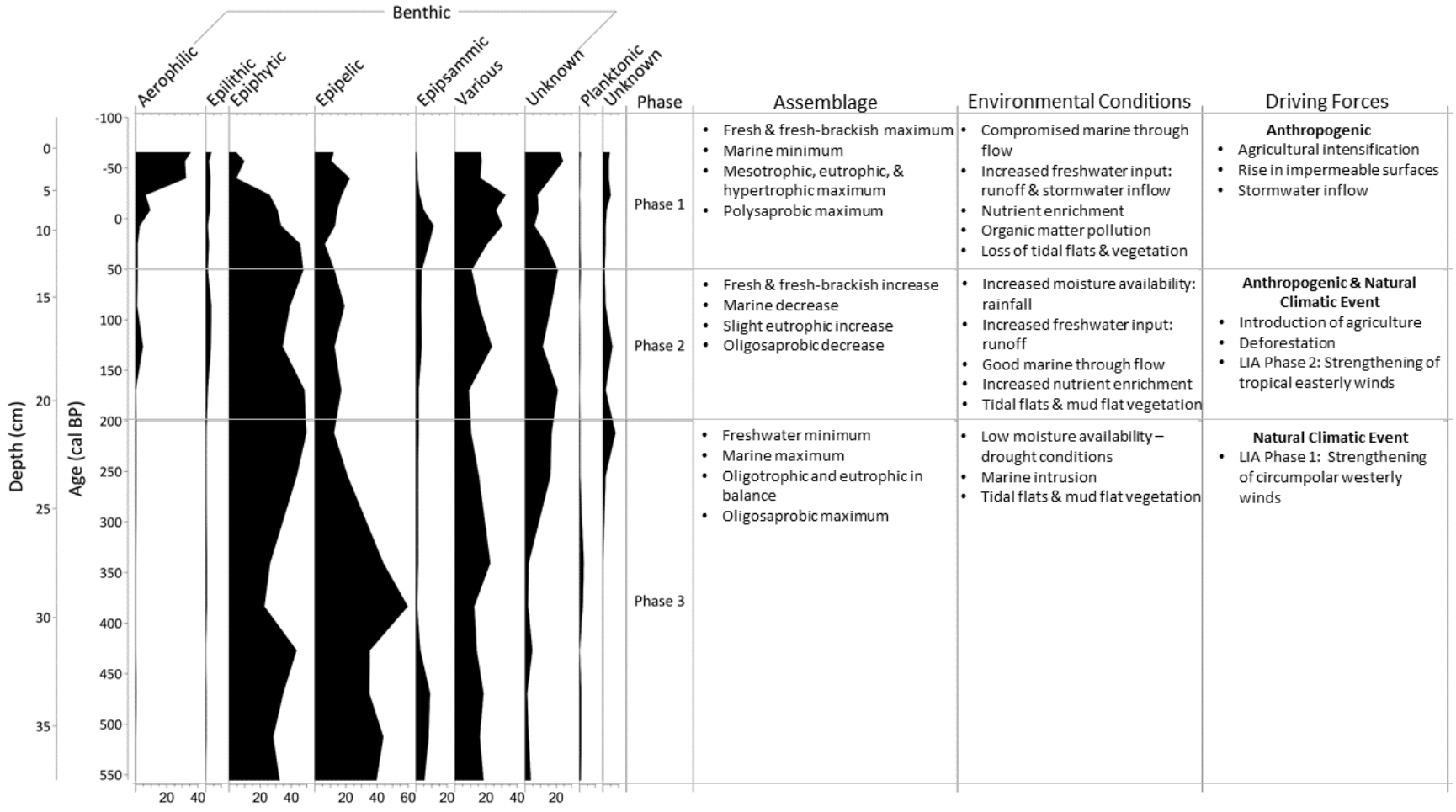

Figure 29. Summary classification of diatoms in KNY19-G based on habitat preferences, in addition to the main assemblage characteristics, inferred environmental conditions, and the driving forces responsible for the discernible environmental change

6.1.1.2. The Ashmead Channel (KNY19-B)

Localised conditions in the Ashmead Channel supported a high biomass and plant material from ~610 to ~470 cal BP in sublittoral estuarine conditions typical of tidal flat and salt marsh environments in near-shore areas. These environmental conditions are consistent with the preferences of epipelic species (Figure 28), such as *D.* (agg) and *Pinnularia yarrensis,* as they secrete a sediment-stabilising extracellular polymeric substance ideal for vegetation growth (Korotky *et al.,* 1999; Méléder *et al.,* 2007; Tsoy *et al.,* 2015; Chiba *et al.,* 2016; Sitoe *et al.,* 2017). As a result, the initial period of KNY19-B's record can be described by shallow waters, sand or tidal flats, and the presence of some macrophytes (Sawai *et al.,* 2001; Katsuki *et al.,* 2012; Chiba *et al.,* 2016; Weilhoefer *et al.*, 2021). This sandy habitat is ideal for the epipsammic species, namely *Catenula adhaerens* and *Plagiogramma* cf. *staurophorum,* which are abundant until ~2005 CE (Figure 28) (Vos and de Wolf, 1988; Sawai *et al.,* 2016; Zalat *et al.,* 2021). The high biomass and presence of aquatic vegetation are counterintuitive to the results of the relative percentage diagrams (Figure 16) and Trophic Diatom Index (TDI) values (Figure 20), which indicate low nutrient conditions and an absence of epiphytic species. Again, it must be noted that the TDI and relative percentage diagrams could be obscured by the overwhelming representation of marine species in the lower reaches during this period, thereby obscuring the actual trophic status. Additionally, wetter conditions occurred during this earlier stage at ~590 cal BP, which predates KNY19-G's recovered depositional period, since the once-off occurrence of fresh-brackish *Achnanthidium biasolettinum* points to increased freshwater inflow from the Bongani River or streams surrounding the Ashmead Channel. Subsequently, the lack of freshwater species indicates that drier environmental conditions persisted until ~250 cal BP. The initial period of this phase of the estuary's development could coincide with somewhat lower hydrodynamic stress as epipelic diatoms tend to increase as sediment grain size decreases, as seen in Figures 15 and 28 (Azovsky *et al.,* 2020). However, the notable presence of allochthonous *P. sulcata* illustrates that lower hydrodynamic stress was minimal, in that the tidal influence remained strong.

The Ashmead Channel is typified by high hydrodynamics in a high-disturbance environment due to the active mixing of the water column resulting from incessant sediment disturbance resulting from tidal action from ~470 cal BP throughout the majority of the record. This is demonstrated by a shift from an epipelic to epipsammic assemblage after ~470 cal BP, as epipsammic species are influenced by high hydrodynamics (Figure 28) (Méléder *et al.,* 2007; Ribeiro *et al.,* 2013; Ubertini *et al.,* 2015; Azovsky *et al.,* 2020). This is due to the fact that epipsammic species attach to the surface of sand grains and are resilient to the incessant and energetic sediment disturbance in the form of burial and

resurfacing of sand grains owing to wave action (Moss, 1977; Scholz and Liebezeit, 2012; Ribeiro *et al.* 2013). This transition from epipelic to coarse-grained sediment preferring epipsammic diatom species is also visible in Figure 15 as a shift from finer-grained sediment towards coarser-grained sediment from ~420 cal BP. This high energy environment is unsurprising, considering that tidal height fluctuations within the lower reaches are usually comparable to that of the ocean and would extend further with the absence of a raised Thesen Island (Whitfield, 1992; Largier *et al.,* 2000; Marker, 2003).

6.1.1.3. The Middle Reaches (KNY19-G)

The middle reaches experienced a weak riverine influence potentially associated with drier conditions from ~550 cal BP until ~250 cal BP. This is substantiated by the low relative percentage of freshwater species at KNY19-G in combination with a dominant marine assemblage (Figure 23), therefore demonstrating strong marine inflow in the middle reaches of the estuary, particularly until ~300 cal BP. Again, contemporary studies have shown that the marine component extends into the upper reaches of the estuary during droughts (Largier *et al.,* 2000). The low flow conditions are accompanied by warm, shallow waters with macrophyte growth and the active mixing of the water column, as indicated by the combination of *D.* (agg) and epiphytic species, such as *Diploneis elliptica* and *C. placentula,* where the presence of *D. elliptica* is very common in estuaries and coastal zones across the globe (Economou-Amilli, 1980; Vos and De Wolf, 1993; Korotky *et al.,* 1997; Tsoy *et al.,* 2015; Hendrarto and Nitisuparjo, 2011; Gomes *et al.,* 2017; Razjigaeva *et al.,* 2020). Generally, it appears as though the latter part of this phase is characterised by the early onset of slightly wetter conditions, as the relative abundance of marine species decreases to give way to the gradual appearance of freshwater species, such as acidophilic *Eunotia* diatom taxa and *Frustulia crassinervia,* specifically at KNY19-G from ~260 cal BP onwards (Figure 23). However, it must be noted that the latter stage of this period relied on only a few samples, therefore it is challenging to discuss this period with certainty.

Eutrophic and oligotrophic species occur in near-similar proportions in the middle reaches (Appendix 3, Figure 38). Essentially, a combination of marine inflow, riverine input, and natural processes could explain the presence of a contrasting nutrient environment. KNY19-G has a large oligotrophic diatom assemblage as a result of the inflow of nutrient-poor marine waters (Allanson *et al.*, 2000), which is responsible for the oligotrophic nature of the estuary. The Knysna River has a higher trophic status compared to the estuary, since it is responsible for introducing nutrients - particularly nitrogen and phosphorus - obtained from higher up in the catchment area, as the estuary is dependent on the river for its nutrient supply (Clark *et al.,* 2002). Additionally, the nutrients could be procured by natural means, since estuaries are naturally productive systems where nutrients are regenerated through

natural means, recycled, and stored in the sediment (Cooper *et al.*, 2010; Trobajo and Sullivan, 2010; Day *et al.,* 2013; Adams *et al.,* 2020).

6.1.2. Phase 2 - Colonial Lagoon: ~200 to ~50 cal BP (~1900 CE)

6.1.2.1. The Ashmead Channel (KNY19-B)

The habitat requirements of epipsammics, including *C. adhaerens, P.* cf. *staurophorum* and *D. minor*, during Phase 2 implies the persistence of warm, shallow waters, and the presence of some macrophytes typical of sand flats and coastal environments (Vos and de Wolf, 1988; Hutchinson *et al.,* 2004; Katsuki *et al.,* 2012; Begun *et al.*, 2015; Sawai *et al.,* 2016; Zalat *et al,* 2021). Furthermore, the epipsammic community is reflected by the high percentage of sand in core KNY19-B between ~200 and ~50 cal BP (Figure 16). A reduction in *P. sulcata* from ~200 cal BP throughout the remainder of the last two phases could indicate a marginally weaker tidal influence, although this seems improbable on the grounds that the epipsammic diatom community illustrates persistently high hydrodynamics (Figure 28), which typifies sandy sediments exposed to high physical stress (Méléder *et al.,* 2007; Scholz and Liebezeit, 2011). Instead, it seems that the disappearance of *P. sulcata* is linked to an increase in nitrogen loads, by reason that the species is prone to poor preservation under these conditions (McQuoid and Nordberg, 2003). The TDI values corroborate the increase in nutrient loads by identifying the first instance of meso-eutrophic conditions in ~1825 CE in the Ashmead Channel, while the diatom record points to the presence of heavy organic pollution in the form of polysaprobic *Sellaphora seminulum* and *N. tenelloides* - two species that are commonly recorded in the literature as typical of eutrophic and polysaprobic environments owing to their high total phosphorus and nitrogen optima (Taylor *et al.*, 2007; Faria *et al.*, 2013; Wilczyñski *et al.*, 2015; Salomoni *et al.*, 2017; Stewart *et al.,* 2018). These changes are either a reflection of natural estuarine processes and natural climate change or anthropogenic activities. In particular, the main anthropogenic activities consisted of the exploitation of indigenous forests in the Knysna area from 1763, the introduction of agriculture (cattle grazing) on Thesen Island in the early 1800s, and the start of the shipping industry from 1817 - all of which could influence the diatom assemblage (Hart and Halkett, 1998; Matthews, 2019; Joubert, 2021) (see subsection 6.2.2.).

6.1.2.2. The Middle Reaches (KNY19-G)

Similar to KNY19-B, the environmental setting during Phase 2 remains comparable to Phase 1, where the dominant species reflect the intermittent subsurface exposure and swamp-like nature of the tidal flats and their well-established mud-flat vegetation community (Sawai and Nagumo, 2003; Nguetsop *et al.,* 2004; Chen *et al.*, 2005; Beltrones and Fuerte, 2006; Cantonati *et al.*, 2012; Chen *et al.,* 2014; Razjigaeva *et al.,* 2014; Mašić and Barudanović, 2020). A higher percentage of finer sediments (Figure 22) in KNY19-G roughly coincides with a sudden increase in freshwater species along with a decline in marine species at ~200 cal BP (Figure 23), potentially linked to the remobilisation of sediments linked to deforestation. Since very coarse and coarse sand dominates the upper estuary (Human *et al.,* 2020), the introduction of finer-grained fluvially derived sediment could be a result of increased freshwater flow from the Knysna River. The notion of increased freshwater inflow is supported by an increase in acidophilic species between ~200 to ~50 cal BP, most of which reached their highest relative abundances by ~1865 CE, which is when a considerably large freshwater pulse entered the system and contributed towards the oligotrophic assemblage. Generally, contemporary studies show that the pH values in the lower, middle, and upper estuary all range between 6.6 and 8, except when acidic inflowing freshwater from the Knysna River decreases the pH in the upper and middle reaches (Russel, 1996). The slight acidy of the river during periods of high freshwater flow is derived from the concentration of humic acids, thereby notably lowering the pH (up to 3.4) (Russel, 1996; Snow, 2007). In addition, species indicative of medium to high current velocity and flow, such as *C. placentula, F. crassinervia,* and *Surirella fastuosa* var. *cuneata,* are present thereby providing further evidence of high freshwater inflow (Pan *et al.,* 1996; Plenković-Mora *et al.,* 2008; Holmes and Taylor, 2015). Notwithstanding the growing freshwater influence, the occurrence of marine species at ~1900 CE demonstrates that salinity inputs remained high due to the lack of obstructions in the estuary and the permanently open mouth.

This phase is characterised by an increase in nutrient loads and organic matter pollution, in comparison to the previous phase, as illustrated by the borderline mesotrophic TDI values (Figure 27). The increase in eutrophic (Appendix 3, Figure 38) and polysaprobic (Appendix 3, Figure 39) species from ~1825 CE onwards, such as *N. tenelloides, Cocconeis scutellum, C. placentula, F. pygmaea,* and *P. frequentissimum,* suggest a highly productive environment that is prone to organic pollution, nutrient enrichment, and instability (Venkateswarlu, 1986; Hillebrand *et al.,* 2000; Taylor *et al.*, 2007; Taylor *et al.,* 2007; Della Bella *et al.,* 2007; Lange *et al.,* 2011; Cantonati *et al.,* 2012; Holmes and Taylor, 2015; Jakovljević *et al.,* 2016; Mathews-Bird *et al.,* 2017). Although *N. tenelloides* is suggestive of

natural local tidal flat conditions and potentially reflective of the forested catchment (Razjigaeva *et al.,* 2014b; Antonelli *et al.,* 2017), its presence alongside species linked to organic pollution indicates that anthropogenic disturbance is influencing the diatom record at KNY19-G from ~1825 CE onwards. This is substantiated by historical records, which state that the first farms along the banks of the Knysna River and estuary were granted to colonialists in the 1770s alongside the ongoing logging and shipping activities (Caveney, 2015; Matthews, 2019; Collinson, 2020; Joubert, 2021) (see subsection 6.2.2.).

Although it cannot be disputed that increased nutrient loads are a result of natural processes and wetter conditions, it must be noted that changing land-use practices associated with the colonial occupation may have influenced the rise in trophic status and increased the rate of organic matter decomposition, as illustrated by the increase in polysaprobic species (Appendix 2, Figure 37; Appendix 3, Figure 39), in the Ashmead Channel and in the middle reaches of the estuary. It is difficult to discern between natural and anthropogenic influence in a system that is prone to natural fluctuations, nonetheless, it is believed that the diatom assemblage is mirroring natural climate change, as well as land-use changes in the form of deforestation, shipping, and agriculture (see sub-section 6.2.2.).

6.1.3. Phase 3 - Anthropogenically Impacted Lagoon: ~1900 to Present

6.1.3.1. The Ashmead Channel (KNY19-B)

~1900 to ~2005 CE

Prior to ~2005 CE, the dominance of epipsammics indicates elevated hydrodynamics in the middle reaches of the estuary (Figure 28). Increased runoff, industrial and agricultural waste products, and stormwater outlets associated with urban expansion introduced freshwater, nutrients, and organic matter into the estuary from ~1930 CE until the present, particularly into the Ashmead Channel (Marker, 2003; Knysna Municipality, 2020), whereas the stabilisation of Thesen Island via infilling in the 1920s hindered throughflow of marine waters (Hart and Halkett, 1998; Clark *et al.,* 2002). In effect, this reduced the marine assemblage in the Ashmead Channel while giving rise to a larger fresh and fresh-brackish assemblage, as well as an increase in eutrophic and hypertrophic species. These alterations likely facilitated the disappearance of marine species, such as *P. yarrensis* and *Lyrella lyra,* in ~1930 CE because these species have narrow ecological preferences and the environmental changes were too sudden and too severe to enable the adaptation - and hence survival - of the species. These anthropogenically-derived inputs triggered an increase in *S. seminulum* in ~1950 CE, which is

characteristic of pollution and high zinc concentrations (De Jonge *et al.*, 2008; Faria *et al.*, 2013; Rimet *et al.*, 2016; Stewart *et al., 2*018; Soeprobowati *et al.*, 2019). Unsurprisingly, high TDI values coincide with the relatively high percentage of *S. seminulum*, thereby further indicating the input of excessive nutrients and organic material during this period. Subsequently, the TDI decreases and is accompanied by an unexpected and drastic decrease in eutrophics between ~2000 to ~2005 CE. This could refer to the impact of water quality control measures or infrastructure upgrades, although this seems unlikely. Instead, this anomaly is more likely related to the vast amount of species with an unknown trophic status classification, consequently creating the illusion of a reduced eutrophic assemblage during this period.

~2010 CE to Present

From ~2010 to present, the Ashmead Channel is marked by the complete disappearance of marine species (*D*. (agg), *Auliscus* cf. *sculptus, P. sulcata,* and *P. delicatulum*) and a reduction in epipsammics typical of tidal flat assemblages - a change that is accompanied by a decrease in the percentage of sand in favour of silt towards the top of the core (Figures 15, 16, and 28). This stands in contrast to the previous phases where estuarine tidal flat species were common. Furthermore, the diatom record points to the loss of aquatic vegetation in the Ashmead Channel, such as *Zostera capensis* (Adams, 2016), as indicated by the decline of the epiphytic *C. costata,* which is a likely pioneer on *Z. marina* (Ruocco *et al.,* 2019).

The diatom record reflects that infrastructure developments, such as bridges and causeways, stormwater drain inflow, recreational boating, wastewater treatment discharge, and sewerage pumps are correlated with a rise in silt, increased freshwater inflow, nutrient enrichment, and organic pollution (Mosisch and Arthington, 1998; Marker, 2003; Knysna Municipality, 2020). This has resulted in a flourishing fresh, fresh-brackish, eutrophic, and polysaprobic diatom community (Figure 16; Appendix 2, Figures 36 and 37). The epipsammics are replaced with epilithics and species with a preference for multiple substrate types, thus reflecting an increase in artificial substrates, such as concrete (Figure 28). The co-occurence of *S. seminulum, N. tenelloides, Nitzschia frustulum,* and *Halamphora coffeaeformis* between ~2010 and ~2019 CE point towards critical levels of organic pollution (likely related to non-compliant discharges from the Knysna WWTW), heavy industrial practices, low to moderate agricultural activity in the estuary (Blinn and Bailey, 2001; Taylor *et al.*, 2007; Delgado *et al.,* 2012; Hafner *et al.,* 2018; Benhassane *et al.,* 2020; Claassens *et al.,* 2020). The prevalence of these species, along with the disappearance of *P. sulcata,* further indicates the high

nitrogen input at the sampling site, as *P. sulcata* is prone to poor preservation under these conditions (McQuoid and Nordberg, 2003). Furthermore, the elevated nutrient inputs are clearly illustrated by the TDI values, thus severely impacting the diatom community and leading to an increase in diversity (Figure 26) (see section 6.4.).

6.1.3.2. The Middle Reaches (KNY19-G)

In comparison to the Ashmead Channel, KNY19-G is more influenced by agricultural activities in the catchment, however, it is also impacted by infrastructure development (such as the opening of the White Bridge in 1955), stormwater inflow, and sewerage pumps (Marker, 2003; Knysna Municipality, 2020). This has resulted in an increase in freshwater and nutrient inputs, which has altered the water chemistry in the middle reaches and caused a reduction in the extent of the lagoon regime, thereby leading to a loss of marine species from ~1960 CE to present, as seen in the Ashmead Channel. The construction of bridges and causeways hinder the throughflow of marine waters to the upper estuary, thus further contributing to the loss of marine species. Similar to the changes transpiring in the Ashmead Channel, the middle reaches also experience unmatched freshwater inputs - resulting from increased runoff and stormwater inflow - specifically in ~1975 CE when freshwater and acidophilic species peak (Figure 23). The drastic increase in freshwater inputs is also noticeable as a rise in the percentage of sand in core KNY19-G (Figure 22), most likely originating via erosion of poorly consolidated sand on the Brenton Dune as a consequence of urban development during this phase (Reddering and Esterhuysen, 1987). The increased nutrient inputs, organic matter pollution, and environmental instability have led to the establishment of opportunistic species, such as *N. tenelloides* and *Nitzschia supralitorea* (particularly from ~1990 CE to present) at the expense of epiphytic species (Figure 29) (Villanueva *et al.,* 2000; Jakovljević *et al.,* 2016; Matthews-Bird *et al.,* 2017; Gastineau *et al.,* 2021). The shift towards opportunistic species is further reinforced by the rapid rise in the eutrophic *Rhopalodia musculus,* since the species is not highly sensitive to anthropogenic stresses (Bush and Colinvaux, 1994; Negus *et al.,* 2020). The nutrient enrichment is also reflected in the highest recorded TDI in ~1990 CE. Initially, the nutrient inputs caused higher species diversity (Figure 26) (see section 6.4), after which there is a reduction in diversity due to increased nutrient enrichment and organic matter pollution favouring opportunistic species.

6.2. DRIVERS OF ENVIRONMENTAL CHANGE

6.2.1. Phase 1: Climate Dynamics and Indigenous Populations (~610 to ~200 cal BP)

The Knysna Estuary is a shallow estuary exposed to daily tidal fluctuations, hence planktonic species are rare and aerophilic species are common due to the fact that they need to survive exposure/ desiccation during low tide. As a result, the only means of detecting rainfall variability in the Knysna Estuary is by employing the freshwater assemblages of KNY19-B and KNY19-G to imply freshwater inputs and hence rainfall. For example, low rainfall will contribute towards low riverine inputs and hence a poorly established freshwater diatom community. This contrasts with palaeolimnological studies that often use the ratio between benthic and planktonic species to indicate lake levels and thus moisture availability (Stager *et al.,* 2013).

Freshwater species were present in very low concentrations from ~610 to ~250 cal BP in both the Ashmead Channel and the middle reaches of the estuary (Figures 16 and 23. Instead, marine species dominated the estuary. As discussed previously, this suggests minimal freshwater inflow under slightly drier conditions. This is consistent with contemporary studies that have shown that the marine component extends into the upper reaches of the estuary during droughts when freshwater inflows are restricted (Largier *et al.,* 2000). The appearance of fresh-brackish species at ~590 cal BP in the Ashmead Channel could indicate a brief period of wetter conditions in the estuary. It is likely that the increased freshwater input is a singular occurrence or evidence of a short-lived period of flooding, seeing that drought conditions predate and succeed the event. Generally, the latter part of this phase (~250 to ~200 cal BP) is characterised by the early onset of slightly wetter conditions, as the relative abundance of marine species decreases to give way to the gradual appearance of freshwater, fresh-brackish, and brackish-fresh species at both KNY19-B and KNY19-G. However, the relatively small dilute community at both sites (in comparison to the following phases) implies that the increase in moisture availability - and thus freshwater inputs via streams, runoff, and the Knysna and Bongani Rivers - was fairly limited during this period and that predominantly arid conditions prevailed.

It is postulated that the Knysna Estuary diatom record is responding to the “Little Ice Age” (LIA) spanning from ~650 to ~90 cal BP (~1300 to ~1850 CE) (Matthews and Briffa, 2005). The term was coined by François Matthes in 1939 and is used to describe relatively recent climate change associated with internal factors (ocean-atmosphere dynamics) or external factors (solar activity and volcanic eruptions) (Nesje and Dahl, 2002; Matthews and Briffa, 2005). Both cores fall within the timeframe of

the LIA. It appears as though the predominantly drier conditions at the Knysna Estuary from ~610 to ~250 cal BP, along with the brief wet period at ~590 cal BP, are consistent with the first phase of the LIA (~650 to ~450 cal BP), by reason that similar responses are recorded in the interior and coastal region of the southern Cape (Talma and Vogel, 1992; Chase *et al.,* 2013; Kirsten, 2014; Wündsch *et al.,* 2016). More specifically, the Cango Cave speleothem oxygen isotope ($\delta^{18}O$) record suggests cooler and drier conditions in the interior of the southern Cape, while carbon ($\delta^{13}C$) and nitrogen ($\delta^{15}N$) isotope data obtained from rock hyrax middens in Seweweekspoort imply increased aridification from ~700 to ~570 cal BP in the summer rainfall zone (SRZ) (Talma and Vogel, 1992; Tyson and Lindesay, 1992; Chase *et al.,* 2013). The brief wet period could have been a result of a major flood event in view of, according to Holmgren *et al.* (1992:304), stable isotope variations from the Makapansgat Cold Air Cave in the Limpopo province indicating that major flood events increased during the aridification associated with the LIA cooling. The mostly dry conditions in the estuary from ~250 to ~200 cal BP coincide with the intermediary phase of the LIA - a two century-long warm episode from ~450 to ~275 cal BP, which is typified by drier conditions along the southern Cape coast (Tyson and Lindesay, 1992; Kirsten, 2008; Kirsten, 2014). In particular, the Knysna estuary diatom record is in agreement with diatom records from the Wilderness Lakes Complex (Eilandvlei, Swartvlei, and Groenvlei), all of which indicate lower lake levels associated with increased aridity between roughly ~500 to ~275 cal BP (Kirsten, 2008; Kirsten, 2014). The slightly drier conditions at the Knysna Estuary during the LIA are a result of the strengthening of the circumpolar westerly winds that expand northward (Tyson and Lindesay, 1992), while tropical disturbances or higher Agulhas Current sea-surface temperatures could have restricted precipitation in the region (Du Plessis *et al.*, 2020). The second cold phase of the LIA is discussed in section 6.2.2., as it corresponds to Phase 2 of the Knysna Estuary's environmental change.

Consequently, it is evident that a natural global climate change event impacted environmental change in the Knysna Estuary during Phase 1 and that the estuary exhibited a regional climatic reaction to the LIA. Although, it must be noted that the area was recurrently occupied by indigenous populations, which also interacted with the landscape during this period (Hart and Halkett, 1998; Sealy, 2003; Keller, 2019). Hunter-gatherers have used fire for millennia in their hunting strategies and to manage the productivity of geophytes, as well as other uses, such as cooking (Deacon, 1983; Esteban *et al.*, 2018; Wadley *et al.,* 2020; Humphrey *et al.*, 2021). If a fire were to get out of hand, the after-effects of the fire have the potential to increase the concentration or nutrient load of water bodies (Ranalli, 2004). Thus far the diatom record and TDI values signal changes in the trophic status or nutrient load of the estuary, however, the changes are not drastic. Although it is difficult to disentangle the effects of natural and human-induced nutrient inputs during this period due to a lack of the combination of

palaeoenvironmental and archaeological records in the region, it is most likely that the hunter-gatherers had a negligible to very low impact on the Knysna Estuary during this phase.

6.2.2. Phase 2: LIA and Colonial Occupation (~1750 to ~1900 CE)

This phase is typified by an increase in moisture availability and the associated rise in freshwater inflow through streams and the Knysna River, as illustrated by the growing freshwater assemblage at KNY19-G, which peaks in ~1865 CE (Figure 23). Subsequently, freshwater inflow conditions roughly return to pre-1865 CE values for the remainder of this phase. Although a slight increase in freshwater and fresh-brackish species are also present in the Ashmead Channel (Figure 16), the increase in moisture availability in the lower estuary is expressed as a rise in nutrient inputs owing to catchment dynamics. Notably, more nutrients are introduced into the system from ~1750 to ~1865 CE onwards through freshwater inflow from streams and the Bongani River during periods of increased rainfall, as illustrated by the TDI values (Figure 20). However, the first farms alongside the Knysna River and estuary were granted to colonists in 1770, therefore it is challenging to identify the source of any nutrient inputs (i.e., natural versus anthropogenic) from here on forth (Caveney, 2015; Collinson, 2020). As a result, it is proposed that the diatom record is roughly responding to the final phase of the LIA (~1680 to ~1860 CE) in combination with the onset of colonial occupation (Tyson and Lindesay, 1992).

It is clear that the second phase of the estuary's environmental development is significantly wetter compared to the pre-colonial phase and that moisture availability increases prior to colonial settlement in the area. Hence, it is suggested that the wetter conditions and increased moisture availability between ~200 cal BP and ~1900 CE are consistent with the later phase of the LIA, as illustrated by palaeoclimatic records of the southern Cape interior (Chase *et al.,* 2013), southern Cape coast (Quick *et al.,* 2018), and potentially the west coast (Stager *et al.,* 2012). In particular, stable isotope variation at Seweweekspoort suggests cooler and wetter conditions at ~1660 CE in the interior of the southern Cape and the SRZ (Chase *et al.,* 2013), while pollen evidence from Eilandvlei recorded humid conditions and increased moisture availability between ~1690 and ~1850 CE (Quick *et al.,* 2018). Similarly, the west coast and winter rainfall zone (WRZ) also experienced wetter conditions during the latter phase of the LIA, as demonstrated by Verlorenvlei's diatom record (Stager *et al.,* 2012). The wetter conditions in the Knysna Estuary could be caused by the strengthening and perturbation of the tropical easterly winds of the general circulation of the atmosphere over southern Africa (Tyson and Lindesay, 1992).

The freshwater peak in ~1865 CE is particularly complex, as this period marks the culmination of the wetter second phase LIA, as well as an intensification in colonial activities. Therefore, deforestation in the catchment could have exacerbated freshwater inflow conditions during a period of wetter conditions under natural climatic conditions (Chase *et al.,* 2013; Stager *et al.,* 2013; Quick *et al.,* 2018), considering that deforestation can lead to increased runoff, erosion, and a rise in organic matter (Benito *et al.,* 2003; Pienitz *et al.*, 2006; Gholami, 2013; Khaleghi, 2017). Consequently, the impact of deforestation could have been instrumental in the freshwater peak in ~1865 CE at KNY19-G, as well as a contributing factor towards the increasingly polysaprobic assemblage denoting an increase in organic matter decomposition. In addition, the influence of deforestation in the catchment is implied by KNY19-G's increase in sedimentation rate from ~1880 CE. This is comparable to a study by Taffs *et al.* (2008) that used the Australian Tuckean Swamp's diatom record to illustrate that the removal of indigenous vegetation cover started in 1855 and led to an increase in freshwater influence due to increased catchment runoff. The estuary's growing α-mesosaprobic to polysaprobic assemblage demonstrates an increase in organic matter decomposition, which is therefore in line with a study illustrating that deforestation during the early colonial settlement period increased the organic matter concentration of Lac Saint-Augustin in Canada (Pienitz *et al.,* 2006). Although, it is highly likely that agriculture also introduced organic matter into the estuary.

The establishment of farms surrounding the upper and lower estuary by the early 1800s are further responsible for introducing nutrients and organic matter into the system, for the reason that cattle faeces is nutrient-rich and can increase the total nitrogen concentration of water (Davies-Colley *et al.,* 2004; Houlbrooke *et al.,* 2004; Caveney, 2015; Collinson, 2020). Therefore, the farms along the banks of the Knysna River in the upper and middle reaches of the estuary could also have been partly responsible for the increasingly eutrophic and polysaprobic assemblage during this phase. The tidal streams flowing through Thesen Island, which at that point was still more of a low sandbank (Figure 30), could have dispersed the nutrients derived from grazing cattle on the island (Hart and Halkett, 1998). Additionally, the estuary was used as a functioning harbour for the transportation of timber from 1817, which contributed to the establishment of a larger and more permanent sawmill (consisting of a steam mill for sawing and milling timber) in 1875, thus further contributing towards nutrient enrichment (Matthews, 2019; Joubert, 2021). As a result, the increase in nutrients would have contributed towards the first instance of meso-eutrophic TDI values in the lower reaches of the estuary in ~1825 CE. Similarly, diatom records from the Ångermanälven Estuary in the Baltic Sea determined that land use change comprised of farming and the subsequent clearing of pine forest during the early onset of human occupation was possibly linked to a shift in eutrophic taxa typical of

anthropogenic influence (Warnock *et al.,* 2018), which is consistent with the Knysna Estuary's increase in the eutrophic *N. tenelloides, N. supralitorea,* and *N. frustulum* - species that reflect human-induced nutrient inputs. Moreover, historical records indicate two major fires in the 1860s and late 1880s, which could also have elevated the nutrient content of the estuary (Hart and Halkett, 1998; Ranalli, 2004; Duncan, 2006).

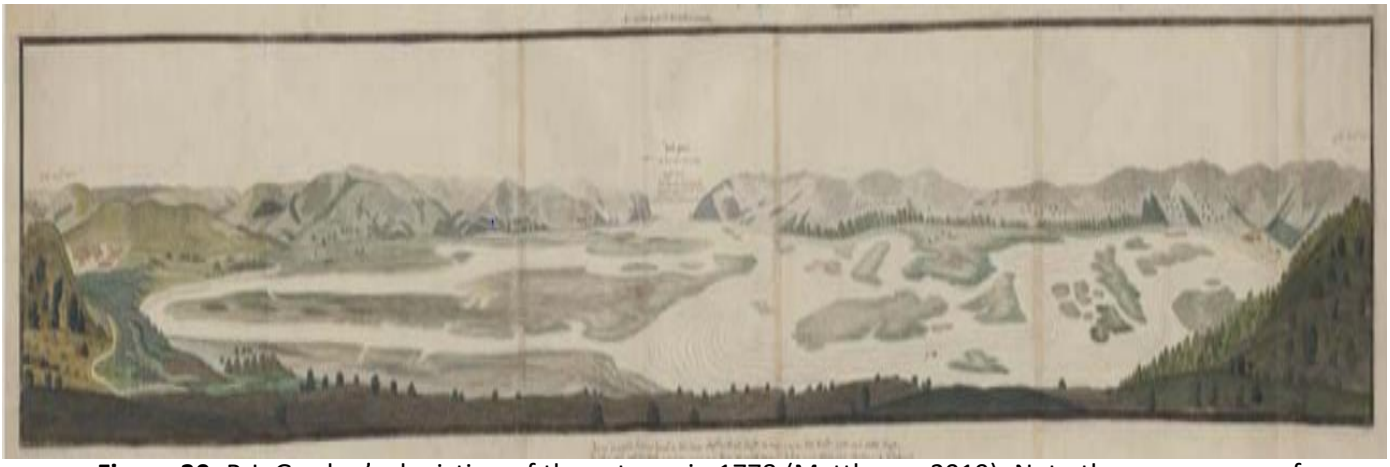

Figure 30. R.J. Gordon's depiction of the estuary in 1778 (Matthews, 2019). Note the appearance of Thesen Island prior to being infilled in the 1920s, thus promoting marine through flow.

Thus, it is evident that a natural climatic event and early colonial land use change, such as intense deforestation and agriculture, can impact environmental conditions within an estuary in terms of freshwater inputs, nutrient increases, and the rise in the rate of organic matter decomposition. However, it is important to note that the population around the Knysna Estuary was still relatively small (over 1000 settlers in 1880) (Caveney, 2015), which explains why the diatom record and TDI values suggest minimal impact during this phase as compared to Phase 3.

6.2.3. Phase 3: Extensive Anthropogenic Forcings (~1900 CE to Present)

6.2.3.1. The Ashmead Channel (KNY19-B)

Epipsammic species - species with a preference for coarse-grained sediment - decreased amidst a rise in siltation rates from ~1930 CE until present (Figure 28). This is likely in reaction to the construction of bridges and causeways across the estuary, as well as raising Thesen Island to facilitate development, which restricted tidal flow and fostered the deposition of finer sediments (Clark *et al.,* 2002; Human *et al.,* 2020). In particular, the Thesen Island causeway is known to have caused siltation and shallowing in the Ashmead Channel (Grindley and Heydorn, 1979; Clark *et al.,* 2002). Moreover, the

decreasing percentage of epipsammics could also be indicative of altered tidal flow regimes - i.e., lower hydrodynamic stress - caused by the obstructions in the estuary, as these species are linked with high hydrodynamics. Additionally, the rise in concrete surfaces around the Ashmead Channel from the 1900s onwards has also affected the epipsammics, seeing that it has provided a niche for epilithic species and species with a preference for various substrates (Figure 28).

The unprecedented increase in freshwater inputs at the expense of marine species in core KNY19-B arose due to the infilling of Thesen Island and hence preventing marine through flow, as well as the vast amount of WWTW effluent and stormwater inflow that enters the Ashmead Channel, as illustrated Figure 31. Urban runoff is further contributing towards freshwater inputs, ultimately owing to the fact that urban growth has increased surface flow and annual runoff from the urban and informal settlements due to a rise in impermeable surfaces, a lack of ecosystem services, and inadequate drainage infrastructure (Gholami, 2013; Adams *et al.*, 2019; O'Donoghue *et al.,* 2021). Prior to urbanisation, runoff would have infiltrated the soil instead of discharging into the estuary (Adams *et al.*, 2019). Apart from introducing large quantities of freshwater, the WWTW, stormwater inflow, and urban runoff has also led to the vast increase in eutrophic species associated with anthropogenic influence and elevated nutrient concentrations most notably *N. tenelloides* and *N. frustulum,* as well as the development of an unnaturally large polysaprobic assemblage, which is a reflection of the decomposition rate of organic matter inputs in the form of sewage. Specifically, the WWTW and urban runoff are the main nutrient and organic matter pollution sources and amount to daily inputs of 6500 m^3 into the Knysna Estuary (Adams *et al.,* 2020). It must be noted that organic matter is also sourced from the ocean (Human *et al.,* 2020), however, marine input alone cannot account for the high organic matter decomposition rates experienced at KNY19-B. To a lesser extent, the urban centre and informal settlements also contribute to the eutrophic and polysaprobic assemblage in various ways, including discharge from industrial and business activities, insufficient wastewater disposal systems, sewer infrastructure discharge and obstruction, wastewater treatment plant operation failure and constraints, and the illegal disposal of materials in stormwater systems or streams (Clark *et al.,* 2002; Knysna Municipality, 2020). Recreational boating may also contribute towards the eutrophic assemblage and high TDI values when sediments release nutrients upon being brought into suspension (Mosisch and Arthington, 1998), while road runoff can also modify the nutrient concentration of the Ashmead Channel (Sriyaraj and Shutes, 2001; Boger *et al.,* 2018).

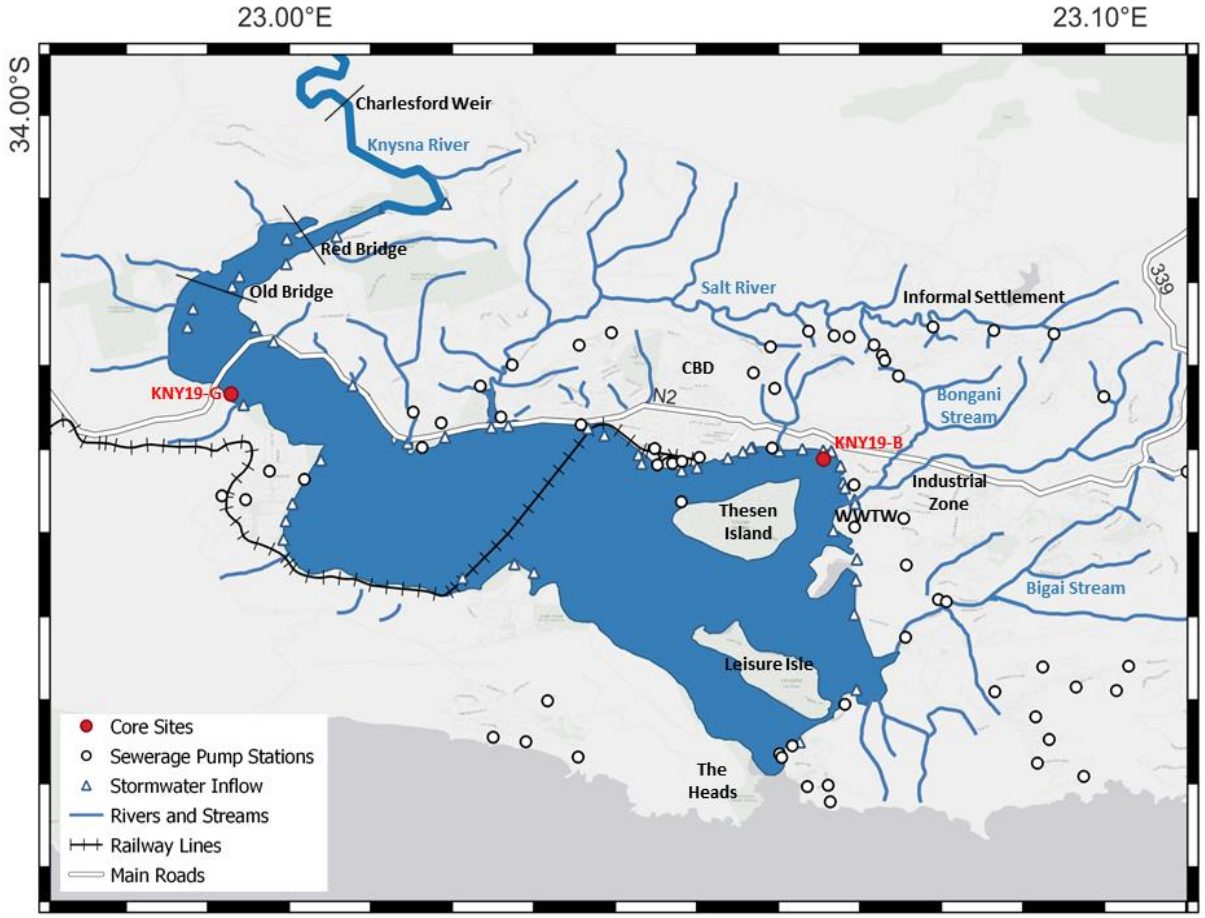

Figure 31. Map of sewage pump stations and stormwater inflow points surrounding the Knysna Estuary.

Interestingly, the diatom record at KNY19-B also points to changes in natural tidal flat vegetation assemblages. The decline in the relative percentage of epiphytic species, such as *C. costata,* from ~2010 CE to present supports studies that describe the loss of *Z. capensis* in the Ashmead Channel (Figure 28) (Adams, 2016). This is substantiated by the growing eutrophic assemblage and high TDI values mirroring an increase in nitrogen and phosphorus loads, resulting in macroalgae blooms that initiated the loss of *Z. capensis* (Adams, 2016; Allanson *et al.,* 2016). Lastly, a decrease of species typical of intertidal flats is indicative of the loss of aquatic vegetation as a consequence of urbanisation and population growth.

6.2.3.2. The Middle Reaches (KNY19-G)

The diatom assemblage reflects an increase in fresh-brackish species and brackish species in favour of marine species and is therefore interpreted as an increase in freshwater inflow. This stands in opposition to studies that have shown that freshwater inflow from the Knysna River has decreased as a consequence of population growth and land use change, as more freshwater is abstracted for municipal consumption and impacted by modified streamflow (Clark *et al.,* 2002; Claassens *et al.,*

2020; O'Donoghue *et al.,* 2021). Instead, the diatom assemblage is recording freshwater inputs in the form of increased runoff from impermeable surfaces and stormwater inputs. This means that the diatom record's ability to display the decrease in fluvial inputs is obscured by the prevalence of various freshwater pulses starting from Phase 2. The freshwater inputs from ~1960 to present have decreased the salinity, which altered the diatom assemblage and led to the exclusion of marine species and species typical of supratidal areas. It is likely that the addition of infrastructure - including causeways, bridges, and the raising of Thesen Island - could have hindered marine through flow to the upper reaches, thereby contributing to the lower percentage of marine species. Simultaneously, these changes have provided artificial substrates for a variety of diatom species, effectively decreasing the number of epiphytic species typical of intertidal flats (Figure 29). This implies that aquatic vegetation was replaced with artificial constructions, which is consistent with the literature, since almost 70% of the Knysna Estuary's supratidal marsh has been lost (Claassens *et al.,* 2020; Raw *et al.,* 2020).

The final phase of the estuary's development is characterised by a highly disturbed ratio of oligotrophic to eutrophic species, as illustrated by the increase in eutrophic, hypereutrophic, and polysaprobic species associated with anthropogenic activity, including *N. tenelloides* and *P. frequentissimum,* particularly from ~1990. During Phase 1 and most of Phase 2, the Knysna River was responsible for introducing natural sources of nutrients derived from the catchment into the estuary (Clark *et al.,* 2002), although it is apparent that natural riverine input alone can no longer be the singular source of nutrients and organic matter (Human *et al.,* 2020). At present, the trophic status of the diatom record indicates that the final phase of the estuary's development is impacted by intensified urbanisation and agricultural practices. In particular, large volumes of nutrients enter the estuary by means of the Knysna River during spring storms when dairy and beef farmers in the catchment use chemical and organic fertilisers (Allanson *et al.,* 2000b; Switzer, 2004; CES, 2007). It is more than likely that the use of inorganic or chemical fertilisers increased between 1950 to 1970, thereby affecting the trophic state of the Knysna River and subsequently impacting the diatom assemblage at KNY19-G (Novotny, 1999; Krausmann *et al.,* 2003; Pienitz *et al.*, 2006; Scanlon *et al.,* 2007; Bouwman *et al.,* 2013). Specifically, Else (2018) suggested that the Charlesford Farm - a farm with 700 cattle and 50 sows - substantially increased the nutrient load of the Knysna River (Charlesford Farm, n.d.). Cattle have been observed grazing in close proximity to KNY19-G (pers. obs.). As previously mentioned, there is a well-established relationship between cattle faeces and increased nutrient concentration (Davies-Colley *et al.,* 2004; Houlbrooke *et al.,* 2004). The current status of the diatom assemblage at KNY19-G is further impacted by sewage pump stations and stormwater inflow points located in close proximity to KNY19-G. Although there are comparatively fewer sewage and

stormwater points surrounding KNY19-G in comparison to the Ashmead Channel (Figure 31), the impact of stormwater inflow and effluent cannot be discredited, considering that the middle reaches are influenced by both point and diffuse sources within the Knysna River catchment (Allanson *et al.,* 2000b). Runoff from impermeable surfaces, such as the N2 highway, cannot be discredited for the reason that road runoff can also modify the nutrient concentration of aquatic bodies (Sriyaraj and Shutes, 2001; Boger *et al.,* 2018).

To summarise, the Knysna Estuary diatom record shows a major increase in the sediment accumulation rate, an expansion of the eutrophic and polysaprobic assemblage in reaction to nutrient and organic pollution, an increase in dilute species, and a decrease in diatom species typical of the original tidal flat environment from ~1900 CE. This is in line with the land use change associated with population growth and urban expansion around the Knysna estuary during the last century. These findings are consistent with extensive change driven by anthropogenic activities that have been observed in many estuaries across the world. For example, sedimentological, geochemical, and diatom records from Dives Estuary in France, Rio de la Plata Estuary in Uruguay, Biscayne Bay in Florida, and Guadiana Estuary in Iberia (Lespez *et al.,* 2010; Delgado *et al.,* 2012; Wachnicka *et al.,* 2013; Perez, García-Rodríguez *et al.*, 2017) all point towards human influence in the past century, most notably in relation to nutrient input and catchment modification. Furthermore, eutrophic diatoms species from the Oder Estuary in the Baltic Sea were found to be indicative of water quality deterioration, particularly with the onset of agricultural fertilisers after World War Two (Andrén, 1999), whereas Taffs *et al.* (2008) demonstrated that the period from 1900 onwards shows a dramatic increase in sedimentation rate with the development of a drainage network, as well as a small trend towards an increasingly freshwater diatom assemblage - all of which are trends that are clearly evident in the Knysna Estuary's diatom record.

6.3. SALINITY AND NUTRIENTS AS THE MAIN STRUCTURAL VARIABLES

The positions of the two core sites reveals a horizontal salinity gradient. KNY19-B is located in closer proximity to the mouth and thus exhibits a large marine assemblage, whereas KNY19-G has a larger freshwater assemblage and lower salinity levels due to freshwater inputs from the Knysna River. The disparate assemblages are an example of how diatoms respond to the competition paradigm under the stress-gradient hypothesis, which states that "high-salinity-tolerant species will occupy those habitats closest to the mouth, while low-salinity-tolerant species with a higher competitive ability will occupy those habitats closest to the river" (Nunes *et al.,* 2021). Salinity has a structuring effect on

diatom assemblages as the salinity gradient functions as a physicochemical barrier for marine and freshwater species by placing environmental stress on marine species (Teske and Woodbridge, 2003). The salinity gradient illustrated by this study is consistent with Largier *et al.* (2000) and Else (2018) who also found evidence of a natural salinity gradient in the Knysna Estuary driven by the tidal mixing and daily freshwater inflows. Similarly, salinity is a primary structuring variable in various other estuarine studies (e.g., Wachnicka *et al.*, 2010; Potapova, 2011; Dalu *et al.*, 2016; Bode *et al.,* 2017; Nunes *et al.,* 2021). As a result, it is not unexpected that salinity is the main structuring variable in the Knysna Estuary, as seen in Figures 17 and 24.

Estuaries are highly productive ecosystems seeing that they receive nutrients naturally from terrestrial and marine inputs, including weathering, upwelling, as well as more recent anthropogenic inputs (O'Boyle and Silke, 2010; Trobajo and Sullivan, 2010; Day *et al.,* 2013; Melo-Magalhães *et al.,* 2016; Adams *et al.,* 2020). Accordingly, it is believed that the results of the PCAs (Figures 17 and 24) are responding to both natural and anthropogenic nutrient inputs, as estuaries are sensitive to nutrient inputs in general (Nodine and Gaiser, 2014). This is in congruence with Else's (2018) research findings stating that nutrients are a secondary structuring variable at the Knysna Estuary. In comparison, other studies also highlight nutrient availability as one of the most influential environmental variables that regulate and structure estuarine diatom communities (e.g., Frankovich *et al.,* 2006; Wachnicka *et al.*, 2010; Kasin, 2011; Nche-Fambo *et al.*, 2015; Kock *et al.*, 2019).

According to Underwood and Provot (2000), it can be challenging to identify the key environmental factors that result in distributional patterns. This is because diatoms in estuaries inhabit a complex environment, since many estuaries have a high covariance of factors, such as inorganic nutrient concentration, organic loads, and salinity (Underwood and Provot, 2000). Therefore, it may be impossible to determine which physicochemical variable diatom species are primarily responding to (Underwood and Provot, 2000; Dalu *et al.*, 2016). Adding to the complexity, natural drivers in estuaries, such as nutrients, can be modified by human activities thus making it challenging to differentiate between natural and anthropological environmental factors (Rovira *et al.*, 2012). Consequently, the dominant diatom species will reflect natural variability whilst simultaneously exhibiting characteristics of anthropogenically impacted areas (Rovira *et al.*, 2012). This could be the case of *N. tenelloides,* which was associated with negative loadings in both cores. On the one hand, *N. tenelloides* is polytrophic and occurs in extremely polluted waters, while on the other hand it is characteristic of shallow water basins and can naturally occur in estuaries without the presence of anthropogenically-derived nutrient pollution (Taylor *et al.*, 2007; Razjigaeva *et al.*, 2014b; Noga *et al.,*

2016). For example, *N. tenelloides* was originally present in trace amounts in the Knysna Estuary prior to colonial settlement as a result of naturally high nutrient loads. Subsequently, *N. tenelloides* increased in abundance in response to anthropological pressures and was found alongside species indicative of anthropogenic influence, such as *S. seminulum* and *N. supralitorea.* Hence, it can be assumed that *N. tenelloides* is more indicative of anthropogenically impacted and extremely polluted waters. It is thus imperative to observe the species in the context of the assemblage and the associated land use changes.

6.4. THE RELATIONSHIP BETWEEN COMMUNITY STRUCTURE AND TROPHIC STATUS

The Shannon-Wiener Diversity Index (H') is closely related to the trophic state of the water body (Table 10), which is indicated by the TDI (Gao and Song, 2005). These indices are mostly used to quantify the effect of specific activities, e.g., agriculture or wastewater treatment, and pollution on water bodies, therefore they can function as an indicator for the modification of ecosystems under nutrient enrichment or pollution (Watt, 1998; Gao and Song, 2005; De la Rey, 2007; Cooper *et al.*, 2010).

Table 10. Trophic status and corresponding species diversity levels according to the Department of Water Affairs and Forestry's (1996) Aquatic Ecosystem Guideline and values obtained from Lemley et al., (2021).

Trophic Status	Species Diversity Levels	H' Values
Oligotrophic	Moderate	(H' > 3)
Mesotrophic	High	(H' 2.5 - 3)
Eutrophic	Low	(H' 2 - 2.5)
Hypertrophic	Very low	(H' < 2)

Overall, the trophic status and diversity values of the Knysna Estuary do not concur with the classical approach to community structure and pollution, which is based on the assumption that diversity indices have an inverse relationship with nutrient values in the water column (Watt, 1998; Blanco *et al.,* 2012; Wu *et al.*, 2014; Lemley *et al.,* 2015; Shibabaw *et al.,* 2021). Essentially, pollution or nutrient enrichment causes low diversity values, as seen in Table 10, in that the most tolerant species outcompete the intolerant taxa to the point where only a few species survive, thus causing a decline in diversity (Van Dam, 1982; Blanco *et al.,* 2012; Lemley *et al.,* 2015). Instead, low diversity scores at the base of core KNY19-B coincide with oligotrophic TDI values (Figures 20 and 27), whereas moderate

values are associated with meso-eutrophic and eutrophic TDI values at the top of the core. Similarly, high diversity scores at the base of KNY19-G correspond with oligotrophic TDI values, while a moderate diversity is concurrent with mesotrophic and meso-eutrophic values. The strong oligotrophic diversity values at the top of the cores are in disagreement with the increasingly eutrophic diatom assemblage observed at both sites. Moreover, both cores' percentage pollution tolerant values (%PTV) did not have a marked increase (PTV% < 20%) (Tables 6 and 9), indicating that the sites are currently free of significant organic pollution. This is somewhat surprising due to the diatom assemblage clearly recording a rise in polysaprobic species, which represents species that are tolerant towards domestic and industrial organic pollution (Harding and Taylor, 2011). However, the increasing influence of organic pollution could manifest as an increase in %PTV in both cores' most recent samples.

These findings are consistent with Babko *et al.* (2020) who found that diversity scores increased with pollution associated with runoff from stormwater systems. Likewise, Watt (1998) found that species diversity in a nutrient-enriched river was higher, while De la Rey *et al.* (2008) used second-degree polynomial multiple regressions to show that high H' and evenness is present in moderate pollution conditions, instead of at unpolluted sites (as would be expected). It is proposed that KNY19-B recent rise in diversity (from ∼2010 CE to Present) in response to nutrient enrichment could be consistent with the intermediate disturbance hypothesis, which states that high species diversity is sustained when a site experiences intermediate pollution levels (Watt, 1998). The diatom assemblage at KNY19-B is potentially reacting to the increasingly dilute and nutrient-rich conditions linked to stormwater inflow and sewage effluent, thus creating a favourable environment for new species and leading to an increase in diversity. Although KNY19-G's most recent samples (∼1990 CE to Present) illustrate a decreasing trend in diversity regarding nutrient enrichment, the diversity values are still high. The trend could allude to the possibility that KNY19-G's most recent samples are responding in accordance with the classical approach or the intermediate disturbance hypothesis associated with moderate pollution conditions. Either way, the amplitude and fluctuation of species diversity during a period of nutrient enrichment could be a sign of an unbalanced or changing environment, which is in line with findings by Cheng *et al.* (2012). Lastly, the rising %PTV is congruous with studies that have illustrated that organic pollutants from sewage effluent increases %PTV and contributes towards increasingly eutrophic conditions (Bellinger *et al.*, 2006)

Bearing the above in mind, it is obvious that the Shannon-Wiener Diversity Index showed no relationship with the TDI. This is due to the non-linear relationship between diversity indices, as well

as the fact that TDI is regarded as more relevant and reliable in lake and river monitoring studies as compared to estuaries (De la Rey *et al.*, 2008; Harding and Taylor, 2011). Moreover, the TDI reduces data into a single value that loses community composition information (Harding and Taylor, 2011). Furthermore, diversity is impacted by various ecosystem processes, such as predation, competition, and habitat harshness, thereby further complicating the use of this index in estuaries (Estrada *et al.,* 2004; Goa and Song, 2005; Armitage *et al.*, 2009). Although caution is advised when using TDI and community structure in tandem, each index by itself may only provide a partial view of environmental conditions. Instead, the combination of these two indices may provide a more holistic view on estuarine development, on the condition that the indices are properly applied.

6.6. CONCLUSIONS

This chapter explores historically recent environmental changes in the Knysna Estuary by utilising fossilised diatoms as biological indicators on environmental conditions alongside historical records.

The Knysna Estuary diatom record illustrates the impact of a global climatic event, which is consistent with various southern Cape palaeoecological records. The diatom record shows that anthropogenically-induced changes were likely first introduced during the period of colonial settlement, whereas the last century is characterised by major shifts in the diatom assemblage in response to land use change and population growth. Unprecedented rates of nutrient enrichment and organic matter inputs could have a detrimental effect on estuarine health if stormwater inputs, runoff (both industrial and agricultural), and sewage effluent are continued to be managed inefficiently. Additionally, it was evident salinity and nutrients are major structural variables in the estuary and that diversity and trophic status indices showed no relationship on the grounds that they provided mixed results that were inconsistent with the diatom species composition.

CHAPTER 7 - CONCLUSIONS

This study aimed to use fossilised diatoms as biological indicators of environmental conditions to explore historically recent changes in the Knysna Estuary. In order to achieve this, shallow cores were obtained from the estuary and an interim chronology was utilised based on ^{14}C and ^{210}Pb dating methods to illustrate the temporal change in the diatom assemblage. Qualitative and statistical analyses enabled the reconstruction of major estuarine changes in relation to salinity, trophic status, and organic matter decomposition. Relative percentage diagrams reveal the extent of changes in the most important environmental variables, whereas statistical analyses, such as Principal Component Analysis, Shannon-Wiener Diversity Index, and Trophic Diatom Index, provide supportive evidence of changing environmental conditions. The outputs, amalgamated alongside historical records, offer a high temporal resolution reconstruction of natural and human-induced environmental change in the estuary.

The Knysna Estuary diatom record serves as the first documentation of environmental change in the estuary's geologically recent past. The following findings are noteworthy:

- The Pre-colonial Lagoon Phase extended from ~610 to ~200 cal BP and is characterised by strong marine inflow, a high hydrodynamic regime, and slightly drier conditions.
- These conditions are consistent with the first and intermediary phase of the LIA, which is in congruence with both interior and coastal palaeoenvironmental records of the southern Cape. Moreover, marine through flow was permitted due to a lack of human-induced alterations.
- The Colonial Lagoon Phase spanned from ~200 to ~50 cal BP (~1900 CE) and is distinguished by a shift towards increased freshwater inflow in the upper reaches, the maintenance of high hydrodynamics in the middle reaches, and the first discernible instance of anthropogenic disturbance.
- The environmental conditions of the estuary during the Colonial Lagoon Phase reflect the second phase of the LIA and are congruent with palaeoecological records from the interior of the southern Cape.
- Since the LIA signal is interwoven with the first perceptible instances of human impacts, it is increasingly difficult to determine the climatic conditions at the estuary. For example, freshwater inputs could be a result of a wetter LIA phase or increased runoff associated with deforestation.

- The Anthropogenically Impacted Lagoon Phase (~1900 CE to Present) is set apart by altered marine through flow, large volumes of freshwater inflow, and an unparalleled rise in nutrient and organic matter inputs.
- Population growth, urbanisation, and the associated land use change caused an increase in freshwater and fresh-brackish inflow, nutrients, and organic matter, all of which is linked to stormwater inflow, ineffective WWTW, and other pollutants (chemical fertilisers and sewage) entering the estuary via streams. Marine through flow is impacted by large-scale construction projects, such as bridges and causeways, as well as raising the level of Thesen Island. Poor tidal flushing and an increasingly eutrophic and polysaprobic assemblage are of major concern.
- Salinity and nutrients are the main structuring variables impacting diatom assemblage composition.
- The Shannon-Wiener Index and Trophic Diatom Index showed no relationship with one another and caution is advised when using these two techniques in an estuarine environment.

7.1. LIMITATIONS AND SUGGESTIONS GOING FORWARD

Estuaries are highly dynamic and complex environments considering that elements such as winds, tidal forces, and fluvial discharge subject them to constant change over a manifold of temporal and spatial scales (Schumann *et al.*, 1999; Cooper *et al.*, 2010; Trobajo and Sullivan, 2010; Gomes *et al.,* 2017). As a result, estuaries are in a constant state of fluctuation, which makes it challenging to conduct research (Trobajo and Sullivan, 2010). Sediment mixing due to biotic (bioturbation by meio- and macrofauna), abiotic (wave or tidal induced), and/or anthropogenic (trawling and anchoring) factors in estuaries have deleterious effects on the temporal variation in sediment cores, thus influencing the results of ^{210}Pb dating (Andersen, 2017; Taffs *et al.*, 2017). Natural physicochemical components of estuaries, such as nutrients, can be altered by anthropological activity, which makes it difficult to differentiate between natural and human-induced stressors (Rovira *et al.*, 2012; Kock *et al.*, 2019). Therefore, despite being proven to be very useful palaeoindicators in estuarine environments, further field and laboratory studies are required to assess the impact of sediment mixing on establishing a reliable chronology, in addition to assessing the application of diatoms as bioindicators in estuaries (Du *et al.*, 2017; Taffs *et al.*, 2017). Although these constraints need to be refined, it is possible to take these limitations into account when interpreting results (Taffs *et al.*, 2017).

In order to better understand the regional effect of the LIA in the YRZ, it would be useful to identify and explore other estuaries located in the YRZ. This can help inform climate model predictions about the future seeing that these models do not currently consider the climatic complexity of palaeoecological records (Stager *et al.,* 2013). Additionally, it would be advantageous to combine the discovery of more archaeological sites in the YRZ with YRZ palaeoecological records as a means of disentangling the impacts of hunter-gatherers (if any) from natural climate change events or natural estuarine variability. Since the relationship between diatom species diversity and trophic status is complex and non-linear (De la Rey, 2008), particularly in estuaries, it might be more beneficial to relate the amplitude and fluctuation in species diversity to changes in water quality, as well as to consider species composition and the occurrence of dominant species (Stevenson, 1984; Trobajo and Sullivan, 2010; Soeprobowati *et al.*, 2020). The TDI has the potential to be incredibly useful and valuable supporting evidence, however, it is imperative to adjust the TDI so that it is suitable for application in estuaries. At present, it is more appropriate for lacustrine and riverine use for the reason that estuaries are naturally productive and nutrient-rich systems.

7.2. IN SUMMARY

First and foremost, this study has provided the first record of change in the Knysna Estuary's microalgae community and their response to environmental stress. This is particularly important as thus far palaeoestuarine science is still developing in the Southern Hemisphere (Taffs *et al.*, 2017). Additionally, by using fossilised diatoms as bioindicators to reconstruct environmental change in the Knysna Estuary, this study has provided potential baseline conditions that can assist in steering estuary restoration decisions (Gillson and Marchant, 2014). Although this aspect falls outside of the scope of this project, it is hoped that this research will ultimately and indirectly contribute towards improved management and rehabilitation of the Knysna Estuary. Furthermore, evidence of climatic changes contributes towards the body of knowledge surrounding the year-round rainfall zone and any potential model predictions for future climate change in the region. The extent of urbanisation and population growth make it near-impossible to expect that conditions can return to normal, however, improved land and stormwater runoff management can go a long way in improving the water quality at the Knysna Estuary (Van Niekerk *et al.,* 2012; Adams, 2016). Lastly, it is imperative to provide adequate flushing toilets and waste disposal to informal settlements, as well as to ensure compliance or improved nutrient removal from the WWTW, as these contaminants ultimately terminate in the estuary (Adams *et al.*, 2019; Claassen *et al.,* 2020; Knysna Municipality, 2020).

CHAPTER 7 - REFERENCES

Adams, J.B., 2016. Distribution and status of Zostera capensis in South African estuaries—a review. *South African Journal of Botany*, *107*, pp.63-73. Available: https://doi.org/10.1016/j.sajb.2016.07.007 [2022, January 27]

Adams, J.B., 2020. Salt marsh at the tip of Africa: patterns, processes and changes in response to climatechange. *Estuarine, Coastal and Shelf Science*, *237*, p.106650. Available: https://doi.org/10.1016/j.ecss.2020.106650 [2022, January 27]

Adams, J.B., Cowie, M. and Van Niekerk, L., 2016. *Assessment of completed ecological water requirement studies for South African estuaries and responses to changes in freshwater inflow*. Pretoria: Water Research Commission. WRC Report No. KV 352/15

Adams, J.B., Snow, G.C. and Veldkornet, D.A. 2012. Chapter 6. Estuarine habitat. In: Van Niekerk, L. and Turpie, J.K. (eds) 2012. South African National Biodiversity Assessment 2011: Technical Report. Volume 3: Estuary Component. CSIR Report Number CSIR/NRE/ECOS/ER/2011/0045/B. Council for Scientific and Industrial Research, Stellenbosch.

Adams, J.B., Pretorius, L. and Snow, G.C., 2019. Deterioration in the water quality of an urbanised estuarywith recommendations for improvement. *Water SA*, *45*(1), pp.86-96. Available: https://doi.org/10.4314/wsa.v45i1.10 [2022, January 27]

Adams, J.B., Taljaard, S., Van Niekerk, L. and Lemley, D.A., 2020. Nutrient enrichment as a threat to the ecological resilience and health of South African microtidal estuaries. *African Journal of Aquatic Science*, *45*(1-2), pp.23-40. DOI: 10.2989/16085914.2019.1677212.

AlgaeBase. n.d. *Species search.* Available: https://www.algaebase.org/search/species/ [2021, June 24].

Allanson, B.R., Human, L.R.D. and Claassens, L., 2016. Observations on the distribution and abundance of a green tide along an intertidal shore, Knysna Estuary. *South African Journal of Botany*, *107*, pp.49-54. Available: https://doi.org/10.1016/j.sajb.2016.02.197 [2022, January 27]

Allanson, B.R., Maree, B. and Grange, N., 2000b. An introduction to the chemistry of the water column of the Knysna Estuary with particular reference to nutrients and suspended solids. *Transactions of the Royal Society of South Africa*, *55*(2), pp.141-162.

Allanson, B.R., Nettleton, J. and de Villiers, C.J., 2000. Benthic macrofauna richness and diversity in the Knysna Estuary: a 50 year comparison. *Transactions of the Royal Society of South Africa*, *55*(2), pp.177-185, DOI: 10.1080/00359190009520442

Andersen, T.J., 2017. Some practical considerations regarding the application of 210 Pb and 137 Cs dating to estuarine sediments. In Applications of Paleoenvironmental Techniques in

Estuarine Studies. K. Weckström, K.M. Sauders, P.A. Gell, C.G. Skilbeck (Eds.), Springer, Dordrecht. pp. 121-140. DOI:10.1007/978-94-024-0990-1_21

Anderson, N.J. and Vos, P., 1992. Learning from the past: diatoms as palaeoecological indicators of changes in marine environments. *Netherland Journal of Aquatic Ecology*, *26*(1), pp.19-30.

Andrén, E., 1999. Changes in the composition of the diatom flora during the last century indicate increased eutrophication of the Oder estuary, south-western Baltic Sea. *Estuarine, Coastal and Shelf Science*, *48*(6), pp.665-676.

Antonelli, M., Wetzel, C.E., Ector, L., Teuling, A.J. and Pfister, L., 2017. On the potential for terrestrial diatom communities and diatom indices to identify anthropic disturbance in soils. *Ecological Indicators*, *75*, pp.73-81. Available: https://doi.org/10.1016/j.ecolind.2016.12.003 [2022, January 27]

Appleby, P.G., 1993. Forward to the lead-210 dating anniversary series. *Journal of Paleolimnology*, *9*(2), pp.155-160.

Armitage, A.R., Gonzalez, V.L. and Fong, P., 2009. Decoupling of nutrient and grazer impacts on a benthic estuarine diatom assemblage. *Estuarine, coastal and shelf science*, *84*(3), pp.375-382. Doi:10.1016/j.ecss.2009.07.001

Atazadeh, I., Sharifi, M. and Kelly, M.G., 2007. Evaluation of the trophic diatom index for assessing water quality in River Gharasou, western Iran. *Hydrobiologia*, *589*(1), pp.165-173. Available: https://doi.org/10.1007/s10750-007-0736-0 [2022, January 27]

Aquino-López, M.A., Blaauw, M., Christen, J.A. and Sanderson, N.K., 2018. Bayesian Analysis of 210Pb Dating. *Journal of Agricultural, Biological and Environmental Statistics*, *23*(3), pp.317-333. Available: https://doi.org/10.1007/s13253-018-0328-7 [2022, January 27]

Aquino-López, M.A., Ruiz-Fernández, A.C., Blaauw, M. and Sanchez-Cabeza, J.A., 2020. Comparing classical and Bayesian 210Pb dating models in human-impacted aquatic environments. *Quaternary Geochronology*, *60*, p.101106. Available: https://doi.org/10.1016/j.quageo.2020.101106 [2022, January 27]

Azovsky, A.I., Mazei, Y.A., Saburova, M.A. and Sapozhnikov, P.V., 2020. Patterns in diversity and composition of the microbenthos of subarctic intertidal beaches with different morphodynamics. *Marine Ecology Progress Series*, *648*, pp.19-38. Available: https://doi.org/10.3354/meps13419 [2022, January 27]

Babko, R., Szulżyk-Cieplak, J., Danko, Y., Duda, S., Kirichenko-Babko, M. and Łagód, G., 2019. Effect of stormwater system on the receiver. *Journal of Ecological Engineering*, *20*(6). Available: https://doi.org/10.12911/22998993/109433 [2022, January 27]

Barsanti, M., Garcia-Tenorio, R., Schirone, A., Rozmaric, M., Ruiz-Fernández, A.C., Sanchez-Cabeza, J.A., Delbono, I., Conte, F., Godoy, J.D.O., Heijnis, H. and Eriksson, M., 2020. Challenges and limitations of the 210Pb sediment dating method: Results from an IAEA modelling

interlaboratory comparison exercise. *Quaternary Geochronology*, *59*, p.101093. Available: https://doi.org/10.1016/j.quageo.2020.101093 [2022, January 27]

Bate, G.C., Smailes, P.A. and Adams, J.B., 2004. *Benthic Diatoms in the Rivers and Estuaries of South Africa: Report to the Water Research Commission*. Water Research Commission.

Bate, G.C., Smailes, P.A. and Adams, J.B., 2013. Epipelic diatoms in the estuaries of South Africa. *Water SA*, *39*(1), pp.105-118. Available: http://dx.doi.org/10.4314/wsa.v37i4.18 [2022, January 27]

Battarbee, R.W., 1984. Diatom analysis and the acidification of lakes. *Philosophical Transactions of the Royal Society of London. B, Biological Sciences*, *305*(1124), pp.451-477.

Battarbee, R.W., Jones, V.J., Flower, R.J., Cameron, N.G., Bennion, H., Carvalho, L. and Juggins, S., 2002. Diatoms. In *Tracking environmental change using lake sediments* (pp. 155-202). Springer, Dordrecht.

Battarbee, R.W., Charles, D.F., Dixit, S.S., and Renberg, I. 2010. *Diatoms as indicators of surface water acidity.* Smol, J.P. and Stoermer, E.F. eds., In The diatoms: applications for the environmental and earth sciences. Cambridge University Press.

Barbier, E.B., Hacker, S.D., Kennedy, C., Koch, E.W., Stier, A.C. and Silliman, B.R., 2011. The value of estuarine and coastal ecosystem services. *Ecological monographs*, *81*(2), pp.169-193.

Begun, A.A., Ryabushko, L.I. and Zvyagintsev, A.Y., 2015. Bacillariophyta of periphyton of navigation buoys in the Posiet bay area (the sea of Japan, Russia). *International Journal on Algae*, *17*(1).

Beiras, R., 2018. *Marine pollution: sources, fate and effects of pollutants in coastal ecosystems*. Elsevier.

Bellinger, B.J., Cocquyt, C. and O'reilly, C.M., 2006. Benthic diatoms as indicators of eutrophication in tropical streams. *Hydrobiologia*, *573*(1), pp.75-87. DOI 10.1007/s10750-006-0262-5

Bellinger, E.G. and Sigee, D.C., 2015. *Freshwater algae: identification, enumeration and use as bioindicators*. John Wiley & Sons.

Beltrones, D.S. and Fuerte, F.L., 2006. Epiphytic diatoms associated with red mangrove (Rhizophora mangle) prop roots in Bahía Magdalena, Baja California Sur, Mexico. *Revista de biologia tropical*, pp.287-297.

Benhassane, L., Oubraim, S., Mounjid, J., Fadlaoui, S. and Loudiki, M., 2020. Monitoring Impacts of Human Activities on Bouskoura Stream (Periurban of Casablanca, Morocco): 3. Bio-Ecology of Epilithic Diatoms (First Results). *Nature Environment & Pollution Technology*, *19*. Available: https://doi.org/10.46488/NEPT.2020.v19i05.016 [2022, January 27]

Benito, E., Santiago, J.L., De Blas, E. and Varela, M.E., 2003. Deforestation of water-repellent soils in Galicia (NW Spain): effects on surface runoff and erosion under simulated rainfall. *Earth SurfaceProcesses and Landforms: The Journal of the British Geomorphological Research Group*, *28*(2), pp.145-155. DOI: 10.1002/esp.431

Bere, T. and Tundisi, J. G., 2011. Diatom-based water quality assessment in streams influence by urban pollution: effects of natural and two selected artificial substrates, São Carlos-SP, Brazil' *Brazilian Journal of Aquatic Science and Technology*, 15(1), p. 54. Doi: 10.14210/bjast.v15n1.p54-63.

Bianchi, T.S. and Allison, M.A., 2009. Large-river delta-front estuaries as natural "recorders" of global environmental change. *Proceedings of the National Academy of Sciences*, *106*(20), pp.8085-8092. Available: www.pnas.orgcgidoi10.1073pnas.0812878106 [2022, January 27]

Blaauw, M., 2010. Methods and code for 'classical'age-modelling of radiocarbon sequences. *Quaternarygeochronology*, *5*(5), pp.512-518. Available: https://doi.org/10.1016/j.quageo.2010.01.002 [2022, January 27]

Blanco, S., Cejudo-Figueiras, C., Tudesque, L., Bécares, E., Hoffmann, L. and Ector, L., 2012. Are diatom diversity indices reliable monitoring metrics?. *Hydrobiologia*, *695*(1), pp.199-206. Available: https://doi.org/10.1007/s10750-012-1113-1 [2022, January 27]

Blewett, S.C. and Phillips, D., 2016. An overview of Cape Fold Belt geochronology: implications for sediment provenance and the timing of orogenesis. *Origin and evolution of the cape mountains and Karoo Basin*, pp.45-55. DOI 10.1007/978-3-319-40859-0_5

Blinn, D.W. and Bailey, P.C., 2001. Land-use influence on stream water quality and diatom communities in Victoria, Australia: a response to secondary salinization. *Hydrobiologia*, *466*(1), pp.231-244.

Bode, A., Varela, M., Prego, R., Rozada, F. and Santos, M.D., 2017. The relative effects of upwelling and river flow on the phytoplankton diversity patterns in the ria of A Coruña (NW Spain). *Marine biology*, *164*(4), p.93. DOI 10.1007/s00227-017-3126-9

Boger, A.R., Ahiablame, L., Mosase, E. and Beck, D., 2018. Effectiveness of roadside vegetated filter strips and swales at treating roadway runoff: A tutorial review. *Environmental Science: Water Research & Technology*, *4*(4), pp.478-486. DOI: 10.1039/C7EW00230K

Boschker, H.T.S., Kromkamp, J.C. and Middelburg, J.J., 2005. Biomarker and carbon isotopic constraints on bacterial and algal community structure and functioning in a turbid, tidal estuary. *Limnology and Oceanography*, *50*(1), pp.70-80.

Bouwman, L., Goldewijk, K.K., Van Der Hoek, K.W., Beusen, A.H., Van Vuuren, D.P., Willems, J., Rufino, M.C. and Stehfest, E., 2013. Exploring global changes in nitrogen and phosphorus cycles in agriculture induced by livestock production over the 1900–2050 period. *Proceedings of the National Academy of Sciences*, *110*(52), pp.20882-20887. Available: http://www.pnas.org/cgi/doi/10.1073/pnas.1012878108 [2022, January 27]

Brabec, K., Zahrádková, S., Pařil, P., Němejcová, D., Kokeš, J. and Jarkovský, J., 2004. Assessment of organic pollution effect considering differences between lotic and lentic stream habitats. In *Integrated assessment of running waters in Europe*, pp. 331-346. Springer, Dordrecht.

Bush, M.B. and Colinvaux, P.A., 1994. Tropical forest disturbance: paleoecological records from Darien, Panama. *Ecology*, *75*(6), pp.1761-1768.

Buzer, J.S. and Sym, S.D., 1983. Diatoms and pollen in a trial core from Sandwich Harbour, South West Africa (Namibia). *British Phycological Journal*, *18*(2), pp.121-129.

Cañedo-Argüelles, M., Kefford, B.J., Piscart, C., Prat, N., Schäfer, R.B. and Schulz, C.J., 2013. Salinisation of rivers: an urgent ecological issue. *Environmental pollution*, *173*, pp.157-167. Available: https://doi.org/10.1016/j.envpol.2012.10.011 [2022, January 27]

Cantonati, M., Angeli, N., Bertuzzi, E., Spitale, D. and Lange-Bertalot, H., 2012. Diatoms in springs of the Alps: spring types, environmental determinants, and substratum. *Freshwater science*, *31*(2), pp.499-524. DOI: 10.1899/11-065.1

Cantwell, M.G., King, J.W., Burgess, R.M. and Appleby, P.G., 2007. Reconstruction of contaminant trends in a salt wedge estuary with sediment cores dated using a multiple proxy approach. *Marine environmental research*, *64*(2), pp.225-246. Available: https://doi.org/10.1016/j.marenvres.2007.01.004 [2022, January 27]

Car, A., Witkowski, A., Jasprica, N., Ljubimir, S., Čalić, M., Dobosz, S., Radić, I.D. and Hrustić, E., 2019. Epilithic diatom communities from areas of invasive Caulerpa species (Caulerpa taxifolia and Caulerpa cylindracea) in the Adriatic Sea, NE Mediterranean. *Mediterranean Marine Science*, *20*(1), pp.151-173. DOI: 10.12681/mms.14330

Caveney, P., 2015. A Brief History of Knysna from 1770 to 1890. *The Heritage Portal,* Available https://www.theheritageportal.co.za/article/brief-history-knysna-1770-1890 [2022, January 27]

Charlesford farm, n.n. About. Available: https://charlesford.co.za/about.php [2022, January 5]

Chase, B.M., Boom, A., Carr, A.S., Meadows, M.E. and Reimer, P.J., 2013. Holocene climate change in southernmost South Africa: rock hyrax middens record shifts in the southern westerlies. *Quaternary Science Reviews*, *82*, pp.199-205. Available: http://dx.doi.org/10.1016/j.quascirev.2013.10.018 [2022, January 27]

Chen, C.P., Gao, Y.H. and Lin, P., 2005. Biomass, species composition and diversity of benthic diatoms in mangroves of the Houyu Bay, China.

Cheng, F., Song, X., Yu, Z. and Liu, D., 2012. Historical records of eutrophication in Changjiang (Yangtze) River estuary and its adjacent East China Sea. *Biogeosciences Discussions*, *9*(6), pp.6261-6291. doi:10.5194/bgd-9-6261-2012

Cheng, F., Yu, Z. and Song, X., 2014. Long-term changes in sedimentary diatom assemblages and their environmental implications in the Changjiang (Yangtze) River estuary, China. *Chinese journal of oceanology and limnology*, *32*(1), pp.155-161.

Chiba, T., Endo, K., Sugai, T., Haraguchi, T., Kondo, R. and Kubota, J., 2016. Reconstruction of Lake Balkhash levels and precipitation/evaporation changes during the last 2000 years from fossil

diatom assemblages. *Quaternary International*, *397*, pp.330-341. Available: https://doi.org/10.1016/j.quaint.2015.08.009 [2022, January 27]

Clark, B.M., Lane, S., Turpie, J.K., van Niekerk, L. and Morant, P.D., 2002. South Africa National Report Phase 1: Integrated Problem Analysis. *Report prepared for GEF MSP Sub-Saharan Africa Project (GF/6010-0016), Cape Town*.

Claassens, L., Barnes, R.S.K., Wasserman, J., Lamberth, S.J., Miranda, N.A.F., Van Niekerk, L. and Adams, J.B., 2020. Knysna Estuary health: ecological status, threats and options for the future. *African Journal of Aquatic Science*, *45*(1-2), pp.65-82. DOI: 10.2989/16085914.2019.1672518

Coastal & Environmental Services. 2007. Knysna Estuary Management Plan – Volume I: Situation Assessment, CES, Grahamstown.

Cohen, A.L. and Tyson, P.D., 1995. Sea-surface temperature fluctuations during the Holocene off the south coast of Africa: implications for terrestrial climate and rainfall. *The Holocene*, *5*(3), pp.304-312.

Coleman, D.C. and Corbin, F.T., 1991. Introduction and ordinary counting as currently used. In *Carbon isotope techniques*. D.C. Coleman & B. Fry, Eds. San Diego: Academic Press, Inc.3-9.

Collinson, S. 2020. *Knysna: 250 Years of History, 1770-2020: a Timeline of Historical Events and Interesting Information that Make Knysna the Town it is Today.* South Africa: Steve Collinson, 2020

Cooper, J.A.G., 2001. Geomorphological variability among microtidal estuaries from the wave-dominated South African coast. *Geomorphology*, *40*(1-2), pp.99-122. Available: https://doi.org/10.1016/S0169-555X(01)00039-3[2022, January 27]

Cooper, S., Gaiser, E. and Wachnicka, A., 2010. Estuarine paleoenvironmental reconstructions using diatoms. *The diatoms: applications for the environmental and earth sciences*, 2nd ed, J.P. Smol & E.F. Stoermer, Eds. Cambridge: Cambridge University Press. 324-345.

Costa, R.M.D., Matos, J.B., Pinto, K.S.T. and Pereira, L.C.C., 2013. Phytoplankton of a dynamic Amazon sandy beach. *Journal of Coastal Research*, (65), pp.1751-1756. DOI: 10.2112/SI65-296

Costanza, R., d'Arge, R., De Groot, R., Farber, S., Grasso, M., Hannon, B., Limburg, K., Naeem, S., O'neill, R.V., Paruelo, J. and Raskin, R.G., 1997. The value of the world's ecosystem services and natural capital. *nature*, *387*(6630), p.253.

Costanza, R., de Groot, R., Sutton, P., Van der Ploeg, S., Anderson, S.J., Kubiszewski, I., Farber, S. and Turner, R.K., 2014. Changes in the global value of ecosystem services. *Global environmental change*, *26*, pp.152-158.

Cressey, M., Dawson, S., White, R. and Anderson, S., 2010. Early Holocene Relative Sea-Level Changes at Clachan Harbour, Raasay, Scottish Hebrides. *Scottish Archaeological Internet Reports*, *31*,pp.473-480.

Dalu, T. and Froneman, P.W., 2016. Diatom-based water quality monitoring in southern Africa: challenges and future prospects. *Water SA*, *42*(4), pp.551-559. Available: http://dx.doi.org/10.4314/wsa.v42i4.05 [2022, January 27]

Dalu, T., Richoux, N.B. and Froneman, P.W., 2016. Distribution of benthic diatom communities in a permanently open temperate estuary in relation to physico-chemical variables. *South African Journal of Botany*, *107*, pp.31-38. Available: https://doi.org/10.1016/j.sajb.2015.06.004 [2022, January 27]

Day Jr, J.W., Yanez-Arancibia, A., Kemp, W.M. and Crump, B.C., 2013. Introduction to estuarine ecology. *Estuarine ecology*, *2*. John Wiley and Sons. pp.1-19

Dearing, J.A., Yang, X., Dong, X., Zhang, E., Chen, X., Langdon, P.G., Zhang, K., Zhang, W. and Dawson, T.P.,2012. Extending the timescale and range of ecosystem services through paleoenvironmental analyses, exemplified in the lower Yangtze basin. *Proceedings of the National Academy of Sciences*, *109*(18), pp.E1111-E1120. Available: https://www.pnas.org/content/pnas/109/18/E1111.full.pdf [2022, January 27]

Deacon, H.J., 1983. Another look at the Pleistocene climates of South Africa. *South African Journal of Science*, *79*(8), pp.325-328.

De la Rey, P.A., Van Rensburg, L. and Vosloo, A., 2008. On the use of diatom-based biological monitoring Part 1: A comparison of the response of diversity and aut-ecological diatom indices to water quality variables in the Marico-Molopo River catchment. *Water Sa*, *34*(1), pp.53-60.

Davies-Colley, R.J., Nagels, J.W., Smith, R.A., Young, R.G. and Phillips, C.J., 2004. Water quality impact of a dairy cow herd crossing a stream. *New Zealand Journal of Marine and Freshwater Research*, *38*(4), pp.569-576. DOI: 10.1080/00288330.2004.9517262

Delgado, J., Boski, T., Nieto, J.M., Pereira, L., Moura, D., Gomes, A., Sousa, C. and García-Tenorio, R., 2012. Sea-level rise and anthropogenic activities recorded in the late Pleistocene/Holocene sedimentary infill of the Guadiana Estuary (SW Iberia). *Quaternary Science Reviews*, *33*, pp.121-141. Available: http://dx.doi.org/10.1016/j.quascirev.2011.12.002 [2022, January 27]

Delgado, C., Pardo, I. and García, L., 2012. Diatom communities as indicators of ecological status in Mediterranean temporary streams (Balearic Islands, Spain). *Ecological indicators*, *15*(1), pp.131-139. Available: https://doi.org/10.1016/j.ecolind.2011.09.037[2022, January 27]

Della Bella, V., Puccinelli, C., Marcheggiani, S. and Mancini, L., 2007. Benthic diatom communities and their relationship to water chemistry in wetlands of central Italy. *Annales de Limnologie-International Journal of Limnology*, 43(2), pp. 89-99.

De Jonge, M., Van de Vijver, B., Blust, R. and Bervoets, L., 2008. Responses of aquatic organisms to metal pollution in a lowland river in Flanders: a comparison of diatoms and macroinvertebrates. *Science of the Total Environment*, *407*(1), pp.615-629. Available: https://doi.org/10.1016/j.scitotenv.2008.07.02 [2022, January 27]

Department of Environmental Affairs. 2015. Guidelines for the Development and Implementation of Estuarine Management Plans in terms of the National Estuarine Management Protocol. Cape Town.

Department of Water Affairs and Forestry. 1996. South African Water Quality Guidelines, Volume 7: Aquatic Ecosystems. Pretoria, South Africa: Department of Water Affairs and Forestry Republic of South Africa.

Desrosiers, C., Leflaive, J., Eulin, A. and Ten-Hage, L., 2013. Bioindicators in marine waters: benthic diatoms as a tool to assess water quality from eutrophic to oligotrophic coastal ecosystems. *Ecological indicators*, *32*, pp.25-34. Available: https://doi.org/10.1016/j.ecolind.2013.02.021 [2022, January 27]

Diatoms of North America. n.d. *Species.* Available: https://diatoms.org/species [2021, June 24].

Dixit, S.S., Smol, J.P., Kingston, J.C. and Charles, D.F., 1992. Diatoms: powerful indicators of environmental change. Environmental science & technology, 26(1), pp.22-33.

Dokulil, M.T., 2003. Algae as ecological bio-indicators. In *Trace metals and other contaminants in the environment*. Vol. 6, pp. 285-327). Elsevier. Markert, B.A., Breure, A.M. and Zechmeister, H.G. eds., 2003. *Bioindicators and biomonitors*. Elsevier.

Duncan, C.E., 2006. *Holocene environmental change and the vegetation community dynamics of the Kynsna forest: pollen and charcoal analysis of sediments from Groenvlei, Southern Cape, South Africa* (Master's thesis, University of Cape Town).

Du, G., Yan, H. and Dupuy, C., 2017. Microphytobenthos as an indicator of environmental quality status in intertidal flats: case study of coastal ecosystem in Pertuis Charentais, France. Estuarine, Coastal and Shelf Science, 196, pp.217-226. DOI: 10.1016/j.ecss.2017.06.031

Du Plessis, N., Chase, B.M., Quick, L.J., Haberzettl, T., Kasper, T. and Meadows, M.E., 2020. Vegetation and climate change during the Medieval Climate Anomaly and the Little Ice Age on the southern Cape coast of South Africa: Pollen evidence from Bo Langvlei. *The holocene*, *30*(12), pp.1716-1727. DOI: 10.1177/0959683620950444

Dürr, H.H., Laruelle, G.G., van Kempen, C.M., Slomp, C.P., Meybeck, M. and Middelkoop, H., 2011. Worldwide typology of nearshore coastal systems: defining the estuarine filter of river inputs to the oceans. *Estuaries and Coasts*, *34*(3), pp.441-458. Available: https://doi.org/10.1007/s12237-011-9381-y [2022, January 27]

Economou-Amilli, A., 1980. Marine Diatoms from Greece. I. Diatoms from the Saronikos Gulf. *Nova Hedwigia*, *32*(1), pp.63-104.

Else, N.E., 2018. Modern diatom distribution patterns and determining factors in the Knysna Estuary in the Western Cape, South Africa (Honours project).

Engelbrecht, C.J. and Engelbrecht, F.A., 2016. Shifts in Köppen-Geiger climate zones over southern Africa in relation to key global temperature goals. *Theoretical and applied climatology*, *123*(1-2), pp.247-261. DOI 10.1007/s00704-014-1354-1

Engelbrecht, C.J., Landman, W.A., Engelbrecht, F.A. and Malherbe, J., 2015. A synoptic decomposition of rainfall over the Cape south coast of South Africa. *Climate Dynamics*, *44*(9-10), pp.2589-2607. DOI 10.1007/s00382-014-2230-5

Esteban, I., Marean, C.W., Fisher, E.C., Karkanas, P., Cabanes, D. and Albert, R.M., 2018. Phytoliths as an indicator of early modern humans plant gathering strategies, fire fuel and site occupation intensity during the Middle Stone Age at Pinnacle Point 5-6 (south coast, South Africa). *PLoS One*, *13*(6), p.e0198558. Available: https://doi.org/10.1371/journal.pone.0198558 [2022, January 27]

Espinosa, M.A. and Isla, F.I., 2015. Modern diatom assemblages in surface sediments from meso-macrotidal estuaries of Patagonia, Argentina. *Pan-American Journal of Aquatic Science,* 10(1), pp.29-43.

Estrada, M., Henriksen, P., Gasol, J.M., Casamayor, E.O. and Pedrós-Alió, C., 2004. Diversity of planktonic photoautotrophic microorganisms along a salinity gradient as depicted by microscopy, flow cytometry, pigment analysis and DNA-based methods. *FEMS Microbiology Ecology*, *49*(2), pp.281-293.

Falkowski, P.G., Katz, M.E., Knoll, A.H., Quigg, A., Raven, J.A., Schofield, O. and Taylor, F.J.R., 2004. The evolution of modern eukaryotic phytoplankton. science, 305(5682), pp.354-360

Faria, D., Guimarães, A.T.B. and Ludwig, T.A.V., 2013. Responses of periphytic diatoms to mechanical removal of Pistia stratiotes L. in a hypereutrophic subtropical reservoir: dynamics and tolerance.*Brazilian Journal of Biology*, *73*(4), pp.681-689. Available: https://doi.org/10.1590/S1519-69842013000400002 [2022, January 27]

Fox, W.M., Johnson, M.S., Jones, S.R., Leah, R.T. and Copplestone, D., 1999. The use of sediment cores from stable and developing salt marshes to reconstruct historical contamination profiles in the Mersey Estuary, UK. *Marine Environmental Research*, *47*(4), pp.311-329. Available: https://doi.org/10.1016/S0141-1136(98)00123-8 [2022, January 27]

Finné, M., Norström, E., Risberg, J. and Scott, L., 2010. Siliceous microfossils as late-Quaternary paleo-environmental indicators at Braamhoek wetland, South Africa. *The Holocene*, *20*(5), pp.747-760. DOI: 10.1177/0959683610362810

Frankovich, T.A., Gaiser, E.E., Zieman, J.C. and Wachnicka, A.H., 2006. Spatial and temporal distributions of epiphytic diatoms growing on Thalassia testudinum Banks ex König: relationships to water quality. *Hydrobiologia,* 569(1), pp.259-271.DOI 10.1007/s10750-006-0136-x

Ganzey, L.A., Razjigaeva, N.G., Nishimura, Y., Grebennikova, T.A., Kaistrenko, V.M., Gorbunov, A.O., Arslanov, K.A., Chernov, S.B. and Naumov, Y.A., 2015. Deposits of historical and paleotsunamis on the coast of Eastern Primorye. *Russian Journal of Pacific Geology*, *9*(1), pp.64-79. DOI: 10.1134/S1819714015010029

Garcia-Rodriguez, F., Puerto, L.D., Venturini, N., Pita, A.L., Brugnoli, E., Burone, L. and Muniz, P., 2011. Diatoms, protein and carbohydrate sediment content as proxies for coastal eutrophication in Montevideo, Rio de la Plata Estuary, Uruguay. *Brazilian Journal of Oceanography*, *59*(4), pp.293-310.

Gastineau, R., Hamedi, C., Hamed, M.B.B., Abi-Ayad, S.M.E.A., Bąk, M., Lemieux, C., Turmel, M., Dobosz, S., Wróbel, R.J., Kierzek, A. and Lange-Bertalot, H., 2021. Morphological and molecular identification reveals that waters from an isolated oasis in Tamanrasset (extreme South of Algerian Sahara) are colonized by opportunistic and pollution-tolerant diatom species. *Ecological Indicators*, *121*, p.107104. Available: https://doi.org/10.1016/j.ecolind.2020.107104 [2022, January 27]

Gasse, F., Barker, P., Gell, P.A., Fritz, S.C. and Chalie, F., 1997. Diatom-inferred salinity in palaeolakes: an indirect tracer of climate change. *Quaternary Science Reviews*, *16*(6), pp.547-563.

Geldenhuys, C.J., 1991. Distribution, size and ownership of forests in the southern Cape. *South African Forestry Journal*, *158*(1), pp.51-66.

Gillson, L. and Marchant, R., 2014. From myopia to clarity: sharpening the focus of ecosystem management through the lens of palaeoecology. *Trends in Ecology & Evolution*, *29*(6), pp.317-325. Available http://dx.doi.org/10.1016/j.tree.2014.03.010 [2022, January 27]

Gao, X. and Song, J., 2005. Phytoplankton distributions and their relationship with the environment in the Changjiang Estuary, China. *Marine Pollution Bulletin*, *50*(3), pp.327-335.

Gholami, V., 2013. The influence of deforestation on runoff generation and soil erosion (Case study: Kasilian Watershed). *Journal of Forest Science*, *59*(7), pp.272-278.

Ghosh, A. and Filipsson, H.L., 2017. Applications of Foraminifera, Testate Amoebae and Tintinnids in Estuarine Palaeoecology. In *Applications of Paleoenvironmental Techniques in Estuarine Studies*. K. Weckström, K.M. Sauders, P.A. Gell, C.G. Skilbeck (Eds.), Springer, Dordrecht. pp. 313-337. DOI: 10.1007/978-94-024-0990-1_21

Goh, K.M., 1991. Carbon Dating. In *Carbon isotope techniques*. D.C. Coleman & B. Fry, Eds. San Diego: Academic Press, Inc 125-145.

Gomes, A., Boski, T., Moura, D., Szkornik, K., Witkowski, A., Connor, S., Laut, L., Sobrinho, F. and Oliveira, S., 2017, April. Modern diatom assemblages as tools for paleoenvironmental reconstruction: a case study from estuarine intertidal zones in southern Iberia. In *EGU General Assembly Conference Abstracts* (p. 7156).

Google Earth V 7.1 (March 31, 2020). *View of core site B*. AfriGIS 2021. https://earth.google.com/web/ [Accessed 22 June 2021].

Google Earth V 7.1 (March 31, 2020). *View of core site G*. AfriGIS 2021. https://earth.google.com/web/ [Accessed 22 June 2021].

Gordon, N., García-Rodríguez, F. and Adams, J.B., 2012. Paleolimnology of a coastal lake on the Southern Cape coast of South Africa: Sediment geochemistry and diatom distribution. Journal of African Earth Sciences, 75, pp.14-24. Available: https://doi.org/10.1016/j.jafrearsci.2012.06.008 [2022, January 27]

Grimm, E.C. 1997. *TlLIA: A Pollen Program for Analysis and Display*. Illinois State Museum, Springfield.

Grimm, E.C., 1987. CONISS: A Fortran 77 program for stratigraphically constrained cluster analysis by the method of incremental sum of squares. Computers & Geosciences, 13, pp.13–35.

Grindley, J.R. and Heydorn, A.E.F., 1979. Man's impact on estuarine environments. *South African Journal of Science*, *75*(12), pp.554-560.

Haberzettl, T., Kirsten, K.L., Kasper, T., Franz, S., Reinwarth, B., Baade, J., Daut, G., Meadows, M.E., Su, Y. and Mäusbacher, R., 2019. Using 210Pb-data and paleomagnetic secular variations to date anthropogenic impact on a lake system in the Western Cape, South Africa. *Quaternary Geochronology*, *51*, pp.53-63. Available: https://doi.org/10.1016/j.quageo.2018.12.004 [2022, January 27]

Hahn, A., Neumann, F.H., Miller, C., Finch, J., Frankland, T., Cawthra, H.C., Schefuß, E. and Zabel, M., 2021. Mid-to Late Holocene climatic and anthropogenic influences in Mpondoland, South Africa. *Quaternary Science Reviews*, *261*, p.106938. Available: https://doi.org/10.1016/j.quascirev.2021.106938 [2022, January 27]

Hammer, Ø., Harper, D.A.T., Ryan, P.D. 2001. PAST: Paleontological Statistics software for education and data analysis. Paleontologia Electronica 4(1): 9 pp.

Harding, W.R., Archibald, C.G.M. and Taylor, J.C., 2005. The relevance of diatoms for water quality assessment in South Africa: A position paper. *Water Sa*, *31*(1), pp.41-46.

Harding, W.R. and Taylor, J.C., 2011. *The South African Diatom Index (SADI): A Preliminary Index for Indicating Water Quality in Rivers and Streams in Southern Africa: Report to the Water Research Commission*. Water Research Commission.

Hart, T. And Halkett, D., 1998. An Assessment Of Heritage Resources On Thesen Island: Knysna.

Harvey, A.L., 2019. *An investigation of the pollution contribution of catchments surrounding the Knysna Estuary, with implications for stormwater management* (Master's thesis, Faculty of Engineering and the Built Environment).

Heaton, T.J., Köhler, P., Butzin, M., Bard, E., Reimer, R.W., Austin, W.E., Ramsey, C.B., Grootes, P.M., Hughen, K.A., Kromer, B. and Reimer, P.J., 2020. Marine20—the marine radiocarbon age

calibration curve (0–55,000 cal BP). *Radiocarbon*, *62*(4), pp.779-820. DOI:10.1017/RDC.2020.68

Hendrarto, I.B. and Nitisuparjo, M., 2011. Biodiversity of benthic diatom and primary productivity of benthic micro-flora in mangrove forests on central Java. *Journal of Coastal Development*, *14*(2),pp.131-140.

Heinsalu, A., Luup, H., Alliksaar, T., Nõges, P. and Nõges, T., 2007. Water level changes in a large shallow lake as reflected by the plankton: periphyton-ratio of sedimentary diatoms. In European Large Lakes Ecosystem changes and their ecological and socioeconomic impacts (pp. 23-30). Springer, Dordrecht.

Hillebrand, H., Worm, B. and Lotze, H.K., 2000. Marine microbenthic community structure regulated by nitrogen loading and grazing pressure. *Marine Ecology Progress Series*, *204*, pp.27-38. Available: http://www.int-res.com/articles/meps2000/204/m204p027.pdf [2022, January 27]

Hoagland, K.D., Rosowski, J.R., Gretz, M.R. and Roemer, S.C., 1993. Diatom extracellular polymeric substances: function, fine structure, chemistry, and physiology. Journal of Phycology, 29(5), pp.537-566.

Hogg, A.G., Hua, Q., Blackwell, P.G., Niu, M., Buck, C.E., Guilderson, T.P., Heaton, T.J., Palmer, J.G., Reimer, P.J., Reimer, R.W. and Turney, C.S., 2013. SHCal13 Southern Hemisphere calibration, 0–50,000 years cal BP. *Radiocarbon*, *55*(4), pp.1889-1903.

Holmes, M. and Taylor, J.C., 2015. Diatoms as water quality indicators in the upper reaches of the Great Fish River, Eastern Cape, South Africa. *African Journal of Aquatic Science*, *40*(4), pp.321-337.DOI: 10.2989/16085914.2015.1086722

Holmgren, K., Karlén, W., Lauritzen, S.E., Lee-Thorp, J.A., Partridge, T.C., Piketh, S., Repinski, P., Stevenson, C., Svanered, O. and Tyson, P.D., 1999. A 3000-year high-resolution stalagmitebased record of palaeoclimate for northeastern South Africa. *The Holocene*, *9*(3), pp.295-309.

Houlbrooke, D.J., Horne, D.J., Hedley, M.J., Hanly, J.A. and Snow, V.O., 2004. A review of literature on the land treatment of farm-dairy effluent in New Zealand and its impact on water quality. *New Zealand Journal of Agricultural Research*, *47*(4), pp.499-511. DOI: 10.1080/00288233.2004.9513617

Hudon, C. and Bourget, E., 1983. The Effect of Light on the Vertical Structure. *Botanica Marina*, *26*, pp.317-330.

Human, L.R.D., Weitz, R., Allanson, B.R. and Adams, J.B., 2020. Nutrient fluxes from sediments pose management challenges for the Knysna Estuary, South Africa. *African Journal of Aquatic Science*, *45*(1-2), pp.1-9. DOI: 10.2989/16085914.2019.1671787

Humphrey, G.J., Gillson, L. and Ziervogel, G., 2021. How changing fire management policies affect fire seasonality and livelihoods. *Ambio*, *50*(2), pp.475-491. Available: https://doi.org/10.1007/s13280-020-01351-7 [2022, January 27]

Hutchinson, I., James, T.S., Clague, J.J., Barrie, J.V. and Conway, K.W., 2004. Reconstruction of late Quaternary sea-level change in southwestern British Columbia from sediments in isolation basins. *Boreas*, *33*(3), pp.183-194. DOI 10.1080/03009480410001299

Istvánovics, V., 2010. Eutrophication of lakes and reservoirs. *Lake Ecosystem Ecology; Elsevier: San Diego, CA, USA*, pp.47-55.

Iurian, A.R., Millward, G., Blake, W. and Hernández, J.A., 2021. Fine-tuning of 210Pb-based methods for dating vegetated saltmarsh sediments. *Quaternary Geochronology*, *62*, p.101153. Available: https://doi.org/10.1016/j.quageo.2021.101153 [2022, January 27]

Jakovljević, O.S., Popović, S.S., Vidaković, D.P., Stojanović, K.Z. and Krizmanić, J.Ž., 2016. The application of benthic diatoms in water quality assessment (Mlava River, Serbia). *Acta Botanica Croatica*, *75*(2), pp.199-205. DOI: 10.1515/botcro-2016-0032.

Jesus, B., Brotas, V., Ribeiro, L., Mendes, C.R., Cartaxana, P. and Paterson, D.M., 2009. Adaptations of microphytobenthos assemblages to sediment type and tidal position. *Continental Shelf Research*, *29*(13), pp.1624-1634. Available: https://doi.org/10.1016/j.csr.2009.05.006 [2022, January 27]

Jiang, H., 1996. Diatoms from the surface sediments of the Skagerrak and the Kattegat and their relationship to the spatial changes of environmental variables. *Journal of Biogeography*, *23*(2), pp.129-137.

Joubert, R., 2021. History of the Overberg, George, Knysna & Tsitsikamma Forests Pre-modern history to 2011. Available: https://www.discover-sedgefield-south-africa.com/support-files/history-of-the-overberg-george-knysna-and--tsitsikamma-forests-pre-modern-to-2011.pdf [2022, January 27]

Kasim, M., 2011. Correlation of environmental factors and diatom assemblages in Akkeshi-Ko Estuary system. *Journal of Coastal Zone Management*, *14*(3), pp.242-254.

Katsuki, K., Seto, K., Noguchi, T., Sonoda, T. and Kim, J., 2012. Effects of regional climate changes on the planktonic ecosystem and water environment in the frozen Notoro Lagoon, northern Japan. *Marine environmental research*, *81*, pp.83-89. Available: https://doi.org/10.1016/j.marenvres.2012.08.007 [2022, January 27]

Keller, H.M., 2019. *The Subsistence Strategies of Middle and Later Stone Age Foragers During Interstadial/Glacial Transitions at Knysna, South Africa* (Doctoral dissertation, University of Colorado at Denver).

Kelly, M.G., 1998. Use of the trophic diatom index to monitor eutrophication in rivers. *Water research*, *32*(1), pp.236-242.

Kelly, M.G. and Whitton, B.A., 1995. The trophic diatom index: a new index for monitoring eutrophication in rivers. *Journal of applied phycology*, *7*(4), pp.433-444.

Khaleghi, M.R., 2017. The influence of deforestation and anthropogenic activities on runoff generation. *Journal of Forest Science*, *63*(6), pp.245-253. doi: 10.17221/130/2016-JFS

Kirchner, G., 2011. 210Pb as a tool for establishing sediment chronologies: examples of potentials and limitations of conventional dating models. *Journal of Environmental Radioactivity*, *102*(5), pp.490-494.

Kirsten, K., 2008. *Holocene environmental change at Groenvlei, Knysna, South Africa: evidence from diatoms*(Masters dissertation, University of Cape Town).

Kirsten, K., 2014. *Late Holocene diatom community responses to climate variability along the southern Cape coastal plain, South Africa* (Doctoral dissertation, University of Cape Town).

Kirsten, K.L., Haberzettl, T., Wündsch, M., Frenzel, P., Meschner, S., Smit, A.J., Quick, L.J., Mäusbacher, R. and Meadows, M.E., 2018. A multiproxy study of the ocean-atmospheric forcing and the impact of sea-level changes on the southern Cape coast, South Africa during the Holocene. *Palaeogeography, Palaeoclimatology, Palaeoecology*, *496*, pp.282-291. Available: https://doi.org/10.1016/j.palaeo.2018.01.045 [2022, January 27]

Kirsten, K.L., Kasper, T., Cawthra, H.C., Strobel, P., Quick, L.J., Meadows, M.E. and Haberzettl, T., 2020. Holocene variability in climate and oceanic conditions in the winter rainfall zone of South Africa—inferred from a high resolution diatom record from Verlorenvlei. *Journal of Quaternary Science*, 35(4), pp.572-581. DOI: 10.1002/jqs.3200

Kock, A., Taylor, J.C. and Malherbe, W., 2019. Diatom community structure and relationship with water quality in Lake Sibaya, KwaZulu-Natal, South Africa. *South African Journal of Botany*, *123*, pp.161-169. Available https://doi.org/10.1016/j.sajb.2019.03.013 [2022, January 27]

Knysna Municipality, 2020, Final Integrated Development Plan 2020-2021 Amended. Available: https://www.cogta.gov.za/cgta_2016/wp-content/uploads/2020/12/Knysna-final_amended__idp_2020_2021.pdf [2022, January 27]

Korotky, A.M., Razjigaeva, N.G., Grebennikova, T.A., Ganzey, L.A., Mokhova, L.M., Bazarova, V.B., Sulerzhitsky, L.D. and Lutaenko, K.A., 1999. Holocene deposits and paleogeography of Kunashir sland (Kurile Islands). *Geology of the Pacific Ocean*, *18*(1), pp.25-40.

Kraaij, T., Baard, J.A., Arndt, J., Vhengani, L. and Van Wilgen, B.W., 2018. An assessment of climate, weather, and fuel factors influencing a large, destructive wildfire in the Knysna region, South Africa. *Fire Ecology*, *14*(2), pp.1-12. Available: https://doi.org/10.1186/s42408-018-0001-0 [2022, January 27]

Krausmann, F., Haberl, H., Schulz, N.B., Erb, K.H., Darge, E. and Gaube, V., 2003. Land-use change and socio-economic metabolism in Austria—Part I: driving forces of land-use change: 1950–1995. *Land use policy*, *20*(1), pp.1-20. Available: https://doi.org/10.1016/S0264-8377(02)00048-0 [2022, January 27]

Lamberth, S.J. and Turpie, J.K., 2003. The role of estuaries in South African fisheries: economic importance and management implications. *African Journal of Marine Science*, *25*, pp.131-157. DOI: 10.2989/18142320309504005

Lange, K., Liess, A., Piggott, J.J., Townsend, C.R. and Matthaei, C.D., 2011. Light, nutrients and grazing interact to determine stream diatom community composition and functional group structure. *Freshwater Biology*, *56*(2), pp.264-278. doi:10.1111/j.1365-2427.2010.02492.x

Lecointe, C., Coste, M. and Prygiel, J., 1993. "Omnidia": software for taxonomy, calculation of diatom indices and inventories management. *Hydrobiologia*, *269*(1), pp.509-513.

Largier, J.L., Attwood, C. and Harcourt-Baldwin, J.L., 2000. The hydrographic character of the Knysna Estuary. *Transactions of the Royal Society of South Africa*, *55*(2), pp.107-122.

Lemley, D.A., Adams, J.B., Taljaard, S. and Strydom, N.A., 2015. Towards the classification of eutrophic condition in estuaries. *Estuarine, Coastal and Shelf Science*, *164*, pp.221-232. Available: https://doi.org/10.1016/j.ecss.2015.07.033 [2022, January 27]

Lemley, D.A., Adams, J.B. and Bate, G.C., 2016. A review of microalgae as indicators in South African estuaries. *South African Journal of Botany*, *107*, pp.12-20. Available: https://doi.org/10.1016/j.sajb.2016.04.008 [2022, January 27]

Lemley, D.A., Lamberth, S.J., Manuel, W., Nunes, M., Rishworth, G.M., Van Niekerk, L. and Adams, J.B., 2021. Effective management of closed hypereutrophic estuaries requires catchment-scale interventions. *Frontiers in Marine Science*, *8*, p.658. Available: https://doi.org/10.3389/fmars.2021.688933 [2022, January 27]

Lespez, L., Clet-Pellerin, M., Davidson, R., Hermier, G., Carpentier, V. and Cador, J.M., 2010. Middle to Late Holocene landscape changes and geoarchaeological implications in the marshes of the Dives estuary (NW France). *Quaternary International*, *216*(1-2), pp.23-40. doi:10.1016/j.quaint.2009.06.018

Lobo, E.A., Wetzel, C.E., Ector, L., Katoh, K., Blanco Lanza, S. and Mayama, S., 2010. Response of epilithic diatom communities to environmental gradients in subtropical temperate Brazilian rivers. *Limnetica*, *29*(2), pp.0323-340. DOI: 10.23818/limn.29.27

Logan, B. and Taffs, K.H., 2013. Relationship between diatoms and water quality (TN, TP) in sub-tropical east Australian estuaries. *Journal of Paleolimnology*, *50*(1), pp.123-137. DOI 10.1007/s10933-013-9708-8

Lombard, A.T., Strauss, T., Vlok, J., Wolf, T. and Cameron, M., 2005. A Rapid Conservation Assessment and Corridor Design for the Knysna Municipality.

Long, A.J. and Tooley, M.J., 1995. Holocene sea-level and crustal movements in Hampshire and Southeast England, United Kingdom. *Journal of Coastal Research*, pp.299-310.

López, G.I., 2017. Grain size analysis. *Encyclopedia of Earth Science Series Encyclopedia of Geoarchaeology Allan S. Gilbert (Volume Ed.) Springer*, pp.341-348.

Lotze, H.K., Lenihan, H.S., Bourque, B.J., Bradbury, R.H., Cooke, R.G., Kay, M.C., Kidwell, S.M., Kirby, M.X., Peterson, C.H. and Jackson, J.B., 2006. Depletion, degradation, and recovery potential of estuaries and coastal seas. *Science*, *312*(5781), pp.1806-1809.

Maboya, M.L., Meadows, M.E., Reimer, P.J., Backeberg, B.C. and Haberzettl, T., 2018. Late Holocene marine radiocarbon reservoir correction for the southern and eastern coasts of South Africa. *Radiocarbon*, *60*(2), pp.571-582.DOI:10.1017/RDC.2017.139

Mann, D.G., 1999. The species concept in diatoms. Phycologia, 38(6), pp.437-495.

Mann, M.E., Zhang, Z., Rutherford, S., Bradley, R.S., Hughes, M.K., Shindell, D., Ammann, C., Faluvegi, G. and Ni, F., 2009. Global signatures and dynamical origins of the Little Ice Age and Medieval Climate Anomaly. *Science*, *326*(5957), pp.1256-1260.

Marker, M.E., 2000. A descriptive account of sand movement in the Knysna Estuary. *Transactions of the Royal Society of South Africa*, *55*(2), pp.129-139.

Marker, M.E., 2003. The Knysna Basin, South Africa: geomorphology, landscape sensitivity and sustainability. *Geographical Journal*, *169*(1), pp.32-42.

Marker, M.E., 2004. Changes in the Salt River, tributary to the Knysna Estuary, South Africa: 1936–1998. *South African Geographical Journal*, *86*(2), pp.131-140.

Marker, M.E. and Holmes, P.J., 2005. Landscape evolution and landscape sensitivity: the case of the southern Cape. *South African Journal of Science*, *101*(1), pp.53-60.

Marker, M.E. and Holmes, P.J., 2010. The geomorphology of the Coastal Platform in the southern Cape. *South African Geographical Journal*, *92*(2), pp.105-116. DOI:10.1080/03736245.2010.522041

Martin, A.R.H., 1956. The ecology and history of Groenvlei. *South African Journal of Science*, *52*(8), pp.187-192.

Martin, A.R.H., 1959. The stratigraphy and history of Groenvlei, a South African coastal fen. *Australian Journal of Botany*, *7*(2), pp.142-167.

Mašić, E. and Barudanović, S., 2020. New data on distribution of Hydrurus foetidus (Villars) Trevisan in freshwater habitats on Vranica Mountain (Bosnia and Herzegovina). *Borziana,* 1, pp.15-33. Available: https://doi.org/10.7320/Borz.001.015 [2022, January 27]

Masisi, L., Nelwamondo, V. and Marwala, T., 2008, November. The use of entropy to measure structural diversity. In *2008 IEEE International Conference on Computational Cybernetics* (pp. 41-45). IEEE.

Matos, J.B., Sodré, D.K.L., Da Costa, K.G., Pereira, L.C.C. and Da Costa, R.M., 2011. Spatial and temporal variation in the composition and biomass of phytoplankton in an Amazonian estuary. *Journal of Coastal Research*, pp.1525-1529.

Matthes, F.E., 1939. Report of committee on glaciers, April 1939. *Eos, Transactions American Geophysical Union*, *20*(4), pp.518-523.

Matthews, S., 2019. Water history–In the footsteps of RJ Gordon Part 2. *Water Wheel*, *18*(1), pp.10-13.

Matthews, J.A. and Briffa, K.R., 2005. The 'Little Ice Age': re-evaluation of an evolving concept. *Geografiska Annaler: Series A, Physical Geography*, *87*(1), pp.17-36. DOI:10.1111/j.0435-3676.2005.00242.x

Matthews-Bird, F., Valencia, B.G., Church, W., Peterson, L.C. and Bush, M., 2017. A 2000-year history of disturbance and recovery at a sacred site in Peru's northeastern cloud forest. *The Holocene*, *27*(11), pp.1707-1719. DOI: 10.1177/0959683617702232.

McGuirk Flynn, A., 2008. Organic matter and nutrient cycling in a coastal plain estuary: carbon, nitrogen, and phosphorus distributions, budgets, and fluxes. *Journal of Coastal Research*, (10055), pp.76-94. DOI: 10.2112/SI55-010.1.

McQuoid, M.R. and Nordberg, K., 2003. The diatom Paralia sulcata as an environmental indicator species in coastal sediments. *Estuarine, Coastal and Shelf Science*, *56*(2), pp.339-354. Available: https://doi.org/10.1016/S0272-7714(02)00187-7 [2022, January 27]

Méléder, V., Rincé, Y., Barillé, L., Gaudin, P. and Rosa, P., 2007. Spatiotemporal changes in microphytobenthos assemblages in a macrotidal flat (Bourgneuf Bay, France) 1. *Journal of phycology*, *43*(6), pp.1177-1190. DOI: 10.1111/j.1529-8817.2007.00423.x

Melo-Magalhães, E.M., do Nascimento Moura, A., Medeiros, P.R.P. and Koening, M.L., 2016. Microphytoplankton biomass and trophic state of the estuarine region of São Francisco River (Northeastern Brazil). *Brazilian Journal of Aquatic Science and Technology*, *20*(2), pp.51-62. DOI:10.14210/bjast.v20n2.

Midgley, J.J., Cowling, R.M., Seydack, A.H.W., van Wyk, G.F. 1997. Forest. In *Vegetation of Southern Africa.* R.M. Cowling, D.M. Richardson, S.M. Pierce, Eds.). Pp.278-295. Cambridge University Press, Cambridge.

Millennium Ecosystem Assessment., 2005. Ecosystems and Human Well-Being: Synthesis. Island Press, Washington, DC. pp.1-155.

Mitlehner, A.G., 1992. Palaeoenvironments of the Hoxnian Nar Valley Clay, Norfolk, England: evidence from an integrated study of diatoms and ostracods. *Journal of Quaternary Science*, *7*(4), pp.335-341.

Montoya Moreno, Y. and Aguirre Ramírez,, N.J., 2013. Knowledge to ecological preferences in a tropical epiphytic algae to use with eutrophication indicators. *Journal of Environmental Protection*, pp.27-35 Available: http://dx.doi.org/10.4236/jep.2013.411A1004 [2022, January 27]

Mosisch, T.D. and Arthington, A.H., 1998. The impacts of power boating and water skiing on lakes and reservoirs. *Lakes & Reservoirs: Research & Management*, *3*(1), pp.1-17.

Moss, B., 1977. Adaptations of epipelic and epipsammic freshwater algae. *Oecologia*, *28*(1), pp.103-108.

Mucina, L., Adams, J.B., Knevel, I.C., Rutherford, M.C., Powrie, L.W., Bolton, J.J., van der Merwe, J.H., Anderson, R.J., Bornman, T.G., le Roux, A. and Janssen, J.A., 2006. Coastal vegetation of South Africa. *The vegetation of South Africa, Lesotho and Swaziland*, pp.658-697.

Nakagawa, T., 2007. PolyCounter ver.1.0 & Ergodex DX-1: a cheap and very ergonomic counter board system. Quaternary International, 167-668(Supplement), pp.3–486

Napier, V.R., Turpie, J.K. and Clark, B.M., 2009. Value and management of the subsistence fishery at Knysna Estuary, South Africa. *African Journal of Marine Science*, *31*(3), pp.297-310. DOI: 10.2989/AJMS.2009.31.3.3.991

Nche-Fambo, F.A., Scharler, U.M. and Tirok, K., 2015. Resilience of estuarine phytoplankton and their temporal variability along salinity gradients during drought and hypersalinity. *Estuarine, Coastal and Shelf Science*, *158*, pp.40-52. Available: http://dx.doi.org/10.1016/j.ecss.2015.03.011 [2022, January 27]

Negus, P.M., Marshall, J.C., Steward, A.L., Mcgregor, G.B. and O'Connor, R.A., 2020. Aquatic biota in hot water: thermal gradients in rheocrene hot spring discharges as analogues for the effects of climate warming. *Knowledge & Management of Aquatic Ecosystems*, (421), p.49-63. Available: https://doi.org/10.1051/kmae/2020042 [2022, January 27]

Nesje, A. and Dahl, S.O., 2003. The 'little ice age'–only temperature?. *The Holocene*, *13*(1), pp.139-145. DOI: 10.1191/0959683603hl603fa

Nguetsop, V.F., Servant-Vildary, S. and Servant, M., 2004. Late Holocene climatic changes in west Africa, a high resolution diatom record from equatorial Cameroon. *Quaternary Science Reviews*, *23*(5-6), pp.591-609. Available: https://doi.org/10.1016/j.quascirev.2003.10.007 [2022, January 27]

Nodine, E.R. and Gaiser, E.E., 2014. Distribution of diatoms along environmental gradients in the Charlotte Harbor, Florida (USA), estuary and its watershed: Implications for bioassessment of salinity and nutrient concentrations. *Estuaries and coasts*, *37*(4), pp.864-879. Available: https://doi.org/10.1007/s12237-013-9729-6 [2022, January 27]

Noga, T., Stanek-Tarkowska, J., Kloc, U., Kochman-Kędziora, N., Rybak, M., Peszek, Ł. and Pajączek, A., 2016. Diatom diversity and water quality of a suburban stream: a case study of the Rzeszów city in SE Poland. *Biodiversity Research and Conservation*, *41*(1), pp.19-34.

Novotny, V., 1999. Diffuse pollution from agriculture—a worldwide outlook. Water science and technology, 39(3), pp.1-13.

Nunes, M., Lemley, D.A., Matcher, G.F. and Adams, J.B., 2021. The influence of estuary eutrophication on the benthic diatom community: a molecular approach. *African Journal of Marine Science*, 43(2). Pp.1-16. DOI: 10.2989/1814232X.2021.1897039

O'Boyle, S. and Silke, J., 2010. A review of phytoplankton ecology in estuarine and coastal waters around Ireland. *Journal of plankton research*, *32*(1), pp.99-118.

O'Donoghue, S., Lehmann, M., Major, D., Major-Ex, G., Sutherland, C., Motau, A., Haddaden, N., Kibria, A.S., Costanza, R., Groves, C. and Behie, A., 2021. Adaptation to climate change in small coastal cities: The influence of development status on adaptation response. *Ocean & Coastal Management*, *211*, p.105788. Available: https://doi.org/10.1016/j.ocecoaman.2021.105788 [2022, January 27]

Ortiz-Burgos S. 2016. Shannon-Weaver Diversity Index. In: Kennish M.J. (eds) Encyclopedia of Estuaries. Encyclopedia of Earth Sciences Series. Springer, Dordrecht

Pan, Y., Stevenson, R.J., Hill, B.H., Herlihy, A.T. and Collins, G.B., 1996. Using diatoms as indicators of ecological conditions in lotic systems: a regional assessment. *Journal of the North American Benthological Society*, *15*(4), pp.481-495.

Patrick, R. 1954. Use of Algae, Especially Diatoms, in the Assessment of Water Quality, in *Biological Methods for the Assessment of Water Quality*, edited by Cairns, J. and Dickson, K. (West Conshohocken, PA: ASTM International, 76-95. Available: https://doi-org.ezproxy.uct.ac.za/10.1520/STP34718S [2022, January 27]

Parsons, M.L., Dortch, Q., Turner, R.E. and Rabalais, N.N., 1999. Salinity history of coastal marshes reconstructed from diatom remains. *Estuaries*, *22*(4), pp.1078-1089.

Pereira, L.C., Monteiro, M.C., Guimarães, D.O., Matos, J.B. and Costa, R.M.D., 2010. Seasonal effects of wastewater to the water quality of the Caeté river estuary, Brazilian Amazon. Anais da Academia Brasileira de Ciências, 82(2), pp.467-478. DOI: 10.2112/SI65-296.

Perez, L., García-Rodríguez, F. and Hanebuth, T.J., 2017. Paleosalinity Changes in the Río de la Plata Estuary and on the Adjacent Uruguayan Continental Shelf over the Past 1200 Years: An Approach Using Diatoms as a Proxy. In *Applications of Paleoenvironmental Techniques in Estuarine Studies.* K. Weckström, K.M. Sauders, P.A. Gell, C.G. Skilbeck (Eds.), Springer, Dordrecht. pp. 529-549. DOI: 10.1007/978-94-024-0990-1_21

Petermann, E., Knöller, K., Rocha, C., Scholten, J., Stollberg, R., Weiß, H. and Schubert, M., 2018. Coupling end-member mixing analysis and isotope mass balancing (222-Rn) for differentiation of fresh and recirculated submarine groundwater discharge into Knysna Estuary, South Africa. *Journal of Geophysical Research: Oceans*, *123*(2), pp.952-970. Available: https://doi.org/10.1002/2017JC013008 [2022, January 27]

Petrov, A. and Nevrova, E., 2007. Database on Black Sea benthic diatoms (Bacillariophyta): its use for a comparative study of diversity pecularities under technogenic pollution impacts. *Ocean Biodiversity Informatics*, *202*(37), pp.153-165.

Pienitz, R., Roberge, K. and Vincent, W.F., 2006. Three hundred years of human-induced change in an urban lake: paleolimnological analysis of Lac Saint-Augustin, Quebec City, Canada. *Botany*, *84*(2), pp.303-320. DOIi:10.1139/B05-152

Plankton Net. n.d. *Index.* Available:
https://planktonnet.awi.de/index.php?contenttype=image_details&itemid=60989#search [2021, June 24]

Plenković-Moraj, A., Kralj, K. and Gligora, M., 2008. Effect of current velocity on diatom colonization on glass slides in unpolluted headwater creek. *Periodicum biologorum*, *110*(3), pp.291-295.

Pollard, M., Whitfield, A.K. and Hodgson, A.N., 2018. Possible influences of a macroalgal bloom in eelgrass beds on fish assemblages in the lower Knysna Estuary, South Africa. *African Journal of Aquatic Science*, *43*(3), pp.319-323. DOI: 10.2989/16085914.2018.1515063

Potapova, M., 2011. Patterns of diatom distribution in relation to salinity. In *The diatom world* (pp. 313-332). Springer, Dordrecht.

Potapova, M.G. and Charles, D.F., 2002. Benthic diatoms in USA rivers: distributions along spatial and environmental gradients. *Journal of biogeography*, *29*(2), pp.167-187.

Quick, L.J., Chase, B.M., Wuendsch, M., Kirsten, K.L., Chevalier, M., Maeusbacher, R., Meadows, M.E. and Haberzettl, T., 2018. A high-resolution record of Holocene climate and vegetation dynamics from the southern Cape coast of South Africa: pollen and microcharcoal evidence from Eilandvlei. *Journal of Quaternary Science*, *33*(5), pp.487-500. DOI: 10.1002/jqs.3028

R Core Team. 2020. R: A language and environment for statistical computing. R Foundation for Statistical Computing, Vienna, Austria. URL https://www.R-project.org/.

Ramsey, C.B., 2009. Bayesian analysis of radiocarbon dates. *Radiocarbon*, *51*(1), pp.337-360. Available :http://dx.doi.org/10.1017/S0033822200033865 [2022, January 27]

Ranalli, A.J., 2004. *A summary of the scientific literature on the effects of fire on the concentration of nutrients in surface waters*. GEOLOGICAL SURVEY RESTON VA.

Raw, J.L., Riddin, T., Wasserman, J., Lehman, T.W.K., Bornman, T.G. and Adams, J.B., 2020. Salt marsh elevation and responses to future sea-level rise in the Knysna Estuary, South Africa. *African Journal of Aquatic Science*, *45*(1-2), pp.49-64. DOI: 10.2989/16085914.2019.1662763

Razjigaeva, N.G., Ganzey, L.A., Grebennikova, T.A., Belyanina, N.I., Lebedev, A.M., Maksimov, F.E. and Kuznetsov, V.Y., 2014. Middle Pleistocene warming phase based on the deposits of a buried oyster reef, Southern Lesser Kuril Islands. *Doklady Earth Sciences*, 455(2), p. 376-382. Springer Nature BV. DOI:10.1134/S1028334X14040102.

Razjigaeva, N.G., Ganzey, L.A., Grebennikova, T.A., Ivanova, E.D., Lyaschevskaya, M.S., Kharlamov, A.A. and Kaistrenko, V.M., 2014b. Deposits of the Tohoku Tsunami (March 11, 2011) in the southern Kuril Islands: Composition and fossils. *Oceanology*, *54*(3), pp.374-386. DOI: 10.1134/S0001437014020209

Razjigaeva, N.G., Ganzey, L.A., Nishimura, Y., Grebennikova, T.A., Sugawara, D., Takashimizu, Y., Lebedev, I.I., Gorbunov, A.O., Arslanov, K.A., Maksimov, F.E. and Petrov, A.Y., 2020. Reconstruction of Late Holocene Extreme Hydrological Events of the Valentin Bay Coast, the Sea of Japan. *Russian Journal of Pacific Geology*, *14*, pp.180-192. Available: https://doi.org/10.1134/S1819714020020086 [2022, January 27]

Reddering, JSV & Esterhuysen, K., 1987. Sediment dispersal in the Knysna estuary: environmental management considerations. *South African journal of geology*, *90*(4), pp.448-457.

Reid, W.V., Mooney, H.A., Cropper, A., Capistrano, D., Carpenter, S.R., Chopra, K., Dasgupta, P., Dietz, T., Duraiappah, A.K., Hassan, R. and Kasperson, R., 2005. *Ecosystems and human well-being Synthesis: A report of the Millennium Ecosystem Assessment*. Pp.1-155 Washington Island Press.

Reid, M.A., Tibby, J.C., Penny, D. and Gell, P.A., 1995. The use of diatoms to assess past and present water quality. *Australian Journal of Ecology*, *20*(1), pp.57-64

Reimer, P.J., Bard, E., Bayliss, A., Beck, J.W., Blackwell, P.G., Ramsey, C.B., Buck, C.E., Cheng, H., Edwards, R.L., Friedrich, M. and Grootes, P.M., 2013. IntCal13 and Marine13 radiocarbon age calibration curves 0–50,000 years cal BP. *radiocarbon*, *55*(4), pp.1869-1887. DOI: 10.2458/azu_js_rc.55.16947

Ribeiro, L., Brotas, V., Rincé, Y. and Jesus, B., 2013. Structure and diversity of intertidal benthic diatom assemblages in contrasting shores: a case study from the Tagus estuary1. *Journal of Phycology*, *49*(2), pp.258-270. DOI: 10.1111/jpy.12031

Rimet, F., Bouchez, A. and Tapolczai, K., 2016. Spatial heterogeneity of littoral benthic diatoms in a large lake: monitoring implications. *Hydrobiologia*, *771*(1), pp.179-193. DOI:10.1007/s10750-015-2629-y

Roffe, S.J., Fitchett, J.M. and Curtis, C.J., 2019. Classifying and mapping rainfall seasonality in South Africa: a review. *South African Geographical Journal= Suid-Afrikaanse Geografiese Tydskrif*, *101*(2), pp.158-174. DOI:10.1080/03736245.2019.1573151

Roffe, S.J., Fitchett, J.M. and Curtis, C.J., 2021. Quantifying rainfall seasonality across South Africa on the basis of the relationship between rainfall and temperature. *Climate Dynamics*, *56*(7), pp.2431-2450. Available: https://doi.org/10.1007/s00382-020-05597-5 [2022, January 27]

Rovira, L., Trobajo, R. and Ibáñez, C., 2012. The use of diatom assemblages as ecological indicators in highly stratified estuaries and evaluation of existing diatom indices. *Marine Pollution Bulletin*,

64(3), pp.500-511. Available https://doi.org/10.1016/j.marpolbul.2012.01.005 [2022, January 27]

Round, F.E., Crawford, R.M. and Mann, D.G., 1990. Diatoms: biology and morphology of the genera. Cambridge University Press.

Ruocco, N., Cavaccini, V., Caramiello, D., Ianora, A., Fontana, A., Zupo, V. and Costantini, M., 2019. Noxious effects of the benthic diatoms Cocconeis scutellum and Diploneis sp. on sea urchin development: Morphological and de novo transcriptomic analysis. *Harmful algae*, *86*, pp.64-73. Available: https://doi.org/10.1016/j.hal.2019.05.009 [2022, January 27]

Russell, I.A., 1997. Water quality in the Knysna estuary. *Oceanographic Literature Review*, *44*(3), pp.271-271.

Russell I.A., Randall R.M. & Kruger, N. 2012. Garden Route National Park, Knysna Coastal Section, State of Knowledge. South African National Parks.

Ryabushko, L.I., Balycheva, D.S. and Ryabushko, V.I., 2017. Microphytobenthos diatoms of the Black Sea: Biodiversity and ecology. *Ecologica Montenegrina*, *14*, pp.48-59.

Salomoni, S.E., Rocha, O. and Torgan, L.C., 2017. Seasonal and spatial variation of the epilithic diatoms: case study of an organic pollution gradient in a subtropical region of southern Brazil. *Acta Limnologica Brasiliensia*, *29*. Available: https://doi.org/10.1590/S2179-975X1816 [2022, January 27]

Salomoni, S.E., Rocha, O., Callegaro, V.L. and Lobo, E.A., 2006. Epilithic diatoms as indicators of water quality in the Gravataí river, Rio Grande do Sul, Brazil. *Hydrobiologia*, *559*(1), pp.233-246. DOI 10.1007/s10750-005-9012-3

Sanders, J.G., Cibik, S.J., D'Elia, C.F. and Boynton, W.R., 1987. Nutrient enrichment studies in a coastal plain estuary: changes in phytoplankton species composition. Canadian Journal of Fisheries and Aquatic Sciences, 44(1), pp.83-90.

Sato, H., Kumano, S., Maeda, Y., Nakamura, T. and Matsuda, I., 1998. The holocene development of Kushu lake on Rebun island in Hokkaido, Japan. Journal of Paleolimnology, 20(1), pp.57-69.

Sawai, Y., 2001. Distribution of living and dead diatoms in tidal wetlands of northern Japan: relations to taphonomy. *Palaeogeography, Palaeoclimatology, Palaeoecology*, *173*(3-4), pp.125-141. Available: https://doi.org/10.1016/S0031-0182(01)00313-3 [2022, January 27]

Sawai, Y., Horton, B.P., Kemp, A.C., Hawkes, A.D., Nagumo, T. and Nelson, A.R., 2016. Relationships between diatoms and tidal environments in Oregon and Washington, USA. *Diatom research*, *31*(1), pp.17-38.

Sawai, Y., Horton, B.P. and Nagumo, T., 2004. The development of a diatom-based transfer function along the Pacific coast of eastern Hokkaido, northern Japan—an aid in paleoseismic studies

of the Kuril subduction zone. *Quaternary Science Reviews*, *23*(23-24), pp.2467-2483. Available: https://doi.org/10.1016/j.quascirev.2004.05.006 [2022, January 27]

Sawai, Y. and Nagumo, T., 2003. Diatom (Bacillariophyceae) flora of salt marshes along the Pacific coast of eastern Hokkaido, northern Japan. *Bulletin of the Nippon Dental University. General education*, *32*, pp.93-108.

Scanlon, B.R., Jolly, I., Sophocleous, M. and Zhang, L., 2007. Global impacts of conversions from natural to agricultural ecosystems on water resources: Quantity versus quality. *Water resources research*, *43*(3), pp.1-18. DOI:10.1029/2006WR005486

Schelske, C.L., Peplow, A., Brenner, M. and Spencer, C.N., 1994. Low-background gamma counting: applications for 210 Pb dating of sediments. *Journal of Paleolimnology*, *10*(2), pp.115-128.

Schumann, E.H., 2000. Oceanic exchanges and temperature variability in the Knysna Estuary. *Transactions of the Royal Society of South Africa*, *55*(2), pp.123-128. DOI: 10.1080/00359190009520438

Schumann, E.H., Largier, J.L. and Slinger, J.H., 1999. Estuarine hydrodynamics. *Estuaries of South Africa*, *3*, pp.27-52. Available: https://doi-org.ezproxy.uct.ac.za/10.1017/CBO9780511525490 [2022, January 27]

Schnurrenberger, D., Russell, J. and Kelts, K., 2003. Classification of lacustrine sediments based on sedimentary components. *Journal of Paleolimnology*, *29*(2), pp.141-154.

Scholz, B. and Liebezeit, G., 2012. Microphytobenthic dynamics in a Wadden Sea intertidal flat–Part I: Seasonal and spatial variation of diatom communities in relation to macronutrient supply. *European Journal of Phycology*, *47*(2), pp.105-119. DOI: 10.1080/09670262.2012.663793

Schröder, M., Sondermann, M., Sures, B. and Hering, D., 2015. Effects of salinity gradients on benthic invertebrate and diatom communities in a German lowland river. *Ecological indicators*, *57*, pp.236-248. Available: https://doi.org/10.1016/j.ecolind.2015.04.038 [2022, January 27]

Sealy, J., 2003. Managing collections of human remains in South African museums and universities: ethical policy-making and scientific value: reviews of current issues and research findings: human origins research in South Africa. *South African journal of science*, *99*(5), pp.238-239.

Shibabaw, T., Beyene, A., Awoke, A., Tirfie, M., Azage, M. and Triest, L., 2021. Diatom community structure in relation to environmental factors in human influenced rivers and streams in tropical Africa. *Plos one*, *16*(2), p.e0246043. Available: https://doi.org/10.1371/journal.pone.0246043 [2022, January 27]

Shirey, P.D., Cowley, D.E. and Sallenave, R., 2008. Diatoms from gut contents of museum specimens of an endangered minnow suggest long-term ecological changes in the Rio Grande (USA). *Journal of paleolimnology*, *40*(1), pp.263-272. DOI 10.1007/s10933-007-9156-4

Sieburth, J.M. and Thomas, C.D., 1973. Fouling on eelgrass (Zostera Marine L.) 1. *Journal of phycology*, *9*(1), pp.46-50.

Simpson, K., 2003. *Foraminiferal species distributions and sedimentological dynamics of the Knysna estuary, South Africa* (Master's thesis, University of Cape Town).

Sitoe, S.R., Risberg, J., Norström, E. and Westerberg, L.O., 2017. Late Holocene sea-level changes and paleoclimate recorded in Lake Lungué, southern Mozambique. *Palaeogeography, palaeoclimatology, palaeoecology*, *485*, pp.305-315. Available: https://doi.org/10.1016/j.palaeo.2017.06.022 [2022, January 27]

Sládeček, V., 1986. Diatoms as indicators of organic pollution. *Acta hydrochimica et hydrobiologica*, *14*(5), pp.555-566.

Snow, G.C., 2007. *Contributions to the use of microalgae in estuarine freshwater reserve determinations* (Doctoral dissertation, PhD thesis, Nelson Mandela Metropolitan University. South Africa).

Soeprobowati, T.R., Hariyati, R. and Gell, P., 2019, May. Paleolimnology Record of Human Impact on a Lake Ecosystem: The Case of Shallow Lakes in Central Java. In *IOP Conference Series: Earth and Environmental Science* (Vol. 276, No. 1, p. 012015). IOP Publishing. doi:10.1088/1755-1315/276/1/012015

Soeprobowati, T.R., Suedy, S.W.A., Lubis, A.A. and Gell, P., 2018. Diatom assemblage in the 24 cm upper sediment associated with human activities in Lake Warna Dieng Plateau Indonesia . *Environmental Technology & Innovation*, *10*, pp.314-323. Available: https://doi.org/10.1016/j.eti.2018.03.007 [2022, January 27]

Sriyaraj, K. and Shutes, R.B.E., 2001. An assessment of the impact of motorway runoff on a pond, wetland and stream. *Environment international*, *26*(5-6), pp.433-439. Available: https://doi.org/10.1016/S0160-4120(01)00024-1 [2022, January 27]

Stager, J.C., Mayewski, P.A., White, J., Chase, B.M., Neumann, F.H., Meadows, M.E., King, C.D. and Dixon, D.A., 2012. Precipitation variability in the winter rainfall zone of South Africa during the last 1400 yr linked to the austral westerlies. *Climate of the Past*, *8*(3), pp.877-887. doi:10.5194/cp-8-877-2012

Stager, J.C., Ryves, D.B., King, C., Madson, J., Hazzard, M., Neumann, F.H. and Maud, R., 2013. Late Holocene precipitation variability in the summer rainfall region of South Africa. *Quaternary science reviews*, *67*, pp.105-120. Available: https://doi.org/10.1016/j.quascirev.2013.01.022 [2022, January 27]

Starratt, S.W., 2007. Diatoms in estuaries and tidal marshes. *The Paleontological Society Papers*, *13*, pp.85-109

Stevenson, R.J., 1984. Epilithic and epipelic diatoms in the Sandusky River, with emphasis on species diversity and water pollution. *Hydrobiologia*, *114*(3), pp.161-175.

Stewart, E.M., Hargan, K.E., Sivarajah, B., Kimpe, L.E., Blais, J.M. and Smol, J.P., 2018. A paleoenvironmental study tracking eutrophication, mining pollution, and climate change in Niven Lake, the first sewage lagoon of Yellowknife (Northwest Territories). *Arctic*, *71*(2), pp.201-217. Available: https://doi.org/10.14430/arctic4720 [2022, January 27]

Stidolph, S.R., Sterrenburg, F.A.S., Smith, K.E.L., and Kraberg, A., 2012. *Stuart R. Stidolph Diatom Atlas: U.S. Geological Survey Open-File Report 2012–1163*. Available: http://pubs.usgs.gov/of/2012/1163/ [2021, June 24]

Storme, A., Bastiaens, J., Crombé, P., Cruz, F., Louwye, S., Verhegge, J. and Deforce, K., 2020. The significance of palaeoecological indicators in reconstructing estuarine environments: a multi-proxy study of increased Middle Holocene tidal influence in the lower Scheldt rive N-Belgium. *Quaternary Science Reviews*, *230*, p.106113. Available: https://doi.org/10.1016/j.quascirev.2019.106113 [2022, January 27]

Spellerberg, I.F. and Fedor, P.J., 2003. A tribute to Claude Shannon (1916–2001) and a plea for more rigorous use of species richness, species diversity and the 'Shannon–Wiener'Index. *Global ecology and biogeography*, *12*(3), pp.177-179.

Switzer, T., 2008. Urea loading from a spring storm—Knysna estuary, South Africa. *Harmful Algae*, *8*(1), pp.66-69. Available: https://doi.org/10.1016/j.hal.2008.08.005 [2022, January 27]

Tagliapietra, D., Sigovini, M. and Magni, P., 2012. Saprobity: a unified view of benthic succession models for coastal lagoons. *Hydrobiologia*, *686*(1), pp.15-28. Available: https://doi.org/10.1007/s10750-012-1001-8 [2022, January 27]

Taffs, K.H., Farago, L.J., Heijnis, H. and Jacobsen, G., 2008. A diatom-based Holocene record of human impact from a coastal environment: Tuckean Swamp, eastern Australia. *Journal of Paleolimnology*, *39*(1), pp.71-82. DOI 10.1007/s10933-007-9096-z

Taffs, K.H., Saunders, K.M. and Logan, B., 2017. Diatoms as indicators of environmental change in estuaries. In *Applications of Paleoenvironmental Techniques in Estuarine Studies.* K. Weckström, K.M. Sauders, P.A. Gell, C.G. Skilbeck (Eds.), Springer, Dordrecht. pp. 277-294. DOI:10.1007/978-94-024-0990-1_21

Talma, A.S. and Vogel, J.C., 1992. Late Quaternary paleotemperatures derived from a speleothem from Cango caves, Cape province, South Africa. *Quaternary Research*, *37*(2), pp.203-213.

Taylor, J.C, Harding, W.R. and Archibald, G.M., 2007. An Illustrated Guide to Some Common Diatom Species from South Africa. Report no. TT282/07. Pretoria: Water Research Commission.

Teichert, N., Borja, A., Chust, G., Uriarte, A. and Lepage, M., 2016. Restoring fish ecological quality in estuaries: implication of interactive and cumulative effects among anthropogenic stressors. *Science of the Total Environment*, *542*, pp.383-393. Available: https://doi.org/10.1016/j.scitotenv.2015.10.068 [2022, January 27]

Temizel, B., Soylu, E. N. and Maraslioglu, F., 2017. Water quality assessment of the Pazarsuyu Stream based on epilithic diatom communities, *Fundamental and Applied Limnology*, 190(3), pp. 189–197. doi: 10.1127/fal/2017/0991.

Teske, P.R. and Wooldridge, T.H., 2003. What limits the distribution of subtidal macrobenthos in permanently open and temporarily open/closed South African estuaries? Salinity vs. sediment particle size. *Estuarine, coastal and shelf science*, *57*(1-2), pp.225-238.

Troels-Smith, J., 1955. Karakterisering af løse jordarter. *Danmarks Geologiske Undersøgelse IV. Række*, *3*(10), pp.1-73.

Trobajo, R. and Sullivan, M.J., 2010. Applied diatom studies in estuaries and shallow coastal environments. In *The diatoms: applications for the environmental and earth sciences*, 2nd ed, J.P. Smol & E.F. Stoermer, Eds. Cambridge: Cambridge University Press. 309-323.

Tsoy, I., Prushkovskaya, I., Aksentov, K. and Astakhov, A., 2015. Environmental changes in the Amur Bay (Japan/East Sea) during the last 150 years revealed by examination of diatoms and silicoflagellates. *Ocean Science Journal*, *50*(2), pp.433-444. Available: http://dx.doi.org/10.1007/s12601-015-0039-8[2022, January 27]

Turpie, J. and Clark, B. 2007. The health statues, conservation importance, and economic value of temperate South African estuaries and the development of a regional conservation plan. *C.A.P.E. Estuaries Conservation Plan*.

Tyson, P.D., 1964. Berg winds of South Africa. *Weather*, *19*(1), pp.7-11.

Tyson, P.D. and Lindesay, J.A., 1992. The climate of the last 2000 years in southern Africa. *The Holocene*, *2*(3), pp.271-278. Available: https://doi.org/10.1177%2F095968369200200310 [2022, January 27]

Ubertini, M., Lefebvre, S., Rakotomalala, C. and Orvain, F., 2015. Impact of sediment grain-size and biofilm age on epipelic microphytobenthos resuspension. *Journal of experimental marine biology and ecology*, *467*, pp.52-64. Available http://dx.doi.org/10.1016/j.jembe.2015.02.007 [2022, January 27]

Underwood, G. J. C.1994. Seasonal and spatial variation in epipelic diatom assemblages in the severn estuary' *Diatom Research*, 9(2), pp. 451–472. doi: 10.1080/0269249x.1994.9705319.

Underwood, G., Phillips, J. and Saunders, K., 1998. Distribution of estuarine benthic diatom species along salinity and nutrient gradients. *European Journal of Phycology*, *33*(2), pp.173-183.

Underwood, G.J. and Provot, L., 2000. Determining the environmental preferences of four estuarine epipelic diatom taxa: growth across a range of salinity, nitrate and ammonium conditions. *European Journal of Phycology*, *35*(2), pp.173-182.

Van Dam, H., Mertens, A. and Sinkeldam, J., 1994. A coded checklist and ecological indicator values of freshwater diatoms from the Netherlands. *Netherland Journal of Aquatic Ecology*, *28*(1), pp.117-133.

Van Damme, S., Struyf, E., Maris, T., Ysebaert, T., Dehairs, F., Tackx, M., Heip, C. and Meire, P., 2005. Spatial and temporal patterns of water quality along the estuarine salinity gradient of the Scheldt estuary (Belgium and The Netherlands): results of an integrated monitoring approach *Hydrobiologia*, *540*(1-3), pp.29-45. DOI 10.1007/s10750-004-7102-2

Van Niekerk, L. and Turpie, J.K. (eds) 2012. South African National Biodiversity Assessment 2011: Technical Report. Volume 3: Estuary Component. CSIR Report Number CSIR/NRE/ECOS/ER/2011/0045/B. Council for Scientific and Industrial Research, Stellenbosch.

Van Wilgen, B.W., 1984. Fire climates in the southern and western Cape Province and their potential use in fire control and management. *South African Journal of Science*, *80*(8), p.358.

Venkateswarlu, V., 1986. Ecological studies on the rivers of Andhra Pradesh with special reference to water quality and pollution. *Proceedings: Plant Sciences*, *96*(6), pp.495-508.

Villanueva, D., Queimaliños, C., Modenutti, B. and Ayala, J., 2000. Effects of fish farm effluents on the periphyton of an Andean stream. *Archive of Fishery and Marine Research/Archiv fur Fischerei und Meeresforschung*, *48*(3), pp.283-294.

Vos, P.C., 1988. Methodological aspects of paleo-ecological diatom research in coastal areas of the Netherlands. *Geologie en Mijnbouw*, *67*, pp.31-40.

Vos, P.C. and De Wolf, H., 1993. Diatoms as a tool for reconstructing sedimentary environments in coastal wetlands; methodological aspects. *Hydrobiologia*, *269*(1), pp.285-296.

Vos, P. C. and De Wolf, H. 1988. Methodological aspects of paleo-ecological diatom research in coastal areas of the Netherlands' *Geologie en Mijnbouw*, 67(1988), pp. 31–40. Available at: http://www.njgonline.nl/publish/articles/000346/article.pdf. [2022, January 27]

Wachnicka, A., Gaiser, E., Collins, L., Frankovich, T. and Boyer, J., 2010. Distribution of diatoms and development of diatom-based models for inferring salinity and nutrient concentrations in Florida Bay and adjacent coastal wetlands of south Florida (USA). *Estuaries and Coasts*, *33*(5), pp.1080-1098. Available: https://doi.org/10.1007/s12237-010-9283-4 [2022, January 27]

Wachnicka, A., Gaiser, E., Wingard, L., Briceño, H. and Harlem, P., 2013. Impact of Late Holocene climate variability and anthropogenic activities on Biscayne Bay (Florida, USA): Evidence from

diatoms. *Palaeogeography, Palaeoclimatology, Palaeoecology*, *371*, pp.80-92. Available: http://dx.doi.org/10.1016/j.palaeo.2012.12.020 [2022, January 27]

Wadley, L., Esteban, I., de la Peña, P., Wojcieszak, M., Stratford, D., Lennox, S., d'Errico, F., Rosso, D.E., Orange, F., Backwell, L. and Sievers, C., 2020. Fire and grass-bedding construction 200 thousand years ago at Border Cave, South Africa. *Science*, *369*(6505), pp.863-866. Available: https://hal.archives-ouvertes.fr/hal-02998410

Walker, M., 2005. Radiometric dating 1: radiocarbon dating. *Quaternary Dating Methods*, pp.17-35.

Wallace, R.B., Baumann, H., Grear, J.S., Aller, R.C. and Gobler, C.J., 2014. Coastal ocean acidification: The other eutrophication problem. *Estuarine, Coastal and Shelf Science*, *148*, pp.1-13. Available: https://doi.org/10.1016/j.ecss.2014.05.027 [2022, January 27]

Wang, L., Mackay, A.W., Leng, M.J., Rioual, P., Panizzo, V.N., Lu, H., Gu, Z., Chu, G., Han, J. and Kendrick, C.P., 2013. Influence of the ratio of planktonic to benthic diatoms on lacustrine organic matter δ13C from Erlongwan maar lake, northeast China. *Organic Geochemistry*, *54*, pp.62-68. Available: https://doi.org/10.1016/j.orggeochem.2012.09.010 [2022, January 27]

Warnock, J.P., Bauersachs, T., Kotthoff, U., Brandt, H.T. and Andrén, E., 2018. Holocene environmental history of the Ångermanälven Estuary, northern Baltic Sea. *Boreas*, *47*(2), pp.593-608. DOI 10.1111/bor.12281

Watson, E.B., Wasson, K., Pasternack, G.B., Woolfolk, A., Van Dyke, E., Gray, A.B., Pakenham, A. and Wheatcroft, R.A., 2011. Applications from paleoecology to environmental management and restoration in a dynamic coastal environment. *Restoration Ecology*, *19*(6), pp.765-775. Doi: 10.1111/j.1526-100X.2010.00722.x

Watt, D.A., 1998. Estuaries of contrasting trophic status in KwaZulu-Natal, South Africa. *Estuarine, Coastal and Shelf Science*, *47*(2), pp.209-216.

Weilhoefer, C.L., Matteucci, C.N. and Turner, F., 2021. Multiple Estuarine Gradients Influencing Tidal Flat Benthic Algal Biomass and Community Structure in the Yaquina Estuary, OR, USA. *Estuaries and Coasts*, pp.1-16. Available: https://doi.org/10.1007/s12237-020-00854-6 [2022, January 27]

Weilhoefer, C.L. and Pan, Y., 2006. Diatom-based bioassessment in wetlands: How many samples do we need to characterize the diatom assemblage in a wetland adequately?. *Wetlands*, *26*(3), pp.793-802.

Weilhoefer, C.L. and Pan, Y., 2007. Relationships between diatoms and environmental variables in wetlands in the Willamette Valley, Oregon, USA. *Wetlands*, *27*(3), pp.668-682.

Whitfield, A.K., 1992. A characterization of southern African estuarine systems. *Southern African Journal of Aquatic Science*, *18*(1-2), pp.89-103.

Wilczyñski, J., Kufel-Diakowska, B., Hromadová, B., Tr¹bska, J., Gawe, A., Trybalska, B., Wojtal, A.Z., Stworzewicz, E. and Miêkina, B., 2015. A Gravettian Site in Southern Poland: Jaksice II.

Witkowski, A., Broszinski, A., Bennike, O., Janczak-Kostecka, B., Jensen, J.B., Lemke, W., Endler, R. and Kuijpers, A., 2005. Darss Sill as a biological border in the fossil record of the Baltic Sea: evidence from diatoms. Quaternary International, 130(1), pp.97-109. Available: https://doi.org/10.1016/j.quaint.2004.04.035 [2022, January 27]

Witkowski, A., Cedro, B., Kierzek, A. and Baranowski, D., 2009. Diatoms as a proxy in reconstructing the Holocene environmental changes in the south-western Baltic Sea: the lower Rega River Valley sedimentary record. In *Palaeolimnological Proxies as Tools of Environmental Reconstruction in Fresh Water* (pp. 155-172). Springer, Dordrecht. DOI 10.1007/s10750-009-9808-7

Witkowski, A., Radziejewska, T., Wawrzyniak-Wydrowska, B., Lange-Bertalot, H., Bąk, M. and Gelbrecht, J., 2011. Living on the pH edge: diatom assemblages of low-pH lakes in Western Pomerania (NW Poland). In *The diatom world* (pp. 365-384). Springer, Dordrecht. DOI 10.1007/978-94-007-1327-7_16

Wolin, J.A. and J.R. Stone, 2010. Diatoms as Indicators of Water-Level Change in Freshwater Lakes. In: The Diatoms Applications to the Environmental and Earth Sciences, E.F. Stoermer and J.P. Smol (eds.), Cambridge University Press. pp.174-185.

World Register or Marine Species. n.d. *Taxa.* Available: https://www.marinespecies.org/aphia.php?p=search [2021, June 24].

Wu, N., Schmalz, B. and Fohrer, N., 2014. Study progress in riverine phytoplankton and its use as bio-indicator–a review. Austin Journal of Hydrology, 1(1), p.9.

Wündsch, M., Haberzettl, T., Kirsten, K.L., Kasper, T., Zabel, M., Dietze, E., Baade, J., Daut, G., Meschner, S., Meadows, M.E. and Mäusbacher, R., 2016. Sea level and climate change at the southern Cape coast, South Africa, during the past 4.2 kyr. *Palaeogeography, Palaeoclimatology, Palaeoecology*, *446*, pp.295-307. Available: http://dx.doi.org/10.1016/j.palaeo.2016.01.027 [2022, January 27]

Yuce, A.M., 2017. Determination of environmental factors and littoral phytoplankton in Izmit Bay. *International Journal of Aquatic Science*, *8*(1), pp.3-8.

Zalat, A.A. and Al-Wosabi, M.A., 2011. Distribution of non-marine diatoms in surface sediments of streams in Socotra Island, Yemen. *QScience Connect*, *2011*(1), p.3.

Zalat, A.A. and Al-Wosabi, M., 2010. Preliminary investigation of diatom taxa distribution in recent surface sediments of Socotra Island (Yemen), Indian ocean. *Egypt Journal of Paleontology*, *10*, pp.49-60.

Zalat, A.A., El-Sheekh, M.M. and Gaballa, M., 2019. Distribution pattern of diatom flora in the surface sediments of Bardawil Lagoon (North Sinai), Egypt. *Thalassas: An International Journal of Marine Sciences*, *35*(2), pp.531-539. Available: https://doi.org/10.1007/s41208-019-00160-4 [2022, January 27]

Zalat, A.A., El-Sheekh, M.M., Ghandour, I.M. and Basaham, A.S., 2021. Diatom Assemblages From Surface Sediments of Two Coastal Lagoons, the Central Part of the Red Sea, Saudi Arabia and Their Associated Environmental Variables. *Thalassas: An International Journal of Marine Sciences*, pp.1-25. Available: https://doi.org/10.1007/s41208-020-00283-z [2022, January 27]

Zalat, A.A. and Al-Wosabi, M., 2010. Preliminary investigation of diatom taxa distribution in recent surface sediments of Socotra Island (Yemen), Indian ocean. *Egypt Journal of Paleontology*, *10*, pp.49-60.

Zhao, B., Kreuter, U., Li, B., Ma, Z., Chen, J. and Nakagoshi, N., 2004. An ecosystem service value assessment of land-use change on Chongming Island, China. *Land Use Policy*, *21*(2), pp.139-148. Available: https://doi.org/10.1016/j.landusepol.2003.10.003 [2022, January 27]

Zong, Y., 1997. Implications of Paralia sulcata abundance in Scottish isolation basins. Diatom Research, 12(1), pp.125-150.

Zong, Y., Kemp, A.C., Yu, F., Lloyd, J.M., Huang, G. and Yim, W.W.S., 2010. Diatoms from the Pearl River estuary, China and their suitability as water salinity indicators for coastal environments. *Marine Micropaleontology*, *75*(1-4), pp.38-49. Available: https://doi.org/10.1016/j.marmicro.2010.02.004 [2022, January 27]

APPENDIX 1: DIATOM PLATES – KNY19-B AND KNY19-G

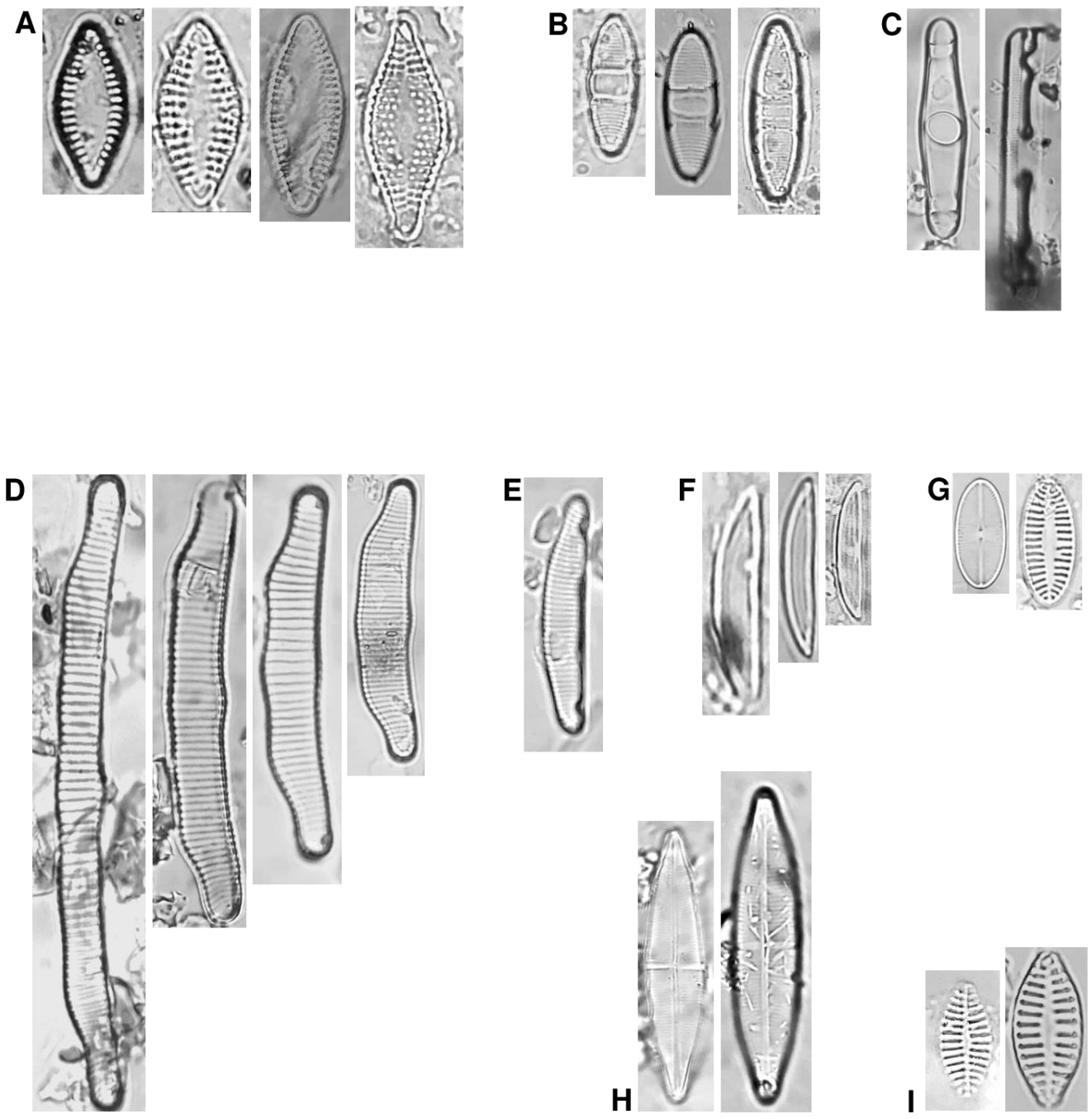

Figure 32. A. *Dimeregramma minor*; **B.** *Plagiogramma* cf. *staurophorum*.; **C.** *Grammatophora oceanica*; **D.** *Eunotia pectinalis var. undulata*; **E.** *E. incisa*; **F.** *Catenula adhaerens*; **G.** *Achnanthes oblongella*; **H.** *A. brevipes*; **I.** *Planothidium delicatulum.* Note that all images were captured at a magnification of 1000x.

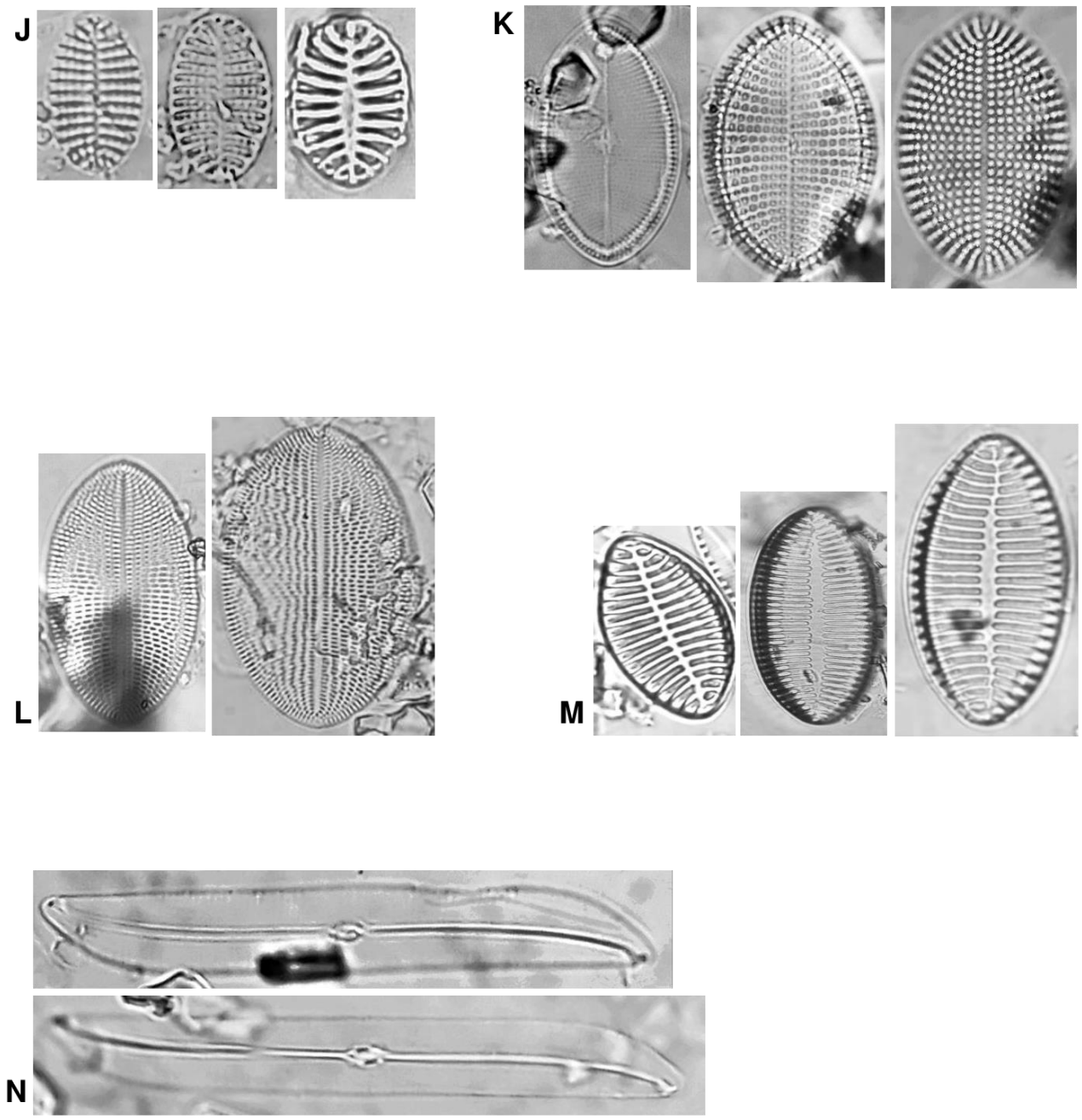

Figure 33. J. *Cocconeis costata*; **K.** *C. scutellum*; **L.** *C. placentula*; **M.** *Giffenia cocconeiformis*; N. *Gyrosigma obtusatum*. Note that all images were captured at a magnification of 1000x.

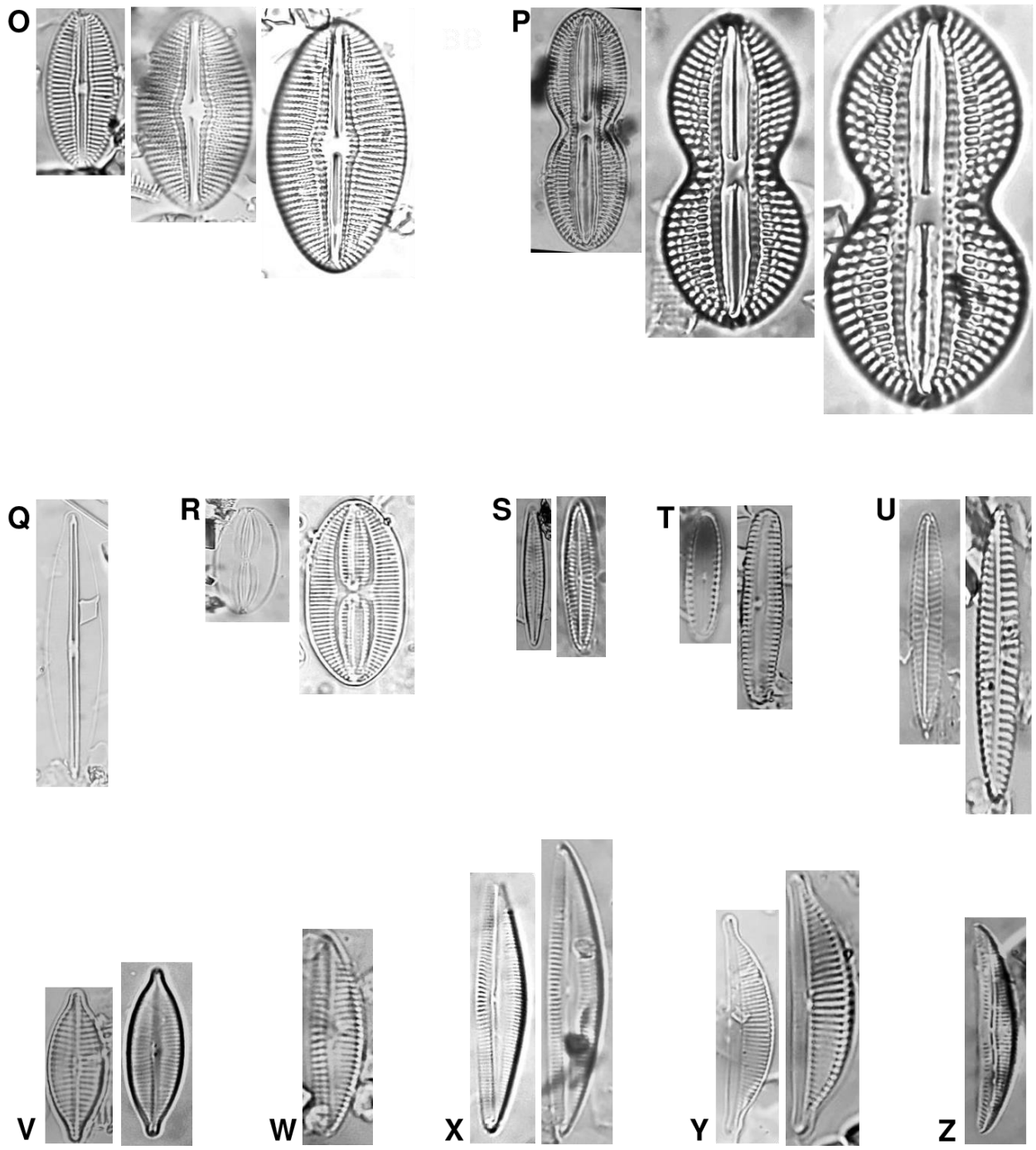

Figure 34. O. *Diploneis elliptica;* **P.** *Diploneis* aggregate (= *Diploneis bombus,* D. *crabro,* D. *interruptus)*; **Q.** *Frustululia crassinervia*; **R.** *Fallacia pygmea*; **S.** *Navicula tenelloides*; **T.** *N. lucens;* **U.** *N. longa;* **V.** *N. germainii*; **W.** *Navicymbula pusilla*; **X.** *Seminavis strigosa*; **Y.** *Halmphora coffeaeformis*; **Z.** *A. helenensis*. Note that all images were captured at a magnification of 1000x.

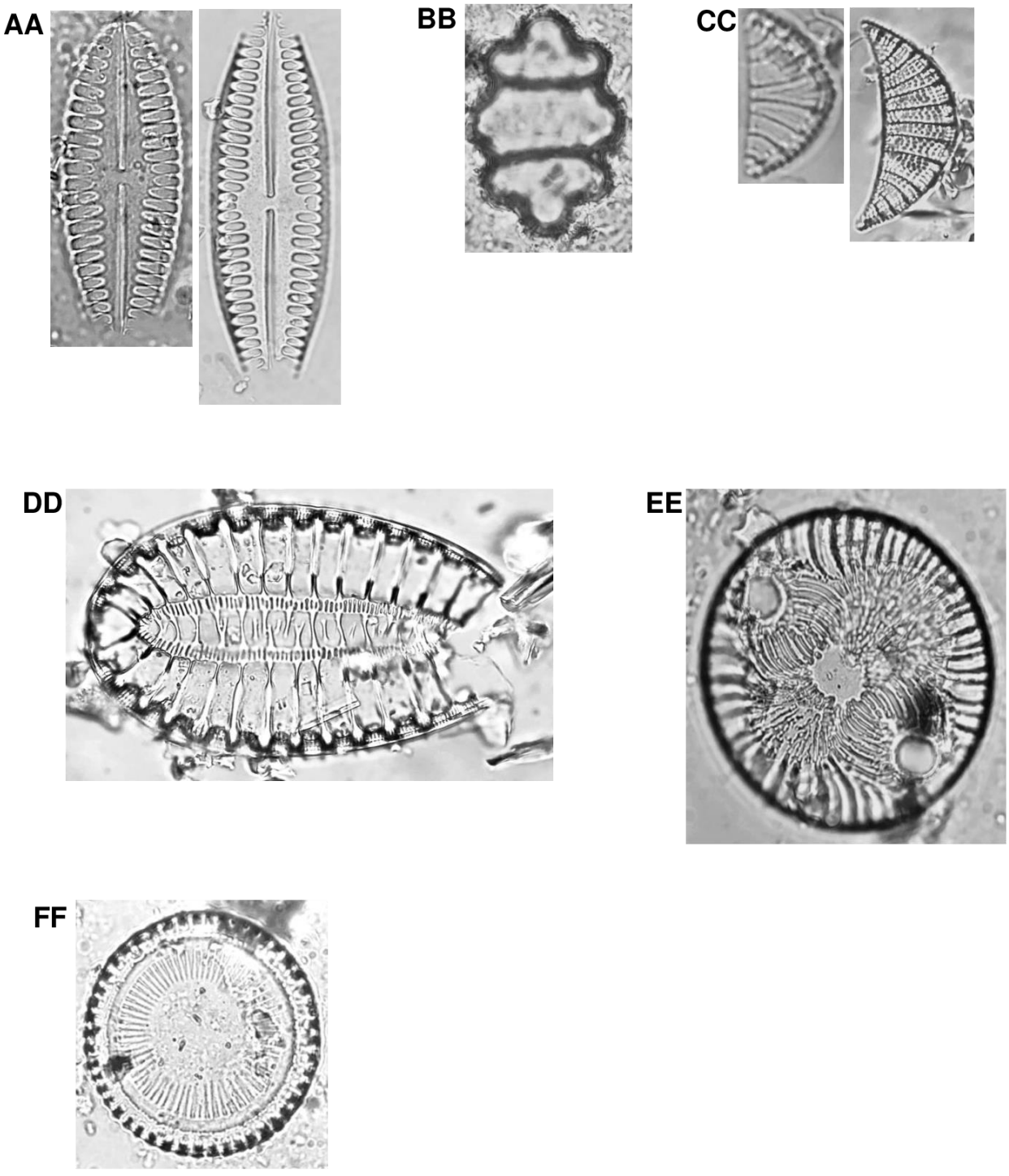

Figure 35. AA. *Pinnularia yarrensis*; **BB.** *Biddulphia pulchella*; **CC.** *Rhopalodia musculus*; **DD.** *Surirella fastuosa var. cuneata*; **EE.** *Auliscus cf. sculptus*; **FF.** *Paralia sulcata.* Note that all images were captured at a magnification of 1000x.

APPENDIX 2: KNY19-B

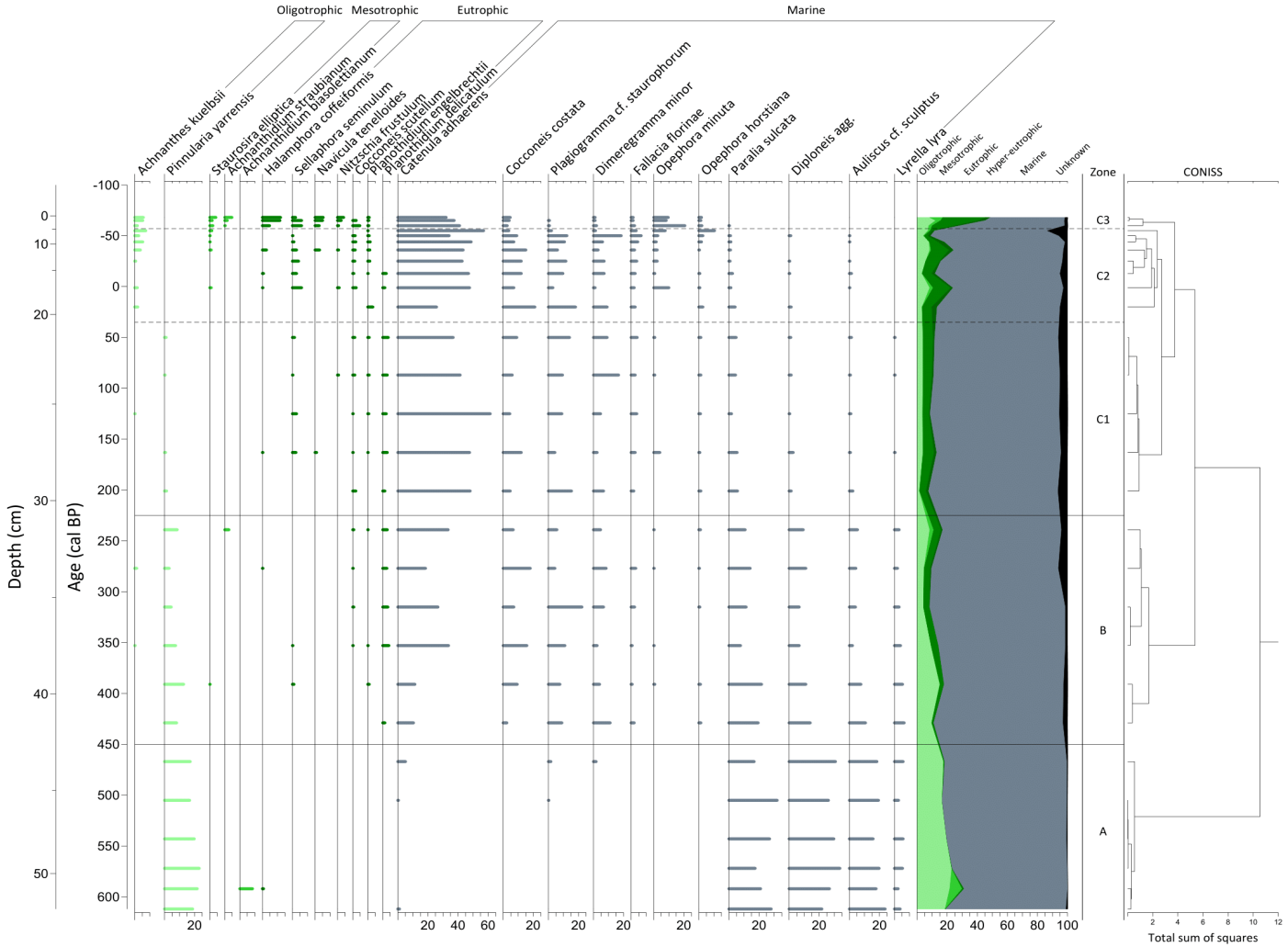

Figure 36. KNY19-B diatom relative percentage diagram against age (cal BP) and depth (cm) where species are grouped according to nutrient preferences.

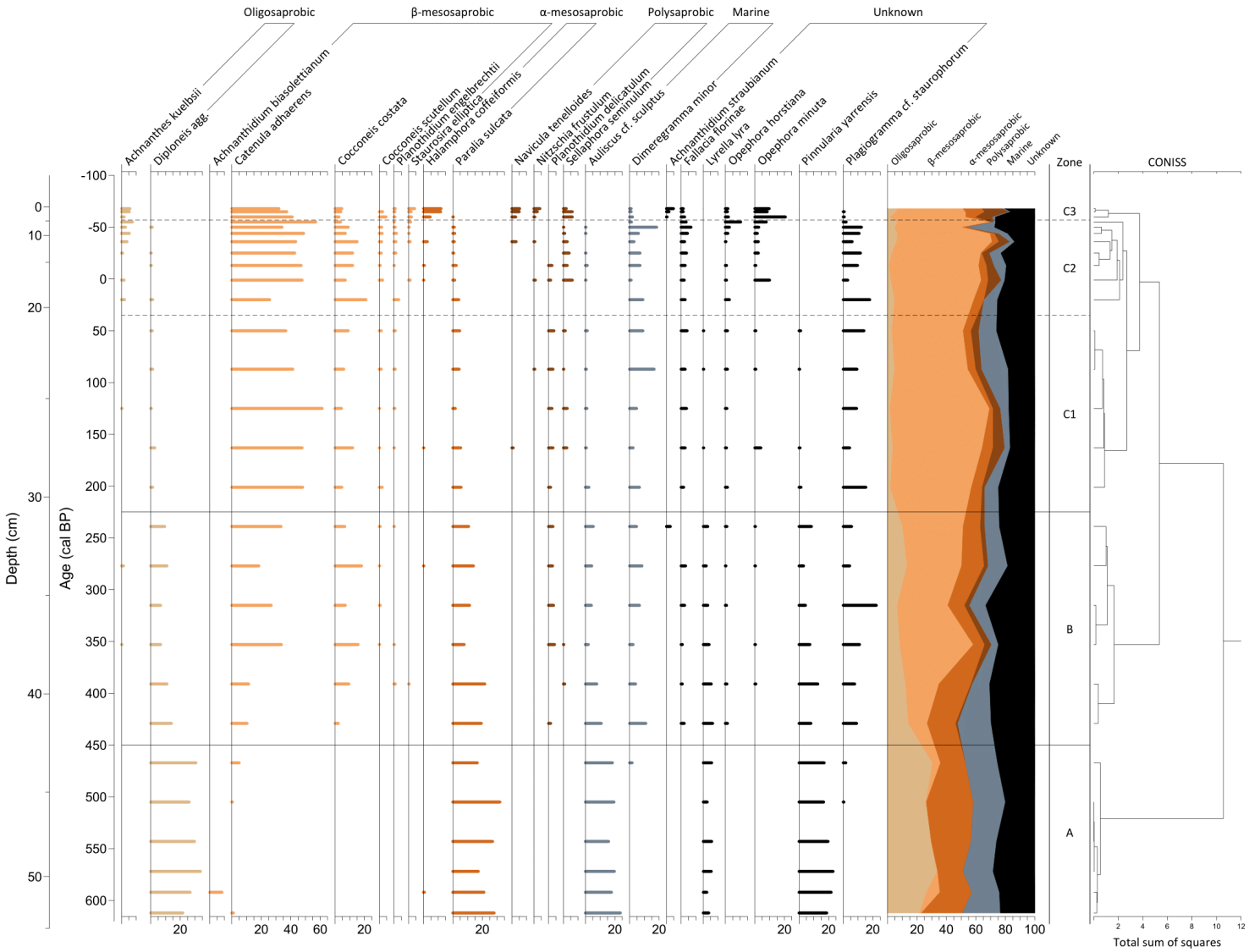

Figure 37. KNY19-B diatom relative percentage diagram against age (cal BP) and depth (cm) where species are grouped according to saprobity preferences

Table 11. Core KNY19-B diatom species and their ecological affinities. Salinity: f = fresh, fb = fresh-brackish, bf = brackish-fresh; b = brackish, mb = marine-brackish, m = marine, u = unknown. Trophic status: o = oligotrophic, m = mesotrophic, e = eutrophic, h = hyper-eutrophic, mar = marine, u = unknown. Saprobity: o = oligosaprobic, bm = β-mesosaprobic, am = α-mesosaprobic, p = polysaprobic, mar = marine, u = unknown. Life form: b = benthic, a = aerophilic, ep = epiphytic, el = epilithic, epp = epipellic, es = epipsammic, p = planktonic, u = unknown

Species Name	Salinity	Trophic status	Saprobity	Life Form
Achnanthes brevipes	fb	e	u	ep
Achnanthes javanica	b	o	u	u
Achnanthes kuelbsii	b	o	o	el
Achnanthes oblongella	fb	o	o	epp
Achnanthidium affine	fb	u	o	u
Achnanthidium biasolettianum	fb	m	bm	b
Achnanthidium eutrophilum	fb	e	u	b
Achnanthidium straubianum	fb	m	u	el
Amphora pediculus	fb	h	bm	el
Aulacoseira subartica cf. subborealis	f	o	o	b-p
Auliscus cf. sculptus	m	mar	mar	es
Catenula adhaerens	m	mar	bm	es
Cocconeis costata	m	mar	bm	epp
Cocconeis distans	m	mar	mar	es
Cocconeis engelbrechtii	b	u	u	ep
Cocconeis pediculus	b	e	bm	ep
Cocconeis placentula	fb	e	bm	ep
Cocconeis placentula var. euglypta	fb	e	bm	ep
Cocconeis scutellum	mb	e	bm	ep/ el
Craticula accomoda	fb	h	p	el
Cyclotella ocellata	f	e	o	p
Dimeregramma minor	m	mar	mar	es
Diploneis (agg) (*= D. bombus, D. crabro, D. interrupta)*	m	mar	o	epp
Diploneis elliptica	fb	o	o	ep
Diploneis smithii	b	u	u	p
Discostella woltereckii	fb	e	am	p
Ehrenbergia granulosa	m	mar	mar	P
Encyonema minutum	f	e	o	ep
Encyonema silesiacum	f	e	u	el
Eolimna minima	fb	e	p	el
Eolimna subminuscula	fb	h	p	el
Eunotia formica	fb	o	o	ep
Fallacia florinae	m	mar	u	es
Fallacia tenera	b	u	u	epp
Fragilaria nanana	f	o	o	P
Giffenia cocconeiformis	m	o	o	b

Species Name	Salinity	Trophic status	Saprobity	Life Form
Grammatophora oceanica	m	mar	mar	ep
Grammatophora undulata	m	mar	Mar	u
Halamphora coffeaeformis	b	e	am	b
Lyrella lyra	m	mar	u	ep
Mastogloia elliptica	b	u	u	ep/ el/ epp
Mayamaea atomus	fb	h	p	a
Navicula bremensis	u	u	u	epp
Navicula cincta	fb	e	am	epp/ ep
Navicula cryptotenella	fb	h	bm	el
Navicula erifuga	b	e	p	u
Navicula germainii	u	e	u	epp
Navicula gregaria	f	h	am	b
Navicula tenelloides	fb	e	p	a
Navicula vandamii	fb	e	u	el/ epp
Nitzschia frustulum	b	e	p	b
Nitzschia littorea	b	u	u	u
Opephora horstiana	mb	u	u	u
Opephora minuta	m	mar	u	es
Paralia sulcate	m	mar	am	p
Pinnularia yarrensis	m	o	u	epp
Plagiogramma cf staurophorum	m	mar	u	es
Planothidium delicatulum	b	e	p	es/ ep
Planothidium engelbrechtii	b	e	bm	ep/ es
Planothidium frequentissimum	fb	h	am	ep/ es
Pseudostaurosira brevistriata	fb	e	bm	ep/ es
Rhopalodia gibba	fb	e	bm	ep
Rhopalodia gibberula	bf	u	u	ep
Rhopalodia musculus	b	u	o	ep
Sellaphora seminulum	f	o	p	el
Staurosira elliptica	fb	m	bm	b
Surirella ovalis	b	e	bm	ep
Tabularia fasciculata	b	e	bm	ep
Terpsinoë musica	bf	u	u	u
Thalassiosira eccentrica	m	mar	mar	u
Triceratium cf scitulum	m	mar	mar	u
Tryblionella apiculata	b	h	p	b
Tryblionella coarctata	b	u	u	b

Table 12. KNY19-B diatom species percentages against depth (cm) and age (cal BP).

Depth (cm)	**0.5**	**1.5**	**3.5**	**5.5**	**7.5**	**9.5**	**11.5**	**13.5**	**15.5**	**17.5**	**19.5**
Age (cal BP)	**-68**	**-65**	**-60**	**-55**	**-50**	**-44**	**-36**	**-25**	**-13**	**1**	**20**
Achnanthes brevipes	0	0	0	0	0	0	0	0	0	0	0
Achnanthes javanica	0	0	0	0	0	0	0	0	0	0	0
Achnanthes kuelbsii	5.67	5.33	1.67	7.33	2.67	5.33	3.67	0.67	0	1.67	2
Achnanthes oblongella	0.67	1	0	0	0	1.33	0.67	0	0	0.67	0
Achnanthidium affine	0	0	0	0	0	0	0	0	0	0	0
Achnanthidium biasolettianum	0	0	0	0	0	0	0	0	0	1.33	0
Achnanthidium biasolettianum	0	0	0	0	0	0	0	0	0	0	0
Achnanthidium eutrophilum	0.33	0.33	0	0	0	0	0	0	0	0	0
Achnanthidium straubianum	4.67	1.67	0.33	0	0	0	0	0	0	0	0
Amphora pediculus	0.33	0	0	0.67	0	2	0	0	0	0	0.67
Aulacoseira subartica f. subborealis	0	0	0	0	0	0	0	0	0.67	0	0
Auliscus cf. sculptus	0	0	0	0	0.33	0.33	0	0.33	1.33	0.33	0
Catenula adhaerens	32.67	37.33	41	57	34	48.67	43.33	42.67	47	47.67	25.67
Cocconeis costata	4.67	4	2.67	3.67	9	7	15	12	12	7	21
Cocconeis distans	0	0	0	0	0	0	0	0.33	0	0	0
Cocconeis engelbrechtii	0	0	0	2.33	0	0	0	0	0	0	1
Cocconeis pediculus	0	0	0	0	0	0	0	0	0	0	0.67
Cocconeis placentula	0	0	0	0	0	0	0.33	1	0.67	0.33	2.33
Cocconeis placentula var. euglypta	1	0.67	0.67	0	0	0.33	0	0	0	0	0
Cocconeis scutellum	0	2.33	4.67	0	1.67	2	1.67	1.33	0.67	2.33	0
Craticula accomoda	0	0.67	1	0	0	0.33	0	0	0	0.33	0
Cyclotella ocellata	0	0	0	0	0	0	0	0.33	0.33	0	0
Dimeregramma minor var. minor	1	1	2	1.33	18.33	6	3	7	7	1	9
Diploneis (agg) (= *D. bombus, D. crabro, D. interrupta)*	0	0	0	0	1	0	0	0.33	0.33	0	1.33

Depth (cm)	**0.5**	**1.5**	**3.5**	**5.5**	**7.5**	**9.5**	**11.5**	**13.5**	**15.5**	**17.5**	**19.5**
Age (cal BP)	**-68**	**-65**	**-60**	**-55**	**-50**	**-44**	**-36**	**-25**	**-13**	**1**	**20**
Diploneis elliptica	0	0	0	0	0	0	0	0	0	0	0
Diploneis smithii	0	0	0	0	0	0	0	0	0.33	0	0
Discostella woltereckii	0	0	0	0	0	0	0	0	0	0	0
Ehrenbergia granulosa	0	0	0	0	0	0	0	0	0	0	0
Encyonema minutum	0	0	0	0	0	0	0.67	0.67	0	0	0
Encyonema silesiacum	0	0	0	0	0	0	0	1.67	0.33	1.67	0
Eolimna minima	0	0	0	0	0	0	0	0.67	0	0	0
Eolimna subminuscula	0	0	0.67	0	0	0	1.33	0.33	0	0	0
Eunotia formica	0	0	0	0	1.33	0	1	0	0	0	0
Fallacia florinae	1.33	1.33	2.33	3.33	6.67	4.33	2.33	3.67	2.67	2	2.67
Fallacia tenera	0	0.67	0	0.33	0	0	0	0	0	0	0
Fragilaria nanana	0	0	0	0	0	0.33	0.33	1	0	0	1.33
Giffenia cocconeiformis	0	0	0	0	0	0	0	0	0	0	0
Grammatophora oceanica	0	0	0	0	0	0	0	0	0	1	0
Grammatophora undulata	0	0	0	0	0	0	0	0	0	0	0
Grammatophora undulata	0	0	0	0	0	0	0	0	0	0	0
Halamphora coffeaeformis	12	11.67	4.67	0	0	0	2.67	0	0.67	0.33	0
Lyrella lyra	0	0	0	0	0	0	0	0	0	0	0
Mastogloia elliptica	0	0	0	0	1	0	0.67	1	1.33	0	0
Mayamaea atomus	1.67	2.33	0.33	0	0	0.33	0	0	0	0	0
Navicula bremensis	0	0	0	0	0	0	0	0	0	1	0
Navicula cincta	0	0	0	0	0	0	0	0	0	2	0
Navicula cryptotenella	0	0	0	0	0	0	0.67	0	0	0	0
Navicula erifuga	1	0.33	0	0.67	0	1	0	0	0	0	0
Navicula germainii	2.67	2	0.67	0.33	0	0	0.33	0.33	0	0.33	0
Navicula gregaria	0	0	0	0	0	0	0	0	0	1	0
Navicula tenelloides	5.33	5	2.67	0	0	0	3	0	0	0	0

Depth (cm)	**0.5**	**1.5**	**3.5**	**5.5**	**7.5**	**9.5**	**11.5**	**13.5**	**15.5**	**17.5**	**19.5**
Age (cal BP)	**-68**	**-65**	**-60**	**-55**	**-50**	**-44**	**-36**	**-25**	**-13**	**1**	**20**
Navicula vandamii	0	0	0	0	0	0	0	0	1	0.67	0
Nitzschia frustulum	4	2.33	0.67	0	0	0	0.67	0	0	1	0
Nitzschia littorea	0	0	0	0	1.67	0	0.67	0	0	0	0
Opehora minuta	9.67	8.33	20.67	7.67	2.67	1.67	2.33	2.33	0.67	10	0
Opephora horstiana	1.67	1.33	2	10.33	2.67	1.67	0.33	0	0.67	0.67	2.67
Paralia sulcate	0	0	0.33	0	1	1.33	1	0.67	2.33	1.33	4
Pinnularia yarrensis	0	0	0	0	0	0	0	0	0	0	0
Plagiogramma cf staurophorum	0	0.67	0.67	2	12.33	10.67	6	11.67	9.67	3	18
Planothidium delicatulum	0	0	0	0	0	0	0	0	2.33	1.33	0
Planothidium engelbrechtii	1	0.67	0.67	0.33	1	1.67	1.33	1.33	0.33	0	3.33
Planothidium frequentissimum	1	1.33	1.67	1	1.67	1.67	1	0.33	2.33	0	3
Pseudostaurosira brevistriata	1.33	0	0	0	0	0.67	0	0	0	0	0
Rhopalodia gibba	0	0	0	0	0	0	0	0.33	0	0	0
Rhopalodia gibberula	0	0	0	0	0	0	0.33	0	0	0	0
Rhopalodia musculus	0	0	0	0	0	0	0	0	0	0	0.33
Sellaphora seminulum	2	6	6	0	0.33	1	2.67	4	2.67	6	0
Staurosira elliptica	4	1.67	2	1.33	0.33	0.33	1	0	0	1	0
Surirella ovalis	0	0	0	0	0	0	0	0	0	0	0
Tabularia fasciculata	0	0	0	0	0	0	1.33	1.67	0	1.67	0
Terpsinoë musica	0	0	0	0.33	0.33	0	0.67	1.33	2.67	0	1
Thalassiosira eccentrica	0.33	0	0	0	0	0	0	0	0	0	0
Triceratium cf scitulum	0	0	0	0	0	0	0	0	0	0	0
Tryblionella apiculata	0	0	0	0	0	0	0	0	0	0.33	0
Tryblionella coarctata	0	0	0	0	0	0	0	1	0	1	0

Depth (cm)	**21.5**	**23.5**	**25.5**	**27.5**	**29.5**	**31.5**	**33.5**	**35.5**	**37.5**
Age (cal BP)	**50**	**87**	**125**	**163**	**201**	**239**	**277**	**315**	**353**
Achnanthes brevipes	0.33	0	0	0	0	0	0	0	0
Achnanthes javanica	0	0	0	0	0	0	0	0	0
Achnanthes kuelbsii	0	0	0.33	0	0	0	1.33	0	0.33
Achnanthes oblongella	0.67	0.67	0.67	0	0	0	0	0	0.67
Achnanthidium affine	0.33	0	0.33	0	0	0	0	0	0
Achnanthidium biasolettianum	0	0	0	0	0	0	0	0	0
Achnanthidium biasolettianum	0	0	0	0	0	0	0	0	0
Achnanthidium eutrophilum	0	0	0	0	0	0	0	0	0
Achnanthidium straubianum	0	0	0	0	0	2.67	0	0	0
Amphora pediculus	0	0	0	0	0	0	0	0	0
Aulacoseira subartica f. subborealis	0	1.33	0	0	0	0	0	0	0
Auliscus cf. sculptus	1.33	0.67	1	0.67	2.33	5.33	4.33	4	2
Catenula adhaerens	36.67	41.33	61.33	47.67	48	33.33	18.33	26.67	33.67
Cocconeis costata	9	6	4.33	12	4.67	6.67	18	7	15.67
Cocconeis distans	0	0	0	0	0	0	0	0	0
Cocconeis engelbrechtii	0	0	0	0	0	0	0	0	0
Cocconeis pediculus	0	0	0	0	0	0	0	0	0
Cocconeis placentula	0.33	0	0.33	0	0.33	0	0	0	0
Cocconeis placentula var. euglypta	0	0	0	0	0	0	0	0	0
Cocconeis scutellum	1.33	1.33	0.33	0.33	2	0.67	0.33	0.67	0.33
Craticula accomoda	0.33	0	0	0	0	0	0	0	0
Cyclotella ocellata	0	0	0	0	0.33	1	0.33	0	0
Dimeregramma minor var. minor	9	16.67	4.67	2.33	6.67	4.67	8.33	6.67	2.33
Diploneis (agg) (= *D. bombus, D. crabro, D. interrupta).*	1	1.33	0.33	2.67	1.33	9.33	11	6.67	6.67
Diploneis elliptica	0	0	0	0	0	0	0	0	0.33
Diploneis smithii	0	0	0	0	0	0	0	0	0

Depth (cm)	**21.5**	**23.5**	**25.5**	**27.5**	**29.5**	**31.5**	**33.5**	**35.5**	**37.5**
Age (cal BP)	**50**	**87**	**125**	**163**	**201**	**239**	**277**	**315**	**353**
Discostella woltereckii	0	0	0	0	0	0	0	0	0
Ehrenbergia granulosa	0.67	0	0	0	0	0	0	0	0
Encyonema minutum	0	0	0	0	0	0	0	0	0
Encyonema silesiacum	0	0	0	0	0	0	0	0	0
Eolimna minima	0	0	0	1	0.33	0	0	0	0
Eolimna subminuscula	0	0	0	0	0	0	0	0	0
Eunotia formica	0	0	0	0	0	0	0	0	0
Fallacia florinae	4	2.67	3.67	2.67	1.67	0	3	2.33	0.67
Fallacia tenera	0.33	0	0	0	0	0	0	0	0
Fragilaria nanana	0	0	0	0	0.33	0	0	0	0
Giffenia cocconeiformis	1	1.33	0	1	0	0	0.33	0	0.33
Grammatophora oceanica	1	0.67	0	0.67	0.33	0	0	0.33	0.33
Grammatophora undulata	0	0	0	0	0	0	0	0	0
Grammatophora undulata	0	0	0	0	0	0	0.33	0	0
Halamphora coffeaeformis	0	0	0	0.33	0	0	0.33	0	0
Lyrella lyra	0.33	0.33	0	0.33	0	3	2	3	4
Mastogloia elliptica	1	1.67	0.67	1	2	0.67	1.33	0.33	0.67
Mayamaea atomus	0	0	0	0	0	0	0	0	0
Navicula bremensis	0.33	0.33	1.67	1	0.33	1	0	0	0
Navicula cincta	0	0	0	0	0	0	0	0	0
Navicula cryptotenella	0	0	0	0	0	0	0	0	0
Navicula erifuga	0	0	0	0.67	0	0	0	0	0.33
Navicula germainii	0	0	0	0	0	0	0	0	0
Navicula gregaria	0	0	0	0	0	0	0	0	0
Navicula tenelloides	0	0	0	1	0	0	0	0	0
Navicula vandamii	0	0	0	0.33	0	0	0	0	0
Nitzschia frustulum	0	0.67	0	0	0	0	0	0	0

Depth (cm)	**21.5**	**23.5**	**25.5**	**27.5**	**29.5**	**31.5**	**33.5**	**35.5**	**37.5**
Age (cal BP)	**50**	**87**	**125**	**163**	**201**	**239**	**277**	**315**	**353**
Nitzschia littorea	0	0	0	0	0	0	0	0	0
Opehora minuta	0.67	0.67	0	4	0	0.33	0.33	0	0.33
Opephora horstiana	1.33	1.33	1	0.67	1.33	1	0.33	0.67	0
Paralia sulcata	4.67	4.33	1.67	5.33	5.67	10.67	14	11.33	7.67
Pinnularia yarrensis	1	0.33	0	0.67	1.33	8.33	3	4.33	7.33
Plagiogramma cf staurophorum	14	9.33	9	4.33	15.33	5.67	4.33	22.33	11
Planothidium delicatulum	3.67	3	2.33	3	1.33	3	2.67	3.33	4
Planothidium engelbrechtii	1	1	0.67	0.33	0	0.33	0	0	0.33
Planothidium frequentissimum	0.67	1	0.67	1.67	1.67	1	1	0	0
Pseudostaurosira brevistriat	0	0	0	0	0	0	0	0	0
Rhopalodia gibba	0	0	0	0	0	0	0	0	0
Rhopalodia gibberula	0	0	0	0	0	0	1.33	0	0.67
Rhopalodia musculus	0	0.33	0	0	0	0	0.33	0	0
Sellaphora seminulum	1.33	0.33	2.67	2.33	0	0	0	0	0.33
Staurosira elliptica	0	0	0	0	0	0	0	0	0
Surirella ovalis	0	0	0	0	0	0	0	0	0
Tabularia fasciculata	0	0	0.67	0.33	0	0	0.33	0	0
Terpsinoë musica	1.33	1	1	1	2	1.33	1.67	0.33	0
Thalassiosira eccentrica	0	0	0	0	0	0	0	0	0
Triceratium cf scitulum	0	0	0	0	0	0	0.33	0	0
Tryblionella apiculata	0	0	0	0	0	0	0	0	0
Tryblionella coarctata	1.33	0.33	0.67	0.67	0.67	0	1	0	0

Depth (cm)	**39.5**	**41.5**	**43.5**	**45.5**	**47.5**	**49.5**	**51.5**	**53.5**
Age (cal BP)	**391**	**429**	**467**	**505**	**543**	**572**	**592**	**612**
Achnanthes brevipes	0	0	0	0	0	0	0	0
Achnanthes javanica	0	1.33	0.67	0	0	0	0	0
Achnanthes kuelbsii	0	0	0	0	0	0	0	0
Achnanthes oblongella	0.67	0	0	0	0	0	0	0
Achnanthidium affine	0	0	0	0	0	0	0	0
Achnanthidium biasolettianum	0	0	0	0	0	0	0	0
Achnanthidium biasolettianum	0	0	0	0	0	0	8.33	0
Achnanthidium eutrophilum	0	0	0	0	0	0	0	0
Achnanthidium straubianum	0	0	0	0	0	0	0	0
Amphora pediculus	0	0	0	0	0	0	0	0
Aulacoseira subartica f. subborealis	0	0	0	0	0	0	0	0
Auliscus cf. sculptus	7.67	10.67	18.33	19.33	15.67	19.67	17.67	23.67
Catenula adhaerens	11.33	10.33	5	0.33	0	0	0	1
Cocconeis costata	9.33	2.33	0	0	0	0	0	0
Cocconeis distans	0	0	0	0	0	0	0	0
Cocconeis engelbrechtii	0	0	0	0	0	0	0	0
Cocconeis pediculus	0	0	0	0	0	0	0	0
Cocconeis placentula	0	0	0	0	0	0	0	0
Cocconeis placentula var. euglypta	0	0	0	0	0	0	0	0
Cocconeis scutellum	0	0	0	0	0	0	0	0
Craticula accomoda	0	0	0	0	0	0	0	0
Cyclotella ocellata	0	0	0	0	0	0	0	0
Dimeregramma minor var. minor	4	11	1.67	0	0	0	0	0
Diploneis (agg) (*= D. bombus, D. crabro, D. interrupta).*	11	14	30.67	26	29.67	33.67	26.67	21.67
Diploneis elliptica	0	0.33	0	0	0	0	0	0
Diploneis smithii	0	0	0	0	0	0	0	0

Depth (cm)	**39.5**	**41.5**	**43.5**	**45.5**	**47.5**	**49.5**	**51.5**	**53.5**
Age (cal BP)	**391**	**429**	**467**	**505**	**543**	**572**	**592**	**612**
Discostella woltereckii	0	0	0.33	0	0	0	0	0
Ehrenbergia granulosa	0	0	0	0	0	0	0	0
Encyonema minutum	0	0	0	0	0	0	0	0
Encyonema silesiacum	0	0	0	0	0	0	0	0
Eolimna minima	0	0	0	0	0	0	0	0
Eolimna subminuscula	0	0	0	0	0	0	0	0
Eunotia formica	0	0	0	0	0	0	0	0
Fallacia florinae	0.67	2	0	0	0	0	0	0
Fallacia tenera	0	0	0	0	0	0	0	0
Fragilaria nanana	0.67	0	0	0	0	0	0	0
Giffenia cocconeiformis	0	0	0	0	0	0	0	0
Grammatophora oceanica	0	1	0.67	0.67	1	0.33	0.67	0.67
Grammatophora undulata	0	0	1	1	0.33	0	0	1
Grammatophora undulata	0	0	0	0	0	0	0	0
Halamphora coffeaeformis	0	0	0	0	0	0	0.67	0
Lyrella lyra	5.33	6.33	5.67	2.67	5.67	5.33	2.33	3.67
Mastogloia elliptica	1	1	0.33	0	0.33	0	0	0
Mayamaea atomus	0	0	0	0	0	0	0	0
Navicula bremensis	0	0	0	0	0	0	0	0
Navicula cincta	0	0	0	0	0	0	0	0
Navicula cryptotenella	0	0	0	0	0	0	0	0
Navicula erifuga	0	0	0	0	0	0	0	0
Navicula germainii	1	0	0	0	0	0	0	0
Navicula gregaria	0	0	0	0	0	0	0	0
Navicula tenelloides	0	0	0	0	0	0	0	0
Navicula vandamii	0	0	0	0	0	0	0	0
Nitzschia frustulum	0	0	0	0	0	0	0	0

Depth (cm)	**39.5**	**41.5**	**43.5**	**45.5**	**47.5**	**49.5**	**51.5**	**53.5**
Age (cal BP)	**391**	**429**	**467**	**505**	**543**	**572**	**592**	**612**
Nitzschia littorea	0	0	0	0	0	0	0	0
Opehora minuta	0.67	0	0	0	0	0	0	0
Opephora horstiana	1	1.33	0	0	0	0	0	0
Paralia sulcate	21.67	19.33	16.67	32	27	17.33	21	28
Pinnularia yarrensis	12.67	8	17	16.67	19.67	23	21.67	18.67
Plagiogramma cf staurophorum	7.67	9	1.67	0.33	0	0	0	0
Planothidium delicatulum	0	1.33	0	0	0	0	0	0
Planothidium engelbrechtii	1	0	0	0	0	0	0	0
Planothidium frequentissimum	0	0	0	0	0	0	0	0
Pseudostaurosira brevistriat	0.67	0	0	0	0	0	0	0
Rhopalodia gibba	0	0	0	0	0	0	0	0
Rhopalodia gibberula	0	0	0	0	0	0	0	0
Rhopalodia musculus	0	0	0	0	0	0	0	0
Sellaphora seminulum	1	0	0	0	0	0	0	0
Staurosira elliptica	0.33	0	0	0	0	0	0	0
Surirella ovalis	0	0	0.33	0	0	0.33	0.67	0.33
Tabularia fasciculata	0	0	0	0	0	0	0	0
Terpsinoë musica	0.67	0.67	0	0.33	0.33	0	0	1
Thalassiosira eccentrica	0	0	0	0	0	0	0	0
Triceratium cf scitulum	0	0	0	0.67	0.33	0.33	0.33	0.33
Tryblionella apiculata	0	0	0	0	0	0	0	0
Tryblionella coarctata	0	0	0	0	0	0	0	0

Table 13. Sample score loadings of the first two statistically significant principal components for KNY19-B.

Age (cal BP)	PC 1	PC 2
-68	-0.06065	0.64166
-65	-0.05938	0.64419
-60	-0.03532	0.29022
-55	-0.01699	0.081659
-50	-0.01064	0.013674
-44	-0.02608	0.19466
-36	-0.01331	0.008181
-25	-0.01304	-0.03807
-13	-0.02029	0.068335
1	-0.01425	-0.04872
20	0.011197	-0.06803
50	-0.00149	-0.073
87	-0.00862	-0.0236
125	0.002782	-0.01665
163	0.018671	-0.06961
201	0.15804	-0.03677
239	0.052539	-0.02912
277	0.083641	-0.0368
315	0.14199	-0.02867
353	0.15725	-0.00945
391	0.33752	0.04991
429	0.33094	0.048839
467	0.39029	0.054746
505	0.457	0.072289
543	0.37025	0.048036
572	0.43315	0.015938

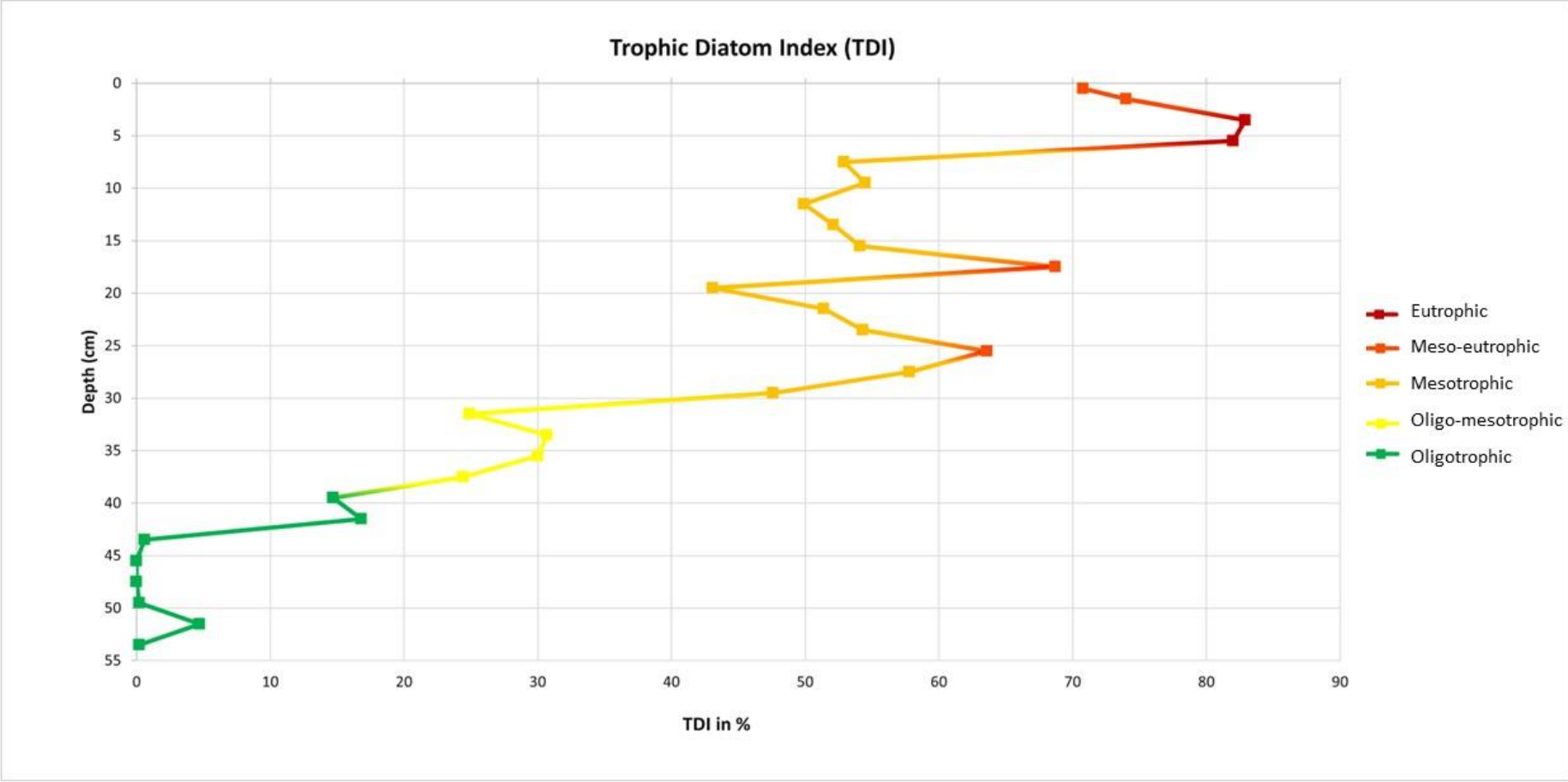

Figure 38. Trophic Diatom Index of KNY19-B against depth.

APPENDIX 3: KNY19-G

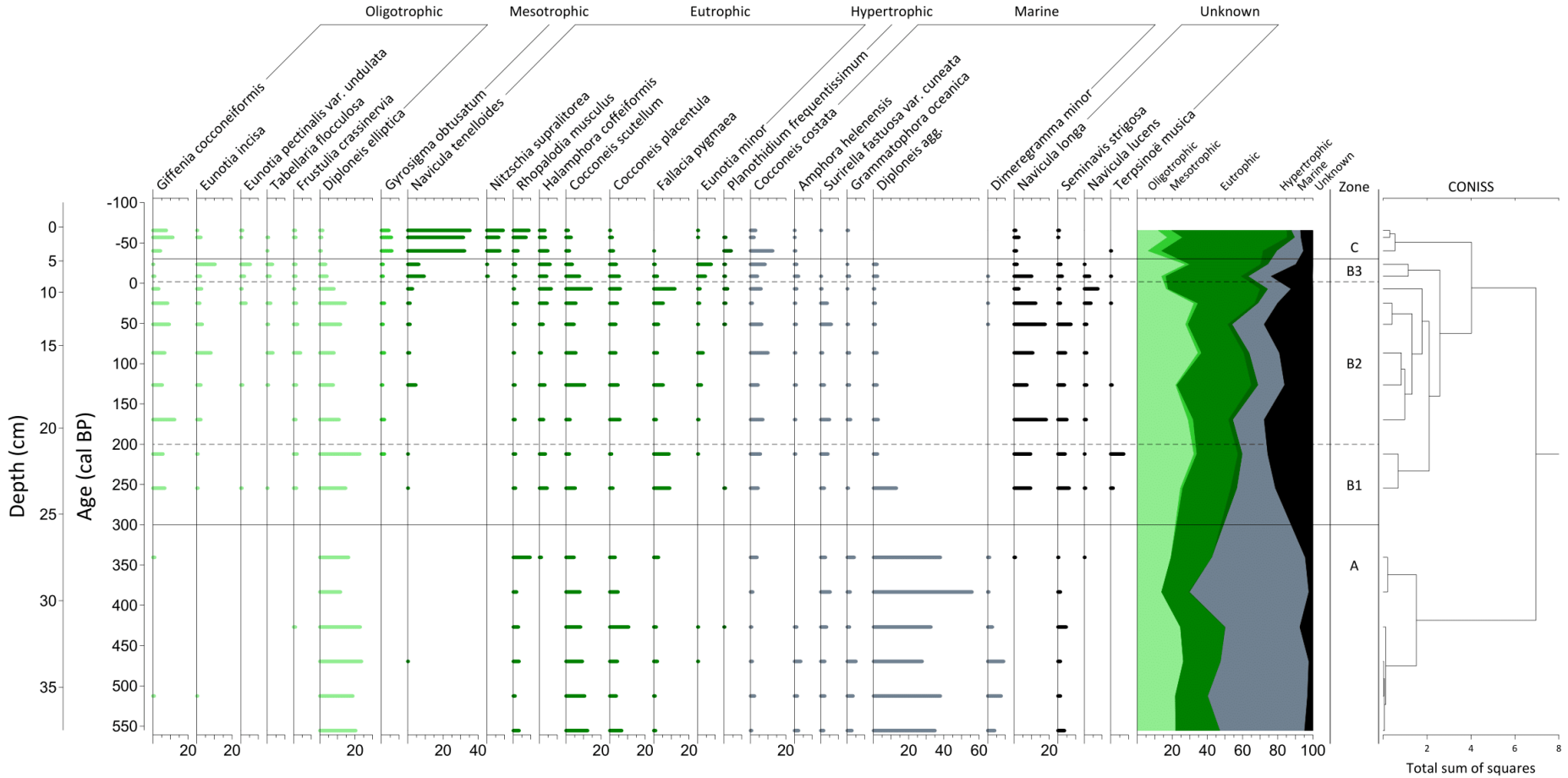

Figure 39. KNY19-G diatom relative percentage diagram against age (cal BP) and depth (cm) where species are grouped according to nutrient preferences.

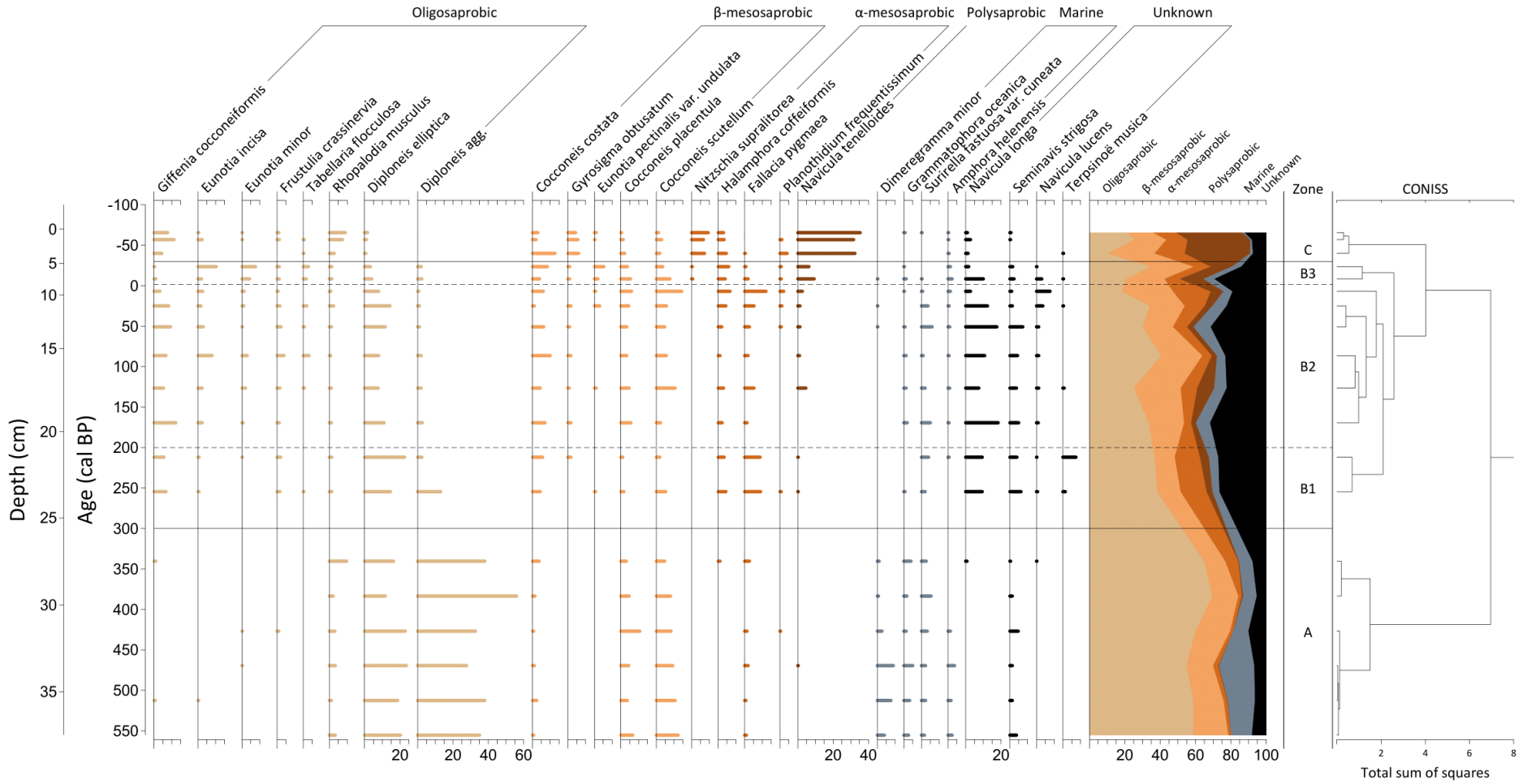

Figure 40. KNY19-G diatom relative percentage diagram against age (cal BP) and depth (cm) where species are grouped according to saprobity preferences.

Table 14. Core KNY19-B diatom species and their ecological affinities. Salinity: f = fresh, fb = fresh-brackish, bf = brackish-fresh; b = brackish, mb = marine-brackish, m = marine, u = unknown. Trophic status: o = oligotrophic, m = mesotrophic, e = eutrophic, h = hyper-eutrophic, mar = marine, u = unknown. Saprobity: o = oligosaprobic, bm = β-mesosaprobic, am = α-mesosaprobic, p = polysaprobic, mar = marine, u = unknown. Life form: b = benthic, a = aerophilic, ep = epiphytic, el = epilithic, epp = epipellic, es = epipsammic, p = planktonic, u = unknown

Species Name	Salinity	Trophy	Saprobity	Life Form
Achnanthes brevipes	fb	e	u	ep
Achnanthes coarctata	f	o	o	ep/ a
Achnanthes fimbriata	u	u	u	el
Achnanthes oblongella	fb	o	o	epp
Achnanthes subaffinis	f	o	o	b
Achnanthes swazi	f	o	u	u
Achnanthidium biasolettianum	fb	m	bm	b
Achnanthidium crassum	fb	m	bm	b
Achnanthidium eutrophilum	fb	e	u	b
Achnanthidium macrocephalum	f	m	bm	b
Achnanthidium petersenii	u	u	u	u
Achnanthidium straubianum	f	m	u	el
Amphora decussata	m	mar	mar	epp
Amphora helenensis	m	mar	mar	epp
Amphora holsatica	b	u	u	epp
Amphora montana	fb	e	bm	b
Amphora pediculus	fb	h	bm	el
Bacillaria paradoxa	b	e	u	epp
Brachysira brebissonii	f	o	o	ep
Brachysira neoexilis	f	m	o	ep
Caloneis linearis	u	u	u	ep
Catenula adhaerens	m	mar	bm	es
Cocconeis costata	m	mar	bm	epp
Cocconeis distans	m	mar	mar	es
Cocconeis heteroidea	m	mar	mar	ep
Cocconeis placentula	fb	e	bm	ep
Cocconeis scutellum	mb	e	bm	ep/ el
Craticula accomoda	fb	h	p	el
Craticula molestiformis	fb	e	p	b
Cyclotella quillensis	b	u	u	p
Delphineis minutissima	m	mar	mar	es
Denticula sundayensis	b	u	u	u
Dimeregramma minor	m	mar	mar	es
Diploneis (agg) (*= D. bombus, D. crabro, D. interrupta).*	m	mar	o	epp
Diploneis elliptica	fb	o	o	ep
Encyonema silesiacum	f	e	u	el

Species Name	Salinity	Trophy	Saprobity	Life Form
Eolimna subminuscula	fb	H	p	el
Epithemia sorex	fb	p	bm	ep
Eunotia exigua	fb	h	am	b
Eunotia flexuosa	f	o	o	ep
Eunotia incisa	f	o	o	ep
Eunotia minor	fb	e	o	ep/ a
Eunotia pectinalis	f	m	bm	ep
Eunotia pectinalis var. undulata	f	o	bm	ep/ a
Eunotia zygodont	f	u	u	ep
Fallacia florinae	m	mar	mar	es
Fallacia monoculata	fb	e	am	b
Fallacia pygmaea	bf	e	am	ep
Fragilaria biceps	fb	e	bm	es
Frustulia saxonica	f	o	o	el
Frustululia crassinervia	f	o	o	ep
Giffenia cocconeiformis	m	o	o	b
Gomphonema gracile	fb	e	o	b
Grammatophora oceanica	m	mar	mar	ep/ p
Gyrosigma obtusatum	f	m	bm	epp
Halamphora coffeaeformis	b	h	am	b
Luticola goeppertiana	fb	h	p	b
Lyrella lyra	m	mar	u	ep
Mastogloia elliptica	b	u	u	ep/ el/ epp
Mastogloia exigua	b	u	u	epp
Mastogloia fimbriata	m	mar	mar	ep
Navicula arvensis var. maior	u	h	p	epp
Navicula cryptotenella	fb	h	bm	el
Navicula germainii	u	e	u	epp
Navicula longa	m	u	u	ep
Navicula lucens	mb	u	u	es
Navicula microcari	fb	u	u	b
Navicula ranomafenensis	u	o	u	u
Navicula schroeteri	b	e	bm	el
Navicula tenelloides	fb	h	p	a
Navicula tripunctata	fb	e	bm	ep/ el
Navicula veneta	bf	h	p	b
Navicymbula pusilla	fb	e	u	u
Nitzschia reversa	u	e	u	b
Nitzschia acicularis	fb	e	am	epp/ p
Nitzschia capitellata	b	h	p	epp
Nitzschia clausii	b	h	am	ell/ epp
Nitzschia frustulum	b	e	p	b
Nitzschia lancettula	u	u	u	p

Species Name	Salinity	Trophy	Saprobity	Life Form
Nitzschia liebertruthii	b	e	bm	u
Nitzschia pura	fb	e	bm	el
Nitzschia sigma	b	e	am	b
Nitzschia supralitorea	fb	e	am	b
Nitzschia umbonate	fb	h	p	el
Opephora horstiana	mb	u	u	u
Paralia sulcate	m	mar	am	p
Pinnularia subcapitata	f	o	o	ep/ el
Pinnularia yarrensis	m	o	u	epp
Plagiogramma cf staurophorum	m	mar	u	es
Planothidium delicatulum	b	e	p	es/ ep
Planothidium engelbrechtii	b	e	bm	ep/ es
Planothidium frequentissimum	fb	h	am	ep/ es
Planothidium rostratum	fb	e	am	es/ ep
Pleurosigma salinarum	b	u	o	b
Raphoneis amphiceros	m	mar	u	es
Rhopalodia musculus	b	e	o	ep/ el
Sellaphora pupula	fb	h	p	epp/ el
Sellaphora seminulum	fb	h	p	el
Sellaphora subhamulata	fb	m	bm	b
Seminavis strigose	mb	u	u	b
Staurosira elliptica	fb	m	bm	b
Surirella fastuosa var. cuneata	m	mar	mar	ep
Tabellaria flocculosa	f	o	o	ep/ p
Tabularia fasciculata	b	e	bm	ep
Terpsinoë musica	bf	u	u	u
Thalassiosira eccentrica	m	mar	mar	u
Tryblionella apiculata	b	h	p	b
Tryblionella coarctata	b	u	u	b
Tryblionella littoralis	b	e	u	epp

Table 15. KNY19-G diatom species percentages against depth (cm) and age (cal BP).

Depth (cm)	**0.5**	**1.5**	**3.5**	**5.5**	**7.5**	**9.5**	**11.5**	**13.5**	**15.5**	**17.5**
Age (cal BP)	**-65.5**	**-57**	**-40**	**-23.5**	**-8.5**	**7**	**25**	**51**	**86.5**	**126.5**
Achnanthes brevipes	0	0	0	1.67	1.67	0.33	1	0.33	0	0.33
Achnanthes coarctata	0	0	0	0	0	0	0	0	0.33	0
Achnanthes fimbriata	0	0	0	0.33	0	0	0	0	0	0.33
Achnanthes oblongella	0.33	0.33	1	1	0	0.67	0.67	0	1.33	1
Achnanthes subaffinis	0	0	0	0	0	0.33	0	0	0	0
Achnanthes swazi	0	0	0	0	0	0	0	0	0.33	0
Achnanthidium biasolettianum	1	0	0	0.67	0.33	0	0.67	0.33	0	0
Achnanthidium crissum	1	0	0	0	0	0.33	0	0	0	0
Achnanthidium eutrophilum	0	0	0	0.33	0	0	0	0	0	0
Achnanthidium macrocephalum	0	0	0	0	0	0	0	0	0.33	0
Achnanthidium petersenii	0	0	0	1.67	0	0.33	1	0.67	0.67	0
Achnanthidium straubianum	0.33	0	0	0	0.67	0	0	0	0	0
Amphora decussata	0	0	0	0.33	0	0	0	0	0	0
Amphora helenensis	0.33	0.33	0.67	1.33	2.33	1.33	0.67	1	0.67	1
Amphora holsatica	0	0	0	0	0.33	0	0	0	0	0
Amphora montana	0	0	0	0	0	0	0	0	0.33	0
Amphora pediculus	0	0	0	0	0	0	0	0	0.33	0
Bacillaria paradoxa	0	0.33	0	0.33	0.33	0	0	0	0.33	0.33
Brachysira brebissonii	0	0	0	1.33	2	0	0.67	0.67	1.33	1
Brachysira neoexilis	0	0	0	0.67	0.33	0	0	0	0	0
Caloneis linearis	0	0	0	0	1	0.33	0	0	0.33	0
Catenula adhaerens	0.33	0.33	0.33	0	0	0.33	0.67	0	0	0.67
Cocconeis costata	3	2	12.67	8.33	4	6	1	6.33	10	4.33
Cocconeis distans	0	0	0	0.33	0.33	0	0	0	0	0

Depth (cm)	**0.5**	**1.5**	**3.5**	**5.5**	**7.5**	**9.5**	**11.5**	**13.5**	**15.5**	**17.5**
Age (cal BP)	**-65.5**	**-57**	**-40**	**-23.5**	**-8.5**	**7**	**25**	**51**	**86.5**	**126.5**
Cocconeis heteroidea	0	0	0	0	0	0	0	0	0	0.33
Cocconeis placentula	0.33	1.33	2	3.67	5.33	6	4.33	3.33	3.33	4.67
Cocconeis scutellum	1.33	3	2	3.67	7.67	14.33	5.67	4.67	5.67	10.67
Craticula accomoda	0	0.33	0.33	0	0	0	0	0	0	0
Craticula molestiformis	0	0	0	0.33	0	0	0	0	0	0
Cyclotella quillensis	0	0	0	0	0.33	0	0	0	0	0
Delphineis minutissima	0	0.33	0.67	1.33	1	2.67	2.67	1	1.67	1
Denticula sundayensis	1.67	1.33	0.67	0	0	0	0	0	0.33	0.67
Dimeregramma minor	0	0	0	0	0.33	0	0.33	0.33	0	0
Diploneis (agg) (= *D. bombus, D. crabro, D. interrupta)*	0	0	0	2	2.33	0.67	1	1	2	2
Diploneis elliptica	1.67	1	0.67	3.33	4	8	14.33	11.67	8	7.67
Encyonema silesiacum	1.33	0	0.33	1.33	0.67	0.33	0.33	0.33	1	1
Eolimna subminuscula	0.33	1.33	1.67	0.67	0	0.33	0	0	0	0.67
Epithemia sorex	0	0	0	0	0.33	0	0.33	0	0	0
Eunotia exigua	0	0	0	0	0	0	0	0	0.67	0
Eunotia flexuosa	0	0	0	0.67	0	0	0	0	0.33	0
Eunotia incisa	0.33	2.33	0	10.33	2	2.67	1.67	3	8	2.33
Eunotia minor	0.33	0.33	0	7.67	4.33	1.33	1	0.33	3	2
Eunotia pectinalis	0	0.67	0	0	0	0	0	0	0	0
Eunotia pectinalis var. undulata	1	0.33	0	5.33	2	0.67	3	0	0	1
Eunotia zygodon	0	0	0	0	0.33	0	0	0	0	0.33
Fallacia florinae	0	0	0	0	0.33	0	0.67	0.67	0	0
Fallacia monoculata	0	0.67	0.33	0.33	0	0	0	0	0	0
Fallacia pygmaea	0	0	0.33	0.67	2	12	5.33	2.67	2	5.33
Fragilaria biceps	0	0	0	0.33	0	0	0	0	0	0
Frustulia saxonica	0	0	0	0	0	0	0	0	0.67	0.33

Depth (cm)	**0.5**	**1.5**	**3.5**	**5.5**	**7.5**	**9.5**	**11.5**	**13.5**	**15.5**	**17.5**
Age (cal BP)	**-65.5**	**-57**	**-40**	**-23.5**	**-8.5**	**7**	**25**	**51**	**86.5**	**126.5**
Frustululia crassinervia	1	1.33	0	1.33	1.33	0.67	1.67	2.33	4	1.67
Giffenia cocconeiformis	7.67	11.33	4.33	0.33	1	3.33	8.33	9.33	6.67	5.33
Gomphonema gracile	0	0	0	0	0	0	0	0	0.33	0
Grammatophora oceanica	0.67	0	0	0.33	1.33	0.33	0	0.67	1.33	1.33
Gyrosigma obtusatum	4.33	5.67	6	1	1	0	1.67	1	1.67	0.67
Halamphora coffeaeformis	3	3.33	4.67	6	4	6.67	4.33	2	1	3
Luticola goeppertiana	0	0	0	0	0	0	0	0.33	0	0
Lyrella lyra	0	0	0	0	0	0	0	0	0	0
Mastogloia elliptica	0	0	0	0	1	0	0	0	0	0.67
Mastogloia exigua	2	0.67	0.67	1	2	0.33	0	0.33	0	0
Mastogloia fimbriata	0	0.33	0.33	0.67	0.33	0	0	0	0	0.67
Navicula arvensis var. maior	0	0	0	0.33	0.33	0	0	0	0	0
Navicula cryptotenella	0.67	0	0	0	0	0.33	0	0.33	0.67	0.33
Navicula germainii	1.67	0.67	1.33	0.67	1	2.67	0.67	2.67	1.67	2.33
Navicula longa	1	2.67	1.33	1.67	10	2.67	12.33	17.67	10.67	7.33
Navicula lucens	0	0	0	0.33	3	7.67	3.67	1.33	1.33	1.33
Navicula microcari	0	0	0	0.33	1.33	0	0	0	0	0
Navicula ranomafenensis	0	0	0	0	0	0	0	0	0	0.33
Navicula schroeteri	0	0	0	0	0.33	0	0	0	0	0
Navicula tenelloides	35.33	31.67	32.33	6.33	9.33	2.67	1.33	1.33	1	4.67
Navicula tripunctata	0	0	0	0	0	0.33	0	0	0	0
Navicula veneta	0	0	0	0.33	0.33	0.33	0	0	0	0
Navicymbula pusilla	2.33	1.33	2	1	1.67	1.33	0.33	0	0	0.33
Nitzschia reversa	0.33	0	0	0	0	0	0	0	0	0
Nitzschia acicularis	0.33	0	0	0.33	0	0	0	0	0	0.33
Nitzschia capitellata	0.33	0.67	0	1	0.67	0	0.33	0	0.33	0
Nitzschia clausii	0	0	0	0	0.33	0.33	0	0	0	0

Depth (cm)	**0.5**	**1.5**	**3.5**	**5.5**	**7.5**	**9.5**	**11.5**	**13.5**	**15.5**	**17.5**
Age (cal BP)	**-65.5**	**-57**	**-40**	**-23.5**	**-8.5**	**7**	**25**	**51**	**86.5**	**126.5**
Nitzschia frustulum	0	0	0	0	0	0	1.33	0.33	0	0
Nitzschia lancettula	0.33	0.33	0	0	0	0	0.33	0	0	0
Nitzschia liebertruthii	0	1	0.33	1	0	0	0	0.33	0.33	2.33
Nitzschia pura	0	0.33	0.33	0	0.33	0	1.67	0.67	0.67	0
Nitzschia sigma	0	0.33	0	0.33	1	0	0.67	2	1.67	0.33
Nitzschia supralitorea	9.33	6.67	7.33	0.33	0.67	0	0	0	0	0
Nitzschia umbonata	0	0	0.33	0	0.67	0.33	0	0	0.33	0.67
Opephora horstiana	0.33	0	0.33	0.33	0.33	0	0	0	0	1
Paralia sulcata	0.33	0	0.33	0	0	0.33	0	0.67	0	0.33
Pinnularia subcapitata	0	0	0	1	0	0	0	0	0	0.33
Pinnularia yarrensis	0	0	0	0	0	0.33	0	0	0.33	0.33
Plagiogramma cf staurophorum	0	0	0	0	0	0.67	0.33	0	0	0
Planothidium delicatulum	0	0	0.67	1	0.33	2.33	0.67	0.33	0.33	1.33
Planothidium engelbrechtii	1	1	1	0.33	0.33	0	0.33	0	0	1
Planothidium frequentissimum	0	1	4	0.67	0.67	2	1	0.67	0	0
Planothidium rostratum	0	0	0	1	0	0	0	0	0	0
Pleurosigma salinarum	1	1	1.67	1	0.67	0	0.67	0.33	0.67	0
Raphoneis amphiceros	0	0	0	0	0	0	0	0.33	0.33	0.67
Rhopalodia musculus	9	7.33	2.67	1.33	1.33	0.67	2.33	1	0.67	1
Sellaphora pupula	0	0	1	0.67	1.33	1.33	0.33	0.33	0	0.33
Sellaphora seminulum	1	0	0	0.33	0	0	0	0	0	0
Sellaphora subhamulata	0.67	0.33	1	0	0	0	0	0	0	0
Seminavis strigosa	0.67	0.33	0	1.67	2.33	1	1.33	7.33	4.33	3.67
Staurosira elliptica	0.33	2	0.67	0	0	0.67	0	0	0	0
Surirella fastuosa var. cuneata	0.33	0	0	0	0.33	0.67	3.67	6	1	2
Tabellaria flocculosa	0	0.67	0.33	3	1.67	0	2	0.67	3.33	0.67
Tabularia fasciculata	0	0	0	0	0	0	0.33	0	0	0.67

Depth (cm)	**0.5**	**1.5**	**3.5**	**5.5**	**7.5**	**9.5**	**11.5**	**13.5**	**15.5**	**17.5**
Age (cal BP)	**-65.5**	**-57**	**-40**	**-23.5**	**-8.5**	**7**	**25**	**51**	**86.5**	**126.5**
Terpsinoë musica	0	0	0.33	0	0.33	0	0.33	0	0	0.67
Thalassiosira eccentrica	0	0	0	1	0	0	0	0	0	0.67
Tryblionella apiculata	0.33	1.33	0.67	0.67	0.33	0	0.33	1	1	2
Tryblionella coarctata	0	0.33	0.33	1.33	0.67	0	0.33	0	0.67	0
Tryblionella littoralis	0	0	0	0	0	1	0.33	0.33	0.67	0.67

Depth (cm)	**19.5**	**21.5**	**23.5**	**27.5**	**29.5**	**31.5**	**33.5**	**35.5**	**37.5**
Age (cal BP)	**169.5**	**212**	**254.5**	**340.5**	**383.5**	**427**	**469.5**	**512.5**	**555.5**
Achnanthes brevipes	0	0.33	2.67	0	0	1.67	1.33	1.67	1.67
Achnanthes coarctata	0	0	0	0	0	0	0	0	0
Achnanthes fimbriata	0	0	0	0	0	0	0	0	0
Achnanthes oblongella	0.67	0.67	0	0	0	0	0	0.33	0
Achnanthes subaffinis	0	0	0	0	0	0	0	0	0
Achnanthes swazi	0	0	0	0	0	0	0	0	0
Achnanthidium biasolettianum	0	0	0	0	0	0	0	0	0
Achnanthidium crassum	0	0	0	0	0	0	0	0	0
Achnanthidium eutrophilum	0	0	0	0	0	0	0	0	0
Achnanthidium macrocephalum	0.33	0	0	0	0	0	0	0	0
Achnanthidium petersenii	0	0	0	0	0	0	0	0	0
Achnanthidium straubianum	0	0	0	0	0	0	0	0	0
Amphora decussata	0	0	0	0	0	0	0	0	0
Amphora helenensis	0.67	0.67	0	0	0	1.33	3.67	1.67	2.33
Amphora holsatica	0	0	0	0	0	0	0	0	0
Amphora montana	0	0	0	0	0	0	0	0	0
Amphora pediculus	0	0	0	0	0	0	0	0	0
Bacillaria paradoxa	0.67	0.67	0	0	0	0	0	0	0
Brachysira brebissonii	0.33	0	0	0	0	0	0	0	0
Brachysira neoexilis	0	0	0	0	0	0	0	0	0
Caloneis linearis	1.67	0.33	0.67	0	0.33	2	0.67	1	1
Catenula adhaerens	0	0.67	0	0	0	0	0	0	0
Cocconeis costata	7	5.67	4.33	3.67	1.33	0.67	1	2.33	0.67
Cocconeis distans	0	0	0	0	0	0	0	0	0
Cocconeis heteroidea	0	0	0	0	0	0	0	0	0

Depth (cm)	**19.5**	**21.5**	**23.5**	**27.5**	**29.5**	**31.5**	**33.5**	**35.5**	**37.5**
Age (cal BP)	**169.5**	**212**	**254.5**	**340.5**	**383.5**	**427**	**469.5**	**512.5**	**555.5**
Cocconeis placentula	5.67	1	1.67	3	4.67	10.67	4.33	3.67	6.67
Cocconeis scutellum	2.33	2	5.33	4.67	8	8.33	9.33	10.67	12.33
Craticula accomoda	0	0	0	0	0	0	0	0	0
Craticula molestiformis	0	0	0	0	0	0	0	0	0
Cyclotella quillensis	0	0	0	0	0	0	0	0	0
Delphineis minutissima	0.33	0.67	0.67	0	0	0	0	0.33	1
Denticula sundayensis	0	0	0	0	0	0	0	0	0
Dimeregramma minor	0	0	0	1	0.67	2.67	9	7.67	4
Diploneis (agg) (= *D. bombus, D. crabro, D. interrupta)*	2.67	2.33	13	38	56	32.67	27.67	38	35
Diploneis elliptica	11	22.67	14.67	16.33	11.67	23	23.67	18.67	20.33
Encyonema silesiacum	1	0	0	0	0	0	0	0	0
Eolimna subminuscula	0	0	0	0	0	0	0	0	0
Epithemia sorex	0	0	0	0	0	0	0	0	0
Eunotia exigua	0	0	0	0	0	0	0	0	0
Eunotia flexuosa	0.33	0.67	0	0	0	0	0	0	0
Eunotia incisa	2.33	0.67	0.67	0	0	0	0	0.33	0
Eunotia minor	0.67	0.33	0	0	0	0.33	0.33	0	0
Eunotia pectinalis	1	0	0.33	0	0	0	0	0	0
Eunotia pectinalis var. undulata	0	0	0.67	0	0	0	0	0	0
Eunotia zygodon	0	0	0	0	0	0	0	0	0
Fallacia florinae	0	0	0	0	0	0	0	0	0
Fallacia monoculata	0	0	0	0	0	0	0	0	0
Fallacia pygmaea	1.33	8.67	9	2.67	0	1.33	2	0.67	1
Fragilaria biceps	0.33	0	0	0	0	0	0	0	0.33
Frustulia saxonica	0.33	0	0	0	0	0	0	0	0
Frustululia crassinervia	1.33	2	1.67	0	0	1	0	0	0

Depth (cm)	**19.5**	**21.5**	**23.5**	**27.5**	**29.5**	**31.5**	**33.5**	**35.5**	**37.5**
Age (cal BP)	**169.5**	**212**	**254.5**	**340.5**	**383.5**	**427**	**469.5**	**512.5**	**555.5**
Giffenia cocconeiformis	12.33	5.67	6.67	1	0	0	0	0.67	0
Gomphonema gracile	0	0	0	0	0	0	0	0	0
Grammatophora oceanica	2	0	0.67	4	1.67	1.33	5	3.33	2.67
Gyrosigma obtusatum	1.67	1.67	0	0	0	0	0	0	0
Halamphora coffeaeformis	2.33	3.33	4.33	1	0	0	0	0	0
Luticola goeppertiana	1	2	0.67	0	0	0	0	0	0
Lyrella lyra	0	0	0	1	0.67	0.33	0.33	0	0
Mastogloia elliptica	0.67	2.67	2	3	0.67	0.67	0.33	0.67	0
Mastogloia exigua	0	0	0	0	0	0	0	0	0
Mastogloia fimbriata	0	0	0.67	0	0	0	0	0	0
Navicula arvensis var. maior	0	0	0	0	0	0	0	0	0
Navicula cryptotenella	0	0	0	0	0	0	0	0	0
Navicula germainii	2.33	0	1.33	0	0	0	0	0	0
Navicula longa	18.33	9.33	9.33	0.67	0	0	0	0	0
Navicula lucens	1	0.33	0.67	0.33	0	0	0	0	0
Navicula microcari	0	0	0	0	0	0	0	0	0
Navicula ranomafenensis	0	0	0	0	0	0	0	0	0
Navicula schroeteri	0	0	0	0	0	0	0	0	0
Navicula tenelloides	0	0.33	0.33	0	0	0	0.33	0	0
Navicula tripunctata	0	0	0	0	0	0	0	0	0
Navicula veneta	0	0	0	0	0	0	0	0	0
Navicymbula pusilla	0	0.33	0.33	0	0	0	0	0	0
Nitzschia reversa	0	0	0	0	0	0	0	0	0
Nitzschia acicularis	0	0	0	0	0	0	0	0	0
Nitzschia capitellata	0.67	0	1.67	0	0	0	0	0	0
Nitzschia clausii	0	0	0	0	0	0	0	0	0
Nitzschia frustulum	0	1.33	0	0.33	0	0	0	0	0

Depth (cm)	**19.5**	**21.5**	**23.5**	**27.5**	**29.5**	**31.5**	**33.5**	**35.5**	**37.5**
Age (cal BP)	**169.5**	**212**	**254.5**	**340.5**	**383.5**	**427**	**469.5**	**512.5**	**555.5**
Nitzschia lancettula	0	0	0	0	0	0	0	0	0
Nitzschia liebertruthii	1.67	0	0	0	0	0	0	0	0
Nitzschia pura	0	0.33	0	0.67	0.67	0	0.33	0.33	0
Nitzschia sigma	0.33	2	0.33	0.67	0	0	0	0.33	0
Nitzschia supralitorea	0	0	0	0	0	0	0	0	0
Nitzschia umbonate	0	0	0.33	0	0	0	0	0	0
Opephora horstiana	0	0.33	0	0	0	0	0	0	0
Paralia sulcate	0	0.33	0.33	2.67	2	0	1	1	0.67
Pinnularia subcapitata	0	0	0	0	0	0	0	0	0
Pinnularia yarrensis	0.33	0	0	2	2.33	0.67	2.67	1.67	1.67
Plagiogramma cf staurophorum	0	0	0	0	0	0	0	0	0
Planothidium delicatulum	0	0.67	0	0	0	0	0	0.33	0
Planothidium engelbrechtii	0	0	0	0	0	0	0	0	0
Planothidium frequentissimum	0	0	0.67	0	0	0.33	0	0	0
Planothidium rostratum	0	0	0	0.33	0	0	0	0	0
Pleurosigma salinarum	0.67	0.67	0	0	0	0	0	0	0
Raphoneis amphiceros	0	0	0	0	0	0	0	0	0
Rhopalodia musculus	1	1.33	1.33	9.67	2	3	3.33	1	3.33
Sellaphora pupula	0	0	0	0	0	0	0	0	0
Sellaphora seminulum	0	0	0	0	0	0	0	0	0
Sellaphora subhamulata	0	0	1	0	0	0	0	0	0
Seminavis strigose	5	4	6.33	0.33	1.33	4.67	1.33	1.33	3.67
Staurosira elliptica	0	0	0	0	0	0	0	0	0
Surirella fastuosa var. cuneata	5	4	2	2.67	5.33	3.33	2.33	2.33	1.67
Tabellaria flocculosa	0	0	0.33	0	0	0	0	0	0
Tabularia fasciculata	0	0	0	0	0	0	0	0	0
Terpsinoë musica	0	7.33	1.33	0	0	0	0	0	0

Depth (cm)	**19.5**	**21.5**	**23.5**	**27.5**	**29.5**	**31.5**	**33.5**	**35.5**	**37.5**
Age (cal BP)	**169.5**	**212**	**254.5**	**340.5**	**383.5**	**427**	**469.5**	**512.5**	**555.5**
Thalassiosira eccentrica	0	0	0	0	0	0	0	0	0
Tryblionella apiculata	1	0.67	0.33	0	0.67	0	0	0	0
Tryblionella coarctata	0.33	0.67	1	0	0	0	0	0	0
Tryblionella littoralis	0.33	0.67	0.67	0.33	0	0	0	0	0

Table 16. Sample score loadings of the first two statistically significant principal components for KNY19-G.

Age (cal BP)	PC 1	PC 2
-65.5	-0.14831	0.59566
-57	-0.13156	0.52648
-40	-0.14522	0.52976
-23.5	0.017916	0.080824
-8.5	0.050713	0.14588
7	0.18701	0.061386
25	0.21574	0.056631
51	0.18114	0.04402
86.5	0.12736	0.020019
126.5	0.1456	0.090103
169.5	0.1679	0.025403
212	0.31146	0.046935
254.5	0.23611	0.035731
340.5	0.24878	0.072152
383.5	0.20703	0.053722
427	0.37736	0.08529
469.5	0.37094	0.09792
512.5	0.30862	0.07334
555.5	0.35215	0.087525

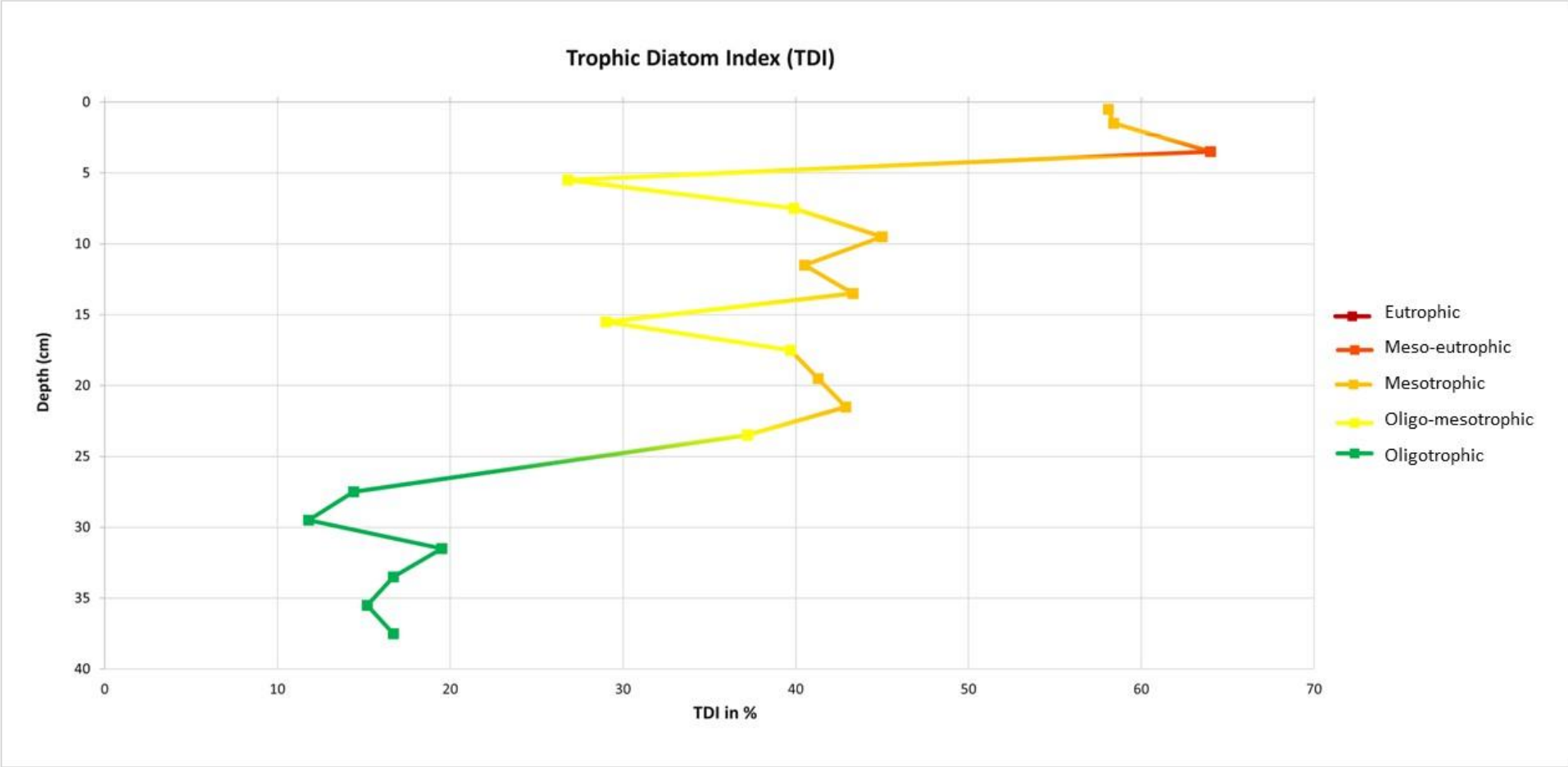

Figure 41. Trophic Diatom Index of KNY19-G against depth.